

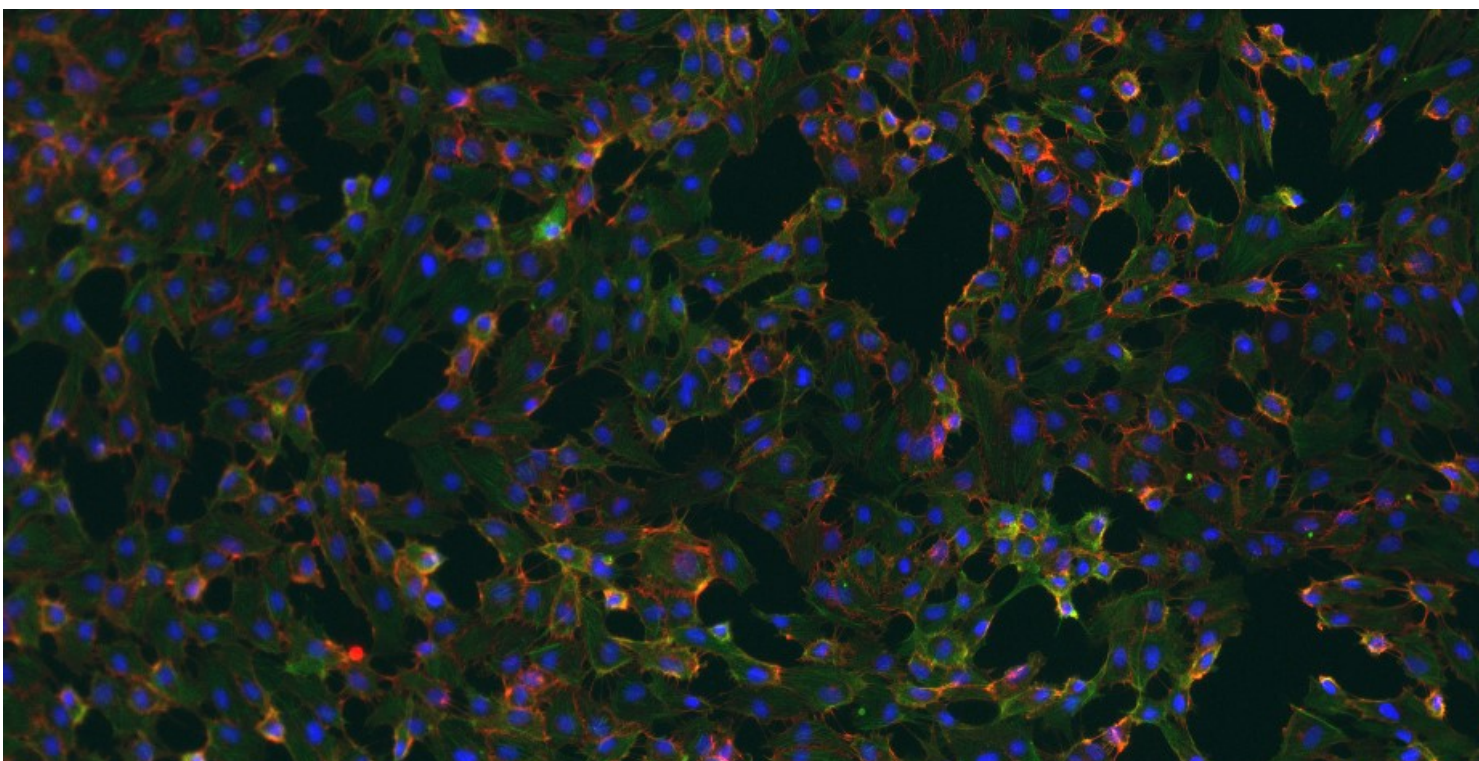
Molecular characterization of endothelial cell response in the context of radiation-induced atherosclerosis

Bjorn Baselet

Août 2017

Thèse présentée en vue de l'obtention du grade
de docteur en Sciences biomédicales et pharmaceutiques

Secteur des sciences de la santé



Acknowledgements

*If I have seen further,
it is by standing on the shoulders of giants.*

– Isaac Newton

Almost four years ago I embarked on a new journey of a lifetime: a PhD research project. While my travel has been turbulent at times, with many ups and downs, at the end of it all I can say that it was worth it. Along the way I had the opportunity to learn a great deal, have new experiences and to meet a lot of warm and kind people. As science is not an individual sport, I devote this section to all giants in my life to whom I owe a big thanks. Because of them, I can see further. Without them, I could never have endured my travel, I could never have withstand rain showers and heavy winds, and I would never have enjoyed the epic mountain views as much. Then again, beauty is also in the travel as the journey is more important than its destination.

Prof. Pierre Sonveaux, my Director. Thank you for accepting me in your lab as your PhD student. I really appreciated your valuable comments and suggestions that helped me in the completion of this thesis. Also a big thanks for sharing your knowledge and expertise.

Dr. An Aerts, my co-Director. Thank you for the support you gave me throughout my PhD work. Thank you for your guidance and our nice discussions.

Prof. Sarah Baatout, head of the Radiobiology Unit. Thank you for your unsurpassed enthusiasm and dedication. I am deeply grateful that you accepted me in your lab as one of your PhD students. Thanks for the nice talks we had and the warm atmosphere you create at our research labs.

Prof. Hans Vanmarcke, Dr. Filip Vanhavere and Dr. Hildegard Vandenhove, my SCK•CEN Superiors. Thank you for giving me the support that made it possible for me to work on my PhD project. Thank you for giving me the opportunity to explore the scientific world.

Prof. Nathalie Delzenne, Prof. Jean-Pascal Machiels, Prof. Bénédicte Jordan and Prof. Sandrine Horman, my accompanying Jury. Thank you for your guidance and continued support throughout my PhD work. Thank you also for the constructive comments and the nice atmosphere during our meetings. And thank you for your thorough and critical evaluation of my PhD thesis.

Prof. Mike Atkinson and Dr. Elke Decrock, my external thesis Jury Members. Thank you for your willingness to be part of my Thesis Jury. Thank you for your constructive comments, thorough reading and critical evaluation of my work.

Dr. Michèle Coeck, Mrs. Griet Vanderperren and other team members of the Centre for Education and Knowledge Management. Thank you for providing the framework that enabled me to perform my PhD. Thanks for your continuous efforts to improve the excellent PhD group atmosphere at SCK•CEN. Thank you for the superb education and training provided.

Mrs. Ilse Beirens, Mr. Roel Dillen, Mr. Pietro Caputo, Mrs. Maud Vanderthommen and other team members of the Communication Services. Thanks for checking and printing all the overdue posters. Thank you for the social events you organized and for the excellent services you provide.

Mr. Bart Marlein, Mr. Michel Doms and other team members of the Dosimetric and Calibration Services. Thank you for your assistance during irradiation experiments. Thank you for your nice chat during the endless waiting.

Mrs. Betty Vandingelen and Mrs. Claude Remacle, our Secretaries from SCK•CEN and UCL. Thank you for being there when I needed assistance or a nice chat. You are one of a kind!

Dr. Hanène Badri, Dr. Kristel Mijndonckx, Dr. Hanane Derradji, Dr. Mieke Verslegers, my office buddies. Thank you very much for your help, advice, mental and scientific support and for being there for me when I needed a talk. I enjoyed every minute sharing a desk with you!

Dr. Roel Quintens, Dr. Marjan Moreels and Dr. Rafi Benotmane, Senior Scientists at the RDB lab. Thank you for your help and assistance during my PhD project. I truly enjoyed working with you.

Dr. Hussein El Saghire, Dr. Charlotte Rombouts, Dr. Annelies Suetens, Dr. Marlies Gijss, Dr. Tine Verreet, Dr. Ellina Macaeva and Mr. Kevin Tabury, my predecessors. Thank you for showing me the way and for convincing me that it could be done. Thank you for all the moments of fun and moral support. I will cherish these moments we spent together.

Mrs. Mieke Neefs, Mrs. Brit Proesmans, Mrs. Lisa Daenen, Mrs. Ilse Coninx, Mrs. Liselotte Leysen, Mrs. Jasmine Buset, Mrs. Ann Janssen, Mrs. Ann Provoost, Mr. Wietse Heylen, Mrs. Arlette Michaux, Mr. Randy Vermeesen and Mrs. Amelie Coolkens, Mr. Thibaut Vazeille, Mrs. Morgane Tardy and Mrs. Marie-Joséphine Fontenille, the world's greatest Lab Technicians. A big thank you for your help and assistance. Thank you for your time and efforts in helping me with experiments.

Dr. Paolo E. Porporato, Dr. Jhudit Pérez-Escuredo, Dr. Jorge Falces, Dr. Andrea Cacace, Dr. Vincent Van Hée, Dr. Martina Sboarina, Mr. Valéry L. Payen, Dr. Amanda Cañas Rodriguez, Dr. Joanna Krzystyniak, Mrs. Debora Grasso, Dr. Lucie Brisson and Mrs. Jessica Vanderstraeten, my dearest colleagues at UCL. Thank you for welcoming me in your warm group. You made me feel at home and supported me in experiments. You made my time at UCL really fun.

Mrs. Raghda Ramadan, Mr. Kai Craenen, Mrs. Noami Daems, Mrs. Katrien Konings, Mrs. André Claude Mbouombouo Mfossa, Mrs. Merel Van Wallegghem, Mrs. Anu Yadav, Mrs. Valérie Van Eesbeeck and Mr. Ali Md Muntasir, my fellow PhD students at SCK•CEN. Thanks for wonderful moments of joy and laughter. I enjoyed our times together in and outside the labs. A big thank you for the nice atmosphere: you are lovely people!

Mr. Niels Belmans, Mrs. Emma Coninx and Mrs. Liese de Ridder, my three master students. It was simply a joy guiding and tutoring you. I could not imagine better master students. Thanks for your assistance during my PhD project and the fun we had in and outside the labs.

Mr. Bart Theuwissen, Mrs. Mieke Thaens, Mrs. Anuschka Vangrinsven, Mrs. Elien Wouters, Mrs. Lotte Proost, my dearest friends. Thank you for your help putting everything in perspective. Thanks for all the fun and the relaxation you gave me!

Mrs. Bo Byloos, my dearest friend and SCK•CEN colleague. If I have to thank you for everything you helped me with, the printing costs of my thesis would be too high. From the moment we met, we connected and found mental support in one another. I enjoyed every conversations we had, every movie we saw and every rollercoaster we've been on. Working together is one of the things I will miss the most at the end of my thesis.

Mrs. Jolien Baselet, my dearest younger sister. You also deserve a big thank you as you supported me throughout this PhD project. Thank you for our relaxing fitness moments, our evening strolls with Tripsy, our lengthy discussions on our future and all the support you gave me during our brother-sister moments.

Mrs. Joke Baselet, Mr. Frank Savelkoul, Mr. Giel Savelkoul and Mr. Gust Savelkoul, my dearest younger sister and family. Thank you for leading the way in having a family. Thank you for the godfatherhood of Gust, my beloved godchild.

Mrs. Isabelle Schelmans and Mr. Johan Baselet, my beloved and dearest parents. Thank you for your continuous support, relaxation and love you gave me day in day out. You showed me the most important things in life and I'm forever grateful for this. Thanks for everything!

Dr. Gerd Devos, my partner. Words cannot describe how much I owe you. You came into my life during my third PhD year. You complete me and make my life more livable and definitely funnier. Thanks to you, I brought my thesis to a successful conclusion. Thank you for your support, time, love and affection. Thank you for being there for me!

Summary

Ionizing radiation is used for radiotherapeutic and diagnostic purposes, which can expose the heart and blood vessels, potentially causing cardiovascular diseases (CVDs). However, dose-dependency and associated molecular mechanisms are still elusive. Our work focused on endothelial cells based on previous information suggesting that ionizing radiation could promote atherosclerosis. We report that a single X-ray dose induces a time- and dose-dependent pro-atherosclerotic phenotype, linked with changes in cell cycle progression and induction of inflammation and senescence. By comparing responses to X-rays and Fe ion, radiation impact was found to be dependent on radiation quality, with a more pronounced and longer lasting response to Fe ions. Altogether, our data provide new molecular information on the causes of radiation-induced CVD and a basis on which to build new knowledge in order to ameliorate the current radiation protection system.

Résumé

Les radiations ionisantes sont utilisées à des fins diagnostiques et thérapeutiques, ce qui peut exposer le cœur et les vaisseaux sanguins, favorisant les maladies cardiovasculaires (CMVs). Or, la dépendance de dose et les mécanismes moléculaires de ces effets sont peu connus. Notre travail s'est intéressé aux cellules endothéliales sur base d'informations suggérant que les radiations ionisantes favorisent l'athérosclérose. Nous rapportons qu'une dose unique de rayons X induit un phénotype pro-athérosclérotique dépendant du temps et de la dose, associé à des changements du cycle cellulaire et à l'induction d'inflammation et de sénescence. La comparaison des réponses aux rayons X et aux ions Fe montre que la qualité des rayons importe, avec des effets plus prononcés et plus longs pour les ions Fe. Nos résultats fournissent donc de nouvelles informations moléculaires relatives aux causes des CMVs radio-induites et une base de travail pour l'amélioration du système de radioprotection actuel.

Samenvatting

Ioniserende straling wordt gebruikt voor radiotherapeutische en diagnostische doeleinden die hart en bloedvaten kunnen blootstellen en zo mogelijks hart- en vaatziekten (HVZ) veroorzaken. Kennis inzake dosisafhankelijkheid en betrokken moleculaire mechanismen is echter minimaal. Ons werk richtte zich op endotheel cellen op basis van voorgaande info die suggereerde dat ioniserende straling atherosclerose bevordert. We melden dat één röntgendosis een tijd- en dosisafhankelijk pro-atherosclerotisch fenotype induceert, gekoppeld aan veranderingen in celcyclus en inductie van ontsteking en senescentie. Tijdens het vergelijken van reacties op röntgenstralen en Fe ionen bleek dat de stralingsimpact afhankelijk was van stralingskwaliteit, met een meer uitgesproken en langdurigere respons op Fe ionen. Onze bevindingen leveren dusdanig nieuwe moleculaire informatie op over de oorzaken van stralingsgeïnduceerde HVZ en kunnen dienen als basis om nieuwe kennis op te bouwen om het huidige stralingsbeschermingssysteem te verbeteren.

Table of contents

Table of contents	7
List of abbreviations.....	11
Introduction Chapter 1. Basic concepts of ionizing radiation.....	19
1.1. What is ionizing radiation?	19
1.2. Radiation metrics.....	19
1.2.1. Measuring and assessing radiation exposure: doses and units	19
1.2.2. Actions of radiation on matter: linear energy transfer and relative biological effectiveness.....	22
1.3. Cancer radiotherapy	23
1.3.1. Radiation treatment is a key player in cancer treatment	23
1.3.2. Oxidative stress	26
1.3.3. DNA damage and repair	31
1.3.4. Cell cycle blockage.....	36
1.3.5. Cell removal.....	37
1.4. Protection against radiation exposure: the current radiation protection system	40
Introduction Chapter 2. Radiation-induced cardiovascular diseases	45
2.1. Cardiovascular diseases - generalities	45
2.2. Epidemiology of irradiation-induced CVD	49
2.3. Physiopathology of radiation-induced CVD	52
2.4. Gaps in the current knowledge of irradiation-induced CVDs	53
Introduction Chapter 3. Endothelial cell responses to ionizing radiation	57
3.1. The vascular endothelium	57
3.2. Physiological functions of endothelial cells	58
3.2.1. Vascular tone regulation	59

3.2.2. Blood coagulation.....	62
3.2.3. Interaction with immune cells.....	64
3.2.4. Vascular permeability.....	65
3.3. Pathological effects of ionizing radiation: endothelial activation and dysfunction.....	67
3.3.1. Endothelial activation: a pro-inflammatory state	68
3.3.2. Deterioration of the vascular tone.....	71
3.3.3. Procoagulatory and prothrombotic phenotype	73
3.3.4. Endothelial cell retraction and death.....	74
3.3.5. Mitochondrial dysfunction	76
3.3.6. Premature endothelial senescence.....	79
3.4. Models to study endothelial cells <i>in vitro</i> and <i>in vivo</i>	81
3.4.1. In vitro endothelial models	81
3.4.2. Ex vivo and in vivo models	86
Aims of the study	93
Results Chapter 1: Functional Gene Analysis Reveals Cell Cycle Changes and Inflammation in Endothelial Cells Irradiated with a Single X-ray Dose in Endothelial Cells Irradiated with a Single X-ray Dose	97
Supplementary figure 1	112
Supplementary figure 2	113
Supplementary figure 3	114
Supplementary figure 4	115
Supplementary figure 5	116
Results Chapter 2: Differential impact of single-dose Fe ion and X-ray irradiation on endothelial cell transcriptomic and proteomic responses	117
Discussion and perspectives	151
1. Dose-, time- and radiation quality-dependent changes in irradiated endothelial cells linked to a pro-atherosclerotic phenotype.....	151

2. Preclinical significance	157
3 Endothelial cells are a critical target for radiation-induced atherosclerosis	160
4. Future directions of research in the field of irradiation-induced atherosclerosis	161
4.1. Novel targets	161
4.2. Biomarkers	161
4.3. Pharmaceutical agents	162
4.4 Impact on clinical practice and radiation protection system	165
5. General conclusion	166
References	169
Annex 1. Curriculum Vitae of Bjorn Baselet.....	221
Annex 2. Online supplementary data related to Results Chapter 1: “Functional gene analysis reveals cell cycle changes and inflammation in endothelial cells irradiated with a single X-ray dose”, by Baselet B <i>et al.</i> , <i>Front. Pharmacol.</i> 2017;8:213.	231
Annex 3. Online supplementary data related to Results Chapter 2: “Differential impact of single-dose Fe ion and X-ray irradiation on endothelial cell transcriptomic and proteomic responses” by Baselet B, <i>et al.</i>	261

List of abbreviations

Abbreviation	Full term
•NO	Nitric oxide
Akt	RAC-alpha serine/threonine-protein kinase
AMPK	Adenosine monophosphate-activated protein kinase
AP-1	Activator protein-1
APAF1	Apoptotic protease-activating factor 1
AT1	Angiotensin II type 1 receptor
ATM	Ataxia telangiectasia mutated
ATR	Ataxia telangiectasia and Rad3-related protein
BAK	Bcl-2 homologous antagonist killer
BAX	Bcl-2-associated X
BH4	Tetrahydrobiopterin
BMI	Body mass index
CaMKII	Ca ²⁺ /calmodulin-dependent protein kinase II
cAMP	Cyclic adenosine monophosphate
CAT	Catalase
CCL2	C-C motif chemokine ligand 2
CCR	C-C chemokine receptor
cGMP	Cyclic guanosine monophosphate
CHK1	Checkpoint kinase 1
CHK2	Checkpoint kinase 2
CI	Confidence interval
CVD	Cardiovascular disease
CXCR	C-X-C motif chemokine receptor
DDB2	Damaged-DNA binding protein 2
DDR	DNA damage response
DNA-PK	DNA-dependent protein kinase
DSB	Double-strand break
EDHF	Endothelium-derived hyperpolarizing factor
EET	Epoxyeicosatrienoic acid
EGF	Epidermal growth factor
ELISA	Enzyme-linked immunosorbent assay
ERR	Excess relative risk
FAD	Flavin adenine dinucleotide
FADD	Fas-associated protein with death domain

FAS	Apoptosis-stimulating fragment
FMN	Flavin mononucleotide
GMP	Guanosine monophosphate
GPx	Glutathione peroxidase
GSH	Glutathione
GSR	Glutathione reductase
GSSG	Glutathione disulfide
HUVEC	Human umbilical vein endothelial cell
ICAM-1	Intracellular cell-adhesion molecule-1
IFN	Interferon
IL	Interleukin
iNOS	Inducible nitric oxide synthase
IκB	Inhibitor of κB
JAK	Janus kinase
JNK	c-Jun N-terminal kinase
Keap1	Kelch-like ECH associated protein 1
LET	Linear energy transfer
LPS	Lipopolysaccharide
MAPK	Mitogen-activated protein kinase
MCP1	Macrophage chemoattractant protein-1
MDC1	Mediator of DNA damage checkpoint protein 1
MIP	Macrophage inflammatory protein
MLCP	Myosin light-chain phosphatase
MPT	Mitochondrial permeability transition
MRN	Mre11-Rad50-Nbs1
NF-κB	Nuclear factor kappa-light-chain-enhancer of activated B cells
nNOS	Neuronal nitric oxide synthase
Nrf2	Nuclear factor (erythroid-derived 2)-like 2
OXPPOS	Oxidative phosphorylation
p16	Cyclin-dependent kinase inhibitor 2A
p21	Cyclin-dependent kinase inhibitor 1
p53	Tumor suppressor protein 53
PCR	Polymerase chain reaction
PDGF	Platelet-derived growth factor
PECAM-1	Platelet endothelial cell adhesion molecule-1

PGI ₂	Prostacyclin
PI3K	Phosphatidylinositol 3 kinase
PKA	Protein kinase A
PKC	Protein kinase C
PKG	Protein kinase G
PP1	Protein phosphatase 1
pRb	Retinoblastoma protein
RaM	Rapid mode of calcium uptake into heart mitochondria
RANTES	Regulated upon activation, normal T cell expressed and secreted
RBE	Relative biological effectiveness
RFN8	Ring finger protein 8
RNS	Reactive nitrogen species
ROS	Reactive oxygen species
SI	International System of Units
SMAD	Mothers against decapentaplegic homolog
SOD	Superoxide dismutase
SSB	Single-strand break
STAT	Signal transducer and activator of transcription
TGFβ	Transforming growth factor β
TNFα	Tumor necrosis factor α
Trx	Thioredoxin
TrxR	Thioredoxin reductase
VCAM-1	Vascular cell-adhesion molecule-1
VE-cadherin	Vascular endothelial cadherin
VSMC	Vascular smooth muscle cell
w _R	Radiation weighting factor
w _T	Tissue weighting factor
XPC	Xeroderma pigmentosum, complementation group C
γH2AX	Phosphorylated Histone H2A variant X

Introduction

Chapter 1

Basic concepts of ionizing radiation

Introduction Chapter 1. Basic concepts of ionizing radiation

1.1. What is ionizing radiation?

From natural to man-made sources, life on earth is exposed on a daily basis to ionizing radiation. Defined as a type of energy released by atoms that travels in the form of electromagnetic waves or particles, this energy can eject tightly bound electrons from the orbit of an atom, causing the atom to become ionized (1). Ionizing radiation can have natural and man-made sources. In nature, one can distinguish 3 main types of ionizing radiation: alpha (α), beta (β) and gamma (γ) radiation. They are all produced by naturally occurring substances with unstable nuclei (*e.g.* cobalt-60 and cesium-137) that spontaneously undergo radioactive decay. During the decay process, energy is lost *via* emission of ionizing radiation in the form of electromagnetic γ -rays and/or charged particles (*e.g.* α - and β -particles) (2). One of the most common man-made forms of ionizing radiation is X-ray radiation. X-rays are in most aspects identical to γ -rays, but differ in origin. While γ -rays are derived from the natural decay of a radioactive elements, X-rays are produced artificially in X-ray generators by directing a stream of high speed electrons at a target material such as gold or tungsten (3). When electrons interact with atomic particles of the target, X-radiation is produced (1). In addition to the most common forms listed above, there are many other forms of ionizing radiation of human or natural origin. Examples are neutrons, accelerated ions and fission fragments (4, 5). These less common forms can have different biological effects, as discussed below, which can be exploited in radiotherapy (6).

1.2. Radiation metrics

1.2.1. Measuring and assessing radiation exposure: doses and units

Radiation is universally present and play many roles integral to the existence of life. Indeed, life may never have emerged on Earth if not for the influence of radiation (7). However, radiation can and have been demonstrated to be dangerous to biological systems. In order to assess the impact of ionizing radiation on health and to set radioprotective guidelines, units to measure dose and its biological effects are required.

The international System of Units (SI) unit of *radioactivity* is the Becquerel (Bq). One Bq is defined as the occurrence of 1 nuclear disintegration per second within a

radioactive source. This unit is not used when studying biological effects because it does not take into account the amount of energy that is deposited in living matter (*e.g.* human body) and that could possibly cause damage (8).

The *absorbed dose* is defined as the amount of energy, originating from any type of ionizing radiation and any irradiation geometry that is absorbed per unit mass of material. The international SI unit for absorbed dose is the Gray (Gy). One Gy represents the absorption of 1 Joule of energy in 1 kilogram of mass (1 J/kg), and provides enough energy to raise the temperature of a kilogram of water by 0.00024 °C. This definition is pure physics, as it does not consider the quality of the ionizing radiation type and the extent of biological damage it inflicts to certain tissues and/or organs. As a result, the terms *equivalent dose* and *effective dose* have been introduced (8).

The *equivalent dose* takes into account the ability of a particular kind of ionizing radiation to cause damage. It is obtained by multiplying the absorbed dose (Gy) with a radiation-weighting factor (w_R), and is defined largely on the basis of the relative biological effectiveness (RBE; see below) of the different radiation types (Table 1). The international SI unit for equivalent dose is the Sievert (Sv) (8).

Table 1. Recommended radiation weighting factors*

Radiation type	w_R
Photons	1
Electrons and muons	1
Protons and charged ions	2
α particles, fission fragments, heavy ions	20
Neutrons	A continuous function of neutron energy

*All values relate to the radiation incident on the body or, for internal radiation sources, emitted from the incorporated radionuclide(s) (8).

The *effective dose* is defined as the weighted sum of all tissue and organ equivalent doses multiplied by their respective tissue-weighting factor (w_T). It expresses the biological effect that a certain type of ionizing radiation has on the human body. w_T values (Table 2) have been defined to represent the contributions of individual

organs and tissues to overall radiation effects on the human body. Similar to the equivalent dose, the effective dose has sievert (Sv) as international SI unit. Care should be taken with w_T values because they constitute an average over both genders and adult ages to reflect the radiation burden to an average human adult (8, 9). Examples of effective doses associated with different sources of ionizing radiation are presented in Table 3.

Table 2 Recommended tissue weighting factors

Tissue	w_T	$\sum w_T$
Bone-marrow (red), colon, lung, stomach, breast, remainder tissues*	0.12	0.72
Gonads	0.08	0.08
Bladder, esophagus, liver, thyroid	0.04	0.16
Bone surface, brain, salivary glands, skin	0.01	0.04
Total		1.00

*Remainder tissues include adrenals, extra-thoracic region, gallbladder, heart, kidneys, lymphatic nodes, muscles, oral mucosa, pancreas, prostate, small intestine, spleen, thymus, uterus/cervix (8).

Table 3: Representative effective doses associated with different sources of ionizing radiation

Source	Effective dose (mSv)*
Dental X-ray	0.005
Radiography chest	0.1
One return flight New-York-London	0.1
Radiography abdomen	1.2
Computed tomography (CT) of head	2
Natural background (per year)	2.4
Mammography	3
CT of chest	7
CT of abdomen	6-10
CT of pelvis	8-10
Coronary CT angiography	12

Myocardial perfusion study	10-29
Myocardial viability study	14-41
Annual occupational dose limit	20
Radiotherapy (delivered in fractions)	40 000 – 70 000

*Doses are whole-body doses, except those of medical exposure, which are delivered to a specific organ. CT: computed tomography. Sv: Sievert. (10-15).

1.2.2. Actions of radiation on matter: linear energy transfer and relative biological effectiveness

Contemporary radiotherapy usually uses conventional X-rays with high energies (4-25 megavolts). However, hadron therapy is gaining momentum in the field of radiotherapy. In this technique, accelerated charged particles are used, such as protons and carbon ions (16). These particles may have a greater biological effect per unit dose than conventional X- and γ -rays, depending on the amount and location of the ionizations they cause. To distinguish between more damaging and less damaging radiation types, the terms *linear energy transfer* (LET) and RBE have been defined (17).

LET is defined as the average energy (in keV) that is lost by an ionizing particle when travelling across a unit length of its trajectory in matter (μm). As such, it describes the density of ionization in a particle track. Electromagnetic X- and γ -rays deposit much of their energy as single isolated ionization and excitation and are, hence, low LET radiation types. For example, approximately 1,000 sparse tracks are produced per Gy of absorbed γ -radiation dose (17) (Figure 1). Ionizing particles, such as α -particles, produce fewer tracks, but intense ionization within each track leads to more severe damage. Hence, they belong to the high LET radiation type. Per Gy of absorbed α -radiation dose, approximately 4 intense ionizing tracks are produced (17).

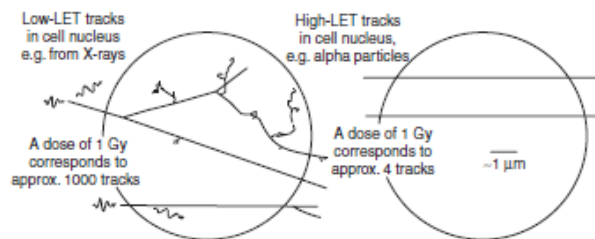


Figure 1. Structure of particle tracks for low-linear energy transfer (LET) radiation (left) and high LET α particles (right). Circles indicate the typical size of mammalian cell nuclei (17).

LET values are directly proportional to induced cell killing and, thus, to biological effectiveness. When measuring the biological effectiveness of certain radiation types, one can quantify their RBE values. RBE is defined as the ratio of the reference absorbed dose of low LET radiation of a standard (X-rays with a LET of $3.5 \text{ keV}/\mu\text{m}$) and the absorbed dose of the radiation type under focus that causes the same amount of biological damage (18). Hence, the higher the RBE value for a given type of radiation, the more damaging this type of radiation is per unit of energy deposited in biological tissues. RBE values are not constant but depend on the biological endpoint, the dose level and LET values (17). In practice, RBE values are represented as regulatory w_R values, which are consensus values adopted by radiation experts (8).

This PhD thesis focuses on cardiovascular effects related to either low LET X-ray radiation (Results Chapter 1) or high LET Fe ion radiation (Results Chapter 2). So far, radiation-induced CVD is assumed to be deterministic in nature, so the amount of energy should be expressed in terms of the absorbed dose (Gy) (19). According to the current consensus, the term “low dose” is defined as a dose of 100 mGy or less throughout this thesis (8, 20).

1.3. Cancer radiotherapy

1.3.1. Radiation treatment is a key player in cancer treatment

Cancer is a growing problem in aging Western populations. Almost 1 out of 3 people in the Western world will indeed be confronted with a cancer diagnosis. Cancer is also currently the second main cause of death in industrialized countries (21).

Several treatment options are available, among which surgery, radiotherapy and chemotherapy are most often used (22). The choice of treatment depends on tumor type, local size of the tumor, the presence of metastasis and general patient characteristics (23). During cancer treatment, half of all patients undergo radiotherapy (22), a treatment option that cures approximately 2 out of 5 cancer patients (24). The majority of patients are treated with external beam radiation therapy, in which a radiation source external to the patient generates X-rays that are directed towards the tumor. A more advanced but less used form of external radiotherapy is particle therapy, which uses beams of accelerated charged heavy particles (such as protons and carbon ions) (16). This type of beams demonstrates improved depth dose characteristics in comparison with low LET radiotherapy (6). In this way, tumors can be irradiated with great precision, minimizing the dose to surrounding healthy tissues. Charged particle beams also induce more damage per unit of dose, *i.e.*, demonstrate a higher RBE compared to conventional low LET X-ray radiotherapy (25, 26). In the context of particle therapy, only protons and carbon ions are used, as they demonstrate biophysical and biological superiority to other charged particles (6, 27). Nevertheless, other charged particles, such as Fe ions, are of concern to space radioprotection as the radiation spectrum of galactic cosmic radiation consists of heavy charged particles, from protons to iron ions (28). Irrespective of the radiation modality used, the ultimate goal of radiotherapy is to deliver a high dose of ionizing radiation to the tumor volume while minimizing the dose to surrounding healthy tissues (29).

A central dogma that stood for many years of radiation biology is that interaction of ionizing radiation with the cell nucleus is responsible for its genotoxic effects (30). Fueling this dogma were experiments in the 1970s that showed that significantly higher radiation doses are needed to kill cells when radiation is targeted selectively to the cytosol in comparison to nucleus (31). In recent years, however, this view has evolved, and while the interaction of ionizing radiation with nucleic acids is certainly critical, studies are looking into other radiation response pathways induced by radiation damage to *e.g.* lipids and proteins (30). When ionizing radiation interacts with biological matter, it can cause damage by interacting directly or indirectly with cellular biomolecules like DNA, proteins or lipids (Figure 2). Cellular damage may then lead to oxidative stress, further DNA damage, cell cycle problems and even cell death, thereby eradicating tumor cells (17). However, not only the tumor but also nonmalignant surrounding tissues

receive a significant radiation dose, which accounts for radiation side effects (32). To enhance the toxicity of radiotherapy for cancer cells and to reduce acute toxic effects on healthy cells, the total therapeutic dose is most often fractionated: it is administered in repeated small fractions over a larger time span. The rationale of fractionation is explained by the 4 R's of modern radiotherapy: repair, redistribution, reoxygenation and repopulation (33). *Repair* mechanisms in cancerous cells are believed to be slower than in normal cells (34). Therefore, with fractionated radiotherapy, all cells can be damaged but irradiation preferentially decreases the number of cancerous cells in the body. Cellular radiosensitivity is dependent on the cell cycle phase: cells in mitosis or late G₂ phase are most sensitive, whereas cells in the late S are most resistant (35). Right after cells are exposed to a single large dose of radiation, a significant percentage of the surviving population is in resistant phases of the cell cycle. Thus, when a second dose is given shortly thereafter, it is less effective in killing cells. However, fractionation can target previously resistant cells as radiation doses are timed apart and cells can *redistribute* through the cell cycle (36). As stated in the oxygen fixation theory, macromolecular damage induced by ionizing radiation is fixed when oxygen is present and may be easily repaired when oxygen levels are below 10 mm Hg, *i.e.*, hypoxia (37, 38). Many tumors contain a mixture of oxygenated and hypoxic cells and further demonstrate dynamic hypoxia as different regions of the tumor intermittently become hypoxic or reoxygenated(35). If the interval between two radiation doses is long enough, *reoxygenation* of the more resistant hypoxic regions takes place due to reduced oxygen demand from dying tumor cells, making them more sensitive to radiotherapy (39). *Repopulation* refers to the rapid proliferation of both surviving tumor cells and normal cells after radiation-induced cell killing (40). When the total treatment time increases, cells have the ability to repopulate the tissue. Single high doses induce more cell killing, but also more acute toxicity to normal tissues. Hence, a trade-off must always be found between tumor cell killing and levels of acute toxicity, allowing the patient to complete the radiotherapy program (41). As such, effective suppression of tumor cell repopulation is a key for the success of radiotherapy (42). The 4 most important biological effects of ionizing radiation exposure, common to all human cells, are discussed below.

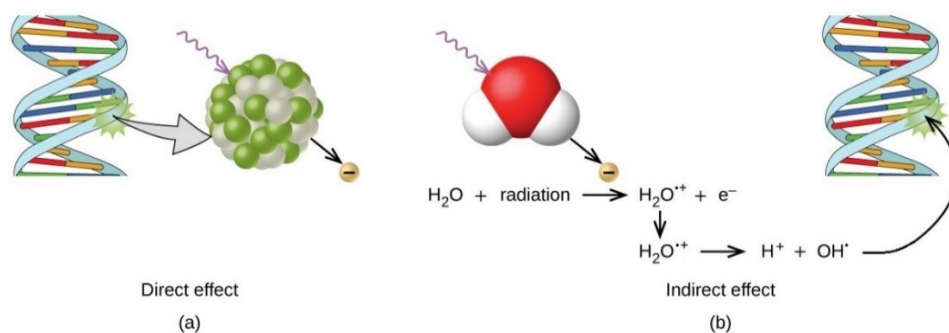


Figure 2. Direct and indirect mechanisms of radiation-induced DNA damage. A. Ionizing radiation can directly damage a biomolecule by ionizing it or breaking its bonds. B. Ionizing radiation can induce water radiolysis, creating an H_2O^+ ion which reacts with H_2O to form a hydroxyl radical. The formed radicals can in turn react with the biomolecule, causing damage indirectly (43).

1.3.2. Oxidative stress

Upon exposure to ionizing radiation, a cell undergoes a stress response within less than a microsecond from the hit. This response is initiated by the biological damage caused by the disruption of atomic structures in a direct and indirect manner (figure 2). The first mode of action represents the direct interaction of radiation with atoms within DNA, lipids, proteins and other cellular components. Direct radiation damage to biomolecules leads to rupture of S-H, O-H, N-H and C-H covalent bonds in backbones and side groups. The formed charged residues are neutralized by the reaction with free radicals and small ions or by reaction with charged groups on same or nearby molecules (44). As a result, cellular damage entails damage to nucleic bases and riboses of the DNA, lipid peroxidation and protein oxidation (30). However, because the largest part of a cell volume is composed of water ($\pm 80\%$), this mode of action is less likely to occur upon contact with ionizing radiation. As a consequence, the most probable way by which ionizing radiation interacts with cellular components is indirectly, after ionization of water molecules. When radiation interacts with water in a cell, water bonds are broken and free radicals are produced in the process of water radiolysis (Figure 3). The radiolytic events typically take place in 3 main stages, all on different time scales: (1) physical stage, (2) physico-chemical stage and (3) chemical stage. In the physical stage, reached about 10^{-16} s after initial matter-ionizing radiation interaction, deposited energy leads to the formation of excited water molecules (H_2O^*) and ionized radical water

molecules (H_2O^+) with the production of sub-excitation electrons (e^-). The 3 initially formed species then react with each other and other molecules at the vicinity of their site of formation during the physico-chemical stage (10^{-15} - 10^{-12} s). Examples of these processes are ion-molecule reactions ($\text{H}_2\text{O}^+ + \text{H}_2\text{O} \rightarrow \text{H}_3\text{O}^+ + \text{HO}\cdot$), dissociative relaxation ($\text{H}_2\text{O}^* \rightarrow \text{HO}\cdot + \text{H}\cdot$) and solvation of electrons ($e^- \rightarrow e^-_{\text{aq}}$). At 10^{-12} - 10^{-6} s after the initial interaction, during the chemical stage, formed species diffuse randomly away from their initial position, where they react with each other and with surrounding molecules (45).

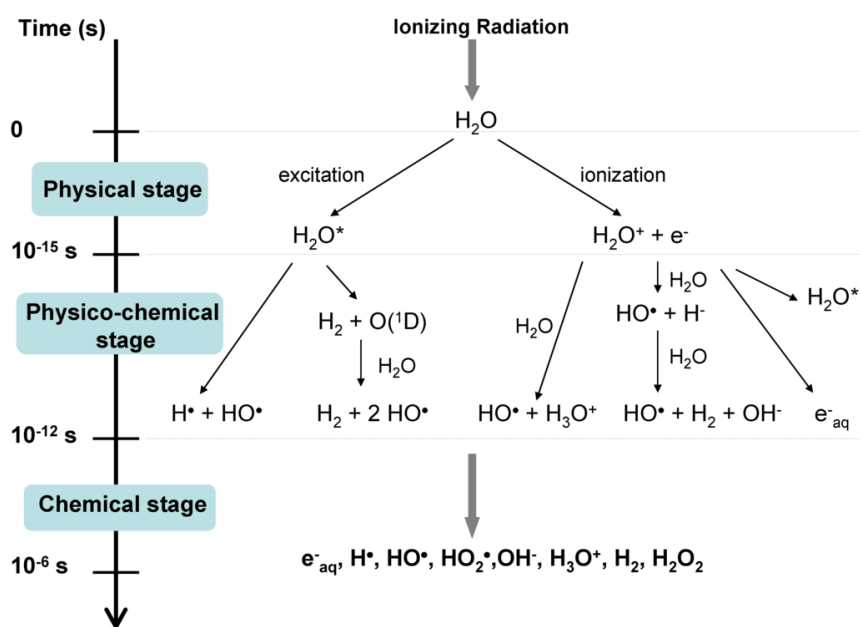


Figure 3. Main reactions occurring during the three stages of water radiolysis. A. During the physical stage (after 10^{-16} s) interaction of ionizing radiation and water leads to the formation of excited water molecules (H_2O^*) and ionized radical water molecules (H_2O^+) with the production of sub-excitation electrons (e^-). B. During the physico-chemical stage (10^{-15} - 10^{-12} s) the 3 initially formed species react with each other and other molecules at the vicinity of their site of formation C. At the chemical stage (10^{-12} - 10^{-6} s), formed species diffuse randomly away from their initial position, where they react with each other and with surrounding molecules (45).

The most abundant type of reactive oxygen species (ROS) formed in a cell after exposure to ionizing radiation is the hydroxyl radical ($\cdot\text{OH}$) (45). With a half-life of 1 ns (46), this short-lived molecule is highly reactive and needs electron pairing for stabilization, enabling harmful oxidizing reactions with cellular components (Figure 4) (47). In addition to $\cdot\text{OH}$, hydrogen peroxide (H_2O_2) and superoxide anion ($\text{O}_2^{\cdot-}$) are produced to a lesser extent as secondary ROS products (48). $\text{O}_2^{\cdot-}$ has a short half-life of 1 μs (46) and needs electron pairing for its stabilization. In contrast, cell membrane-permeable H_2O_2 is less reactive, with a half-life of 1 ms (49) as it does not readily oxidize biological molecules (50). The biological hazard of H_2O_2 largely arises from its conversion to $\cdot\text{OH}$ by interaction with a range of transition metal ions, during so-called Fenton reactions, of which iron is probably the most important *in vivo* (51). In addition to ROS, reactive nitrogen species (RNS) are produced and contribute to radiation damage. For example, highly reactive peroxy nitrite anions (ONOO^-) are generated from the reaction of $\text{O}_2^{\cdot-}$ with nitric oxide ($\cdot\text{NO}$) produced by nitric oxide synthases (52). Collectively, ROS and RNS can cause lipid peroxidation, protein oxidation, oxidative alterations to both genomic and mitochondrial DNA and can inactivate enzymes (47). However, cellular injury only occurs when ROS and/or RNS levels saturate enzymatic and non-enzymatic antioxidant defense systems in cells. This state is known as oxidative stress (53). Paradoxically, at lower, physiological levels, ROS and RNS are known to be important signaling molecules that ensure the integrity and fitness of living organisms (54, 55). Best characterized intracellular sources of endogenous ROS are the electron transport chain in mitochondria and NADPH oxidase family members. Other known sources of ROS are xanthine oxidase, nitric oxide synthase, cyclooxygenases, cytochrome P450 and lipoxygenases (56). As examples of signaling roles of RNS and ROS, NO plays an important role in blood pressure control (described in Introduction Chapter 3) and hydrogen peroxide is involved in microbial killing, since it is used to generate hypochlorous acid inside macrophages and neutrophils (57). Still, ionizing radiation-induced ROS differ from endogenously produced ROS in their concentration, micro-distribution and timing. In particular, irradiation instantaneously induces clustered radical production and clustered damage. Moreover, it mainly generates $\cdot\text{OH}$, whereas endogenous ROS sources such as mitochondria chronically produce superoxide anions and H_2O_2 as single molecules (47).

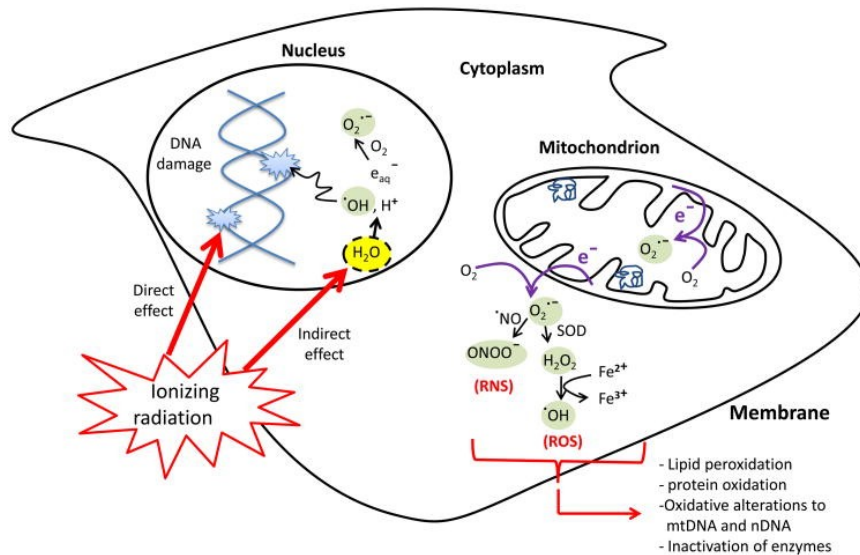


Figure 4. Direct and indirect cellular effects of ionizing radiation on macromolecules. Absorption of ionizing radiation by living cells disrupts atomic structures, producing chemical and biological changes, directly or indirectly through water radiolysis and generation of reactive chemical species by stimulation of oxidases and nitric oxide synthases. Ionizing radiation may also disrupt mitochondrial functions, thereby significantly contributing to persistent alterations of lipids, proteins, nuclear DNA (nDNA) and mitochondrial DNA (mtDNA) (47).

Regulation of the cellular redox state is vital for cellular viability, activation, proliferation and function. Cells have developed antioxidant systems that include enzymatic and nonenzymatic antioxidants that can effectively block the harmful effects of ROS by removing free radical intermediates, thereby inhibiting oxidation reactions. In mammalian cells, the enzymatic defense system consists mainly of superoxide dismutases (SOD), catalase (CAT), glutathione peroxidase (GPx) and glutathione reductase (GSR) (58). SODs catalyze the dismutation reaction of $O_2^{\cdot-}$ to H_2O_2 (Figure 5a) and is the body primary antioxidant defense mechanism since it further prevents free radical production. Three SOD isoforms exist, differing in their metal ion cofactor and cellular location. SOD1 or manganese (Mn) SOD is found in the mitochondrion, SOD2 or copper-zinc (Cu/Zn) SOD is present in the cytosol and SOD3 or extracellular copper-zinc (Cu/Zn) SOD is present in extracellular fluids such as plasma, lymph and synovial fluid (59). Both CAT and GPx catalyze the decomposition of H_2O_2 to water, but they differ in reaction mechanisms. CAT acts

on H_2O_2 by a porphyrin heme at its active site (Figure 5b), whereas GPx has selenocysteine residues at its active site and requires glutathione (GSH) as a cofactor (Figure 5c). During the reduction of H_2O_2 to water by GPx, glutathione is oxidized to glutathione disulfide (GSSG). In order to regenerate GSH, GSSG is reduced by glutathione reductase (GSR) with use of NADPH (Figure 5d) (60). Another essential antioxidant system is that of thioredoxin (Trx), in which reduced Trx catalyzes the reduction of oxidized cysteines or disulfides of many oxidized proteins, and directly quenches $\text{O}_2^{\cdot-}$ and scavenges $\cdot\text{OH}$ (Figure 5e) (61). Resulting oxidized Trx is reduced to Trx by thioredoxin reductase (TrxR) in combination with NADPH (62). However, Trx performs most of its antioxidant functions through peroxiredoxins (Prx), also called thioredoxin peroxidases (Figure 5e) (63). Prx uses cysteine residues as reducing equivalents to directly reduce peroxides, such as H_2O_2 and alkyl hydroperoxides (64). The oxidized form of Prx can then be reduced by reacting with Trx (65, 66).

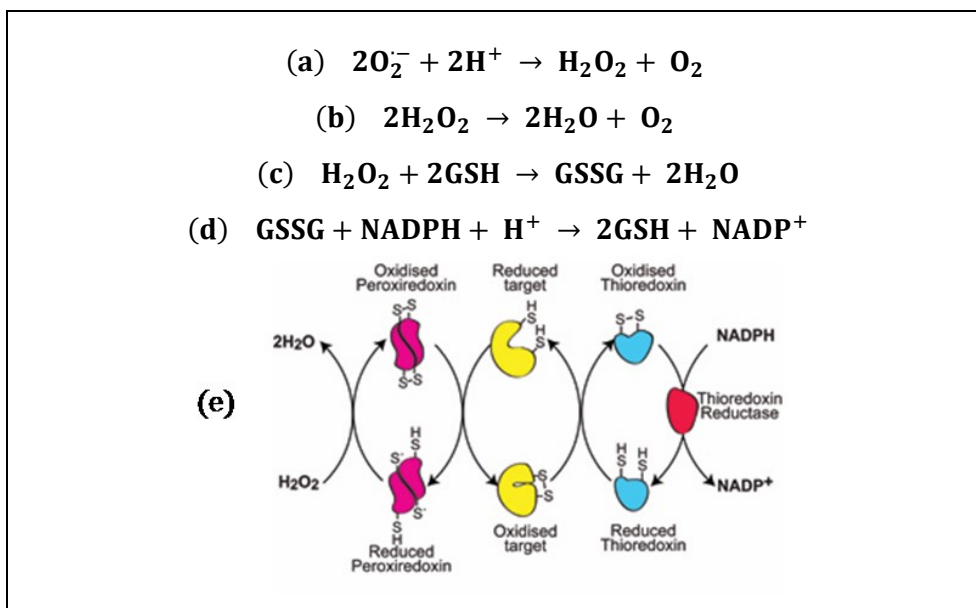


Figure 5. Reaction mechanisms of the main enzymatic radical scavengers: Superoxide dismutase (a), catalase (b), glutathione peroxidase (c), glutathione reductase (d) and peroxiredoxin/thioredoxin (e) (67).

In addition to the above-mentioned enzymatic systems, a range of low-molecular-weight nonenzymatic antioxidants play a role in redox regulation. One of the most important nonenzymatic cellular antioxidants is water-soluble GSH, present in millimolar concentrations in the cytosol and other aqueous phases. While GSH is used as a cofactor by GPx, as mentioned above, it can also directly react with free radicals, especially $\cdot\text{OH}$, by donating a hydrogen atom from its thiol group (60, 68, 69). Other compounds include ascorbic acid (vitamin C) (70, 71), α -tocopherol (vitamin E) (72), melatonin (73), polyphenols such as carotenoids and flavonoids (74), uric acid (75), bilirubin (76) and serum albumin and hemoglobin (77). In general, water-soluble antioxidants (*e.g.* ascorbic acid) react with oxidants in the cytosol and blood plasma, whereas lipid-soluble antioxidants (*e.g.* α -tocopherol) protect cell membranes from lipid peroxidation (78).

In contrast to the well-studied ROS removal systems, the mechanisms that protect mammalian cells from harmful RNS effects remain to be clarified. Nonenzymatic protection may be provided by the compounds listed above, such as GSH, uric acid, β -carotene and vitamins C and E, as well as by the elimination of NO by its rapid reaction with hemoglobin in the blood (79). Potential enzymatic defense systems able to remove RNS consist of thioredoxin (80), GPxs (81), SODs (directly or by removal of $\text{O}_2^{\cdot-}$) (82) and γ -glutamyl transpeptidase (83).

1.3.3. DNA damage and repair

Ionizing radiation directly or indirectly induces a wide range of DNA lesions in a cell. Examples of such lesions are base damage (depurination, depyrimidation and base oxidation), destruction of the sugar phosphate backbone, DNA crosslinks and DNA breaks (single-strand breaks [SSBs] or double-strand breaks [DSBs]) (Figure 6). DNA damage is considered to be the most harmful effect of radiation exposure on cells (84). In particular, DSBs, if not repaired properly, are the most cytotoxic type of DNA damage because they can cause mutations, gross chromosomal aberrations, cell death, and can be responsible for the onset of diseases associated with genomic instability like cancer (84). Occurrence of DNA damage is, however, not specific for radiation exposure; it frequently arises from endogenous sources (such as spontaneous deamination of cytosine (85) and superoxide produced by the electron transport chain as a side-product of cellular metabolism (86)) and exposure to other genotoxic agents, such as UV light and cisplatin (85). To handle

damage, cells have evolved a signaling network, the DNA damage response (DDR), that responds to certain kinds of DNA damage in order to either repair it or trigger apoptosis. DDR is composed of different pathways that repair all kinds of DNA damage, such as nucleotide modifications, DNA crosslinks and SSBs (87). These lesions can be repaired quite quickly (88). DDR comprises (i) sensor proteins that recognize abnormally structured DNA and initiate the signaling cascade, (ii) transducer proteins that transmit and intensify the signal and (iii) effector proteins that carry out crucial functions for repair (Figure 7). Of the various forms of damage induced by ionizing radiation, DSBs are considered to be the main cytotoxic lesions, since inaccurate repair or lack of repair of DSB can lead to mutations or cell death (89). Furthermore, experimental evidence exists for a causal link between the DSB generation and induction of mutations and chromosomal translocations with tumorigenic potential (90-92). Hence, in this section, only the DDR following DSBs will be discussed

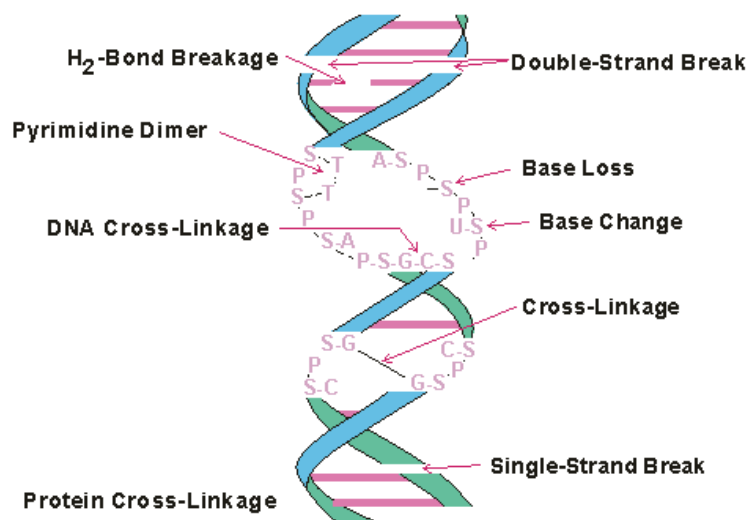


Figure 6. Radiation damage to DNA. Direct or indirect interaction of DNA with ionizing radiation induces the formation of different DNA adducts, comprising base loss, base change, crosslinks, single-strand breaks and double-strand breaks (93).

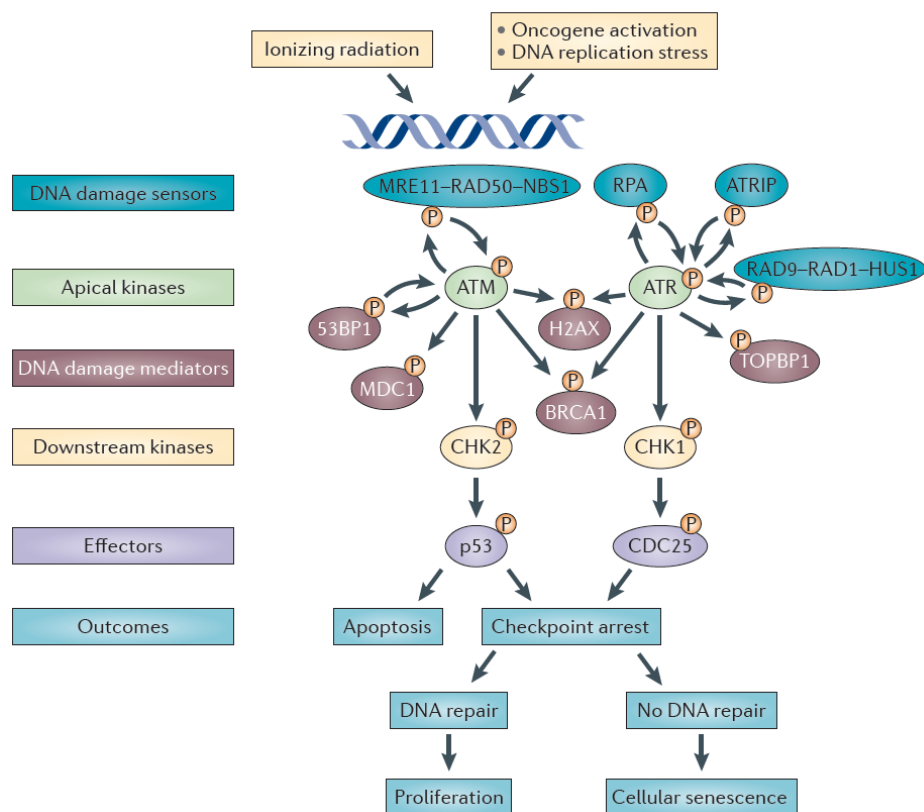


Figure 7. General organization of double-strand break response. The presence of a DSB is recognized by a DNA damage sensor, which transmits the signal to a series of downstream effector molecules through a transduction cascade of DNA damage mediators, to activate signaling mechanisms for cell-cycle arrest and induction of repair, senescence or cell death (94).

DSBs in an irradiated nucleus can be sensed by several pathways in which different proteins, ataxia telangiectasia mutated (ATM), DNA-dependent protein kinase (DNA-PK) and ataxia telangiectasia and Rad3-related protein (ATR), are recruited to the DSB site (95). These 3 major DSB-sensing molecules all have the potential of phosphorylating histone H2A variant H2AX on serine 139 (human sequence), which is designated γ H2AX (96). Bulking of γ H2AX generates foci that provide a high-affinity binding site for downstream factors, such as p53 binding protein 1 (53BP1). In nuclei of unperturbed cells, 53BP1 is evenly dispersed. Upon DSB formation, 53BP1 is relocated to the damaged region in order to promote end-joining of distal DNA ends (Figure 8) (88). In addition, DSB foci also attract other repair proteins,

such as BRCA1, and open the chromatin structure by histone acetylation in order to allow efficient repair (97, 98). Of interest, visualization of γ H2AX and 53BP1 foci by immunochemistry has emerged as an extremely sensitive approach to monitor DSBs (99, 100). It has indeed been established that generated foci closely correlate with the amount of DSBs in the nucleus, and their loss with DNA damage repair. The high sensitivity of this method makes it very useful in low-dose radiobiology (101, 102). A drawback of the use of γ H2AX to visualize DSBs and their repair is that it also gets recruited to replication-associated SSBs (103) and at sites of early apoptotic DNA breakage (104). Colocalization of γ H2AX with 53BP1 foci is assumed to better reflect DSBs (103, 105) because 53BP1 is not retained at sites of SSBs (106) nor at early apoptotic DNA breakage (107). Scoring of colocalized 53BP1/ γ H2AX foci can thus rule out any misclassification, making it very useful for signal validation.

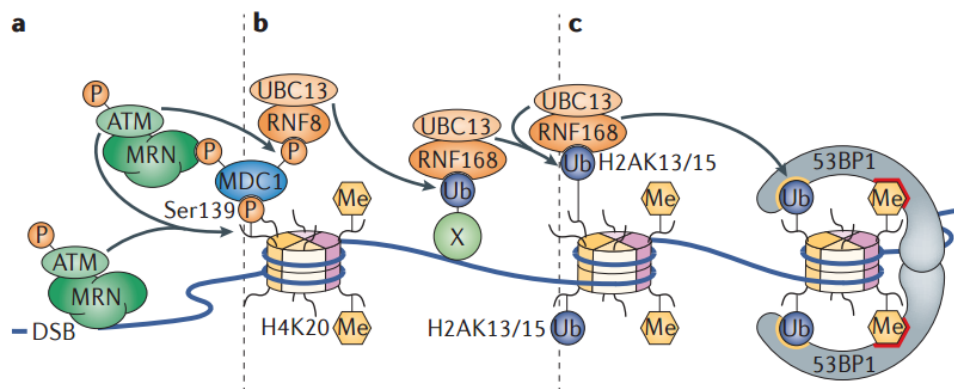


Figure 8. Signal transduction pathway leading to the accumulation of γ H2AX and 53BP1 at a DSB site. (A) DSB lesion is sensed by the Mre11-Rad50-Nbs1 (MRN) complex and recruits active ATM monomers. ATM phosphorylates H2AX at serine 139 to generate γ H2AX. (B-C) Recruitment of ring finger protein 8 (RNF8) by mediator of DNA damage checkpoint protein 1 (MDC1) leads to ubiquitylation of histones that recruits 53BP1 (108).

In addition to γ H2AX at the DSB site, ATM and ATR also phosphorylate tumor suppressor protein p53 and checkpoint kinases 1 and 2 (CHK1 and 2). As guardian of the genome (109), p53 plays a fundamental role in DDR: as a transcription factor, it promotes the transcription of genes essential for cell cycle arrest (*e.g.* cyclin-dependent kinase inhibitor 1 [p21] and 2A [p16]), apoptosis (*e.g.* Bcl-2-associated X [Bax] and Bcl-2 homologous antagonist killer [Bak]) and DNA damage repair (*e.g.* damaged-DNA binding protein 2 [DDB2] and Xeroderma pigmentosum, complementation group C [XPC]) (87). Furthermore, CHK1 and 2 are effector

proteins that are essential in halting cellular proliferation (110). If DSB cannot be repaired, p53 initiates apoptosis (see below).

After recruitment of DSB-associated proteins, repair is carried out *via* homologous recombination (HR) or non-homologous end-joining (NHEJ) (Figure 9). The former uses intact sister chromatid as a template to repair the damaged site, allowing error-free repair during late S and G2 phases of the cell cycle. The latter pieces DNA ends together without homologous DNA strand template, making it error-prone but operable at any cell cycle stage (111). NHEJ is the main DSB repair pathway in irradiated cells (111). It provides rapid restoration of DNA integrity without requiring far-reaching chromatin changes. Comparatively, HR is required for more complex lesions, SSBs and DSBs induced by replication fork stalling or collapse and in heterochromatic regions (111). It repairs DSBs with slow kinetics.

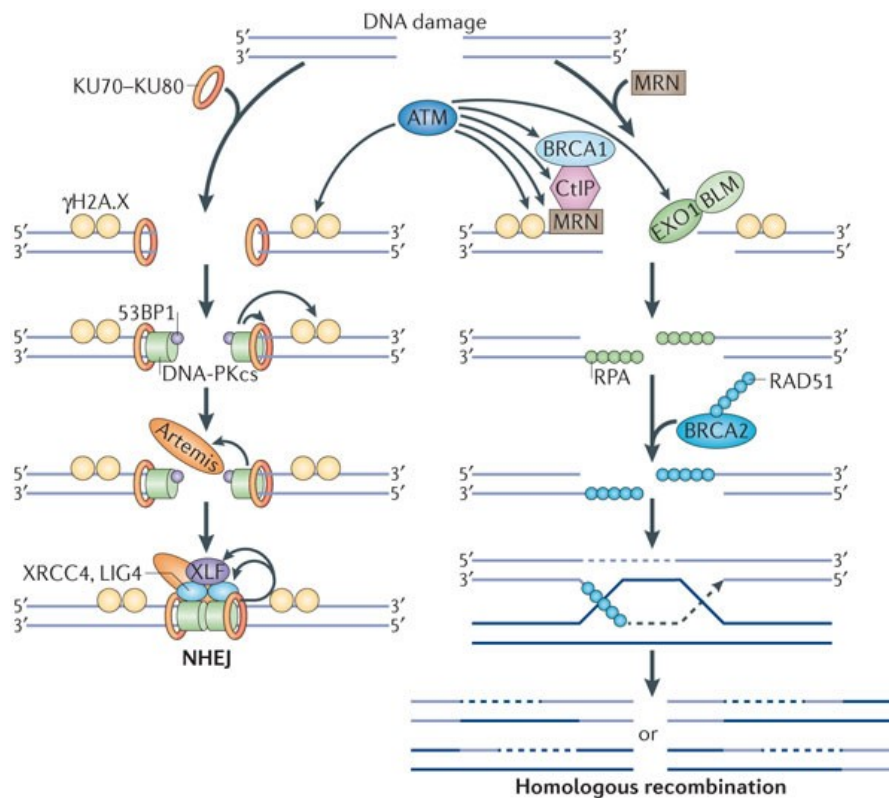


Figure 9. DSB repair pathways in mammals. DSBs are predominantly repaired by error-prone non-homologous end-joining (NHEJ), or by error-free homologous recombination (HR) (112).

1.3.4. Cell cycle blockage

With the aim of providing time to activate cellular repair mechanisms and to protect genetic material, cells are halted in their proliferation when DNA damage is detected. Cell cycle blockage requires a tight coordination of cell cycle checkpoints. Three checkpoints exist: G1/S, intra-S and G2/M. Regulation of these checkpoints occurs *via* the activity of cyclins and cyclin-dependent kinases (CDKs). Differentially expressed throughout the different cell cycle stages, cyclins bind to and activate CDKs, thereby inducing the phosphorylation of factors that regulate cell cycle progression (Figure 10). During DDR, the DSB machinery targets cyclins and CDKs to halt the cell cycle at a given checkpoint. For example, ATM signaling at DSB sites recruits and activates MDM2, p53 and CHK2. When p53 is phosphorylated by ATM/ATR, it induces p21 expression and subsequently inactivates the cyclinD/CDK4/CDK6 complex, which blocks G1/S transition (113). Features of cell cycle checkpoints, like the amount of DSBs necessary to induce arrest and the duration of the arrest, depend on cell type (114, 115). Furthermore, the amount of damage and the cell cycle status at the moment of irradiation also determine cell fate. Cells are found to be more sensitive to radiation-induced DNA damage when they are in G2 or M phase (116).

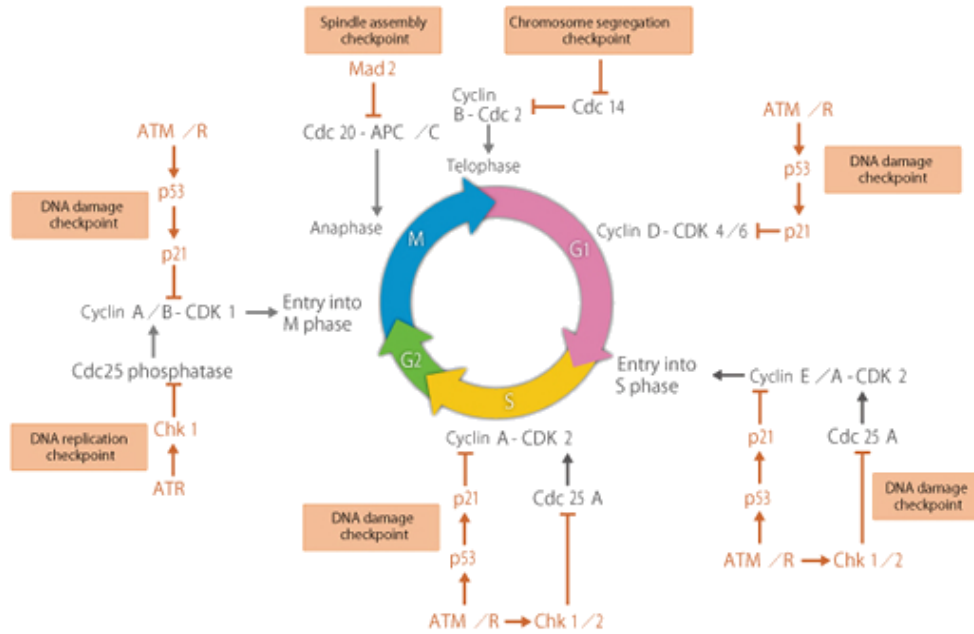


Figure 10: Checkpoint control of the cell cycle. During exposure to ionizing radiation, ATM and ATR signaling induces cell cycle arrest to ensure fidelity of DNA replication and chromosome segregation and to prevent progression through the cell cycle until critical processes have been completed (117).

1.3.5. Cell removal

When genome integrity is too severely compromised to be repaired, cells can be eliminated through various ways. In essence, there are four main possibilities: necrosis, autophagy, senescence and apoptosis (118). Necrosis is a form of non-programmed cell death that occurs when cells are acutely depleted of energy or direct cellular trauma, resulting in loss of cell membrane integrity and uncontrolled release of cellular constituents to the extracellular space (119). Autophagy is a process during which a cell degrades its own components through the action of lysosomes in order to generate metabolic substrates and intermediates (120). Senescence is described as biological aging, during which cells have an ever-lasting G1 arrest mediated by p53/p21 and p16/retinoblastoma protein (pRb) signaling (118). Both pathways can be induced by senescence signals such as telomere attrition, oxidative stress and DNA damage. The resulting accumulation of p16 and p21 lead to inhibition of pRb phosphorylation, leading to decreased expression of

G1 cyclins and, ultimately, cell cycle arrest (121-123). Mitotic catastrophe results from improper distribution of chromosomes during mitosis. Molecular events that govern mitotic catastrophe, in particular those that link the detection of mitotic failure to the engagement of apoptotic or necrotic machineries, are still incompletely understood (124).

The most common way of cell elimination following irradiation is programmed cell death or apoptosis (125). When the amount of DNA damage is too high or when DNA damage is too complex to be repaired, constitutive phosphorylation of p53 activates the apoptosis program. Depending on the amount of activated p53 and on the duration of its activation, damaged cells initiate apoptosis through intrinsic or extrinsic pathways (125). This eventually results in activation of caspases (118), a family of proteases that ensure that cellular proteins are degraded in a controlled fashion with minimal effects on surrounding tissues (126). Ionizing radiation mostly induces the intrinsic apoptotic pathway (127) (Figure 11). In this pathway, transcription of pro-apoptotic genes (*e.g.* *BAX*) and inhibition of anti-apoptotic gene (*e.g.* *BCL-2*) transcription is induced by p53. These transcriptional changes lead to changes in the inner mitochondrial membrane that result in the opening of the mitochondrial permeability transition (MPT) pore and loss of the mitochondrial transmembrane potential. As a result, the outer mitochondria membrane loses its integrity, causing cytochrome c release in the cytosol, which consequently activates caspase 9 and 3 (87, 128).

Depending on the dose and cell type, ionizing radiation can also induce the extrinsic apoptotic pathway and the membrane stress pathway (127). The extrinsic pathway executes radiation-induced apoptosis by signaling through death receptors that belong to the tumor necrosis factor receptor super family (129, 130). Irradiation-induced P53 activation increases the transcription and triggers the rapid transport to the cell membrane of death receptors apoptosis-stimulating fragment (FAS), DR5 and FAS ligand (FASL) (131, 132). As a consequence, FAS cell surface death receptor-associated death domain (FADD) is recruited to death receptors and caspase-8 is activated to form the death-inducing signaling complex. Caspase-8 then activates procaspases 3, 6 and 7 (133). In contrast to DNA damage-dependent intrinsic and extrinsic pathways, activation of the membrane stress pathway does not involve p53 (127). Indeed, lipid oxidative stress following radiation-induced ROS exposure directly account for activation of sphingo-myelinase (134, 135), a membrane-bound

enzyme that hydrolyzes sphingomyelin in the plasma membrane and releases ceramide (136-138). Ceramide is a second messenger that activates the RAC1/MEKK pathway, resulting in direct activation of caspases 1, 3 and 6 (Figure 11) (139).

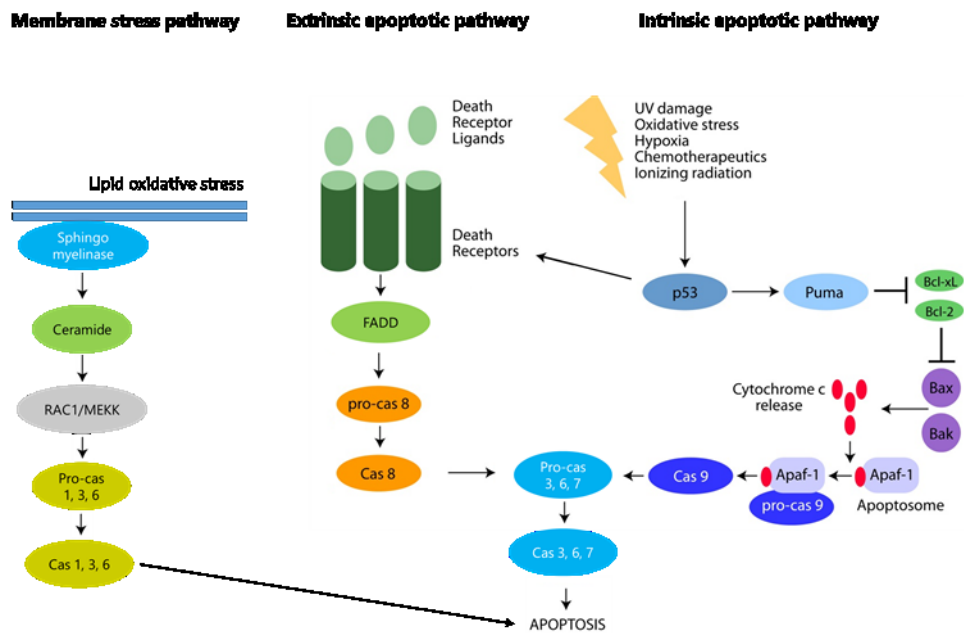


Figure 11. The three major apoptotic pathways. *Membrane stress pathway.* Lipid oxidative stress, results in the production of ceramide following sphingomyelinase activation. Consequent RAC1/MEKK pathway stimulation activates the caspase system. *Extrinsic apoptotic pathway.* P53 activation triggers the expression of death receptors at the cell membrane and the recruitment of FADD. Binding of death receptor ligands to death receptors results in activation of caspase 8 and effector caspases 3, 6 and 7. *Intrinsic apoptotic pathway.* Persistent activation of p53 decreases anti-apoptotic and increases pro-apoptotic protein levels in the cell. These changes lead to a loss of mitochondrial membrane integrity and cytochrome c release. Cytochrome c activates the caspase system that ultimately degrades cellular proteins. Adapted from (140).

1.4. Protection against radiation exposure: the current radiation protection system

Short after the discovery of ionizing radiation by Röntgen in 1895, detrimental effects of ionizing radiation became apparent and people tried to protect themselves (141). Nowadays the International Committee on Radiation Protection (ICRP) and the US National Committee on Radiation Protection (NCRP) aim to protect people by advising the means for achieving this, *e.g.* regulatory and guidance limits (8, 142).

The major question that keeps radiation protection bodies busy and that became the foundation of radiation protection guidelines worldwide is “How much is harmful?”. This question is particularly relevant for low dose exposures for which health impact is not yet fully elucidated. Although a large number of epidemiological and radiobiological studies have been performed to date in order to investigate the effects of low doses of ionizing radiation (143-164), accurate risk assessment is not yet available (14). Current guidelines for protection against low radiation dose exposures are based on cancer risk estimates from epidemiological studies. As discussed in Introduction Chapter 2 of this thesis, cohorts include atomic bomb survivors, occupationally exposed people, patients (diagnostics or therapeutics) and environmentally exposed people (165). In general, an excess cancer risk can be statistically evidenced for doses above 100 mGy. Nevertheless, doses below 100 mGy are inconclusive due to 2 practical limits of epidemiological studies: low statistical power that generates random errors and demography that gives rise to systematic errors. Due to a high natural incidence of cancer, a lifetime follow-up of larger cohorts would be needed to quantify excess cancer risks due to a low dose of ionizing radiation. This is practically infeasible. Furthermore, confounding factors, such as lifestyle risk factors for CVD, can hamper accuracy to confidently detect a small increase in cancer mortality (discussed in Section 2.4). Any inadequacy in matching between control and study groups may give rise to a bias that cannot be reduced merely by expanding the size of the groups (166). As a consequence, risk assessment in the low dose region (< 100 mGy) is based on extrapolations made from high dose risk estimates (167). For cancer, it is widely accepted that the tumorigenic risk increases with radiation dose without the presence of a threshold dose; the stochastic linear non-threshold (LNT) model. This

assumption implies that no dose is absolutely safe, resulting in implementation of the "as low as reasonable achievable" principle (168, 169).

In contrast to cancer, non-cancer diseases are not seen as health risks following exposure to low doses of ionizing radiation. Consequently, they are believed to have a threshold dose below which no significant adverse risks are induced (deterministic linear threshold model) (8, 170). This idea has been challenged by epidemiological findings showing an excess risk of non-cancer diseases following exposure to doses lower than previously thought (151, 171). Epidemiological evidence suggests an excess risk of CVD mortality above 0.5 Gy (151, 171). For doses below 0.5 Gy, the dose-risk relationship is still unclear. However, if the relationship proves to be without a threshold, this may have considerable impact on the current radiation protection system, since the overall excess mortality risk following low dose exposure could double (172).

Chapter 2

Radiation-induced cardiovascular diseases

Introduction Chapter 2. Radiation-induced cardiovascular diseases

2.1. Cardiovascular diseases - generalities

CVDs are the leading cause of mortality and morbidity worldwide. They globally account for approximately 30-50% of all deaths (173). In Belgium, 17.25% of all male deaths and 12.27% of all female deaths under the age of 65 are caused by CVDs. In 2015, 95,329 new cases in males and 91,763 new cases in females were diagnosed with CVD in Belgium, leading to a total of 1,030,616 males (12,295/100,000) and 1,038,886 females (9,621/100,000) with CVD. Moreover, on a daily basis in 2013, 328 antihypertensive drugs and 130 cholesterol-lowering drugs were prescribed per 1,000 people in Belgium (174).

CVDs are multifactorial in nature, with both fixed and lifestyle-associated risk factors, including unbalanced diet, low physical activity, smoking, alcohol use, hypertension, high total cholesterol, high fasting plasma glucose, high body mass index (BMI), male gender, age, family history of premature coronary disease and genetic background (173-175). Total health care cost for CVDs in the year 2015 in Europe amounted to a staggering € 110,809,465, which is € 218 per capita and a total of 8% of the health care expenditure. In Belgium, the total health care costs amounted to € 2,421,246, representing € 216 per capita and a total of 6% of the health care expenditure (174).

Until mid-1960s, the heart was thought to be a relatively radioresistant organ. Even as recent as in the 1980s, the issue of whether radiation exposure promotes coronary artery disease was controversial, and a relationship was not established until mid to late 1990s (176). Ionizing radiation-related CVDs comprise a broad range of different clinical manifestations that depend on various elements, such as radiation dose, exposure frequency, exposed heart volume, age at exposure, latency of disease, length of follow-up and other risk factors such as smoking and unbalanced diet (177). Major clinical manifestations of radiation-related CVDs are pericarditis, congestive heart failure and coronary artery disease. Furthermore, valvular disease, arrhythmias and conduction abnormalities may also be caused by ionizing radiation at > 10 years after exposure to high doses of ionizing radiation (generally higher than 40 Gy) (147, 178, 179). Because they are the main scope of this thesis, coronary artery disease and its main culprit, atherosclerosis, are discussed in more details below.

Coronary artery disease is defined as an obstruction of the blood flow in coronary arteries due to narrowing that restricts blood and oxygen supply to the heart. Coronary artery disease manifests in 2 forms: (i) a mild form leading to angina where the reduced blood flow results in discomfort and (ii) a severe form leading to myocardial infarction or heart attack when blockage is severe. The major cause of coronary artery disease is atherosclerosis, a chronic inflammatory disease of the arterial wall in which the buildup of plaques in the intima impairs normal vascular functioning (180). Development and progression of atherosclerosis is a complex process with many players (Figure 12). Despite advances that led to many compelling hypotheses about the pathophysiology of atherosclerotic lesion formation and of complications such as myocardial infarction, definitive evidence to confirm that processes such as lipoprotein oxidation, inflammation and immunity have a crucial involvement in human atherosclerosis is still lacking (181).

According to the current concept, atherogenesis, *i.e.*, the development of atheromatous plaques in the inner lining of arteries, starts after initial qualitative changes in the monolayer of endothelial cells that lead to endothelial activation and dysfunction (181, 182). When arterial endothelial cells are subjected to irritant stimuli caused *e.g.* by dyslipidemia, hypertension or pro-inflammatory agents, activated endothelial cells start to express adhesion molecules that capture leukocytes on their surfaces (Figure 12) (181, 183). First, adhesion molecules P-selectin and E-selectin are expressed on the membrane of endothelial cells that are able to bind selectin P ligand on the surface of circulating monocytes. As a result, monocytes adhere loosely in a rolling fashion on the endothelium. Then, firmer interaction is accomplished with binding of endothelial integrins vascular cell-adhesion molecule-1 (VCAM-1) and intracellular cell-adhesion molecule-1 (ICAM-1) to lymphocyte function-associated antigen 1 (LFA-1) and very late antigen-4 (VLA-4), respectively, on the monocyte surface. In a final step, adherent monocytes migrate into the subendothelial space using diapedesis, under the influence of chemoattractant molecules. During diapedesis interaction of chemokine macrophage chemoattractant protein-1 (MCP-1), which is recognized by the C-C chemokine receptor 2 (CCR2) on monocytes, is important. Other chemoattractants that may play a role in monocyte recruitment to nascent plaques include interleukin (IL)-8 and its C-X-C motif chemokine receptor 2 (CXCR2), together with macrophage inflammatory proteins (MIP) 1 α and 1 β and the protein regulated upon activation normal T cell expressed and secreted (RANTES), all of which bind to C-C chemokine

receptor 5 (CCR5) on the monocyte surface (181, 182). In contrast to CCR2, the main function of CCR5 is to recruit monocytes from the circulating blood: CCR5 and its ligands act mainly on macrophages within the plaque (184). In parallel, changes of endothelial permeability and extracellular matrix composition promote the entry and retention of cholesterol-containing low-density lipoprotein (LDL) particles in the arterial wall. Once monocytes are resident in the arterial wall, they differentiate into tissue macrophages and start taking up LDL particles, leading to the formation of foam cells. These macrophages produce pro-inflammatory agents that stimulate the proliferation and migration of vascular smooth muscle cells (VSMCs) that are either resident in the tunica intima or present in the tunica media. Main pro-inflammatory cytokines released by macrophages are tumor necrosis factor α (TNF α) and IL-1 β that activate nuclear factor kappa-light-chain-enhancer of activated B cells (NF- κ B) transcription factor, resulting in the activation of many pro-inflammatory pathways that support endothelial proliferation, T cell activation, enhanced expression of adhesion molecules on both leukocytes and endothelial cells and neutrophil attraction and activation. In addition, IFN γ is released that upregulates the expression of IL-1, platelet-activating factor and H₂O₂ by macrophages. Further important cytokines are IL-10, an anti-inflammatory cytokine, and transforming growth factor- β (TGF- β), shown to induce secretion of platelet-derived growth factor (PDGF) by macrophages. PDGF triggers VSMC proliferation. VSMCs also produce collagen and elastin, which form a fibrous cap that covers the plaque. Underneath, a collection of foam cells can be found, among which some die and discharge lipids in the extracellular space. Inefficient clearing of these dead cells along with their extracellular lipids can promote their accumulation as a lipid-rich pool, the necrotic core. The fibrous cap, as such, functions to protect this highly thrombogenic core against exposure to blood. The plaque itself can lead to 2 major clinical manifestations. Either it can keep on growing, leading to blood flow limitation and tissue ischemia, or it can form thrombi after disruption, leading to partial or complete blood vessel occlusion, resulting in a heart attack or stroke (181-183).

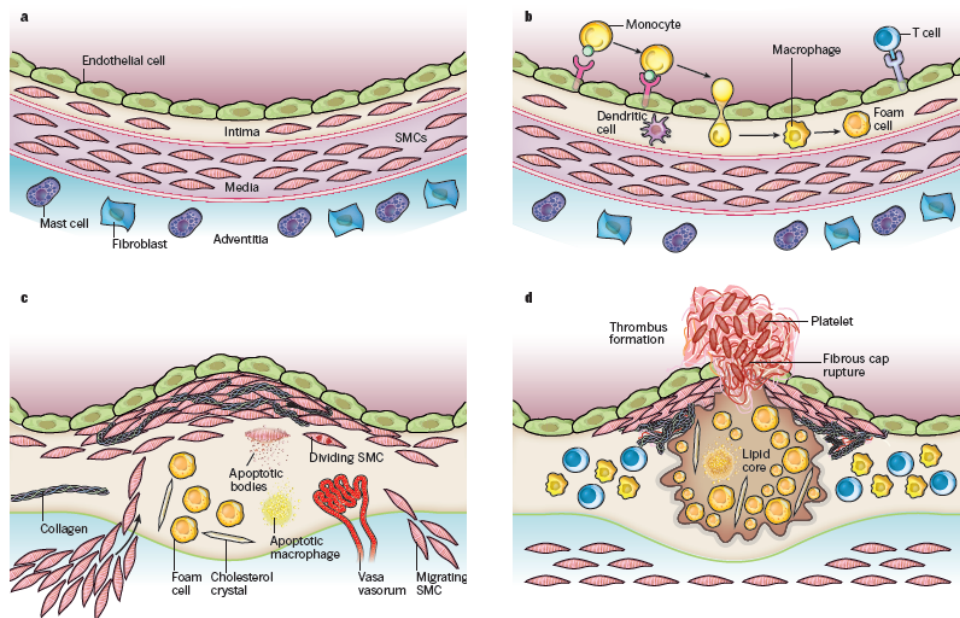


Figure 12. Schematic overview of the development of an atherosclerotic lesion. A. A normal artery is composed of 3 layers: the inner layer with endothelial cells in contact with the blood compartment, the middle layer with vascular smooth muscle cells (VSMCs) and the outer layer with mast cells, nerve endings and microvessels. **B.** After an initial qualitative change in the endothelium, activated endothelial cells express adhesion molecules onto which blood leukocytes adhere, and initiate the directed migration of bound leukocytes into the intima. Intimal monocytes mature into macrophages and take up lipids, yielding foam cells. **C.** Lesion progression includes transmigration of VSMCs from the tunica media into the intima, VSMC proliferation in the intima and enhanced production of extracellular matrix molecules collagen, elastin and proteoglycans. In advanced lesions, macrophages, foam cells and VSMCs can die, resulting in an extracellular pool of lipids and dead/dying cells in the central region of the plaque, denoted as the lipid or necrotic core. Advanced plaques also contain cholesterol crystals and microvessels. **D.** Plaque rupture by physical disruption of the fibrous cap of the atherosclerotic plaque induces thrombosis. This induction is mediated by the contact of blood coagulation components with tissue factors in the plaque interior, resulting in a thrombus that may extend in the vessel lumen, thereby impeding the blood flow (181).

2.2. Epidemiology of irradiation-induced CVD

Almost 1 out of 3 people will develop cancer in the Western world (22), and about 50 to 60% of all cancer patients undergo radiotherapy with radiation doses averaging 1.8 - 2 Gy per fraction (185). During radiotherapy treatment of tumors located in the mediastinal region of the human body (breast, lung and esophageal cancers), the heart and its blood vessels incidentally receive a part of the therapeutic radiation dose (163). Exposure of the cardiovascular system to these therapeutic doses is known to be associated with CVDs. The first epidemiological evidence of this association came from radiation-treated Hodgkin's lymphoma survivors in the 1960s. In a study of 258 patients followed for a median of 14.2 years (range 0.7-26.2) after radiotherapy, cumulative risk for ischemic event increased from 6.4% (95% Confidence interval [CI]. 3.8 ± 10.7) at 10 years to 21.2% (95% C.I. 15 ± 30) at 20-25 years after radiotherapy treatment. Risk for myocardial infarction was 3.4% (95% C.I. 1.6 ± 7.0) at 10 years and 14.2% (95% C.I. 9 ± 22) at 20-25 years, and risk for ischemic cardiac mortality was 2.6% (95% CI 1.1 ± 6.1) at 10 years and 10.2% (95% CI 5.3 ± 19) at 25 years (186) (Figure 13A). Later, in the study of Darby *et al.*, 2,168 breast cancer patients were followed between 5 and more than 20 years after radiotherapy. These authors reported that women irradiated for left breast cancer (estimated mean heart dose 6.6 Gy) had higher rates of major coronary events than women irradiated for right breast cancer (estimated mean heart dose 2.9 Gy; $P = 0.002$). Excess relative risk (ERR), a measure that quantifies how much the level of risk among persons with a given level of exposure exceeds the risk of non-exposed persons (187), for major coronary events was 7.4% per Gy (95% CI, 2.9–14.5) when all follow-up times and breast cancer patients were included (171) (Figure 13B). Further evidence came from patients with peptic ulcers, a disease that was treated with radiotherapy from the 1930s until late 1960s. In a study of 3,719 peptic ulcer patients, the relative risk of mortality following coronary heart disease was 1.24 (95% CI, 1.04 – 1.47) at 10 or more years after radiotherapy (150). Additional proofs of increased risk of CVDs after high dose exposure were provided during the follow-up of Japanese atomic bomb survivors. During a 53 years follow-up of 86,611 life span study cohort members, excess relative risk for death from heart disease per Gy was 0.14 (CI 0.06 – 0.23) (151) (Figure 13C). Although there is a large number of epidemiological studies showing a clear excess of CVD risk above 0.5 Gy, they are of limited use for quantitative risk assessment because individual dosimetry has yet to be performed (152). In addition, even if an adverse effect can

be evidenced at relatively high doses of ionizing radiation, mechanisms by which therapeutic doses of radiation affect the cardiovascular system are still not completely understood (145).

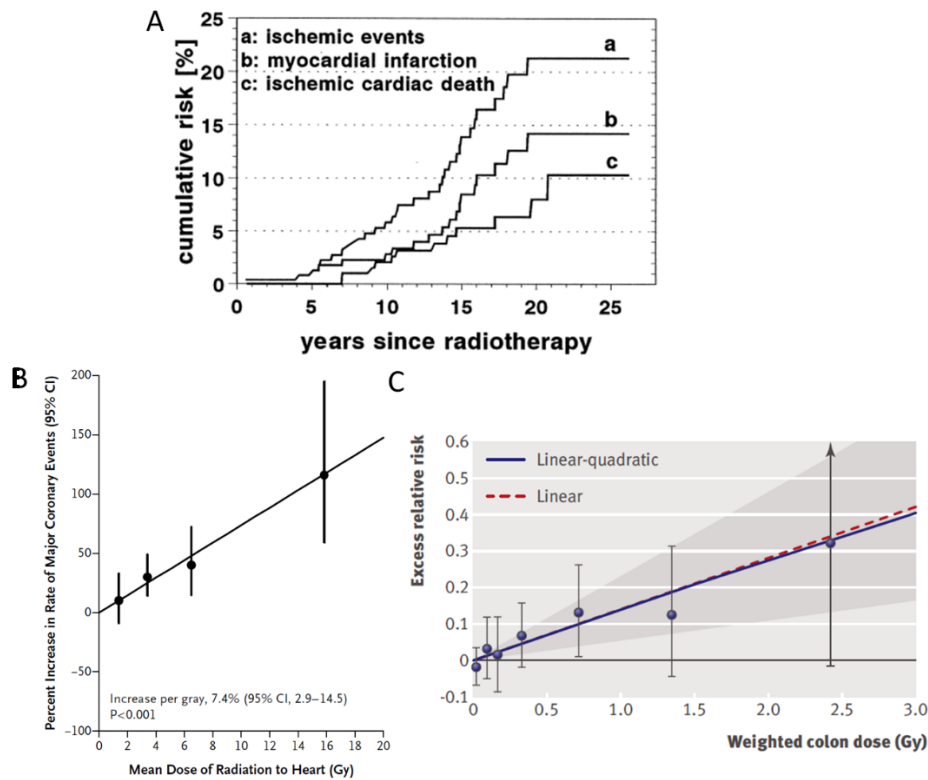


Figure 13. Epidemiological evidence for an increased risk of CVDs after exposure to ionizing radiation. **A.** Cumulative risk curves for the occurrence of cardiac events in Hodgkin lymphoma survivors (186). **B.** Rate of major coronary events according to mean radiation dose to the heart given during breast cancer radiotherapy, as compared with the estimated rate with no radiation exposure to the heart (171). **C.** Excess relative risk for death from heart disease in Japanese atomic bomb survivors. Shaded area is the 95% confidence region for the fitted lines (151).

When the heart receives a radiation dose lower than 0.5 Gy, epidemiological evidence is less strong than for higher doses. The most informative cohort in this respect is composed of Japanese atomic bomb survivors. It is of high value for low dose epidemiology as a source for risk estimation due to its large size, the presence of both sexes and all ages, and because irradiated people have well-characterized

individual dose estimates (153). Studies in occupationally exposed individuals are also of interest as they generally involve relatively low doses received during repeated exposures. Examples of such cohorts are nuclear industry workers from 15 countries (the 15-country study) (154), the UK national registry of radiation workers (155), the national dose registry of Canada (156), the Chernobyl liquidator cohort (157) and the Mayak cohort (158-160). The last cohort is composed of workers from Mayak PA, the first and largest Russian nuclear factory for plutonium production where the majority of workers were exposed to IR during the first period of its operation (188). In addition, data can also be acquired from environmentally exposed groups, such as settlements located at the vicinity of the Techa River (161) and the Semipalatinsk nuclear test area (162).

When taking into account all epidemiological data on CVDs effects of ionizing radiation, a small but highly statistically significant ERR of 0.09 per Gy (95% CI 0.07, 0.12) was observed at doses higher than 0.5 Gy (Table 4) (152). In addition, ERR of circulatory disease mortality was estimated at 0.08 (95% CI 0.04 – 0.12). In other words, receiving 1 Gy of ionizing radiation to the heart and its blood vessels increases the risk of CVD mortality with 8% in comparison to non-exposed people. This assumed risk is rather large and may therefore have serious implications for public health. Indeed, considering the high background rate of CVD, the absolute number of excess cases could be substantial (189). In order to find an association between low-level radiation exposure and CVD risk in a general unselected population, this meta-analysis was extended by Little *et al.* (172). When taking into account 717,660 individuals from the Japanese atomic-bomb survivors and occupational and environmental exposure studies listed above, a statistically significant ERR coefficient of 0.10 (95% CI 0.05 - 0.15) for coronary artery disease was observed as a result of exposure to low-level radiation more than 5 years prior to death (172). A linear association between ERR and radiation dose was assumed even in the low dose range because there was little evidence of nonlinearity in the dose-response curve for CVD in Japanese atomic-bomb survivors (151, 190) and in Mayak workers (158). Authors further argued that the consistency of ERR/Gy between Japanese atomic bomb survivors with moderate radiation doses (151, 190) and occupational cohorts with low doses was used to support the notion of a linear relationship between ERR of CVD mortality and low doses of ionizing radiation (172). In a more recent analysis of the Life Span Study cohort of atomic bomb survivors with 105,444 subjects, the shape of the dose response curve for

solid cancer incidence was found to be significantly different for males *versus* females ($P = 0.02$). For females, the dose response was consistent with linearity, but for males it best fitted a linear-quadratic model (191). If this were to be confirmed, the overall excess risk of CVD-associated mortality after exposure to low doses of radiation would be about twice that associated to radiation-induced cancers, which ranges from 4.2% to 5.6% per Sv for the cohort populations discussed above (172, 192), and it would further be different between both sexes.

Table 4. Aggregate excess relative risks per Sv of circulatory disease in published medium and low dose (<5 Gy) epidemiological datasets *

Endpoint	Studies included	ERR Sv ⁻¹ (with 95% CI)
Heart	Darby <i>et al</i> (1987), Talbott <i>et al</i> (2003), Yamada <i>et al</i> (2004), Carr <i>et al</i> (2005), Ivanov <i>et al</i> (2006), Kreuzer <i>et al</i> (2006), Vrijheid <i>et al</i> (2007), Azizova and Muirhead (2009) + Azizova <i>et al</i> (2010), Shimizu <i>et al</i> (2010)	0.09 (0.05, 0.12)
Stroke	Darby <i>et al</i> (1987), Yamada <i>et al</i> (2004), Ivanov <i>et al</i> (2006), Kreuzer <i>et al</i> (2006), Vrijheid <i>et al</i> (2007), Azizova and Muirhead (2009), Muirhead <i>et al</i> (2009), Shimizu <i>et al</i> (2010)	0.21 (0.16, 0.27)
Morbidity	Yamada <i>et al</i> (2004), Ivanov <i>et al</i> (2006), Azizova and Muirhead (2009) + Azizova <i>et al</i> (2010)	0.10 (0.07, 0.13)
Mortality	Darby <i>et al</i> (1987), Davis <i>et al</i> (1989), Talbott <i>et al</i> (2003), Carr <i>et al</i> (2005), Kreuzer <i>et al</i> (2006), Vrijheid <i>et al</i> (2007), Muirhead <i>et al</i> (2009), Shimizu <i>et al</i> (2010)	0.08 (0.04, 0.12)
Total	Darby <i>et al</i> (1987), Davis <i>et al</i> (1989), Talbott <i>et al</i> (2003), Yamada <i>et al</i> (2004), Carr <i>et al</i> (2005), Ivanov <i>et al</i> (2006), Kreuzer <i>et al</i> (2006), Vrijheid <i>et al</i> (2007), Azizova and Muirhead (2009), Azizova <i>et al</i> (2010), Muirhead <i>et al</i> (2009), Shimizu <i>et al</i> (2010)	0.09 (0.07, 0.12)

* ERR, Excess relative risk; CI, Confidence interval. From reference (152).

2.3. Physiopathology of radiation-induced CVD

Following radiotherapy of the thoracic part of the human body for mediastinal lymphoma, breast, lung and esophageal cancers, the heart incidentally receives a

part of the therapeutic dose (163). As indicated in the epidemiology section, high dose radiation exposure to the heart and its vessels is associated with a risk of radiation-induced CVD (151, 171, 172). In this context, coronary artery disease is considered to be the major cardiovascular complication (145, 147, 171). Two observations have been reported to explain which molecular and cellular mechanisms account for increased morbidity and mortality of coronary artery disease following radiation exposure. First, radiation can influence the pathogenesis of age-related atherosclerosis, thereby accelerating the development of atherosclerosis in coronary arteries (145). Second, damage to the heart microvasculature can reduce blood flow to the myocardium, causing myocardial ischemia that promotes acute infarction (147). Because endothelial activation and dysfunction are major causes of atherosclerosis, much of current radiobiological research is exploring the molecular and phenotypic effects of ionizing radiation in endothelial cells in the context of radiation-induced CVD (181, 183). These aspects are discussed in Introduction Chapter 3. It should be noted, however, that there are also other clinical manifestations of radiation-related CVDs, such as pericarditis and congestive heart failure (147, 178). Radiation-induced pericarditis is caused by damage to the cardiac microvascular network in combination with fibrosis of cardiac venous and lymphatic channels. This ultimately leads to accumulation of a fibrin-rich exudate in the pericardium, causing pericardial tamponade. Congestive heart failure is attributed to radiation-induced fibrosis of the myocardium, which ultimately leads to decreased elasticity and extensibility of cardiac walls, thereby reducing the ejection fraction (177).

2.4. Gaps in the current knowledge of irradiation-induced CVDs

Available epidemiological studies have limited statistical power to detect a possible excess risk of CVD following exposure to radiation doses lower than 0.5 Gy. Limited power is due both to the high background level of CVD in studied populations and to the existence of many potentially confounding risk factors [10]. For example, occupational studies have to deal with the "healthy worker" effect, and the study of A-bomb survivors with the "healthy survivor" effect. Both selection effects occur when healthy individuals with lower mortality and morbidity rates are selectively retained at a specific site (work and living area, respectively) where they accumulate higher doses and therefore confound the dose-risk relationship (154). Other potential confounders in epidemiological studies are lifestyle risk factors for

CVD (*e.g.* smoking, alcohol consumption, obesity, diabetes, hypertension) (152, 172), prognosis of cancer treatment regimens (147), distribution of the dose range, accuracy of dosimetry, duration of follow-up after exposure and correct assignment of the cause of mortality (189). For these reasons, the number of people needed to quantify the excess risk of a dose < 0.5 Gy is unfeasibly high. In the context of radiation-related cancer, for example, a cohort of 5 million people would be needed to quantify the excess risk of a 10 mGy dose, assuming that the excess risk is in proportion to the dose (12). Moreover, CVD may occur a long time after exposure to doses smaller than 30 Gy (approx. 10 - 30 year lag) (147, 193, 194). As a result, a long follow-up period of time is needed to determine the nature and magnitude of risks following individual exposure to lower doses.

Despite the fact that epidemiological studies have led to significant insights in radiation-related CVD risk, there are still many uncertainties that need to be addressed. Does CVD risk occur only above a specific dose? Is the latency of CVD development dependent on the dose? Are there sensitive targets in the heart and vasculature? Does radiation exposure affect CVD incidence or progression, or both? Is there a difference between single dose, fractionated and chronic exposure? To provide a more accurate dose risk assessment in order to improve the current radiation protection system, these questions need to be answered.

Classical epidemiological studies are not adapted to provide answers to these questions. There is, therefore, a clear need for more detailed epidemiological studies that would be capable of addressing potential confounding factors and selection biases that could influence results. Furthermore, there is a particular need for a better understanding of the biological and molecular mechanisms responsible for the association between CVD and ionizing radiation. Hence, a more directed approach is required, such as molecular epidemiology that integrates epidemiology and biology (172). Radiobiological research is thus essential for the understanding of radiation-related CVD risk, both at high and low doses. In other words, accurate risk estimation will be possible only based on comprehensive biological and molecular understanding of what ionizing radiation does to the cardiovascular system.

Chapter 3

*Endothelial cell responses to ionizing
radiation*

Introduction Chapter 3. Endothelial cell responses to ionizing radiation

The endothelium, which forms a thin layer of cells that lines the interior of the heart and blood vessels as well as the lymphatics, plays a complex role in vascular biology. It contributes to key aspects of vascular homeostasis and is also involved in pathophysiological processes, such as thrombosis, inflammation and hypertension. In this chapter, we will summarize and describe current knowledge about endothelial cell function in physiological conditions and endothelial cell activation and dysfunction after radiation exposure. We will also review pharmacological strategies that are currently under investigation to selectively target endothelial cells in order to protect against and mitigate radiation-induced cardiovascular injuries.

3.1. The vascular endothelium

In humans, all tissues depend on blood supply mediated by the circulatory system; arteries that divide in arterioles and transport the blood away from the heart; capillaries that enable the exchange of blood components with tissues; and venules that merge to form veins and carry the blood back to the heart, to the exception of veins of the portal system that carry blood from the digestive tract to the liver. Arteries share general structural features (Figure 14): a lumen; an inner layer, the *tunica intima*, composed of a specialized simple squamous epithelium called the endothelium, its basement membrane and a distinct layer of elastic fibers known as the internal elastic membrane; an intermediate layer, the *tunica media*, composed of VSMCs supported by a framework of collagenous fibers called the external elastic membrane; and an outer layer, the *tunica adventitia* or *externa*, that contains connective tissue (195). In veins, the *tunica media* is much thinner than in arteries and does not always contain VSMCs. Capillaries only comprise a *tunica intima* and pericytes, *i.e.*, contractile cells that attach to endothelial cells. The vascular endothelium consists of an estimated 2.5×10^{12} endothelial cells and accounts for about 2.6% of the total amount of cells present in the human body (196). In a 70-Kg adult, they cover a surface of more than 1,000 m² and account for a weight over 100 g (197). For many years after its discovery in the 1800s, the endothelium was believed to be a mere inert, semipermeable barrier between circulating blood and underlying subendothelial tissues. Numerous subsequent studies have led to the current view of the endothelium as a dynamic

heterogeneous, distributed organ with essential secretory, synthetic, metabolic and immunologic functions (198). In the presence of irritant stimuli, such as dyslipidemia (199, 200), hypertension (201-204) and pro-inflammatory agents (205-208), the normal physiological functions of the arterial endothelium are adversely affected (209, 210), starting a chain of molecular changes that lead to atherosclerosis and CVDs, including coronary artery disease, carotid artery disease, peripheral artery disease and ischemic stroke (195, 211, 212). Most important endothelial functions are addressed below along with the consequences of radiation exposure.

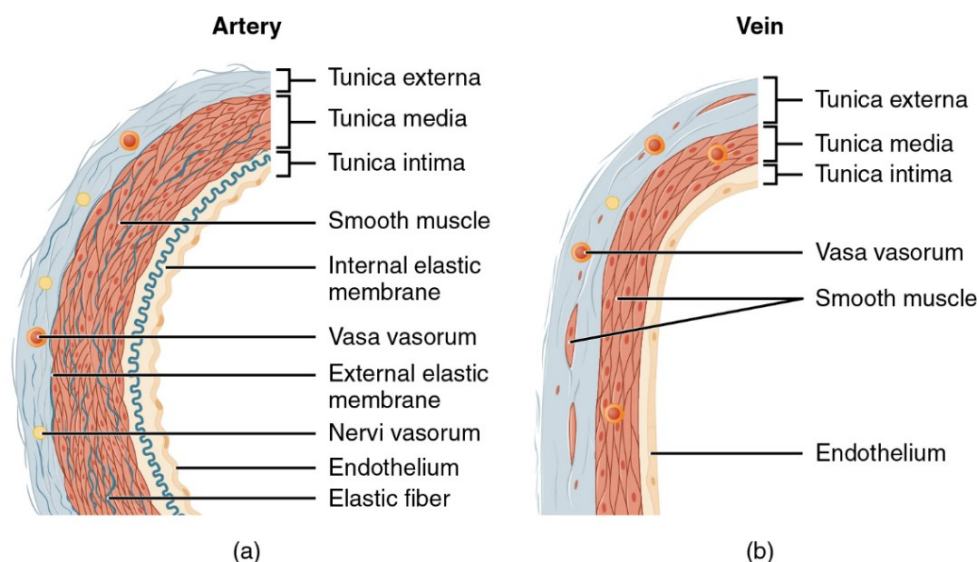


Figure 14. The general structure of large arteries and veins. A, Large arteries are composed of a *tunica externa* composed of connective tissue, a large *tunica media* consisting of smooth muscle supported by collagenous fibers, and a *tunica intima* that contains the endothelium supported by a basement membrane and elastic fibers. B, Large veins demonstrate the same three layers, but have a thinner *tunica media* with less smooth muscle (213).

3.2. Physiological functions of endothelial cells

Assisted by their capacity to sense and respond to mechanical and biochemical stimuli, endothelial cells play an active and critical role in the physiologic regulation of (i) the vascular tone, (ii) blood coagulation, (iii) inflammation and (iv) vascular permeability.

3.2.1. Vascular tone regulation

In 1980, the endothelium was found to secrete a factor that relaxes VSMCs (214). Later, this factor was identified as free radical gas NO (215, 216). In endothelial cells, NO is synthesized when endothelial nitric oxide synthase (eNOS) converts *L*-arginine to *L*-citrulline (217) in the presence of molecular oxygen and six cofactors: tetrahydrobiopterin (BH₄), NADPH, flavin adenine dinucleotide (FAD), flavin mononucleotide (FMN), heme and calmodulin (218). The enzymatic activity of eNOS is regulated by Ca²⁺ and calmodulin (Figure 15). Elevated intracellular Ca²⁺ concentrations enhance the affinity of calmodulin for NOS, resulting in calmodulin binding, which is required for catalytic activity (219). Caveolin-1, the main caveolae coat protein, is also known to bind and tonically inhibit eNOS (220-222). As an allosteric modulator, heat shock protein 90 activates eNOS (223) by displacing caveolin-1 (221). In addition, eNOS activity can be enhanced by phosphorylation on its serine (Ser) 1177 residue, stimulating the electron flux within the reductase domain and increasing Ca²⁺ sensitivity (224, 225). Ser1177 is mainly phosphorylated during shear stress by protein kinase A (PKA), during insulin signaling by RAC-alpha serine/threonine-protein kinase (Akt) and adenosine monophosphate-activated protein kinase (AMPK), during bradykinin signaling by Ca²⁺/calmodulin-dependent protein kinase II (CaMKII), and during estrogen and vascular endothelial growth factor (VEGF) signaling by Akt (226). Another functionally important phosphorylation site in human eNOS is threonine 495. Thr495 is a negative regulatory site as its phosphorylation is associated with decreased electron flux and enzymatic activity due to interference with the binding of calmodulin. Thr495 is phosphorylated by protein kinase C (PKC) and dephosphorylated by protein phosphatase 1 (PP1). Dephosphorylation of Thr495 is associated with stimuli that elevate intracellular Ca²⁺ concentrations. Other phosphorylation sites are Ser114, Ser633, Tyr81 and Tyr657. Consequences of the phosphorylation on these sites are still under investigation (227). Besides eNOS, two other NOS isoforms exist: neuronal NOS (nNOS) and inducible NOS (iNOS). nNOS is constitutively expressed and was first discovered in the brain. However, it can also be found in the spinal cord, sympathetic ganglia and adrenal glands, peripheral nitrergic nerves, epithelial cells of lungs, uterus, and stomach, kidney macula densa cells, and pancreatic islet cells (228). In contrast to eNOS and nNOS, iNOS levels can be induced in virtually all cells by pro-inflammatory stimuli lipopolysaccharide (LPS) and/or cytokines IL-1 β , IFN β , IFN γ , TNF α and IL-6 (226, 228), resulting in activation of Janus kinase/signal

transducers and activators of transcription (JAK/STAT), NF- κ B and mitogen-activated protein kinase (MAPK) pathways (229).

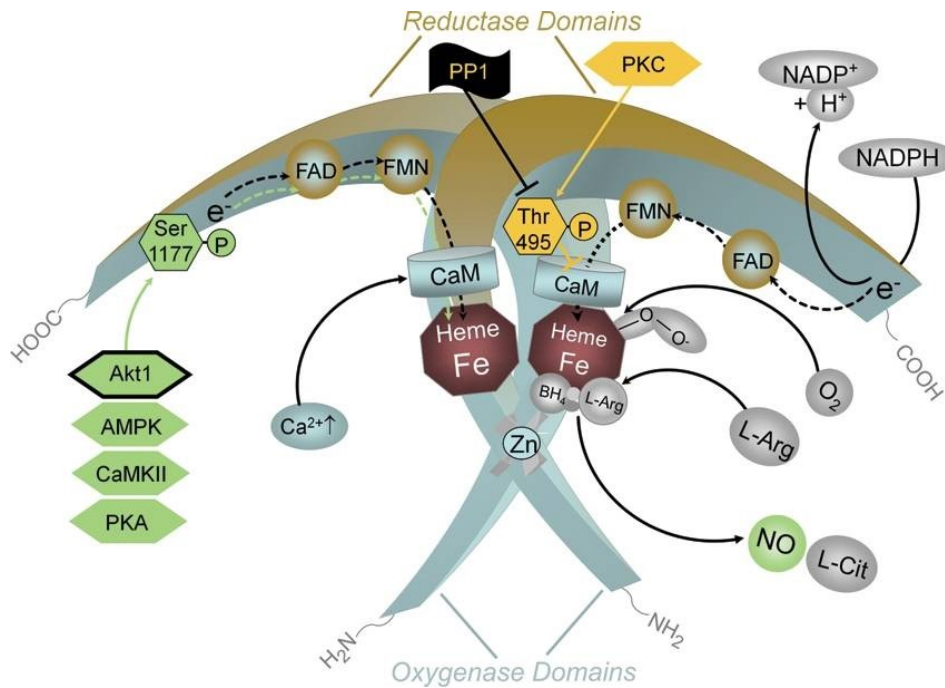


Figure 15. Regulation of endothelial NOS activity by intracellular Ca^{2+} and phosphorylation. Increased levels of Ca^{2+} enhance calmodulin binding and activate eNOS. In addition, eNOS activity is regulated by phosphorylation on serine 1177, resulting in increased enzymatic activity, and by phosphorylation on threonine 495, resulting in decreased enzymatic activity. Not shown is the inhibitory interaction of eNOS with caveolin-1 (226).

Activation of eNOS by either Ca^{2+} -dependent or Ca^{2+} -independent mechanisms occurs after shear stress (230) and contact with a wide variety of vasodilators such as acetylcholine (231), angiotensin II (232), thrombin (233), ATP (234, 235) and bradykinin (236). Once activated, NO diffuses to VSMCs and activates soluble guanylate cyclase, which results in cyclic guanosine monophosphate (GMP) production and subsequent vasodilation (237). However, NO is not the sole endothelium-derived vasodilator. Endothelial cells also generates prostacyclin (PGI_2) (238) capable of relaxing VSMCs. PGI_2 acts mainly on prostacyclin receptor,

stimulating G protein-coupled increase in cAMP and protein kinase A activation, resulting in decreased intracellular Ca^{2+} levels. PGI_2 also inhibits Rho kinase, leading to activation of myosin light-chain phosphatase (MLCP), which initiates VSMC relaxation (239). In addition, endothelium-dependent hyperpolarization (EDH) is triggered by increased cytoplasmic Ca^{2+} levels in endothelial cells (240). This causes the opening of Ca^{2+} -activated potassium channels expressed by endothelial and smooth muscle cells, leading to hyperpolarization of VSMC membranes, closing of their voltage-operated Ca^{2+} channels, reduced cytoplasmic Ca^{2+} levels and, consequently, VSMC relaxation (241-243). EDH responses are caused by a number of factors, namely epoxyeicosatrienoic acids (EETs), electrical communication through gap junctions, endothelium-derived K^+ , hydrogen sulfide and endothelium-derived H_2O_2 (242, 243).

Endothelial cells also produce vasoconstrictor endothelin in response to physical (*e.g.* shear stress, hypoxia) or chemical (*e.g.* thrombin, cytokines) agents (244). By interaction with specific endothelin receptor subtypes (ET-A, -B and -C) on VSMCs, endothelin binding leads to MAPK and phosphatidylinositol 3-kinase (PI3-K)/Akt signaling, resulting in increased cytoplasmic Ca^{2+} levels and vasoconstriction (245). In addition to vascular tone regulation, several vasoactive substances, including NO (246), endothelin (245) and angiotensin II (247), also play a role in the regulation of VSMC proliferation. NO inhibits VSMC proliferation *via* cGMP-dependent and -independent pathways. In the cGMP-dependent manner, NO activates guanylate cyclase, leading to cGMP formation with subsequent inhibition of epidermal growth factor (EGF) signaling (248, 249). Furthermore, guanylate cyclase has been shown to interact with chromosomes (250) and to modulate chromatin folding (251) during mitosis. In the cGMP-independent manner, NO can induce nitrosative stress, leading to S-nitrosylation of Ras (252) and 26S proteasome (253), thereby inducing proliferative VSMC arrest. Endothelin induces VSMC proliferation by potentiation of platelet-derived growth factor (PDGF) signaling (254), transactivation of EGF receptor (EGFR) (255) and binding to its ET receptors, resulting in MAPK signaling and, consequently, cell proliferation (256, 257). Angiotensin II binding to angiotensin II type 1 (AT1) receptors on VSMCs activates MAPK and PI3K intracellular signaling, and transactivates EGFR (258). It must also be noted that there is substantial crosstalk and interaction between several vasoactive substances produced by the endothelium (259). For example, thrombin stimulates both endothelin synthesis and the release of prostacyclin, which oppose each other

actions (260, 261). Hence, the overall response is the net result of complex interaction between several vasoactive pathways. Moreover, the responsiveness and relative importance of these pathways may vary from one vascular bed to another and can further be altered by pathophysiological processes (262).

In addition to the interplay between endothelial cells and VSMCs during vascular tone regulation in large blood vessels, pericytes regulate the vascular diameter of capillaries and capillary blood flow (263). Similar to VSMCs, pericytes contract in reaction to a number of vasoactive substances, including endothelin-1 (264) and angiotensin II (265), and relax in reaction to prostacyclin (264) and NO (266). In contrast to VSMCs, however, pericytes are more sensitive to the metabolic demand of cell and induce vasodilation in response to additional stimuli: acid extracellular pH (267), lactate (268) and adenosine (269).

3.2.2. Blood coagulation

The intimal surface of healthy endothelium has anticoagulant, antithrombotic and fibrinolytic activities. This is first achieved by the endothelial secretion of a variety of molecules important for the regulation of blood coagulation and platelet functions, among which major agents are prostacyclin and NO. Both synergistically act on blood platelets, activating adenylate cyclase and guanylate cyclase to increase intracellular cAMP and cGMP content, respectively (Figure 16). As a result, PKA and protein kinase G (PKG) phosphorylate a number of substrate proteins in blood platelets, resulting in inactivation of small G-proteins of the Ras and Rho families, inhibition of the release of Ca^{2+} from intracellular stores, and modulation of actin cytoskeleton dynamics (270-272). These responses prevent platelet adhesion, granule release and aggregation. Prostacyclin and NO are produced in response to a wide range of vasoactive substances, some of which are also involved in the coagulation process (*e.g.* bradykinin and thrombin) or secreted by aggregating platelets (*e.g.* ATP) in order to limit the intravascular extent of forming thrombi (262). Besides secretion, the endothelium also maintains blood fluidity by promoting the activity of the protein C/protein S pathway (273) in the blood. Protein C is a zymogen present in the blood. Activated protein C (APC) is a strong inhibitor of blood coagulation as it inhibits two essential blood coagulation cofactors: factors Va and VIIIa. Protein C is activated when thrombin binds to thrombomodulin present at the outside of endothelial cells. This activation process

is approximately 20-fold enhanced when protein C is bound to the endothelial cell protein C receptor. Once APC is released in the blood, it forms a complex with protein S that is produced by the endothelial cells, and then inactivates factors Va and VIIIa (273-275). The endothelium also inhibits blood coagulation by providing antithrombin, the main site of inactivation of active thrombin (276), by synthesizing tissue factor pathway inhibitor (277) and by endocytosis of factor Xa (278). In addition to regulating blood fluidity, the endothelium also promotes fibrinolysis by releasing urokinase (279) and tissue-type plasminogen activator (280). Both allow the proteolytic cleavage of plasminogen into plasmin, which digests the fibrin network present in thrombi, thereby degrading them. While the former is only synthesized by activated endothelial cells, the latter is constitutively released into the blood stream (281). Upon vessel injury or inflammation, endothelial properties change in order to promote platelet aggregation and clot formation. This is done by the release of procoagulant/prothrombotic factors and by inhibition of anticoagulant pathways (282). In this respect, endothelial cells synthesize platelet-activating factor that stimulates platelet adhesion to endothelial cells (283). Furthermore, endothelial cells are a main bodily source of von Willebrand factor (vWF) (284), a procoagulant protein that binds to and stabilizes coagulation factor VIII and is essential for platelet binding to exposed extracellular matrix components upon blood vessel damage (285). When stimulated, endothelial cells also synthesize and express tissue factor at their surface, which initiates the extrinsic coagulation pathway (286, 287). In this pathway, tissue factor expression activates factor VII, resulting in activation of factor X and the consequent formation of thrombin. As a serine protease, thrombin is able to cleave fibrinogen to produce fibrin, the building block of a blood clot (195).

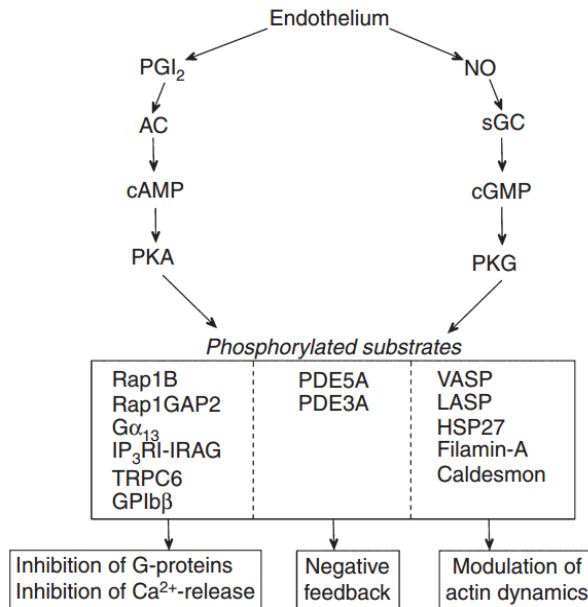


Figure 16. Action of prostacyclin and NO on the cAMP/cGMP signaling network of platelets. Endothelial cells release prostacyclin (PGI₂) and NO and activate adenylate cyclase (AC) and soluble guanylate cyclase (sGC), respectively. Resulting cAMP and cGMP stimulate cAMP-dependent protein kinase A (PKA) and cGMP-dependent protein kinase G (PKG). Substrate phosphorylation results in inhibition of platelet activation, granule release, adhesion and aggregation. GP, glycoprotein; HSP27, heat shock protein 27; IP₃-R, inositol 1,4,5-trisphosphate receptor; LASP, Lim and SH3 domain protein; TRPC6, transient receptor potential channel 6; VASP, vasodilator-stimulated phosphoprotein. Figure adapted from (272).

3.2.3. Interaction with immune cells

During inflammation, a complex interplay takes place between leukocytes and endothelial cells, which is aimed to destroy, dilute or wall-off both the injurious agent and the injured tissue. In acute forms, it can be life preserving, but inappropriate, excessive or chronic inflammation leads to pathological situations (288). As a consequence, the inflammatory process is tightly controlled by numerous cellular players and mediators. Endothelial cells are among main players during the inflammatory process as they are involved in recruitment of inflammatory cells to sites of tissue injury or infection (289). Endothelial cells integrate signals from their environment, such as pro-inflammatory cytokines TNF-

α and interleukin IL-1, and LPS (290). Subsequent NF- κ B activation (288) results in the upregulation of adhesion molecules (291) (*cf.* Introduction Chapter 2) and in the production and release of cytokines (*e.g.* IL-1 and TNF- α) and chemokines (*e.g.* IL-8 and CCL2) by endothelial cells, which serve as communication signals to leukocytes (292-295). (Figure 17).

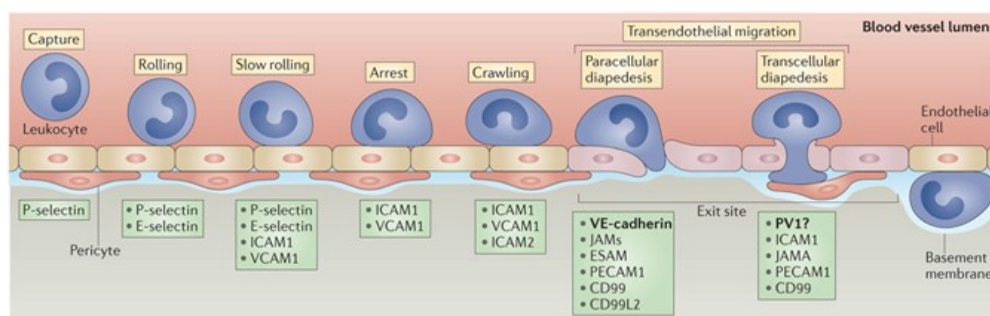


Figure 17. Role of endothelial adhesion molecules during leukocyte adhesion and extravasation. Circulating leukocytes undergo a multistep process of rolling, slow rolling, arrest, adhesion and spreading, and finally transendothelial migration to reach sites of inflammation (296).

3.2.4. Vascular permeability

The endothelium is a selective barrier for blood-tissue exchanges of molecules, thereby controlling tissue oncotic pressure, nutrient delivery and cell extravasation (297, 298). To form this barrier, adhesion molecules present on the surface of juxtaposed endothelial cells bind to each other and form a seal, restricting transendothelial passage (paracellular pathway). The permeability of this barrier varies according to the types of junctions that are present in each tissue type, and is dependent on swift alterations in response to physical forces and biological signals. The type of junction dictates pore size and, hence, the size of molecules that can pass (299). Two types intercellular junctions have been characterized in the endothelium: adherens and tight junctions. Adherens junctions are the most ubiquitous type of endothelial cell-cell junction as they are found in most vascular beds (298, 300). In endothelial cells, they are formed by VE-cadherin anchored to a network of intracellular catenins (β -catenin, γ -catenin, p-120 catenin) that interact

with the actin cytoskeleton (301, 302) (Figure 18). Adherens junctions have a mean pore size of approximately 3 nm (298, 300), making them non-permeant to large macromolecules, such as albumin (69 kDa; molecular radius 3.6 nm). As a consequence, they determine the selectivity of the endothelial barrier to macromolecules in many organs and tissues (298, 300). Tight junctions are less common in the vasculature and can only be found in specialized tissues (*e.g.* blood-brain (303), blood-retinal (304) and blood-testes barriers (305)). Tight junctions confer an additional barrier function, preventing the passage of much smaller molecules (< 1 kDa) and even restricting the flow of small inorganic ions. Hence, they have a mean pore size of approximately 1 nm (306, 307). Tight junctions are mainly composed of occludins bound to cytosolic proteins (*e.g.* ZO-1 and ZO-2) to tightly link the plasma membranes of two juxtaposed cells (308) (Figure 18). Other components are junctional adhesion molecule (JAM) and claudins (309). There are two additional structures found in endothelial cell-cell junctions that are not considered to be determinant of paracellular permeability: gap junctions and fenestrations in discontinuous endothelium. Gap junctions are formed by the interaction of two hexameric connexins from opposing cells, of which endothelial cells are known to express Cx37, Cx40 and Cx43 (310) (Figure 18). By providing an intercellular gateway, gap junctions allow the passage of small molecular weight solutes (*e.g.* second messengers, Ca²⁺ and inositol trisphosphate) between neighboring cells, thereby enabling intercellular communication (311). Fenestrations allow the passage of very large solutes (50 – 100 nm) in specialized tissues such as kidneys, liver and spleen. However, they are of minimal importance in the permeability regulation of common blood vessels (299).

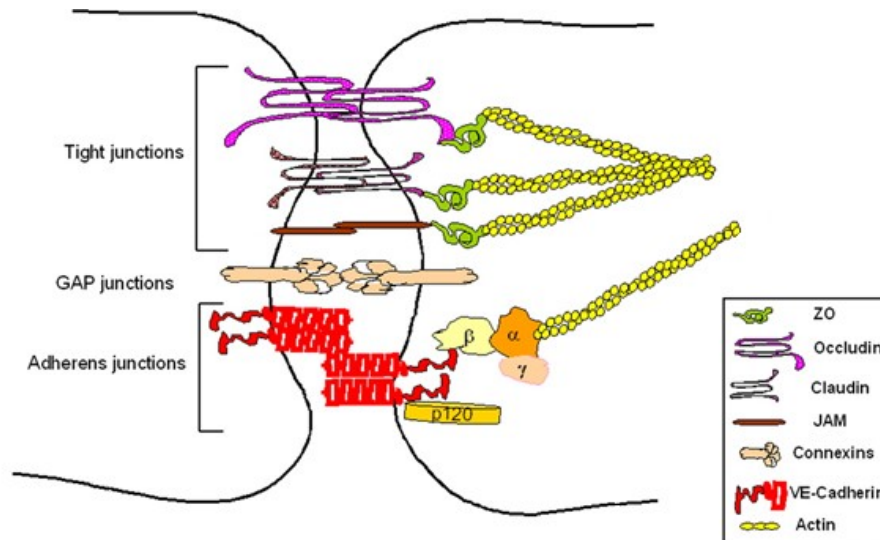


Figure 18. Structural organization of inter-endothelial cell junctions. Tight junctions are formed by occludins, claudins and JAMs, whereas VE-cadherin is required for the formation of adherens junctions. Connexins form gap junctions (298).

3.3. Pathological effects of ionizing radiation: endothelial activation and dysfunction

When cells are exposed to ionizing radiation, they undergo a stress response within less than a microsecond after the hit (47). This response is initiated by the biological damage caused by the disruption of atomic structures, as discussed in Introduction Chapter 1. As a result, endothelial activation occurs, causing the quiescent phenotype to switch towards a pro-inflammatory one. When exposure is prolonged and/or repeated, it can exhaust the protective physiological effect of the endothelium, leading to endothelial dysfunction (312). This pathological state can thus be seen as a maladaptive response to pathological stimuli and refers to a failure of the endothelium to perform its normal, physiologic functions (313). As a result, deterioration of the vascular tone, blood hemostasis problems, inflammation and edema occur at the site of the affected endothelium (314). Because the endothelium is a key integrator of vascular risk, pathogenic signals, including ionizing radiation, may converge to produce several pathological conditions (313), atherosclerosis being a typified example (262). In the sections below, we summarize current knowledge on the effects of ionizing radiation

exposure on the different aspects of endothelial activation and dysfunction. However, it should be noted that it is difficult to draw general conclusions about the adverse events discussed below because the current literature often describes different cell lines, different timepoints and different radiation doses.

3.3.1. Endothelial activation: a pro-inflammatory state

Endothelial cell activation can be defined by the manifestation of a pro-inflammatory phenotype characterized by the expression of chemokines, cytokines and adhesion molecules that facilitate the recruitment and attachment of circulating leukocytes on the vascular wall (312). Endothelial cells are typically activated by pro-inflammatory cytokines TNF- α and IL-6 released by immune cells upon contact with pathogens (315). After ionizing radiation exposure, however, endothelial cell activation occurs in a sterile environment without the presence of pathogens, *i.e.*, sterile inflammation. One of the possible causes of sterile inflammation is oxidative stress, a recognized consequence of endothelial cell exposure to radiation (1, 316-318). Besides reacting with cellular biomolecules, ROS directly activate redox-sensitive transcription factors nuclear factor (erythroid-derived 2)-like 2 (Nrf2), activator protein 1 (AP-1) and NF- κ B (319). Nrf2 is a master regulator of gene expression linked to protein products involved in the removal of ROS, and is known to enhance cellular antioxidant capacity. In the presence of ROS, the cytosolic repressor Kelch-like ECH associated protein 1 (Keap1) is dissociated from Nrf2, followed by nuclear translocation and subsequent DNA binding of Nrf2 on its target genes. These genes code a set of enzymes involved in antioxidant mechanisms, including NADP(H):quinone oxidoreductase-1, SOD, glutathione S-transferase, heme-oxygenase-1, and γ -glutamyl cysteine ligase (319, 320). AP-1 is a heterodimeric transcription factor composed of members of the Jun, Jun dimerization, FOS and related activating transcription partner families (321, 322). Depending on its composition, it plays a role in the expression of several genes involved in cellular differentiation, proliferation and apoptosis. Examples of AP-1-target genes are TGF α , TGF β and IL2 (321). Activation of AP-1 during oxidative and inflammatory stimuli is predominantly mediated by MAPK signaling (319). NF- κ B is another heterodimeric redox-regulated transcription factor that remains sequestered in the cytoplasm as an inactive complex with its inhibitory counterpart inhibitor of κ B (I κ B). Inflammatory and/or oxidative stimuli activate a series of upstream kinases, such as MAPKs, I κ B kinase, PKC and PI3K, which then activate NF-

κ B by phosphorylation-mediated degradation of I κ B. Activated NF- κ B translocates to the nucleus and induces the expression of a wide array of genes regulating pro-inflammatory mediators TNF- α , IL-8, IL-1, iNOS and cyclooxygenase-2 (319). In endothelial cell, NF- κ B is involved in the transcriptional regulation of most cytokines and adhesion molecules (323-327). Another possible cause of endothelial activation is the release of damage-associated molecular patterns (DAMPs) by stressed and dying cells. Tissue injury emits DAMPs that serve as danger signals to activate danger control (*i.e.* inflammation for host defense). DAMPs can either be intracellular molecules that signal cell stress and necrosis (high-mobility group box 1 [HMGB1], histones, purine metabolites, uric acid, S100 proteins, heat shock proteins and DNA/RNA outside nucleus or mitochondria), matrix constituents that signal extensive matrix remodeling (hyaluronan fragments, glycosaminoglycan fragments) and luminal factors that signal barrier destruction (uromodulin, oxidized LDL). DAMPs activate toll-like receptors, purinergic receptors and inflammasomes in parenchymal cells and leukocytes. DAMP binding on endothelial cells upregulates pro-inflammatory signaling pathways that lead to NF- κ B, MAPK, NF- κ B and interferon regulatory factor 3 (IRF3) signaling (328, 329), resulting in expression of adhesion molecules (ICAM-1, VCAM-1, E-selectin) and the release of cytokines (IL-6, IL-8, CCL2, IFN γ) (315, 330-333). In this respect, exposure to ≥ 2 Gy of X-rays was found to induce a dose-dependent *in vitro* and *in vivo* release of HMGB1 (334), known to induce endothelial expression of IL-6, CCL2, ICAM-1 and VCAM-1 (335). Moreover, NF- κ B signaling was found to be upregulated in irradiated arteries of patients treated with radiotherapy, even months or years after radiation exposure (336).

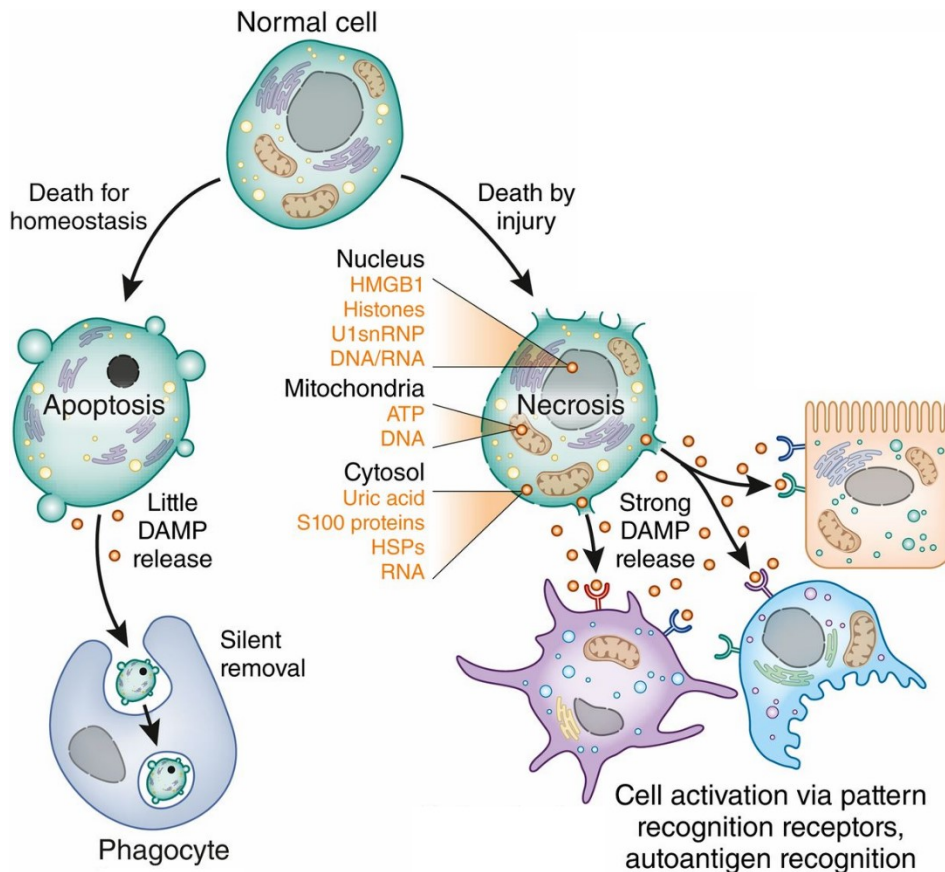


Figure 19. Intracellular damage-associated molecular patterns are released from injured and necrotic cells. Normal cells undergo apoptosis, which maintains inner and outer membranes to avoid DAMP release. Cellular injury followed by stress and necrosis releases intracellular DAMPs from various cellular compartments. U1snRNP, U1 small nuclear ribonucleoprotein; NADPH, NAD phosphate dehydrogenase; CYPD, cyclophilin D, GPX-4, glutathione peroxidase 4; HSP, heat shock protein (337).

In general, high doses of ionizing radiation (> 2 Gy) induce endothelial activation. Endothelial adhesion molecules ICAM-1, VCAM-1 and E-selectin are upregulated in a time- and dose-dependent manner (145, 338), in part due to NF- κ B activation (339). Furthermore, cytokines IL-6 and IL-8 as well as TGF- β were shown to increase after exposure to high doses of ionizing radiation (340, 341). In obese ApoE^{-/-} mice, a 14 Gy exposure induced an inflammatory phenotype, accelerating atherosclerotic plaque formation and rupture (342). In addition, atomic bomb survivors, who are

more prone to the development of atherosclerosis (151), demonstrated signs of general inflammation, with increased levels of IL-6 and C-reactive protein (CRP) (343). Comparatively, the effects of low doses (≤ 2 Gy) of ionizing radiation on endothelial activation are still under debate. A decrease in endothelial ICAM-1 and E-selectin expression has been observed after exposure to 0.3 and 1 Gy (338), which caused decreased endothelial adhesiveness to monocytes (338, 344). This anti-inflammatory effect of low-dose radiation, which was confirmed by others (318, 345-350), requires a pre-activation of endothelial cells with pro-inflammatory stimuli TNF- α , IL-1 β or LPS. When these mice were exposed to low amounts of ^{137}Cs delivered in the drinking water, the pro-inflammatory plaque phenotype was also diminished (351). The dampening effect of radiation exposure on endothelial activation has been used for decades for the treatment of benign inflammatory diseases (352, 353). Today, the use of low dose radiotherapy for the treatment of chronic inflammatory diseases is rare due to the debate on possible cancer and non-cancer risks (349).

It must be emphasized that endothelial cell activation is a normal part of bodily defense mechanisms. In physiological circumstances, it draws immune cells to sites of infection or tissue injury. The difference between normal physiological and detrimental pathological activation of the endothelium lies in the nature, extent, duration and combination of pro-inflammatory stimuli. As a consequence of prolonged and/or repeated exposure to a combination of cardiovascular risk factors, the protective effect of endogenous anti-inflammatory systems of endothelial cells can ultimately be depleted, resulting in endothelial dysfunction (312).

3.3.2. Deterioration of the vascular tone

One of the key consequences of endothelial dysfunction is impairment of endothelium-dependent vasodilation due to reduced bioavailability of vasodilators, particularly NO, and/or to elevated levels of endothelium-derived contracting factors, *i.e.* endothelins, prostaglandin and thromboxane (314, 354-357). The role of NO and its reactive intermediates in the endothelial radiation response largely remains an open question (358). What is known is that, after exposure of endothelial cells to ionizing radiation, NO is rapidly deactivated by superoxide radicals, resulting in the formation of vasotoxic peroxynitrites (359). Irradiation-

induced oxidative stress also causes eNOS uncoupling due to inadequate availability of redox-sensitive cofactor BH₄, resulting in eNOS-dependent production of superoxide and diminished release of NO (360). From 1 to 4 days after irradiation, doses of 6 Gy and higher were found to promote eNOS expression and activity, leading to NO production and NO-induced angiogenesis with a concomitant increase in tumor blood flow (361-363). eNOS activation after endothelial irradiation depends on components of the DNA damage response pathway, namely ATM and heat-shock protein 90, which phosphorylate Ser1179 of eNOS, leading to enhanced eNOS activity (364). However, most of endothelial DNA damage signaling ceases within 24 h after irradiation (365), explaining why irradiation acutely but not chronically enhances NO availability. At later time-points, endothelium-dependent vasodilation is compromised. Timing also depends on the dose and on the nature of the irradiated endothelial bed. For example, reduced endothelium-dependent vasodilation was found in rabbit carotid arterial rings 20 h after irradiation with 8 and 16 Gy (366), in rabbit ear arteries 1 week after irradiation with 10, 20 and 45 Gy (367, 368), in rabbit aorta 9 days after whole-body irradiation with 1, 2 and 4 Gy (369), in the rat prostate vasculature 5 months after irradiation with 10 and 20 Gy (370) and in rat aorta 6 months after irradiation with 15 Gy (371). In humans, endothelium-dependent vasodilation was found to be impaired both *in vitro* and *in vivo* in carotid arteries 4 to 6 weeks after neck irradiation (total pre-operative dose of radiation averaged 47.9±2.8 Gy) (372). In addition, impaired endothelium-dependent vasodilation of axillary arteries was reported in breast cancer radiotherapy patients more than 3 year after radiotherapy (no average dose assigned) (373).

As mentioned in 3.2.1., NO is not the sole vasoactive substance produced and released by the endothelium. The production of prostacyclin, a potent endothelium-derived vasodilator, is also affected by radiation exposure. Basal prostacyclin release was found to be unaffected in irradiated human umbilical vein endothelial cells (HUVECs) at doses up to 25 Gy (374). However, when endothelial cells were stimulated with exogenous arachidonic acid, a precursor of endothelial prostacyclin, prostacyclin levels decreased 15 min after irradiation (375), increased within 1 day after irradiation (376-380) and then decreased again thereafter in a radiation dose-dependent way (374, 378, 381, 382). The short-term stimulatory effect of radiation on prostacyclin production is believed to be caused by oxidative stress (383, 384) and cell damage (378). EDH-related signaling was unaffected after

endothelial irradiation, thereby serving as a reserve defense mechanism for vasorelaxation (369, 385). Conversely, levels of vasoconstrictor endothelin-1 were increased after *in vitro* (386, 387) and *in vivo* (388, 389) radiation exposure with doses ranging from 0.2 to 20 Gy. In addition, the endothelial production and release of vasoconstrictor angiotensin II by endothelial cells, in bovine pulmonary arterial endothelial cells and HUVECs (390, 391) and in pulmonary endothelial cells collected from irradiated rats (392, 393) increased dose- and time-dependently starting 24 h after exposure to 5-30 Gy. Overall, one can conclude that endothelial irradiation induces initial vasodilation during the first couple of days after irradiation, followed by chronic vasoconstriction with compromised endothelium-dependent vasodilation.

Besides affecting the endothelial compartment of blood vessels, ionizing radiation can also directly affect VSMCs. When irradiated in culture in the absence of endothelial cells, VSMCs underwent decreased proliferation after a 1.25-20 Gy exposure (394-396), with a reduction of viable cells only 15 days after exposure (395, 396). The surviving VSMCs demonstrated reduced contractility (396), but maintained a contractile phenotype after exposure to 10-20 (397). In contrast, when VSMCs were cocultured with endothelial cells and both were irradiated together with 2-10 Gy, VSMCs changed from a normal contractile to a fibrogenic phenotype (341) associated with the pathogenesis of atherosclerosis (398). Fibrosis was induced by TGF β released by irradiated endothelial cells, resulting in mothers against decapentaplegic (SMAD) signaling in VSMCs (341). Exposure to 6 Gy also mediated increased myofilament Ca²⁺ sensitivity in isolated rat thoracic aortic VSMCs 9 and 30 days after exposure (399, 400). Furthermore, oxidative stress has been shown to induce vasoconstriction by promoting Ca²⁺ release from VSMC intracellular stores (401) and by upregulating VSMC proliferation by either their secretion of cyclophilin A (402) or by the binding of oxidative stress products hydroperoxyoctadecadienoic acids and 4-hydroxy-2-nonenal to VSMCs (403, 404).

3.3.3. Procoagulatory and prothrombotic phenotype

In addition to altered vascular tone, vascular damage shifts the homeostatic balance towards a procoagulant and prothrombotic endothelial cell phenotype (405). Because prostacyclin and NO are the main anticoagulatory agents secreted by endothelial cells (406), their decreased production after radiation exposure

results in platelet aggregation and blood clot formation. However, molecular mechanisms responsible for loss of endothelial thromboresistance are more complex. The irradiated endothelium indeed increases the synthesis of tissue factor (407, 408), vWF (409-413) and platelet-activating factor (414), while reducing thrombomodulin production (145, 415, 416), prostacyclin receptor production (375, 384, 417) and its fibrinolytic activity (418-420). These changes promote platelet adhesion and aggregation and the development of platelet-fibrin thrombi (421-424). Cytokines produced during endothelial activation (*e.g.* IL-6 and CCL2) further affect hemostasis by inducing the expression of tissue factor, tissue plasminogen activator, thrombomodulin and vWF (425-427). In this context, irradiation with 14 Gy was shown to induce atherosclerotic plaques with an inflammatory phenotype prone to hemorrhage in ApoE^{-/-} obese mice (342), which may accelerate atherosclerosis (428).

3.3.4. Endothelial cell retraction and death

Besides edema formation in surrounding tissues caused by endothelial inflammation and tissue injury (429, 430), exposure to radiation doses as low as 2 Gy can induce a transient and rapid decrease in the integrity of *in vitro* human endothelial barriers through cell detachment and loss of PECAM-1 (431, 432). Rapid loss of endothelial monolayer integrity depends on cytoskeletal reorganization due to actin stress fiber formation and redistribution of VE-cadherin junctions, resulting in endothelial retraction (433-436). At higher doses, a more direct cause of increased vascular permeability is of course endothelial cell death (437, 438). Sensitivity of endothelial cells to ionizing radiation can be assessed by clonogenic assays, the method of choice to determine cell reproductive death after treatment with ionizing radiation (439) (Figure 20). Radiosensitivity varies between endothelial cells from different vascular beds, with HUVECs being the most sensitive and human hepatic sinusoidal endothelial cells (HHSEC) being the most radioresistant (440). In addition, radiosensitivity depends on radiation quality, with the RBE of α -particles estimated at 5.5 and 4.6 for 10% survival of A549 cells and EA.hy926 cells, respectively. Doses as low as 0.125 Gy can reduce the surviving fraction of EA.hy926 cells (441). Doses higher than 5 Gy induce endothelial cell apoptosis by the production of ceramide (442, 443). Ceramide activates stress activated c-Jun N-terminal kinases (JNKs), resulting in the conversion of sphingomyelin to ceramide by neutral sphingomyelinase and the subsequent

activation of caspase-3 (444, 445). In addition, endothelial apoptosis at doses higher than 5 Gy can also be induced by persistent DNA damage, resulting in p53 accumulation and activation of the caspase pathway (446, 447). Mechanisms behind endothelial cytotoxicity of lower doses are less known. For example, apoptotic EA.hy926 cell death was not increased after exposure to 0.2 Gy, but well after exposure to 5 Gy (448). In another study, TNF- α -activated endothelial cells were shown to have a discontinuous induction of apoptosis, with a relative maximum at 0.3 and 3 Gy and a relative minimum at 0.5 Gy (346). In addition, our group observed a dose-dependent increase in endothelial cell apoptosis from 0.5 Gy in HUVECs and from 0.1 Gy in EA.hy926 cells (449). *In vivo*, compromised barrier function is involved in the pathogenesis of vascular failure, including atherosclerosis (314, 450, 451).

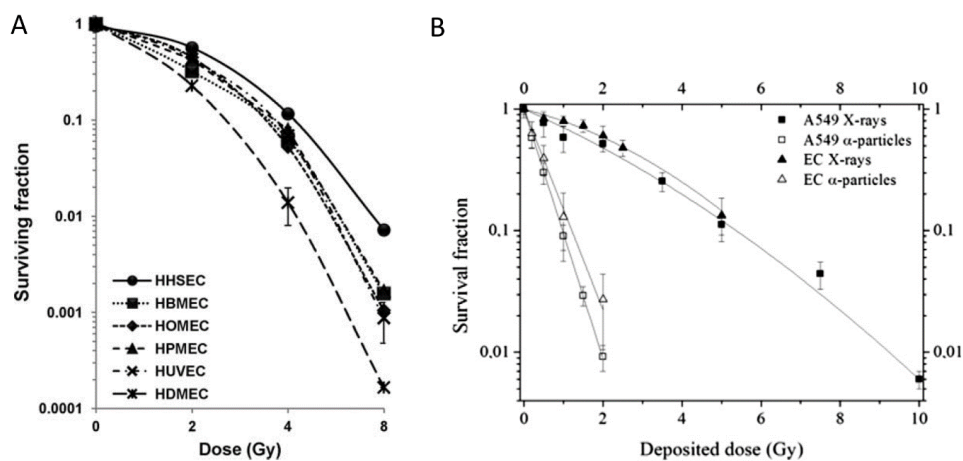


Figure 20. Effect of ionizing radiation on the clonogenic survival of normal endothelial cells from diverse human organs. **A.** Survival fraction of endothelial cells was assessed after clonogenic assays performed 14 days post-irradiation in human hepatic sinusoidal endothelial cells (HHSECs), human brain microvascular endothelial cells (HBMECs), human ovarian microvascular endothelial cells (HOMECs), human pulmonary endothelial cells (HPMECs), human umbilical vein endothelial cells (HUVECs), human dermal microvascular endothelial cells (HDMECs) (440). **B.** Survival fraction was assessed after clonogenic assays performed 11 days post-irradiation. Assays were performed with EA.hy926 cells (EC) derived from fusion of HUVEC with A549 cells (441).

3.3.5. Mitochondrial dysfunction

Recent years have seen increasing interest for radiation-induced mitochondrial dysfunction as a cause of endothelial dysfunction in the context of atherosclerosis (452-456). In most mammalian cells, mitochondria are primarily considered as the major suppliers of cellular energy in the form of ATP by oxidative phosphorylation (OXPHOS) (455). However, mitochondria only have a modest number in endothelial cells (454, 457) and produce a low proportion of total amount cellular energy (458-460). Thus, endothelial mitochondria are more likely to primarily serve as important signaling organelles (461). Apart from metabolic integration, mitochondria are involved in oxidative stress signaling, Ca^{2+} regulation and control of cell death. As a byproduct of OXPHOS, a small amount of O_2 undergoes monoelectronic reduction mainly at complexes I and III of the mitochondrial electron transport chain, resulting in the generation of $\text{O}_2^{\cdot-}$. As a result, mitochondria are a main generation site of ROS within a cell (86). The formed $\text{O}_2^{\cdot-}$ is converted to H_2O_2 by SOD2 inside mitochondria, which is able to activate redox-sensitive transcription factors Nrf2, AP-1 and NF- κ B (319). Normal cytosolic Ca^{2+} concentrations are maintained approximately 10,000 times lower than extracellular Ca^{2+} concentrations by plasma membrane and endoplasmic reticulum Ca^{2+} ATPases. Because these transport proteins require ATP for Ca^{2+} transport, mitochondria are indirectly involved in this form of Ca^{2+} regulation (462, 463). In addition, mitochondria can also directly sequester Ca^{2+} and, thereby, regulate intracellular concentrations by their inner membrane uniporter rapid mode of Ca^{2+} uptake into heart mitochondria (RaM), which is driven by the proton electrochemical potential. Conversely, mitochondria release Ca^{2+} via the $2\text{Na}^+/\text{Ca}^{2+}$ - and $2\text{H}^+/\text{Ca}^{2+}$ -exchanger. Increased mitochondrial Ca^{2+} activates dehydrogenase enzymes in mitochondria and increases ATP synthase activity, leading to increased NADH and ATP production (464). Importantly, mitochondria are also central executioners of apoptosis. In normal state, anti-apoptotic proteins of Bcl-2 family, located on the outer mitochondrial membrane, inhibit pro-apoptotic effector proteins BAX and BAK. In response to cytotoxic stress, BCL-2 homology 3 (BH3)-only proteins inhibit BCL-2 proteins, resulting BAX and BAK activation. BAX and BAK form oligomers that permeabilize the mitochondrial outer membrane, mediating the release of cytochrome c into the cytosol (465, 466). Cytosolic cytochrome c promotes the activation of caspase 9 by apoptotic protease activating factor 1 (APAF1), which in turn activates effector caspases that induce cell death (467). Dysregulation of these vital functions can promote endothelial

inflammation, apoptosis and senescence, which are all linked to the development and progression of atherosclerosis (438, 454-456, 468).

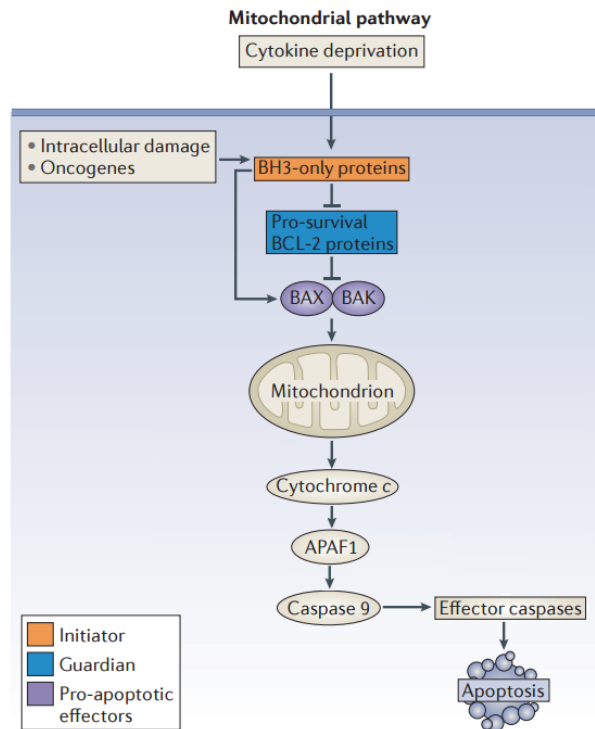


Figure 21. Mitochondria-mediated pathways in apoptosis. Diverse cytotoxic stimuli, including oncogenic stress, intracellular damage and cytokine deprivation, engage the mitochondrial pathway by induction of BCL-2 homology 3 (BH3)only proteins (initiators). These BH3-proteins inhibit prosurvival BCL-2-like proteins (guardians), thereby enabling activation of proapoptotic effectors BAX and BAK, which then disrupt the mitochondrial outer membrane and release cytochrome c. Released cytochrome c promotes caspase 9 activation *via* apoptotic protease activating factor 1 (APAF1), converging at effector caspases (caspase 3, caspase 7 and caspase 6). Figure adapted from (469).

Because mitochondria are the biggest cellular source of ROS (438, 470, 471), they are closely related to oxidative stress signaling. At relatively low levels, mitochondria-derived ROS are signaling molecules that support normal or compensatory cellular functions involved in hypoxic adaptation, immunity, cellular differentiation and longevity (472). However, excessive mitochondrial ROS levels

can cause oxidative stress (455). This is problematic because mitochondria themselves are critical target of ROS (473). In general, after cellular exposure to ionizing radiation, antioxidant supply quickly becomes compromised, leading to a rapid decline of reduced GSH levels [*e.g.* 10 Gy, murine testis (474)]. In an effort to combat oxidative challenge, ROS and RNS activate cellular transcription factors, Nrf2, NF- κ B and AP-1, resulting in increased expression of ROS-detoxifying enzymes catalase, SOD, GPx, GST and heme oxygenase-1 (475-477). Nrf2 is believed to be the main regulator of cellular resistance to pro-oxidants. Because Nrf2 controls basal and induced expression of an array of antioxidant response element-dependent genes, including heme oxygenase-1, MnSOD and GPx (478, 479), it is not surprising that this factor is induced after radiation exposure in both normal and cancerous cells (0.05 Gy – 8 Gy) (476, 480, 481). Nrf2 also confers cellular radioresistance (482-485) by mediation DNA repair and oxidative defense in both normal and cancerous cells (481, 486). In addition, Nrf2 upregulation has been implicated in oxidative stress-induced endothelial dysfunction (487). Because Nrf2 mediates gene expression resulting in both high NADPH production and the production, regeneration and utilization of GSH, Trx and Prx, upregulation of Nrf2 leads to increased levels of these antioxidants after irradiation (0.25 - 20 Gy) in lymphocytes and glioma cells (488, 489). Of note, elevated levels of several mammalian Prx isoforms have been evidenced after a 10 Gy radiation exposure of mouse testis and liver, further enhancing cellular defense mechanisms (474, 490-492). Both cumulative and acute radiation exposure can disrupt the cellular redox balance. However, oxidative stress only prevails when pro-oxidant levels eventually overwhelm cellular antioxidant systems, an event marked by enzyme inactivation, a low GSH/glutathione disulfide ratio and a decreased pool of low molecular weight antioxidants. The consequence of such redox imbalance is manifested by modifications of nucleic acids, lipids, protein, and other biomolecules (30, 475).

If radiation doses are high enough to overwhelm cellular antioxidant responses, oxidative stress can induce mitochondrial dysfunction. As a consequence, radiation-induced oxidative stress that normally disappears within seconds after exposure (473) can lead to the initiation of a self-amplifying cycle, giving rise to long-term ROS production (493) and concomitant mitochondrial dysfunction (438). During this process, mitochondrial DNA seems to be particularly sensitive to oxidative damage because of its limited DNA repair capacity, lack of protective histones, a high exon to intron ratio and its close proximity to the electron transport

chain (494). In agreement, a range of studies demonstrated changes in mitochondrial function and number after exposure of cells or tissues to high doses of ionizing radiation (495-498). Doses of 5-20 Gy of γ radiation were found to induce a dose-dependent increase in ROS levels with a decrease in mitochondrial activity (499, 500). Furthermore, 15 Gy of X-rays induced persistent oxidative stress in endothelial cells, linked to mitochondrial dysfunction and premature senescence (501). Effects of low radiation doses have been less studied on mitochondrial dysfunction in endothelial cells. Doses of 1.5, 4 and 10 Gy were found to influence mitochondrial membrane potential in HUVECs 2 days after exposure. While mitochondrial potential reached back control level by day 5 and 6 in 1.5 and 4 Gy irradiated cells, respectively, 10 Gy resulted in persistently decreased mitochondrial activity (500). In another example, the respiratory capacity of cardiac mitochondria was significantly reduced 40 weeks after local heart irradiation of ApoE^{-/-} mice with a single X-ray dose of 2 Gy (502). In addition, 0.1 and 0.5 Gy were found to reduce mitochondrial pathways in murine hippocampus and cortex (503).

3.3.6. Premature endothelial senescence

Aging of the vascular system predisposes the cardiovascular system to the development of diseases, even in the absence of other risk factors (504). On a cellular level, vascular aging corresponds to endothelial cell senescence (505, 506), a phenomenon that refers to irreversible arrest of endothelial cell renewal. At a molecular level, senescence is induced and maintained by p53 and p16-Rb pathways that inhibit cell cycle progression (Figure 22) (507). Both pathways are activated either during attrition of telomeres, referred to as replicative senescence (508, 509), or during stress situations independently of telomere shortening, referred to as stress-induced premature senescence (510). For instance, limited availability of nutrients and growth factors, chromatin perturbations, improper cell contacts and oxidative stress prematurely induce senescence (511). Oxidative stress is of special importance because it induces and accelerates senescence at multiple molecular levels: accelerated telomere shortening (511), induction of DNA damage leading to p53 activation (122), and NO scavenging decreasing its bioavailability (512), all leading to mitochondrial dysfunction (513).

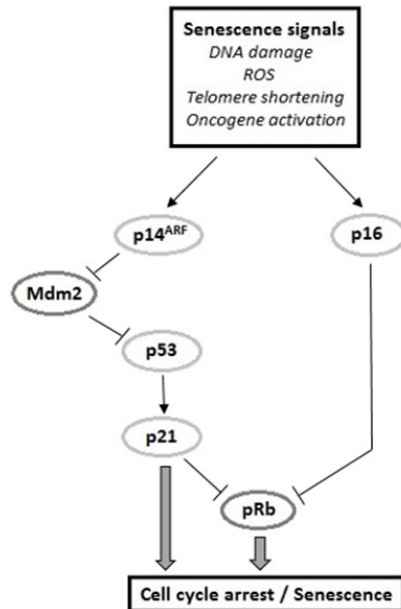


Figure 22. Pathways involved in the induction of senescence. Senescence signals, including DNA damage, ROS and telomere attrition, can affect cell cycle progression by activating the p53 and p16-Rb pathways. From reference (514).

Endothelial senescence is currently emerging as a contributor to the pathogenesis of atherosclerosis through ROS production, decreased NO availability and increased production of pro-inflammatory molecules IL-6, IL-1, IL-8, CCL2, ICAM-1 (513, 515, 516). All these molecules indeed contribute to development and progression of atherosclerosis (468, 513), as indirectly evidenced by the presence of senescent endothelial cells in human atherosclerotic plaques (515). These results have to be taken with caution: identification of senescent endothelial cells suggests an association with atherosclerosis but cannot be used to evidence a causal relationship between endothelial senescence and development and/or progression of atherosclerosis. Considering that ionizing radiation induces oxidative stress (511, 517), DSBs (518) and telomere shortening (517), it is not surprising that it constitutes a stressor that can evoke premature senescence in cells. Several *in vitro* studies demonstrated that high dose (4-50 Gy) radiation exposure (519-525) and chronic radiation exposure to low doses (526-528) induces premature endothelial cell senescence.

3.4. Models to study endothelial cells *in vitro* and *in vivo*

3.4.1. *In vitro* endothelial models

The first successful cultivation of endothelial cells was reported nearly 4 decades ago (529). Until recently, progress in the knowledge of endothelial pathophysiology has been mainly a consequence of investigations performed with endothelial cells in culture (530). A wide and diverse range of primary endothelial cell cultures exists, which are classified according to (i) their source, (ii) whether they were initially derived from arteries, capillaries or veins, and (iii) whether they are from the macrovascular or microvascular beds (531). The most commonly used primary cell culture is HUVECs because they are relative easy to obtain and exhibit endothelial properties intermediate between macro- and microvasculature (532). Other common primary endothelial cell cultures from human origin are human aortic endothelial cells (HAEC), human coronary artery endothelial cells (HCAEC), human iliac vein endothelial cell (HIVEC), human microvascular endothelial cell (HMVEC), human placental endothelial cell (HPEC) and human pulmonary aortic endothelial cell (HPAEC). Primary cell culture models of animal-derived endothelial cells also exist from bovine, murine and rodent sources. Examples include bovine aortic endothelial cells (BAEC), bovine pulmonary artery endothelial cells (BPAEC), mouse aortic endothelial cells (MAEC), rat aortic endothelial cells (RAOEC) and rabbit aortic endothelial cells (RAEC) (532-535). Classification based on origin has been put in place to account for structural and functional heterogeneity of endothelial cells throughout the human vasculature. The endothelial phenotype can indeed differ depending on the organ of origin, the segment of the vascular tree and even between neighboring cells in the same organ and vessel type (536, 537). Endothelial cell heterogeneity is mediated by two mechanisms: differences in the endothelial microenvironment and epigenetics. As blood vessels are distributed throughout the human body, their endothelium is exposed to a wide variety of tissue microenvironments. Furthermore, site-specific properties are epigenetically fixed and do not change in respect to their extracellular environment (Figure 23) (538).

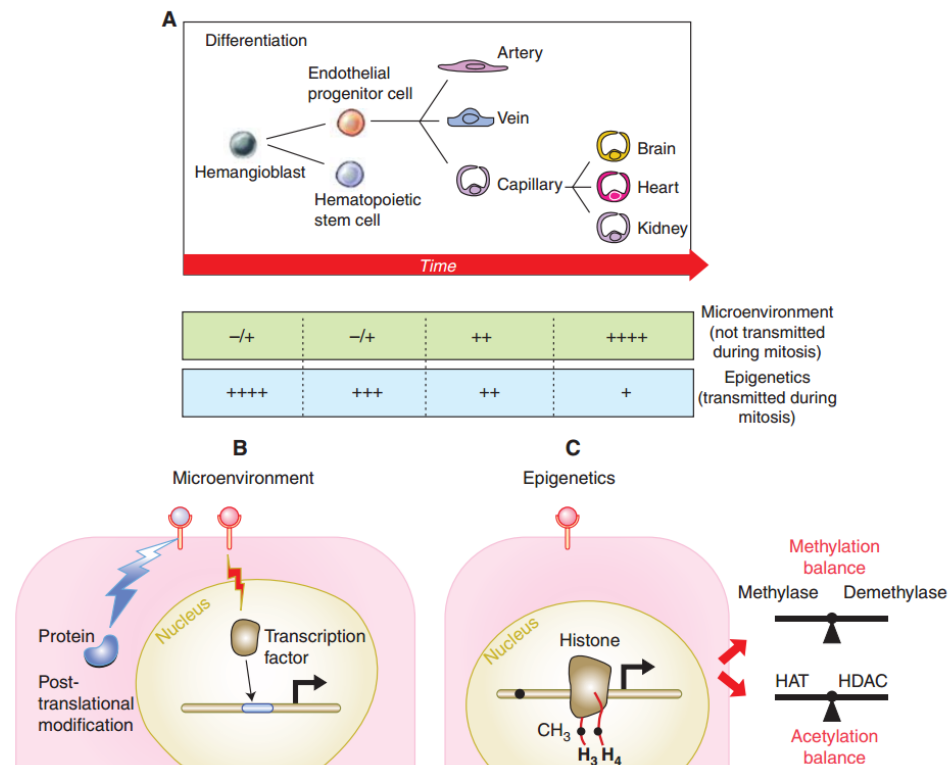


Figure 23. Microenvironment and epigenetics as a cause of endothelial cell heterogeneity.

A. Endothelial progenitor cells are formed by hemangioblasts and are able to differentiate into endothelial cells of arteries, veins and capillaries. The hypothetical relative role of microenvironment and epigenetics in mediating cell type-specific phenotypes is shown. **B.** Nonheritable changes can be mediated in endothelial cells by factors from the microenvironment, by receptor-mediated posttranslational modifications of proteins (e.g. phosphorylation of a signal intermediate) and transcription factor-dependent induction of gene expression. **C.** Epigenetics mediate heritable changes in endothelial cell phenotype by DNA methylation (●), histone methylation (CH₃, ●) and histone acetylation (red lines) that affect gene expression. The amount of methylation is regulated by methylases and demethylases, whereas acetylation of histones is controlled by a balance between histone acetyltransferases (HAT) and histone deacetylases (HDAC) (538).

Drawbacks of primary endothelial cell cultures are their limited replicative life span, loss of primary cell characteristics and responsiveness to stimuli and variation between different donors (532). As a consequence, the need for standardized experimental conditions and reproducible results led to the production of

immortalized, well-characterized endothelial cell lines that stably express a variety of endothelial cell properties (532). The most commonly used cell line is Ea.Hy926, created by the fusion of HUVECs with human lung carcinoma A549 cells (539). These cells overcome replicative senescence, but immortality often results in a gain of tumor cell traits and loss of the primary endothelial cell characteristics (532). This is in contrast to the ideal endothelial cell line that would retain all primary cell characteristics, such as ICAM-1 and VE-cadherin expression, with limited tumor cell traits (532). In this PhD project, Est2 telomerase-immortalized human coronary artery endothelial cells were used because they have a stable genome, were shown to have a similar response to ionizing radiation compared to their primary counterparts (519), have a normal cobblestone morphology, express key endothelial phenotypic markers, including PECAM-1 and VE-cadherin, and take up acetylated LDL (Figure 24). Our choice to use endothelial cells derived from coronary arteries was based on the *in vivo* observation that radiation exposure of the heart during radiotherapy (mean doses to the whole heart was 4.9 Gy [range 0.03 - 27.72 Gy]) accelerates age-related atherosclerosis of coronary endothelial cells, leading to coronary artery disease (171).

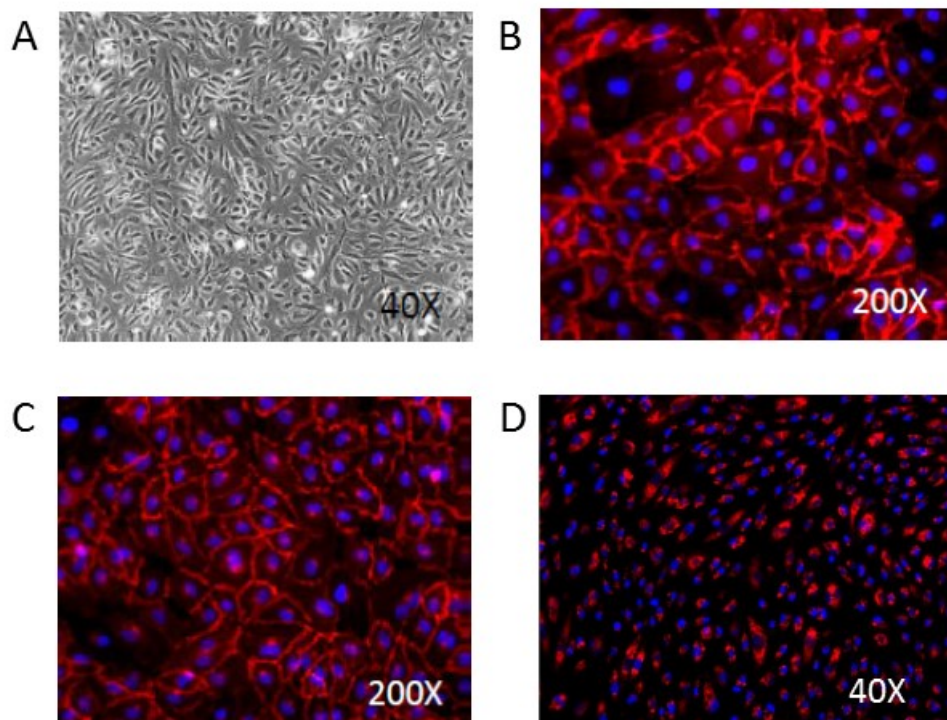


Figure 24. Expression of endothelial phenotypical markers by Est2 telomerase-immortalized human coronary artery endothelial cells. A. Phase contrast of endothelial cells demonstrating cobblestone morphology. B. Immunocytochemical staining for PECAM-1 (red), showing its location at intercellular endothelial junctions. C. Immunocytochemical staining for VE-cadherin (red), showing its location at the endothelial intercellular junctions. D. Uptake of acetylated-low density lipoprotein (Ac-LDL) by endothelial cells. Blue, nuclear staining (DAPI). Courtesy of Dr. Kenneth Raj and Dr. Donna Lowe.

Although very useful, *in vitro* endothelial models are not representative of the *in vivo* situation. In recent years, advances have been made with the development of *in vitro* coculture and 3D models that mimic *in vivo* complexity. For the aim of studying different aspects of the pro-atherosclerotic phenotype, vascular cocultures provide interactions between endothelial cells and supportive VSMCs, pericytes, fibroblasts, monocytes and/or macrophages (540-543). Another level of complexity is added in 3D models, allowing to study cell-to-cell and cell-extracellular matrix interactions, as well as influences of the microenvironment (Figure 25) (544). Examples of 3D endothelial models are the vasculogenic model,

combining one type of endothelial cell with extracellular matrix-mimicking material (e.g. gelatin, matrigel), and spheroids that consist of heterogeneous spherical aggregates of endothelial cells with or without the addition of mural cells, which resemble a tube-like structure (Figure 26) (544, 545). A drawback shared by these more advanced models and 2D cultures is that culture conditions are optimized to support fast endothelial proliferation rather than maintenance of a quiescent endothelial cell phenotype as can be normally found *in vivo* (406). In normal physiological conditions, endothelial cells are indeed almost all quiescent (546), owing to reversible growth/proliferation arrest due to contact inhibition that blocks mitogenic inactivity (547). Because radiation sensitivity varies throughout the cell cycle, with the late S phase being the most radiation resistant, this could influence cellular outcome after irradiation (116).

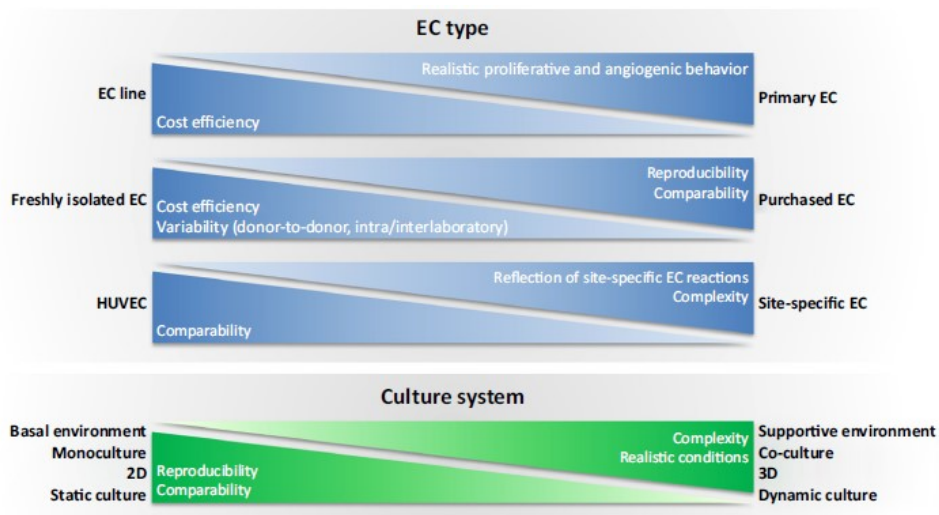


Figure 25. Advantages and drawbacks of different endothelial cell types and culture systems. Primary endothelial cell cultures demonstrate a realistic proliferative and angiogenic behaviour, but fail to be cost efficient. Purchase of endothelial cells gives reproducibility and comparability in the data, but is a costly affair. While HUVECs are comparable to endothelial cells throughout the vascular tree, site-specific endothelial cells should be used when looking for site-specific reactions. Lastly, simple 2D cultures are reproducible and comparable, but fail to represent a realistic condition and the complexity present in the human body. EC, endothelial cells (531).

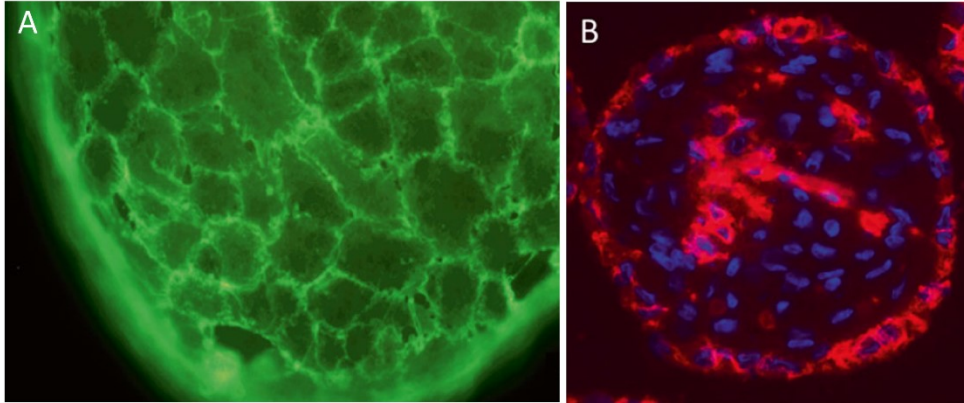


Figure 26. Spheroid-based *in vitro* model of a co-culture composed of endothelial and vascular smooth muscle cells. A. PECAM-1-specific green fluorescence on the surface of spheroids confirms the endothelial identity of the cobblestone-like cells. **B.** A cross-section of co-culture spheroids reveals that PECAM-1-positive endothelial cells (red) are mostly distributed at the spheroid border (548).

3.4.2. *Ex vivo* and *in vivo* models

The use of *in vitro* models provides a great deal of experimental control, but fail to replicate complex cell–cell and cell–matrix interactions that occur *in vivo* and play a central role in the pathogenesis of atherosclerosis. In order to bridge the gap between *in vitro* and *in vivo* research, *ex vivo* organ culture models can account for complex interactions. *Ex vivo* models can be used in the atherosclerosis field to elucidate vascular wall responses to pathophysiologic mechanical forces and biological processes thought to be involved in atherogenesis, including oxidative stress and cytokine production (549). In one of these models, explanted vessel segments of animal (commonly used are canine, bovine, porcine, rat and mouse) or human origin are put in tissue baths (37°C, oxygenated, physiological salt solution) and loaded onto myographs, able to record tension under isometric conditions (wire myographs) or diameter changes under isobaric conditions (pressure myographs; Figure 27) (549-551). Compounds can be added directly to the tissue bath, and vessel tension or diameter changes can be monitored. In this model, de-endothelialization can be applied to confirm the role of endothelial cells in the contraction of explanted vessels (552, 553). In the context of atherosclerosis, myography is mainly used to piece together the complex interaction of mechanical stresses in the vascular environment and oxidative stress (549). Blood vessel explants can also provide a more complete picture of angiogenic processes during aortic ring assays. When compared to the cell culture-based assays, these assays

have the advantage to allow analysis of cellular proliferation, migration, tube formation, micro-vessel branching, perivascular recruitment and remodeling (554). Because neovascularization plays a major role in plaque growth and instability, aortic rings assays have found their place in atherosclerotic research (555). In addition to myographs and ring assays, explants can also be kept in culture with or without addition of compounds to study their behavior in the context of atherosclerosis. Interestingly, a plaque culture model to study human atherosclerotic lesion biology *ex vivo* was recently described (556). Working with fresh human plaques obtained from patients undergoing endarterectomy (removal of atheromatous plaque material) or coronary artery bypass grafting, cut explants are stored in cell culture medium in addition to compounds of interest. After incubation, explants can be used in a variety of analytical techniques, such as polymerase chain reaction (PCR), immunohistochemistry, western blotting, flow cytometry and enzyme-linked immunosorbent assay (ELISA).

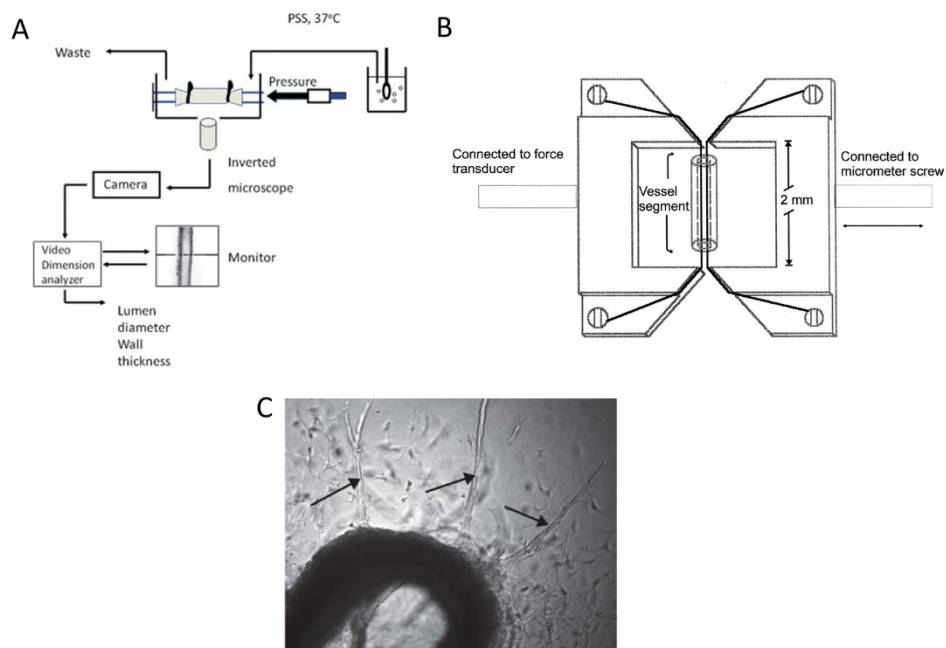


Figure 27. *Ex vivo* blood vessel models. **A.** Typical set-up of a wire myograph. Blood vessel explants are mounted between two glass cannulae in a pressure myograph chamber. Arteries are continuously superfused with gassed physiological salt solution (PSS), in which compounds can be mixed. A video tracer system and dimension analyzer allows the continuous measurement of luminal diameter and left and right wall thickness (557). **B.** Typical set-up of a pressure myograph. Blood vessel explants are mounted on two wires, of which one is coupled to a micrometer screw to regulate basal wall tension and the other is

coupled to a force transducer able to measure changes in explant wall tension following the addition of compounds of interest (558). C. Phase-contrast images of aortic rings embedded in extracellular matrix, showing microvessel outgrowth (black arrows) (554).

Better than *ex vivo* models, a number of animal models have been used for understanding the mechanisms involved in both induction and regression of atherosclerotic lesions. The ideal animal model of atherosclerosis should develop the various stages of the disease, from initial fatty streak to plaque rupture and thrombosis. In addition to close resemblance to the human condition, availability and affordability determines model selection. However, each of the current animal models has some limitations and only replicates part of the atherosclerotic process. The most common animal model of atherosclerosis is the mouse, thanks to its relative low cost, ease of housing, short reproductive cycle, availability of full genomic sequence and associated editing tools. Because wild-type mice are resistant to atherosclerosis due to low LDL plasma levels, genetically modified models were developed that include ApoE^{-/-} and LDL receptor knock out mice (559, 560). These models, however, do not demonstrate coronary lesions and plaque instability, making them useful to study atherogenesis only. Rabbit models develop atherosclerotic lesions either as a result of a high-cholesterol diet or after continuous intimal injury (*e.g.* balloon angioplasty) (561). Lesions resemble human plaques in respect to their inflammatory components, but are mainly formed by VSMCs. By comparison, porcine models spontaneously develop atherosclerosis, which can be accelerated by feeding pigs with an atherogenic diet, *i.e.*, containing high amounts of saturated fat and cholesterol. They develop lesions in their coronary arteries and demonstrate a human-like lipoprotein profile (562-564). When diabetes is induced by injection of beta-cell cytotoxin streptozotocin in combination with a high fat diet, porcine plaques resemble those of human coronary arteries in all their complexity (565). However, these models are expensive, and only a limited number of genetic models are available (566). Lastly, non-human primates are also attractive models to study human atherosclerosis because they have human-like lipoprotein profiles, develop atherosclerosis spontaneously and even acquire myocardial infarctions (567). However, the high cost of experiments, difficulties in handling these animals and ethical issues hamper the use of non-human primates for atherosclerosis research (566, 567).

Differences between cell culture models, animal models and actual atherosclerosis in humans by no means indicate that studies using simple models should be discarded, nor does it mean that the molecular and biological mechanisms identified to be associated to pathophysiology are invalid. Data acquired with *in vitro*, *ex vivo* and *in vivo* models that mimic human atherosclerosis, however, require careful interpretation, recognition of their limitations and, whenever possible, confirmation on human material and/or in patients. Endothelial cell cultures and experimental atherosclerosis in animals allow rigorous testing of mechanistic hypotheses, but do not entirely mimic the human condition (181).

Aims of the study

Aims of the study

The ultimate goal of radiation-induced CVD risk research is to improve assessment and protection of cardiovascular-related health risks associated with exposure to ionizing radiation. CVD is known to occur at radiation doses higher than 0.5 Gy, as evidenced by epidemiological studies with atomic bomb survivors (151) and breast cancer patients (171) (Figure 28). Current understanding is that high dose radiation exposure is associated with age-accelerated atherosclerosis and defects to the heart microvasculature, eliciting CVD (145, 147). However, biological and molecular mechanisms remain elusive. Moreover, limitations of epidemiological studies also make it extremely difficult to directly quantify health risks for low-dose radiation exposure (12). As a consequence, researchers are deemed to rely on radiobiological evidence and biophysical arguments to verify the potential occurrence of radiation risks and to substantiate epidemiological evidence with molecular findings for radiation effects at low doses. The overall aim of our study was to identify molecular and phenotypic responses of endothelial cells to ionizing radiations. First, we aimed to identify molecular mechanisms potentially accounting for the CVD in irradiated endothelial cells. We focused on endothelial activation and dysfunction, two major events linked to the pathogenesis of atherosclerosis (181, 183). Second, in view of the increasing use of charged particle beams in radiotherapy (568), we aimed to determine if molecular mechanisms related to radiation-induced CVD depend on radiation quality. For this reason, the molecular effects of Fe ion irradiation on endothelial cells were compared to those elicited by X-rays. Our experimental data offer an insight into the molecular causes of radiation-induced CVD, which may constitute a basis for ultimately ameliorating radiation protection and for the development of countermeasures for radiation-exposed individuals.

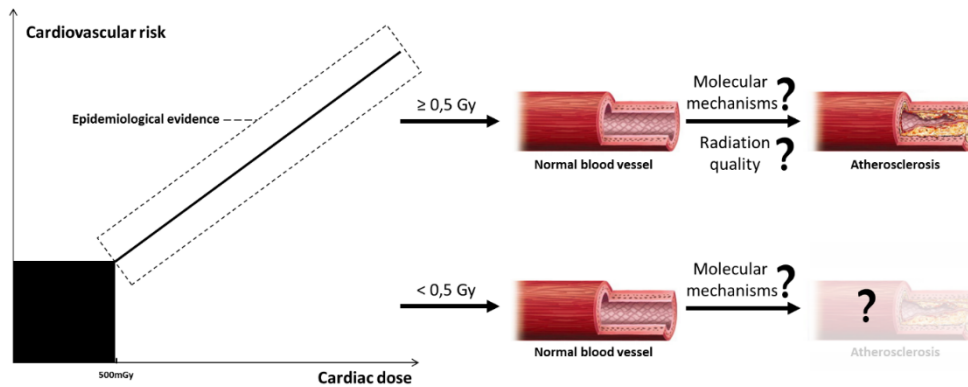


Figure 28. Schematic representation of this PhD project aims. Epidemiological evidence suggests induction of CVDs linked to atherosclerosis above irradiation doses of 0.5 Gy, but does not provide molecular mechanisms nor information about possible dependency on radiation quality. Due to limitations of epidemiological studies, cardiovascular effects of radiation doses below 0.5 Gy are difficult to detect and still constitute a black box of the current radiation protection system. Our aims are to identify molecular mechanisms potentially accounting for the CVD in irradiated endothelial cells and to determine if these mechanisms depend on radiation quality.

Results

Chapter 1

Functional Gene Analysis Reveals Cell
Cycle Changes and Inflammation in
Endothelial Cells Irradiated with a Single
X-ray Dose



Functional Gene Analysis Reveals Cell Cycle Changes and Inflammation in Endothelial Cells Irradiated with a Single X-ray Dose

Bjorn Baselet^{1,2}, Niels Belmans^{1,3}, Emma Coninx¹, Donna Lowe⁴, Ann Janssen¹, Ariette Michaux¹, Kevin Tabury^{1,5}, Kenneth Raj⁴, Roel Quintens¹, Mohammed A. Benotmane^{1†}, Sarah Baatout^{1,6†}, Pierre Sonveaux^{2†} and An Aerts^{1*†}

¹Radiobiology Unit, Belgian Nuclear Research Centre (SCK•CEN), Institute for Environment, Health and Safety, Mol, Belgium, ²Institut de Recherche Expérimentale et Clinique (IREC), Pole of Pharmacology & Therapeutics, Université catholique de Louvain, Brussels, Belgium, ³Faculty of Medicine and Life Sciences, Biomedical Research Institute, Hasselt University, Hasselt, Belgium, ⁴Centre for Radiation, Chemical and Environmental Hazards, Public Health England, Didcot, UK, ⁵Biomedical Engineering Program and Department of Mechanical Engineering, University of South Carolina, Columbia, SC, USA, ⁶Department of Molecular Biotechnology, Ghent University, Ghent, Belgium

OPEN ACCESS

Edited by:

Olivier Cuvillier,
Centre National de la Recherche
Scientifique, France

Reviewed by:

Franz Rödel,
University Hospital Frankfurt, Germany
Alexandros G. Georgakilas,
National Technical University of
Athens, Greece

*Correspondence:

An Aerts
an.aerts@sckcen.be

[†]Co-last authors.

Specialty section:

This article was submitted to
Pharmacology of Anti-Cancer Drugs,
a section of the journal
Frontiers in Pharmacology

Received: 11 January 2017

Accepted: 05 April 2017

Published: 25 April 2017

Citation:

Baselet B, Belmans N, Coninx E,
Lowe D, Janssen A, Michaux A,
Tabury K, Raj K, Quintens R,
Benotmane MA, Baatout S,
Sonveaux P and Aerts A (2017)
Functional Gene Analysis Reveals Cell
Cycle Changes and Inflammation in
Endothelial Cells Irradiated with a
Single X-ray Dose.
Front. Pharmacol. 8:213.
doi: 10.3389/fphar.2017.00213

Background and Purpose: Epidemiological data suggests an excess risk of cardiovascular disease (CVD) at low doses (0.05 and 0.1 Gy) of ionizing radiation (IR). Furthermore, the underlying biological and molecular mechanisms of radiation-induced CVD are still unclear. Because damage to the endothelium could be critical in IR-related CVD, this study aimed to identify the effects of radiation on immortalized endothelial cells in the context of atherosclerosis.

Material and Methods: Microarrays and RT-qPCR were used to compare the response of endothelial cells irradiated with a single X-ray dose (0.05, 0.1, 0.5, 2 Gy) measured after various post-irradiation (repair) times (1 day, 7 days, 14 days). To consolidate and mechanistically support the endothelial cell response to X-ray exposure identified via microarray analysis, DNA repair signaling (γ H2AX/TP53BP1-foci quantification), cell cycle progression (BrdU/7AAD flow cytometric analysis), cellular senescence (β -galactosidase assay with CPRG and IGFBP7 quantification) and pro-inflammatory status (IL6 and CCL2) was assessed.

Results: Microarray results indicated persistent changes in cell cycle progression and inflammation. Cells underwent G1 arrest in a dose-dependent manner after high doses (0.5 and 2 Gy), which was compensated by increased proliferation after 1 week and almost normalized after 2 weeks. However, at this point irradiated cells showed an increased β -Gal activity and IGFBP7 secretion, indicative of premature senescence. The production of pro-inflammatory cytokines IL6 and CCL2 was increased at early time points.

Conclusions: IR induces pro-atherosclerotic processes in endothelial cells in a dose-dependent manner. These findings give an incentive for further research on the shape of the dose-response curve, as we show that even low doses of IR can induce premature endothelial senescence at later time points. Furthermore, our findings on

the time- and dose-dependent response regarding differentially expressed genes, cell cycle progression, inflammation and senescence bring novel insights into the underlying molecular mechanisms of the endothelial response to X-ray radiation. This may in turn lead to the development of risk-reducing strategies to prevent IR-induced CVD, such as the use of cell cycle modulators and anti-inflammatory drugs as radioprotectors and/or radiation mitigators.

Keywords: X-ray, endothelium, atherosclerosis, cardiovascular disease, cell cycle

INTRODUCTION

At higher doses of ionizing radiation (>0.5 Gy), epidemiological data show a significant excess risk of late occurring cardiovascular disease (CVD; Hildebrandt, 2010; Shimizu et al., 2010; Darby et al., 2013). The term CVD encompasses coronary heart disease and peripheral arterial disease, and is most often related to atherosclerosis (Lusis, 2000). In the clinics, these doses are used in 50 to 60% of all cancer patients during radiotherapy (Gottfried et al., 1996). During these treatments, normal surrounding tissues also receive a part of the dose. For example, the mean dose of radiation to the heart during breast cancer radiotherapy ranges from 0.03 to 27.72 Gy, with an overall average of 4.9 Gy (Darby et al., 2013). Still, knowledge of the underlying biological and molecular mechanisms of radiation-induced CVD is limited (Little et al., 2008; Hildebrandt, 2010) and should be complemented with experimental findings.

In addition to higher doses, low doses of ionizing radiation (≤ 0.1 Gy Fazel et al., 2009) are also increasingly used in the clinics, mainly for diagnostic medical purposes (UNSCEAR, 2008). Consequently, the possibility of an excess risk of CVD following exposure to ionizing radiation is of great societal concern. However, the current radiation protection system is based on the assumption that there is a threshold at 0.5 Gy where epidemiological evidence for non-cancer effects is suggestive (Hildebrandt, 2010). Indeed, over recent years, a growing body of epidemiological data suggested an excess risk of late occurring CVD at much lower doses, without a clear-cut threshold (Hildebrandt, 2010; Shimizu et al., 2010; Darby et al., 2013). However, due to a lack of statistical power, these data are suggestive rather than persuasive.

The mechanisms by which radiation causes CVD are at present unknown, but radiation acts, at least in part, by causing or promoting atherosclerosis (Borghini et al., 2013). Atherosclerosis is a multifactorial disease characterized by a chronic inflammatory process of the arterial wall. It is believed to be initiated by irritative stimuli (e.g., hypertension, dyslipidemia, and pro-inflammatory mediators) leading to endothelial dysfunction (Libby et al., 2011), a pathological state characterized by the loss of endothelial functions that are normally in place to maintain vascular integrity (Hirase and Node, 2012). This dysfunctional state induces a pro-inflammatory reaction in the endothelium, triggering the expression of adhesion molecules such as selectin P and intracellular adhesion molecule 1 (ICAM1; Collins et al., 2000) and the secretion of cytokines such as C-C Motif Chemokine

Ligand 2 (CCL2; Boring et al., 1998) and interleukin-6 (IL6) (Schieffer et al., 2004). These molecules mediate the attachment of circulating monocytes and lymphocytes, driving the intimal immune cell infiltration. Eventually, a chronic inflammatory reaction ensues, resulting in the formation of an atheroma filled with foam cells and a necrotic core (Weber and Noels, 2011). By using bioinformatics and metanalytical approaches, knowledge on the molecular networks that are common in ionizing radiation, immune and inflammatory responses is emerging (Georgakilas et al., 2015). These studies will further help to understand the underlying molecular mechanisms of radiation-induced inflammatory reactions and will help to explain the pathogenesis of radiation-induced CVD.

In the radiobiological context, endothelial cells have been proposed to be a critical target in radiation-induced CVD (Little et al., 2008; Hildebrandt, 2010). Indeed, exposure of the vascular endothelium to IR can result in endothelial cell dysfunction (Bhattacharya and Asaithamby, 2016), a well-established cardiovascular risk factor that promotes the development and progression of atherosclerosis (Vita and Keane, 2002; Widmer and Lerman, 2014). Although the mechanisms of radiation-induced CVD are far from being understood, inflammatory processes seem to be involved. Following irradiation, upregulation of several pro-inflammatory molecules by endothelial cells has been observed. For example, the expression of ICAM1 and selectin P increased after irradiation in both *in vitro* and *in vivo* experiments (Gallo et al., 1997; Hallahan and Virudachalam, 1997a,b; Van Der Meer et al., 1999; Haubner et al., 2013). Furthermore, endothelial cells upregulate the secretion of several pro-inflammatory cytokines, such as IL6 and CCL2, after irradiation (Van Der Meer et al., 1999; Haubner et al., 2013).

In this study, we tried to find molecular evidence for the presence of an excess risk of CVD following exposure of endothelial cells to low single X-ray doses (0.05 and 0.1 Gy), a caveat in current radiobiological knowledge. Furthermore, we aimed to identify underlying biological and molecular mechanisms of radiation-induced CVD after exposure of endothelial cells to a single X-ray dose (0.05, 0.1, 0.5, 2 Gy). Compared to the existing knowledge, our study looks at longer time spans after radiation exposure combined with the use of human coronary artery endothelial cells. These endothelial cells are linked to coronary artery disease, observed after radiation exposure during radiotherapy in females with breast cancer (Darby et al., 2013). Endothelial cells were irradiated with a single X-ray dose (0.05, 0.1, 0.5, 2 Gy) and transcriptomic changes were

measured after various post-irradiation (repair) times (1 day, 7 days, 14 days). We report that a single X-ray dose induces dose- and time-dependent transcriptional changes associated with atherosclerosis-related processes in immortalized human coronary artery endothelial cells.

MATERIALS AND METHODS

Cells and Irradiation

Human telomerase-immortalized coronary artery endothelial (TICAE) cells (ECACC) were grown in Human MesoEndo Endothelial Cell Medium (Cell Applications) and cultured at 37°C with 5% CO₂ in a humidified incubator as described elsewhere (Lowe and Raj, 2014). Cells were irradiated at >95% confluence with a dose rate of 0.50 Gy/min, using an AGO HS320/250 X-ray cabinet (only for microarray samples; 250 kV, 13 mA, 1.5 mm Al, and 1.2 mm Cu) or an Xstrahl RX generator (for validation samples; 250 kV, 12 mA, 3.8 mm Al, and 1.4 mm Cu). Cells were not passaged during experiments, but medium was changed thrice per week.

Microarrays

Total RNA of TICAE cells was extracted according to manufacturer's instructions using the AllPrep DNA/RNA/protein mini kit (Qiagen). RNA was quantified using a NanoDrop Spectrophotometer and its quality assessed with an Agilent 2100 Bioanalyzer. Samples with a RNA integrity number >8 were used for hybridization onto Affymetrix Human Gene 2.0 ST arrays, following manufacturer's instructions. Raw data were uploaded to the Partek Genomics Suite (version 6.6) and normalized using a customized Robust Multi-chip Analysis algorithm (background correction for entire probe sequence, quantile normalization, log₂ transformation of intensity signals). Data are available in the ArrayExpress database (<http://www.ebi.ac.uk/arrayexpress>; accession number E-MTAB-5054).

Functional Enrichment Analysis

Functional gene enrichment was performed and visualized using GOrilla (Eden et al., 2007, 2009). Settings were: organism: *Homo sapiens*; running mode: two unranked lists of genes (target list: differentially expressed genes, background list: genes expressed above background in at least 33% of all samples); *P*-value threshold: 0.001. To exclude redundant gene ontology terms, results were reduced using REVIGO (Rudjer Boskovic Institute, Croatia) with an authorized similarity of 0.4 (Supek et al., 2011). Gene Ontology version used was go_201507-termdb.obo-xml.gz (<http://archive.geneontology.org/full/2015-07-01/>).

Transcription Factor Binding Site Enrichment Analysis

Chromatin immunoprecipitation (ChIP) enrichment analysis was performed with Enrichr (Icahn School of Medicine at Mount Sinai, USA) to identify transcription factors that were enriched for target genes within the list of differentially expressed genes (Chen et al., 2013; Kuleshov et al., 2016). Databases from all species, cell types and ChIP methods were interrogated.

Reverse Transcription Quantitative PCR (RT-qPCR)

RT-qPCR analysis was performed as previously described (Verreert et al., 2015) on a 7,500 Fast Real-Time PCR system (Applied Biosystems). Gene expression was normalized to reference genes *RAP2C* and *INPP1*. Gene expression ratios were calculated using the Pfaffl method (Pfaffl, 2001). Data were normalized to the values of the respective control samples at the same time point (either 1 day, 7 days, 14 days) and presented as the average expression ratio.

DNA Double Strand Break Repair Kinetics

To identify DNA double strand breaks (DSBs) and early DNA damage repair response, cells were stained for phosphorylated histone H2AX (γ H2AX) and tumor suppressor p53-binding protein 1 (TP53BP1). After irradiation, cells were fixed (2% PFA), permeabilized (0.25% Triton X-100 in PBS), blocked (1% normal goat serum [Thermo Fisher] in Tris-NaCl [Perkin Elmer]) and probed with primary anti- γ H2AX (1/300; Merck-Millipore #05-636) and anti-TP53BP1 (1/1,000; Novus Biologicals #NB100-304) antibodies (1 h, 37°C). After washing, cells were incubated with 1 μ g/ml DAPI and secondary Alexa Fluor 488 and 568 (Life technologies) antibodies (1 h, 37°C). Cells on slides were visualized with an Eclipse Ti microscope (NIKON) equipped with a 40 \times Plan Fluor objective (NA 0.6) and an Andor Ixon EMCCD camera. Twelve fields (z-stack of 9 planes axially separated by 1 μ m) were captured per replicate with a lateral spacing of 500 μ m. Images were analyzed with Fiji software (Schindelin et al., 2012) using the Cellblocks toolbox (De Vos et al., 2010). In brief, software allowed to analyze each nucleus based on the DAPI signal using Gaussian filtering and region of interest identification. Within each nucleus, pixel size and intensity emitted from the Alexa 488 (γ H2AX) and Alexa 568 (TP53BP1) fluorochromes along with their overlap were analyzed, after which the foci number per nucleus was determined in a fully automatic manner using a predefined threshold algorithm combined with multi-scale Laplacian filtering. Settings used were triangle threshold algorithm with a Laplacian scale of 2 and a minimum foci size of 3 pixels. Six biological replicates were screened per condition, and a minimum of 200 nuclei were analyzed per replicate.

Cell Cycle

TICAE cells were treated with 10 μ M of BrdU for 1 h, followed by ethanol fixation for a minimum of 24 h. Cells were permeabilized and stained with rat anti-BrdU antibody (AbD Serotec, #OBT0030CX) and 10 μ g/ml 7-amino-actinomycin D (Sigma-Aldrich). Samples were run on a BD Accuri C6 flow cytometer, with a maximum flow speed of 300 events/s.

Senescence

To determine senescence-associated β -galactosidase activity, cells were lysed in M-PER reagent (ThermoFisher Scientific). Lysates were incubated at 37°C for 18 h in reaction buffer (1 mM MgCl₂, 2 mM chlorophenolred- β -D-galactopyranoside in 50 mM phosphate buffer, pH 6.0). Reaction was stopped by adding 1 M of Na₂CO₃, and absorbance was measured at 570 nm.

Multiplex Bead Array

C-C motif chemokine 2 (CCL2), interleukin 6 (IL6) and insulin-like growth factor binding protein 7 (IGFBP7) levels in cell culture supernatants were analyzed using a multiplex magnetic bead array (R&D systems). Assays were performed according to manufacturer's instructions. Samples were run on a Luminex 200 and analyzed with xPONENT 3.1 (Luminex Corporation).

Statistics

Data show means \pm SEM. Microarray data were filtered to exclude genes expressed below the background signal in at least 67% of all samples and analyzed using two-way ANOVA. Differentially expressed genes were identified as those with a fold change $>|1.5|$ and $P < 0.05$ after correction for multiple testing according to Benjamini and Hochberg (Benjamini and Hochberg, 1995). Other data were analyzed using two-way ANOVA with Bonferroni *post-hoc* test. $P < 0.05$ was considered statistically significant.

RESULTS

Irradiation with 0.5 and 2 Gy Alters Gene Expression in Endothelial Cells

Amongst other cardiovascular effects, radiation exposure has been shown to accelerate age-related atherosclerosis leading to coronary artery disease (Darby et al., 2013). Since endothelial cell dysfunction is a well-established risk factor of atherosclerosis (Vita and Keane, 2002; Widmer and Lerman, 2014), we tested whether irradiation of endothelial cells with a single X-ray dose (0.05, 0.1, 0.5, 2 Gy) measured after various post-irradiation (repair) times (1 day, 7 days, 14 days) could activate pro-atherosclerotic processes *in vitro*. We observed dose- and time-dependent changes in gene expression using a genome-wide gene expression analysis. Differentially expressed genes are listed in Supplementary Tables 1–3, and their number is shown in Table 1. Single X-ray doses of 0.05 and 0.1 Gy did not affect gene expression at any of the investigated time points. In contrast, a single X-ray dose of either 0.5 or 2 Gy induced marked and comparable (Supplementary Figure 1) differences in gene expression detected on day 1 post-irradiation. While the response was essentially transient at 0.5 Gy, a large number of genes were still differentially expressed in TICAE cells 7 and 14 days after irradiation with a single X-ray dose of 2 Gy.

TABLE 1 | Irradiation with a single dose of X-rays induces differential gene expression in TICAE cells.*

	1 day	7 days	14 days
0.05 Gy	0	0	1 (–1)
0.1 Gy	0	0	1 (–1)
0.5 Gy	162 (+22/–140)	2 (+1/–1)	4 (–4)
2 Gy	522 (+107/–415)	129 (+79/–50)	59 (+41/–18)

*TICAE cells were analyzed at the indicated time points after irradiation with a single dose of X-rays. Changes are shown compared to sham irradiation, as described in Materials and Methods ($n = 3$). Numbers between brackets indicate up (+) and/or down (–) regulated genes per condition.

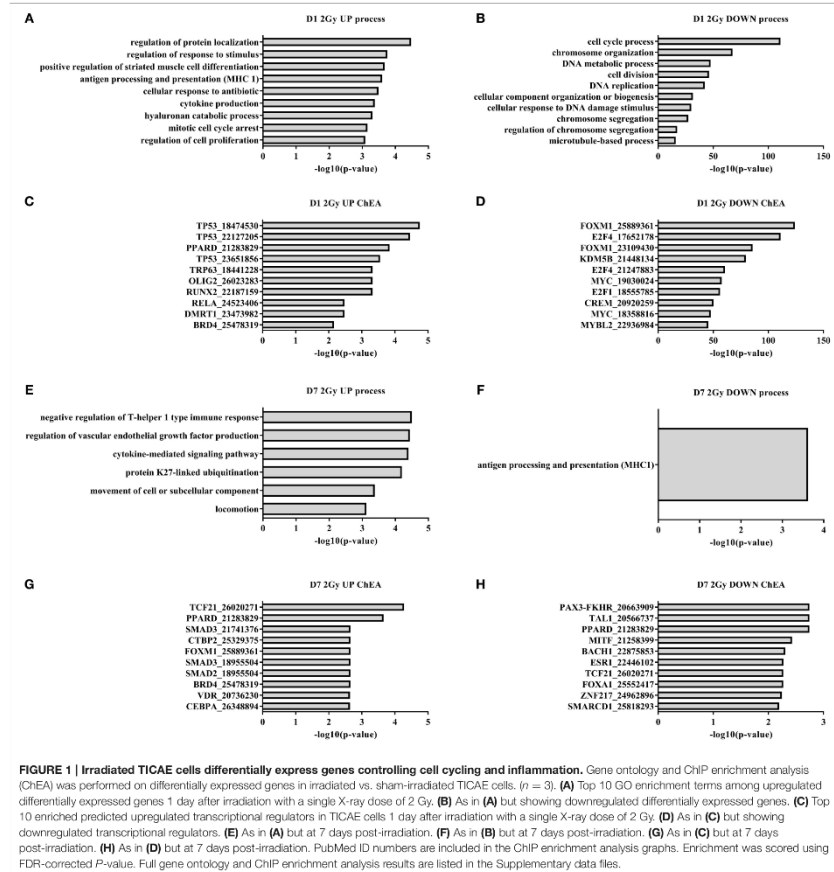
Irradiation of Endothelial Cells Represses the Expression of Genes Involved in Cell Cycling and Induces Inflammation

Functional enrichment analysis revealed that, 1 day after exposure to a single X-ray dose of 2 Gy, the upregulated differentially expressed genes were involved in cell cycle arrest and cytokine production and the downregulated ones in cell cycle-related processes such as mitotic cell cycle, chromosome organization and microtubule dynamics (Figures 1A,B). ChIP enrichment analysis was then used to identify transcription factors that control sets of differentially expressed genes. The identified transcription factors were shown to regulate cell cycle responses to DNA damage [such as p53 (Lane, 1992), Myc (Wasylishen and Penn, 2010), FOXM1 (Zona et al., 2014) and members of the E2F family (Bertoli et al., 2013)] and cytokine production (RELA and NF- κ B; Magné et al., 2006) (Figures 1C,D).

At day 7 and 14 after exposure to a single X-ray dose of 2 Gy, 129 and 59 genes were differentially expressed, respectively (Table 1). On day 7, gene ontology analysis highlighted inflammation-related processes, including induction of the negative regulation of T-helper 1 type immune response, cytokine-mediated signaling and suppression of MHC1 antigen processing and presentation (Figures 1E,F). ChIP enrichment analysis identified several inflammation-associated transcription factors (Figures 1E,G), among which PPAR δ , known to regulate multiple pro-inflammatory pathways (Barish et al., 2008), endothelial cell proliferation and angiogenesis (Piqueras et al., 2007) and SMAD2/3, involved in TGF β signaling (Derynck and Zhang, 2003). Furthermore, transcription factors vitamin D receptor, which promotes autophagy and cell survival pathways (Uberti et al., 2014), and BACH1, involved in oxidative stress response and cell-cycle progression (Wang et al., 2016a), were identified. Although not listed in the top 10, members of the E2F and p53 families of transcription factors were also identified (Supplementary data files), indicating a persistent cell cycle response. On day 14 following the exposure to a single X-ray dose of 2 Gy, no enrichment of transcription factors or gene ontology terms was identified.

Ionizing Radiation Causes a Dose-Dependent Repression of the Expression of Genes Controlling Mitotic Endothelial Cell Proliferation

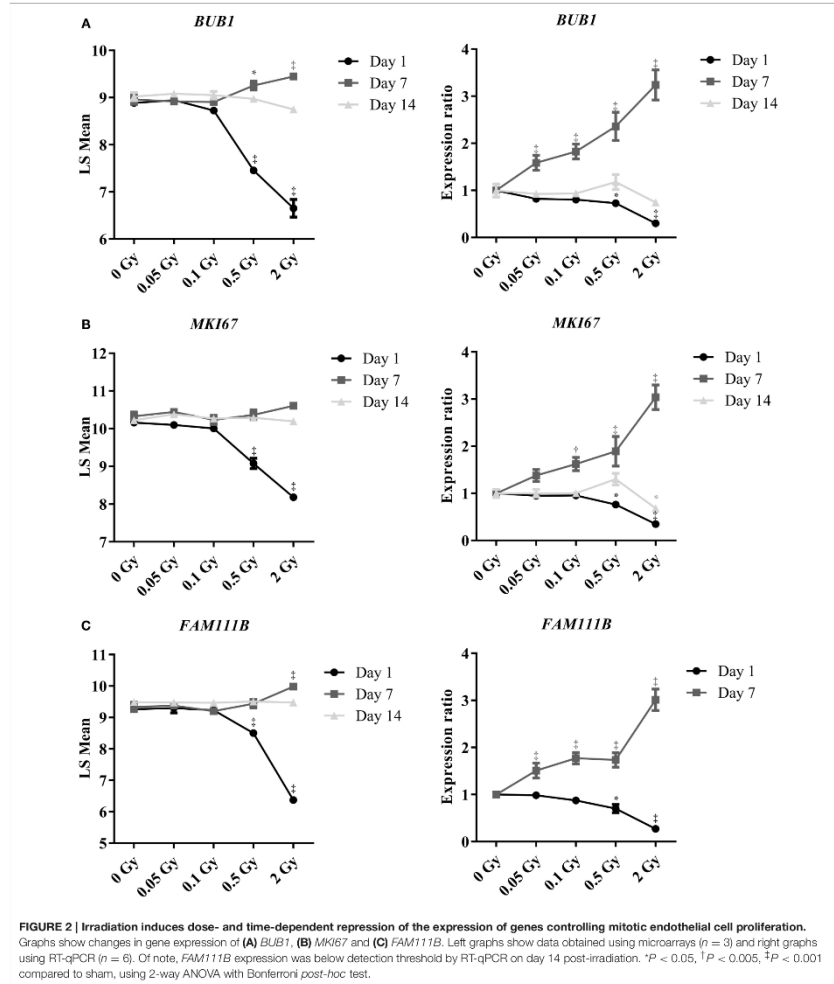
To confirm the effect of a single X-ray dose on the proliferation of endothelial cells, as observed in the microarray data, we performed RT-qPCR analysis on independent samples. *BUB1*, *FAM111B* and *MKI67* genes were selected for their involvement in mitotic cell cycle progression: *BUB1* is a mitotic checkpoint kinase (Bolanos-Garcia and Blundell, 2011), *MKI67* encodes proliferation marker Ki67 (Gerdes et al., 1983) and *FAM111B* has an unknown function but could be related to DNA replication (Aviner et al., 2015). Microarray and RT-qPCR data matched for *BUB1* (Figure 2A), *MKI67* (Figure 2B) and *FAM111B* (Figure 2C), with a significant decrease in gene



expression at a single X-ray dose of 0.5 or 2 Gy on day 1 post-irradiation, followed by a slight increase on day 7 and a return to basal expression on day 14. However, contrary to microarray results, RT-qPCR indicated a dose-dependent increase in the expression of all three genes at all irradiation doses on day 7 post-irradiation. This could be due to differences in the normalization technique used in the assays (Morey et al., 2006).

Radiation Exposure Activates DNA Damage Signaling, Induces an Acute G1 Arrest and Leads to Premature Senescence

To consolidate and mechanistically support the endothelial cell response to a single X-ray dose exposure identified during microarray analysis, we performed immunocytochemical

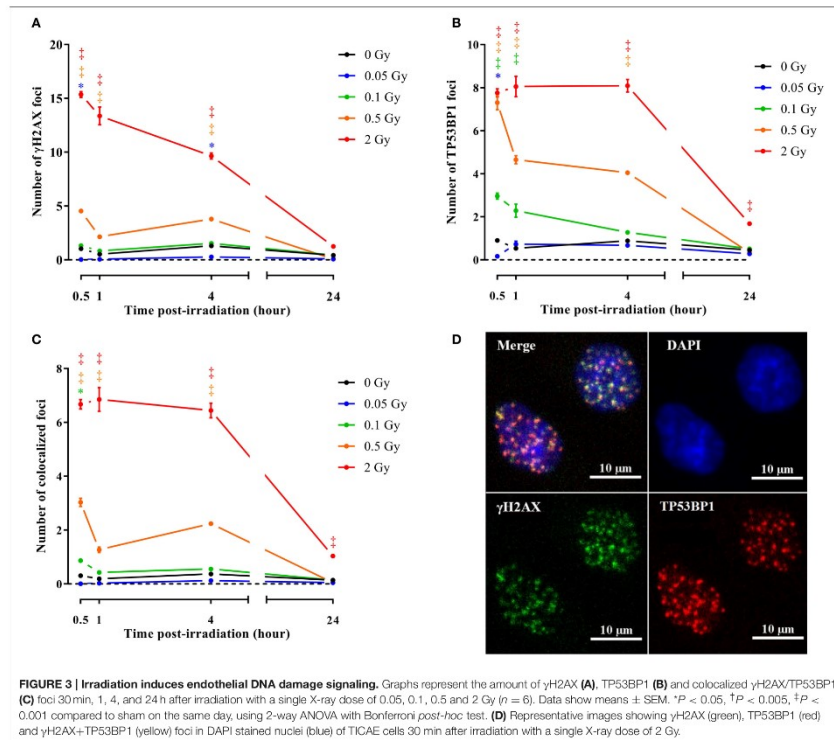


stainings for γ H2AX and TP53BP1, two markers of DNA DSB repair (Wang et al., 2014) that interact during DNA damage response and are linearly related to DSB number and radiation

dose (Wang et al., 2014; Kleiner et al., 2015). Irradiation with a single X-ray dose rapidly and dose-dependently increased the number of γ H2AX, TP53BP1 and colocalized γ H2AX+TP53BP1

foci (Figures 3A–D, Supplementary Figures 2–5). Foci numbers were maximal 30 min to 1 h after irradiation, followed by an almost complete decline at 24 h, except for 2 Gy where residual foci were probably indicative of lethal DNA damage (Banáth et al., 2010). To study the effect of a single X-ray dose on cellular proliferation, we performed a cell cycle analysis to study the cell cycle progression. On day 1 after irradiation, we detected a dose-dependent increase in the percentage of cells in G0/G1 and a decrease in the percentage of cells in S and G2/M phases, indicating that the cells arrested at the G1 checkpoint (Figure 4A). On day 7 post-irradiation, cells reached a state of contact inhibition and were mostly in G0/G1 in the sham condition. Irradiated cells displayed a cell cycle profile similar to that of control cells, except for the 2 Gy dose, where significantly more cells

were in S phase and less in G0/G1, indicating higher cellular proliferation. Increased proliferation was presumably due to the absence of contact inhibition resulting from cell death, as well as a longer and stronger G1 arrest induced at day 1. On day 14 post-irradiation, we detected no difference for sham-irradiated cells vs. cells irradiated with a single dose of 0.05, 0.1 and 0.5 Gy. Compared to sham, endothelial cells irradiated with a single X-ray dose of 2 Gy still had a disturbed cell cycle progression with more cells in G0/G1 and less in G2/M, which may be indicative of premature senescence. In accordance, all radiation doses increased senescence-associated β -galactosidase activity (Dimri et al., 1995; Figure 4B) and insulin-like growth factor-binding protein 7 (IGFBP7) secretion (Wajapeyee et al., 2008; Figure 4C) in TICAE cells on day 14 post-irradiation.



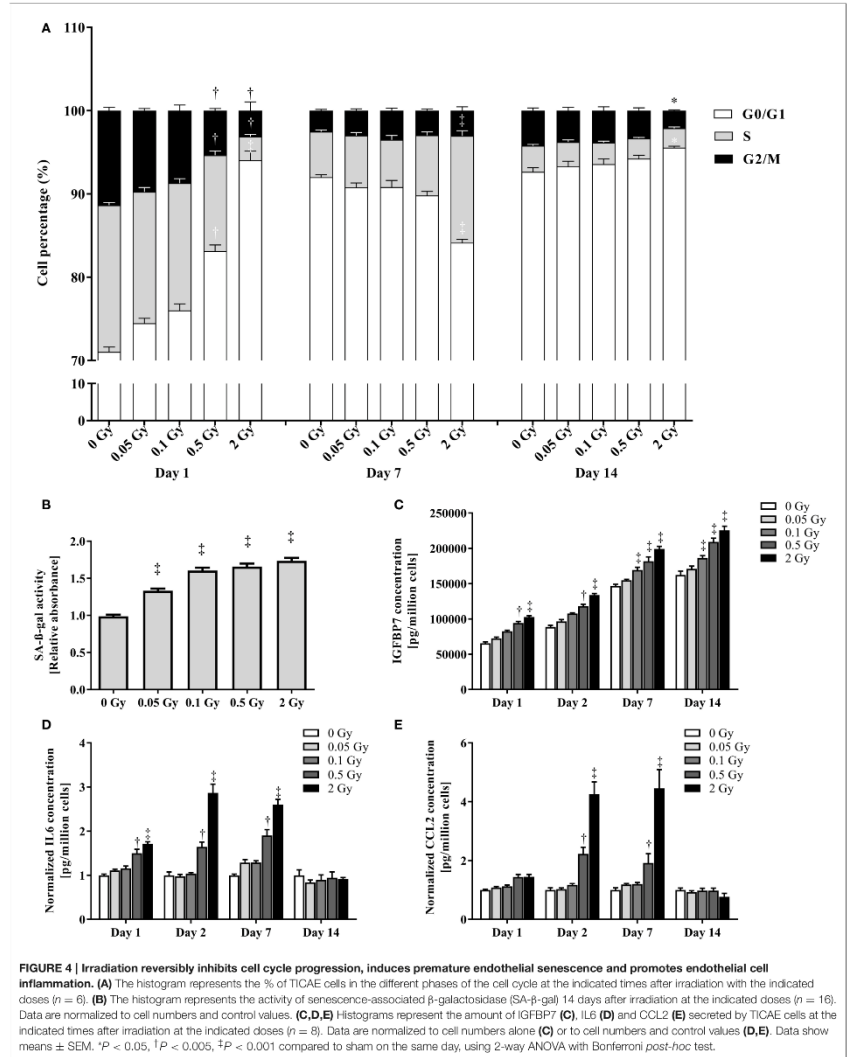


FIGURE 4 | Irradiation reversibly inhibits cell cycle progression, induces premature endothelial senescence and promotes endothelial cell inflammation. (A) The histogram represents the % of TICAE cells in the different phases of the cell cycle at the indicated times after irradiation with the indicated doses ($n = 6$). **(B)** The histogram represents the activity of senescence-associated β -galactosidase (SA- β -gal) 14 days after irradiation at the indicated doses ($n = 16$). Data are normalized to cell numbers and control values. **(C,D,E)** Histograms represent the amount of IGFBP7 **(C)**, IL6 **(D)** and CCL2 **(E)** secreted by TICAE cells at the indicated times after irradiation at the indicated doses ($n = 8$). Data are normalized to cell numbers alone **(C)** or to cell numbers and control values **(D,E)**. Data show means \pm SEM. * $P < 0.05$, † $P < 0.005$, ‡ $P < 0.001$ compared to sham on the same day, using 2-way ANOVA with Bonferroni post-hoc test.

Irradiation Induces IL6 and CCL2 Expression in Endothelial Cells

To confirm the induction of inflammation in irradiated TICAE cells, we focused on two pro-inflammatory cytokines involved in atherosclerosis: IL6 (Schuett et al., 2009) and CCL2 (Harrington, 2000). On days 1, 2 and 7 post-irradiation, IL6 secretion was significantly increased in endothelial cells irradiated with a single X-ray dose of 0.5 and 2 Gy (Figure 4D), while CCL2 secretion increased on days 2 and 7 post-irradiation following a single X-ray dose of 0.5 and 2 Gy (Figure 4E). Both pro-inflammatory cytokines returned to control levels after 14 days, thus indicating the presence of transient radiation-induced inflammation.

Altogether, gene expression, cell cycle and cytokine analysis unraveled an altered proliferation and an increased inflammatory state in endothelial cells at 1, 2, and 7 days after exposure to a single X-ray dose. At 14 days post-irradiation, cellular proliferation and inflammatory state reverted back to levels similar to those observed in non-irradiated (control) samples. However, at this time point the endothelial cells irradiated with a single X-ray dose, ranging from 0.05 to 2 Gy, demonstrated an increased senescence-associated- β -galactosidase activity and IGFBP7 secretion, indicative of premature senescence at all doses under investigation.

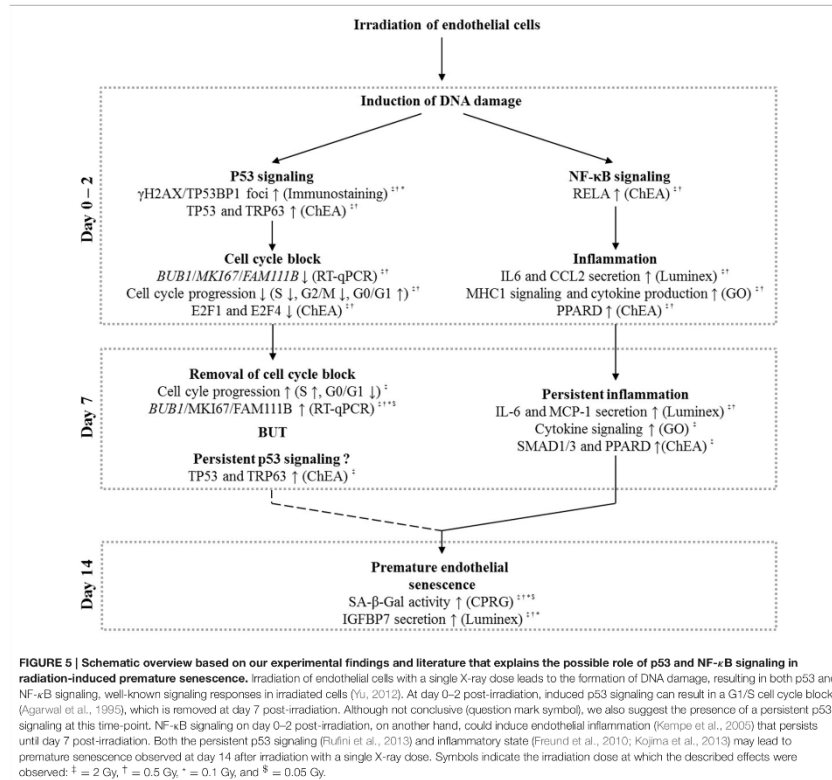
DISCUSSION

Our study aimed at investigating whether endothelial cell irradiation induced pro-atherosclerotic processes as suggested by epidemiological data (Shimizu et al., 2010; Darby et al., 2013). Furthermore, we aimed to determine whether low doses (0.05 and 0.1 Gy; doses received during serial diagnostics) of ionizing radiation could induce the same effects as those observed at higher doses (0.5 and 2 Gy; doses received on healthy tissues during radiotherapy) of ionizing radiation. We report dose- and time-dependent repression of endothelial cell cycling with an increased senescence-associated β -galactosidase activity and inflammatory cytokine secretion (Figure 5). These changes are indicative of a pro-atherosclerotic phenotype in endothelial cells.

A predominant effect of IR exposure is cell cycle arrest. Accordingly, in endothelial cells we showed that irradiation with a single X-ray dose ≥ 0.5 Gy represses the expression of genes that support cell cycle progression. We evidenced a G1 arrest 1 day after single dose irradiation with 0.5 and 2 Gy of X-rays. G1 arrest generally results from p53 activation in response to DNA damage (Bernhard et al., 1995), which was evidenced with enrichment analysis and the formation of γ H2AX and TP53BP1 foci. To determine the complexity of the DNA damage after exposure to ionizing radiation, future studies should look at the colocalization between DSB and non-DSB damage (Nikitaki et al., 2016). G1 arrest was followed by a progressive restoration of cell cycling for all doses, except for 2 Gy where cell cycling restoration was followed by an additional G1 arrest, which coincided with increased senescence-associated β -galactosidase activity and IGFBP7 secretion. Thus, exposure to a single X-ray dose induced markers linked to senescence, even at a dose as low as 0.05 Gy. Persistent p53 family signaling due to persistent DNA damage, as seen in our enrichment analysis at day 7, could be responsible

for premature senescence (Rufini et al., 2013). Our findings at low doses of X-rays are consistent with previous studies having evidenced premature senescence at higher doses in the same cell line (Lowe and Raj, 2014) and upon chronic exposure to low dose rates in different endothelial cells (Yentrapalli et al., 2013a,b; Rombouts et al., 2014). Senescent endothelial cells are shown to be present in human atherosclerotic plaques (Minamino et al., 2002) and are emerging as a contributor to the pathogenesis of atherosclerosis (Wang et al., 2016b). Therefore, premature senescence could play a role in radiation-induced CVD (Wang et al., 2016b), and research with cell cycle modulators as radioprotectors is warranted. However, there is no universal marker or hallmark of senescence identified so far that is entirely specific to the senescent state of a cell. Furthermore, not all senescent cells express all the possible senescence markers identified so far. As a consequence, future studies are needed to corroborate our *in vitro* findings in other *in vitro* as well as *in vivo* models. These studies should use highly sensitive techniques adapted to determine the presence of endothelial cell senescence even at low doses of ionizing radiation. One of such innovative and highly sensitive dyes is Sudan-Black-B, a specific lipofuscin stain that can be used to detect both replicative and stress-induced senescence independently of sample preparation (Evangelou et al., 2017).

Inflammation plays a pivotal role in the development, progression and final outcome of atherosclerosis (Libby, 2002). In this study, we evidenced radiation-induced inflammation in endothelial cells after exposure to a single X-ray dose of 0.5 and 2 Gy. Although the cause of this pro-inflammatory reaction is not entirely clear, the release of damage-associated molecular patterns (DAMPs) by stressed and apoptotic cells could be involved. One of the DAMPs released by apoptotic cells, called HMGB1, has been described to induce IL6 and CCL2 secretion as well as the expression of ICAM1 and VCAM1 in endothelial cells (Sun et al., 2013). Binding of these DAMPs to Toll-like receptors on endothelial cells upregulates pro-inflammatory signaling molecules such as NF- κ B (Fiuza et al., 2003). In accordance, transcriptional regulation by pro-inflammatory factors RELA and PPAR δ , negative regulation of the T-helper 1 type immune response, suppression of MHC1 antigen processing and presentation, and cytokine-mediated signaling were detected with enrichment analyses. Inflamed endothelial cells initiate the formation of atherosclerotic plaques by attracting leukocytes and enabling their extravasation and migration (Libby, 2002). After activation, leukocytes form a dynamic and multilateral relationship with the vascular wall cells, ultimately driving and determining the course of the disease (Libby, 2002). Accordingly, we detected increased levels of pro-atherosclerotic and pro-inflammatory cytokines IL6 and CCL2 in endothelial cells after irradiation with a single X-ray dose of 0.5 and 2 Gy. IL6 contributes to plaque initiation and destabilization via a variety of mechanisms that include the release of other pro-inflammatory cytokines, prothrombotic mediators, acute phase reactants and lipoprotein oxidation (Schuett et al., 2009). CCL2 recruits monocytes into the subendothelial cell layer, a key step in the initiation and development of plaques (Harrington, 2000). Similar to our data, other endothelial cell types were found to produce significant amounts of pro-inflammatory molecules



such as IL6, IL8, ICAM1 and VCAM1 following irradiation with a single X-ray dose of 2 Gy (Van Der Meeren et al., 1999; Haubner et al., 2013). However, these studies did not address long-term effects of radiation exposure. The significance of an inflammatory reaction in irradiated endothelial cells has yet to be determined as it could induce adverse effects on the vascular function (Hingorani et al., 2000; Paoletti et al., 2004). In this context, previous *in vivo* experiments indicated that irradiation predisposes ApoE^{-/-} obese mice to atherosclerotic plaques with an inflammatory phenotype prone to hemorrhage (Stewart et al., 2006). These prothrombotic changes may also accelerate atherosclerosis (Hoving et al., 2012). Interestingly, inflammation has also been identified as a cause of cellular senescence (Freund et al., 2010), and IL6 has been shown to induce senescence in

fibroblasts through IGFBP-related processes (Kojima et al., 2013). We found similar responses in endothelial cells.

The current study used telomerase-immortalized human coronary artery endothelial cells. These endothelial cells are not tumorigenic (unpublished data), were shown to have a similar response to IR compared to their primary counterparts (Lowe and Raj, 2014) and display all major endothelial phenotypic markers, such as von Willebrand factor, PECAM1 and cadherin-5 (unpublished data). However, one must stress that our *in vitro* study did not integrate several biological aspects related to the complexity of the development of radiation-induced CVD in humans. For example, not only macrovascular (e.g., coronary arteries) but also microvascular injury could be at the basis of radiation-induced CVD (Darby et al., 2010). In the context of

the ProCardio FP7 project, our findings will be integrated with other *in vitro*, *in vivo* and epidemiological data to increase our understanding of radiation-induced CVD.

In conclusion, we found that exposure of endothelial cells to a single X-ray dose induces a dose- and time-dependent cell cycle arrest, senescence and inflammation. These findings are indicative of the activation of pro-atherosclerotic processes and bring insights into the underlying molecular mechanisms of the endothelial response to X-ray irradiation. Although we cannot conclude that there is no threshold effect of irradiation-induced cardiovascular risk, our findings give an incentive for further research on the shape of the dose-response curve. Future research should also explore fractionated radiotherapy in its clinical mode and should further investigate the link between the possible release of DAMPs by irradiated endothelial cells and their response to radiation. Elucidation of the role of inflammation and premature senescence after radiation exposure, their timing and their involvement in the onset, progression and outcome of human atherosclerosis is now warranted in order to optimize the radiation protection system and to devise cardiovascular risk-reducing strategies if necessary. Optimization could be sought in the field of modern radiotherapy techniques, which reduce the dose to the normal tissues (MacDonald et al., 2013; Beck et al., 2014; Ngwa et al., 2014), and radiation protectants or mitigators that could reduce the deleterious effects of irradiation on the normal tissues (Raviraj et al., 2014).

AUTHOR CONTRIBUTIONS

BB performed microarray analysis (functional enrichment analysis and transcription factor binding site enrichment analysis), RT-qPCR experiments, cell cycle analysis, senescence assays and multiplex bead array analysis. Furthermore, he performed (statistical) analysis of all the data provided in this manuscript. NB helped BB during RT-qPCR experiments, DNA double strand break repair assays, cell cycle analysis and senescence assays. EC stained and quantified DNA double strand break repair kinetics. DL and KR created and validated the human coronary artery endothelial cell line. Microarrays were performed by AJ and AM. KT performed multiplex bead arrays.

REFERENCES

- Agarwal, M. L., Agarwal, A., Taylor, W. R., and Stark, G. R. (1995). p53 controls both the G2/M and the G1 cell cycle checkpoints and mediates reversible growth arrest in human fibroblasts. *Proc. Natl. Acad. Sci. U.S.A.* 92, 8493–8497. doi: 10.1073/pnas.92.18.8493
- Aviner, R., Shenoy, A., Flroy-Stein, O., and Geiger, T. (2015). Uncovering hidden layers of cell cycle regulation through integrative multi-omic analysis. *PLoS Genet.* 11:e1005554. doi: 10.1371/journal.pgen.1005554
- Banath, J. P., Klokoy, D., MacPhail, S. H., Banuelos, C. A., and Olive, P. L. (2010). Residual gammaH2AX foci as an indication of lethal DNA lesions. *BMC Cancer* 10:4. doi: 10.1186/1471-2407-10-4
- Barish, G. D., Atkins, A. R., Downes, M., Olson, P., Chong, L. W., Nelson, M., et al. (2008). PPARdelta regulates multiple proinflammatory pathways to suppress atherosclerosis. *Proc. Natl. Acad. Sci. U.S.A.* 105, 4271–4276. doi: 10.1073/pnas.0711875105
- Beck, R. E., Kim, L., Yue, N. J., Haffty, B. G., Khan, A. J., and Goyal, S. (2014). Treatment techniques to reduce cardiac irradiation for breast cancer patients

assisted during microarray analysis (functional enrichment analysis and transcription factor binding site enrichment analysis) and RT-qPCR primer design. BB, NB, EC, DL, KT, KR, RQ, MB, SB, PS, and AA helped with data interpretation, scientific guidance and preparation of the manuscript.

FUNDING

This work was funded by EU FP7 DoReMi network of excellence (grant #249689), EU FP7 project ProCardio (grant #295823), the Belgian Federal Agency for Nuclear Control FANC-AFCN (grant #CO-90-13-3289-00) and the Belgian Fonds National de la Recherche Scientifique (F.R.S.-FNRS). BB, NB, and EC are supported by a doctoral SCK•CEN grant. PS is a F.R.S.-FNRS Senior Research Associate. Funding sources had no role in study design, data collection analysis and interpretation, the writing and submission of the manuscript for publication.

ACKNOWLEDGMENTS

Authors thank Bart Marlein and Ludo Melis for their continued assistance during X-irradiation at SCK•CEN and Winnok de Vos for the Cellblocks toolbox used in FIJI.

SUPPLEMENTARY MATERIAL

The Supplementary Material for this article can be found online at: <http://journal.frontiersin.org/article/10.3389/fphar.2017.00213/full#supplementary-material>

Supplementary Data Sheet 1 | Irradiated TICAe cells differentially express genes controlling cell cycling and inflammation. ChIP enrichment analysis (ChEA) was performed on differentially expressed genes in irradiated versus sham-irradiated TICAe cells ($n = 3$). Full list of the enriched predicted upregulated and downregulated transcriptional regulators in TICAe cells at the indicated times after irradiation and at the indicated doses.

Supplementary Data Sheet 2 | Irradiated TICAe cells differentially express genes controlling cell cycling and inflammation. Gene ontology enrichment analysis was performed on differentially expressed genes in irradiated versus sham-irradiated TICAe cells ($n = 3$). Full list of the GO enrichment terms among upregulated and downregulated differentially expressed genes in TICAe cells at the indicated times after irradiation and at the indicated doses.

- treated with breast-conserving surgery and radiation therapy: a review. *Front. Oncol.* 4:327. doi: 10.3389/fonc.2014.00327
- Benjamini, Y., and Hochberg, Y. (1995). Controlling the false discovery rate - a practical and powerful approach to multiple testing. *J. R. Stat. Soc. Ser. B Methodol.* 57, 289–300.
- Bernhard, E. J., Maity, A., Muschel, R. J., and McKenna, W. G. (1995). Effects of ionizing radiation on cell cycle progression. *Rev. Radiat. Environ. Biophys.* 34, 79–83. doi: 10.1007/BF01275210
- Bertoli, C., Skotheim, J. M., and de Bruin, R. A. (2013). Control of cell cycle transcription during G1 and S phases. *Nat. Rev. Mol. Cell Biol.* 14, 518–528. doi: 10.1038/nrm3629
- Bhattacharya, S., and Asathambay, A. (2016). Ionizing radiation and heart risks. *Semin. Cell Dev. Biol.* 58, 14–25. doi: 10.1016/j.semcdb.2016.01.045
- Bolanos-Garcia, V. M., and Blundell, T. L. (2011). BUB1 and BUBR1: multifaceted kinases of the cell cycle. *Trends Biochem. Sci.* 36, 141–150. doi: 10.1016/j.tibs.2010.08.004
- Borghini, A., Gianicolo, E. A., Picano, E., and Andreassi, M. G. (2013). Ionizing radiation and atherosclerosis: current knowledge and future

- challenges. *Atherosclerosis* 230, 40–47. doi: 10.1016/j.atherosclerosis.2013.06.010
- Boring, L., Gosling, J., Cleary, M., and Charo, I. F. (1998). Decreased lesion formation in CCR2^{-/-} mice reveals a role for chemokines in the initiation of atherosclerosis. *Nature* 394, 894–897. doi: 10.1038/29788
- Chen, F. Y., Tan, C. M., Kou, Y., Duan, Q., Wang, Z., Meirelles, G. V., et al. (2013). Enrichr: interactive and collaborative HTML5 gene list enrichment analysis tool. *BMC Bioinformatics* 14:128. doi: 10.1186/1471-2105-14-128
- Collins, R. G., Velji, R., Guevara, N. V., Hicks, M. J., Chan, L., and Beaudet, A. L. (2000). P-Selectin or intercellular adhesion molecule (ICAM)-1 deficiency substantially protects against atherosclerosis in apolipoprotein E-deficient mice. *J. Exp. Med.* 191, 189–194. doi: 10.1084/jem.191.1.189
- Darby, S. C., Cutter, D. J., Boerma, M., Constone, L. S., Fajardo, L. F., Kodama, K., et al. (2010). Radiation-related heart disease: current knowledge and future prospects. *Int. J. Radiat. Oncol. Biol. Phys.* 76, 656–665. doi: 10.1016/j.ijrobp.2009.09.064
- Darby, S. C., Iwertz, M., McGale, P., Bennet, A. M., Blom-Goldman, U., Bronnum, D., et al. (2013). Risk of ischemic heart disease in women after radiotherapy for breast cancer. *N. Engl. J. Med.* 368, 987–998. doi: 10.1056/NEJMoa12.09825
- Derynck, R., and Zhang, Y. F. (2003). Smad-dependent and Smad-independent pathways in TGF-beta family signalling. *Nature* 425, 577–584. doi: 10.1038/nature02006
- De Vos, W. H., Van Neste, L., Dieriks, B., Joss, G. H., and Van Oostveldt, P. (2010). High content image cytometry in the context of subnuclear organization. *Cytometry A* 77, 64–75. doi: 10.1002/cyto.a.20807
- Dimri, G. P., Lee, X., Basile, G., Acosta, M., Scott, G., Roskelley, C., et al. (1995). A biomarker that identifies senescent human cells in culture and in aging skin in vivo. *Proc. Natl. Acad. Sci. U.S.A.* 92, 9363–9367. doi: 10.1073/pnas.92.20.9363
- Eden, E., Lipson, D., Yegor, S., and Yakhini, Z. (2007). Discovering motifs in ranked lists of DNA sequences. *PLoS Comput. Biol.* 3:e39. doi: 10.1371/journal.pcbi.0030039
- Eden, E., Navon, R., Steinfeld, L., Lipson, D., and Yakhini, Z. (2009). GOrilla: a tool for discovery and visualization of enriched GO terms in ranked gene lists. *BMC Bioinformatics* 10:48. doi: 10.1186/1471-2105-10-48
- Evangelou, K., Lougiakis, N., Rizou, S. V., Kotsinas, A., Kletsas, D., Muñoz-Espín, D., et al. (2017). Robust, universal biomarker assay to detect senescent cells in biological specimens. *Aging Cell* 16, 192–197. doi: 10.1111/acel.12545
- Fazel, R., Krumholz, H. M., Wang, Y., Ross, J. S., Chen, J., Ting, H. H., et al. (2009). Exposure to low-dose ionizing radiation from medical imaging procedures. *N. Engl. J. Med.* 361, 849–857. doi: 10.1056/NEJMoa0901249
- Fiuzza, C., Bustin, M., Talwar, S., Tropea, M., Gerstenberger, E., Shelhamer, J. L., et al. (2003). Inflammation-promoting activity of HMGB1 on human microvascular endothelial cells. *Blood* 101, 2652–2660. doi: 10.1182/blood-2002-05-1300
- Freund, A., Orjalo, A. V., Desprez, P. Y., and Campisi, J. (2010). Inflammatory networks during cellular senescence: causes and consequences. *Trends Mol. Med.* 16, 238–246. doi: 10.1016/j.molmed.2010.03.003
- Gallo, R. L., Dorschner, R. A., Takahama, S., Klagsbrun, M., Eriksson, E., and Bernfield, M. (1997). Endothelial cell surface alkaline phosphatase activity is induced by IL-6 released during wound repair. *J. Invest. Dermatol.* 109, 597–603. doi: 10.1111/1523-1747.ep12337529
- Georgakilas, A. G., Psalidas, A., Louka, M., Nikitaki, Z., Vouras, C. E., Bagos, P. G., et al. (2015). Emerging molecular networks common in ionizing radiation, immune and inflammatory responses by employing bioinformatics approaches. *Cancer Lett.* 368, 164–172. doi: 10.1016/j.canlet.2015.03.021
- Gerdes, J., Schwab, U., Lemke, H., and Stein, H. (1983). Production of a mouse monoclonal antibody reactive with a human nuclear antigen associated with cell proliferation. *Int. J. Cancer* 31, 13–20. doi: 10.1002/ijc.2910310104
- Gottfried, K. L., D., Penn, G., and U. S. Nuclear Regulatory Commission (1996). *Medical Use Program, and Institute of Medicine (U.S.). Committee for Review and Evaluation of the Medical Use Program of the Nuclear Regulatory Commission. Radiation in Medicine: a Need for Regulatory Reform.* Washington, DC: National Academy Press.
- Hallahan, D. E., and Virudachalam, S. (1997a). Intercellular adhesion molecule 1 knockout abrogates radiation induced pulmonary inflammation. *Proc. Natl. Acad. Sci. U.S.A.* 94, 6432–6437. doi: 10.1073/pnas.94.12.6432
- Hallahan, D. E., and Virudachalam, S. (1997b). Ionizing radiation mediates expression of cell adhesion molecules in distinct histological patterns within the lung. *Cancer Res.* 57, 2096–2099.
- Harrington, J. R. (2000). The role of MCP-1 in atherosclerosis. *Stem Cells* 18, 65–66. doi: 10.1634/stemcells.18-1-65
- Haubner, F., Leyh, M., Ohmann, E., Pohl, F., Pranti, L., and Gassner, H. G. (2013). Effects of external radiation in a co-culture model of endothelial cells and adipose-derived stem cells. *Radiat. Oncol.* 8:66. doi: 10.1186/1748-717X-8-66
- Hildebrandt, G. (2010). Non-cancer diseases and non-targeted effects. *Mutat. Res.* 687, 73–77. doi: 10.1016/j.mrfmmm.2010.01.007
- Hingorani, A. D., Cross, J., Kharbanda, R. K., Mullen, M. J., Bhagat, K., Taylor, M., et al. (2000). Acute systemic inflammation impairs endothelium-dependent dilatation in humans. *Circulation* 102, 994–999. doi: 10.1161/01.CIR.102.9.994
- Hirase, T., and Nade, K. (2012). Endothelial dysfunction as a cellular mechanism for vascular failure. *Am. J. Physiol. Heart Circ. Physiol.* 302, H499–H505. doi: 10.1152/ajpheart.00325.2011
- Hoving, S., Heeneman, S., Gijbels, M. J., Te Poele, J. A., Visser, N., Cleutjens, J., et al. (2012). Irradiation induces different inflammatory and thrombotic responses in carotid arteries of wildtype C57BL/6J and atherosclerosis-prone ApoE(-/-) mice. *Radiother. Oncol.* 105, 365–370. doi: 10.1016/j.radonc.2012.11.001
- Kemp, S., Kestler, H., Isar, A., and Wirth, T. (2005). NF-kappaB controls the global pro-inflammatory response in endothelial cells: evidence for the regulation of a pro-atherogenic program. *Nucleic Acids Res.* 33, 5308–5319. doi: 10.1093/nar/gki836
- Kleiner, R. E., Verma, P., Molloy, K. R., Chait, B. T., and Kapoor, T. M. (2015). Chemical proteomics reveals a gammaH2AX-53BP1 interaction in the DNA damage response. *Nat. Chem. Biol.* 11, 807–814. doi: 10.1038/nchembio.1908
- Kojima, H., Inoue, T., Kunimoto, H., and Nakajima, K. (2013). IL-6-STAT3 signaling and premature senescence. *JAKSTAT* 2:e25763. doi: 10.4161/jkst.25763
- Kuleshov, M. V., Jones, M. R., Rouillard, A. D., Fernandez, N. F., Duan, Q., Wang, Z., et al. (2016). Enrichr: a comprehensive gene set enrichment analysis web server 2016 update. *Nucleic Acids Res.* 44, W90–W97. doi: 10.1093/nar/gkw377
- Lane, D. P. (1992). Cancer, p53, guardian of the genome. *Nature* 358, 15–16. doi: 10.1038/358015a0
- Libby, P. (2002). Inflammation in atherosclerosis. *Nature* 420, 868–874. doi: 10.1038/nature01323
- Libby, P., Ridker, P. M., and Hansson, G. K. (2011). Progress and challenges in translating the biology of atherosclerosis. *Nature* 473, 317–325. doi: 10.1038/nature10146
- Little, M. P., Tawn, E. J., Tzoulaki, I., Wakeford, R., Hildebrandt, G., Paris, F., et al. (2008). A systematic review of epidemiological associations between low and moderate doses of ionizing radiation and late cardiovascular effects, and their possible mechanisms. *Radiat. Res.* 169, 99–109. doi: 10.1667/RR1070.1
- Lowe, D., and Raj, K. (2014). Premature aging induced by radiation exhibits pro-atherosclerotic effects mediated by epigenetic activation of CD44 expression. *Aging Cell* 13, 900–910. doi: 10.1111/acel.12253
- Lusis, A. J. (2000). Atherosclerosis. *Nature* 407, 233–241. doi: 10.1038/nar29.9.e45
- MacDonald, S. M., Jimenez, R., Paetzold, P., Adams, J., Beatty, J., DeLaney, T. F., et al. (2013). Proton radiotherapy for chest wall and regional lymphatic radiation: dose comparisons and treatment delivery. *Radiat. Oncol.* 8:71. doi: 10.1186/1748-717X-8-71
- Magné, N., Toulon, R. A., Bottero, V., Didelot, C., Houtte, P. V., Gerard, J. P., et al. (2006). NF-kappaB modulation and ionizing radiation: mechanisms and future directions for cancer treatment. *Cancer Lett.* 231, 158–168. doi: 10.1016/j.canlet.2005.01.022
- Minamino, T., Miyauchi, H., Yoshida, T., Ishida, Y., Yoshida, H., and Komuro, I. (2002). Endothelial cell senescence in human atherosclerosis: role of telomere in endothelial dysfunction. *Circulation* 105, 1541–1544. doi: 10.1161/01.CIR.0000013836.85741.17
- Morcy, J. S., Ryan, J. C., and Van Dolah, F. M. (2006). Microarray validation: factors influencing correlation between oligonucleotide microarrays and real-time PCR. *Biol. Proced. Online* 8, 175–193. doi: 10.1251/bpo126
- Nikitaki, Z., Nikolov, V., Mavragani, I. V., Mladenov, E., Mangelis, A., Laskaratou, D. A., et al. (2016). Measurement of complex DNA damage induction and repair in human cellular systems after exposure to ionizing radiations of varying linear energy transfer (LET). *Free Radic. Res.* 50(Suppl 1), S64–S78. doi: 10.1080/10715762.2016.1232484

- Ngwa, W., Kumar, R., Sridhar, S., Korideck, H., Zygmanski, P., Cormack, R. A., et al. (2014). Targeted radiotherapy with gold nanoparticles: current status and future perspectives. *Nanomedicine* 9, 1063–1082. doi: 10.2217/nmm.14.55
- Paoletti, R., Gotto, A. M. Jr., and Hajjar, D. P. (2004). Inflammation in atherosclerosis and implications for therapy. *Circulation* 109(23 Suppl. 1), II20–26. doi: 10.1161/01.cir.0000131514.71167.2e
- Pfaffl, M. W. (2001). A new mathematical model for relative quantification in real-time RT-PCR. *Nucleic Acids Res.* 29:45. doi: 10.1093/nar/29.9.e45
- Piqueras, L., Reynolds, A. R., Hodivala-Dilke, K. M., Alfranca, A., Redondo, J. M., Hatae, T., et al. (2007). Activation of PPARbeta/delta induces endothelial cell proliferation and angiogenesis. *Arterioscler. Thromb. Vasc. Biol.* 27, 63–69. doi: 10.1161/01.ATV.0000259972.83623.61
- Raviraj, J., Bokkasam, V. K., Kumar, V. S., Reddy, U. S., and Suman, V. (2014). Radiosensitizers, radioprotectors, and radiation mitigators. *Indian J. Dent. Res.* 25, 83–90. doi: 10.4103/0970-9290.131142
- Rombouts, C., Aerts, A., Quintens, R., Baselet, B., El-Saghire, H., Harms-Ringdahl, M., et al. (2014). Transcriptomic profiling suggests a role for ICBP5 in premature senescence of endothelial cells after chronic low dose rate irradiation. *Int. J. Radiat. Biol.* 90, 560–574. doi: 10.3109/09553002.2014.905724
- Rufini, A., Tucci, P., Celardo, I., and Melino, G. (2013). Senescence and aging: the critical roles of p53. *Oncogene* 32, 5129–5143. doi: 10.1038/onc.2012.640
- Schieffer, B., Selle, T., Hilfiker, A., Hilfiker-Kleiner, D., Grote, K., Tietge, U. J., et al. (2004). Impact of interleukin-6 on plaque development and morphology in experimental atherosclerosis. *Circulation* 110, 3493–3500. doi: 10.1161/01.CIR.0000148135.08582.97
- Schindelin, J., Arganda-Carreras, I., Frise, E., Kaynig, V., Longair, M., Pietzsch, T., et al. (2012). Fiji: an open-source platform for biological-image analysis. *Nat. Methods* 9, 676–682. doi: 10.1038/nmeth.2019
- Schuetz, H., Luchtefeld, M., Grothusen, C., Grote, K., and Schieffer, B. (2009). How much is too much? Interleukin-6 and its signalling in atherosclerosis. *Thromb. Haemost.* 102, 215–222. doi: 10.1160/th09-05-0297
- Shimizu, Y., Kodama, K., Nishi, N., Kasagi, F., Suyama, A., Soda, M., et al. (2010). Radiation exposure and circulatory disease risk: Hiroshima and Nagasaki atomic bomb survivor data, 1950–2003. *BMJ* 340:b5349. doi: 10.1136/bmj.b5349
- Stewart, F. A., Heeneman, S., Te Poele, J., Kruse, J., Russell, N. S., Gijbels, M., et al. (2006). Ionizing radiation accelerates the development of atherosclerotic lesions in ApoE^{-/-} mice and predisposes to an inflammatory plaque phenotype prone to hemorrhage. *Am. J. Pathol.* 168, 649–658. doi: 10.2353/ajpath.2006.050409
- Sun, W., Jiao, Y., Cui, B., Gao, X., Xia, Y., and Zhao, Y. (2013). Immune complexes activate human endothelium involving the cell-signaling HMGB1-RAGE axis in the pathogenesis of lupus vasculitis. *Lab. Invest.* 93, 626–638. doi: 10.1038/labinvest.2013.61
- Supek, F., Bošnjak, M., Skunca, N., and Šmuc, T. (2011). REVIGO summarizes and visualizes long lists of gene ontology terms. *PLoS ONE* 6:e21800. doi: 10.1371/journal.pone.0021800
- Uberti, F., Lattuada, D., Morsanuto, V., Nava, U., Bolis, G., Vacca, G., et al. (2014). Vitamin D protects human endothelial cells from oxidative stress through the autophagic and survival pathways. *J. Clin. Endocrinol. Metab.* 99, 1367–1374. doi: 10.1210/je.2013.2013
- UNSCEAR (2008). *Sources and Effects of Ionizing Radiation. Annex A: Medical Radiation Exposures.*
- Van Der Meeren, A., Squiban, C., Gourmelon, P., Lafont, H., and Gaugler, M. H. (1999). Differential regulation by IL-4 and IL-10 of radiation-induced IL-6 and IL-8 production and ICAM-1 expression by human endothelial cells. *Cytokine* 11, 831–838. doi: 10.1006/cyto.1999.0497
- Verreert, T., Quintens, R., Van Dam, D., Verslegers, M., Tanori, M., Casciati, A., et al. (2015). A multidisciplinary approach unravels early and persistent effects of X-ray exposure at the onset of prenatal neurogenesis. *J. Neurodev. Disord.* 7:3. doi: 10.1186/1866-1955-7-3
- Vita, J. A., and Keaney, J. F. Jr. (2002). Endothelial function: a barometer for cardiovascular risk? *Circulation* 106, 640–642. doi: 10.1161/01.CIR.0000028581.07992.56
- Wajapeyee, N., Serra, R. W., Zhu, X., Mahalingam, M., and Green, M. R. (2008). Oncogenic BRAF induces senescence and apoptosis through pathways mediated by the secreted protein IGFBP7. *Cell* 132, 363–374. doi: 10.1016/j.cell.2007.12.032
- Wang, H., Adhikari, S., Butler, B. F., Pandita, T. K., Mitra, S., and Hegde, M. L. (2014). A perspective on chromosomal double strand break markers in mammalian cells. *Jacobs J. Radiat. Oncol.* 1:003.
- Wang, X., Liu, J., Jiang, L., Wei, X., Niu, C., Wang, R., et al. (2016a). Bach1 Induces Endothelial Cell Apoptosis and Cell-Cycle Arrest through ROS Generation. *Oxid. Med. Cell. Longev.* 2016:6234043. doi: 10.1155/2016/6234043
- Wang, Y., Boerma, M., and Zhou, D. (2016b). Ionizing Radiation-Induced endothelial cell senescence and cardiovascular diseases. *Radiat. Res.* 186, 153–161. doi: 10.1667/RR14445.1
- Wasylshen, A. R., and Penn, L. Z. (2010). Myc: the beauty and the beast. *Genes Cancer* 1, 532–541. doi: 10.1177/1947601910378024
- Weber, C., and Noels, H. (2011). Atherosclerosis: current pathogenesis and therapeutic options. *Nat. Med.* 17, 1410–1422. doi: 10.1038/nm.2538
- Widmer, R. J., and Lerman, A. (2014). Endothelial dysfunction and cardiovascular disease. *Glob. Cardiol. Sci. Pract.* 2014, 291–308. doi: 10.5339/gcsp.2014.43
- Yentrapalli, R., Azimzadeh, O., Barjaktarovic, Z., Sarioglu, H., Wojcik, A., Harms-Ringdahl, M., et al. (2013a). Quantitative proteomic analysis reveals induction of premature senescence in human umbilical vein endothelial cells exposed to chronic low-dose rate gamma radiation. *Proteomics* 13, 1096–1107. doi: 10.1002/pmic.201200463
- Yentrapalli, R., Azimzadeh, O., Sriharshan, A., Malinowsky, K., Merl, J., Wojcik, A., et al. (2013b). The PI3K/Akt/mTOR pathway is implicated in the premature senescence of primary human endothelial cells exposed to chronic radiation. *PLoS ONE* 8:e70024. doi: 10.1371/journal.pone.0070024
- Yu, H. (2012). Typical cell signaling response to ionizing radiation: DNA damage and extranuclear damage. *Chin. J. Cancer Res.* 24, 83–89. doi: 10.1007/s11670-012-0083-1
- Zona, S., Bella, L., Burton, M. J., Nestal de Moraes, G., and Lam, E. W. (2014). FOXM1: an emerging master regulator of DNA damage response and genotoxic agent resistance. *Biochim. Biophys. Acta* 1839, 1316–1322. doi: 10.1016/j.bbagr.2014.09.016

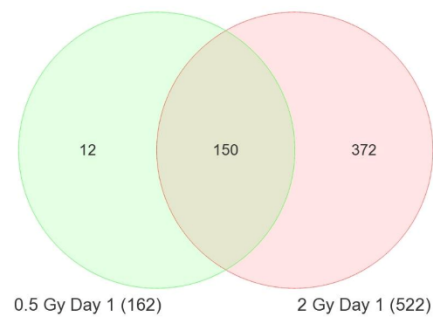
Conflict of Interest Statement: The authors declare that the research was conducted in the absence of any commercial or financial relationships that could be construed as a potential conflict of interest.

Copyright © 2017 Baselet, Belmans, Coninx, Lowe, Janssen, Michaux, Tabury, Raj, Quintens, Benotmane, Baatout, Sonveaux and Aerts. This is an open-access article distributed under the terms of the Creative Commons Attribution License (CC BY). The use, distribution or reproduction in other forums is permitted, provided the original author(s) or licensor are credited and that the original publication in this journal is cited, in accordance with accepted academic practice. No use, distribution or reproduction is permitted which does not comply with these terms.

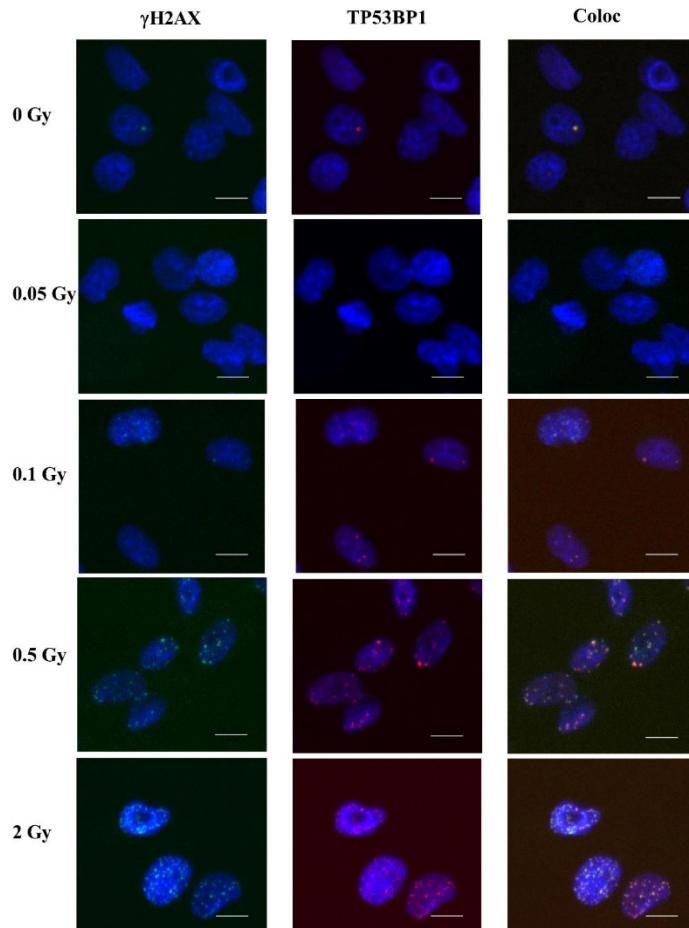
*Supplementary Material***Functional Gene Analysis Reveals Cell Cycle Changes and Inflammation in Endothelial Cells Irradiated with a Single X-ray Dose**

Bjorn Baselet^{1,2}, Niels Belmans^{1,3}, Emma Coninx¹, Donna Lowe⁴, Ann Janssen¹, Arlette Michaux¹, Kevin Tabury^{1,5}, Kenneth Raj⁴, Roel Quintens¹, Abderrafi Mohammed Benotmane^{1,5}, Sarah Baatout^{1,6,5}, Pierre Sonveaux^{2,5} An Aerts^{1,5,*}

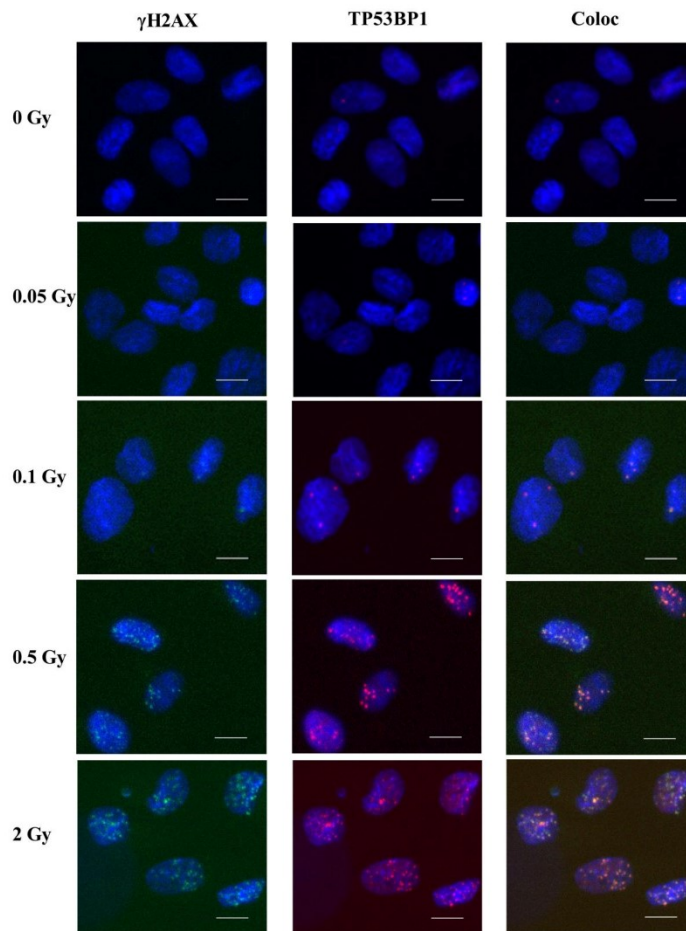
* Correspondence: An Aerts: an.aerts@sckcen.be

0.5 Gy Day 1 vs. 2 Gy Day 1

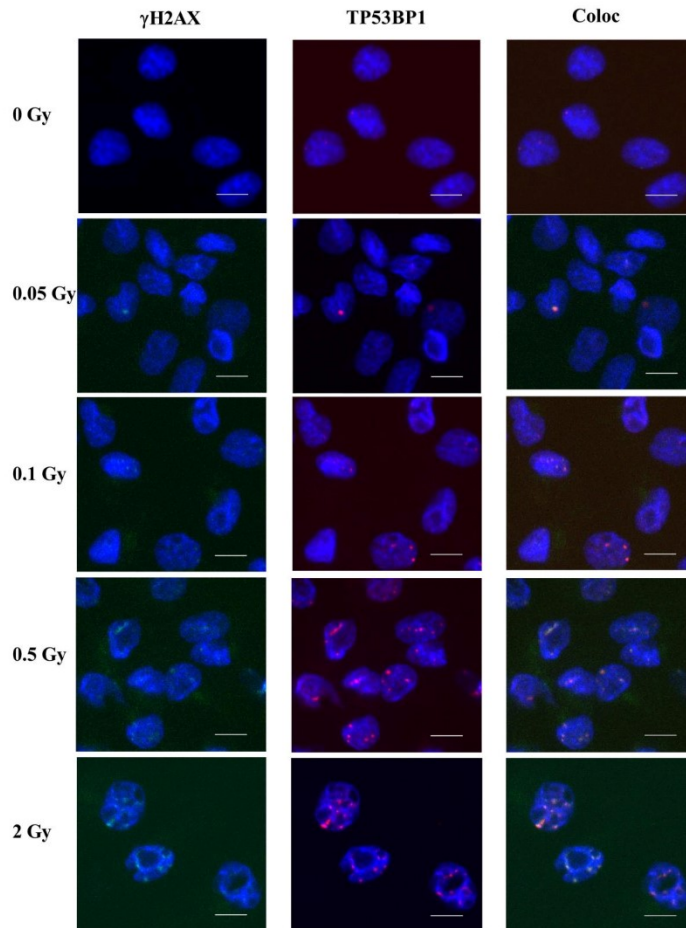
Supplementary Figure 1. Venn diagram showing the overlap after 1 day between the differentially expressed genes in TICAE cells irradiated with a single X-ray dose of 0.5 Gy and 2 Gy.



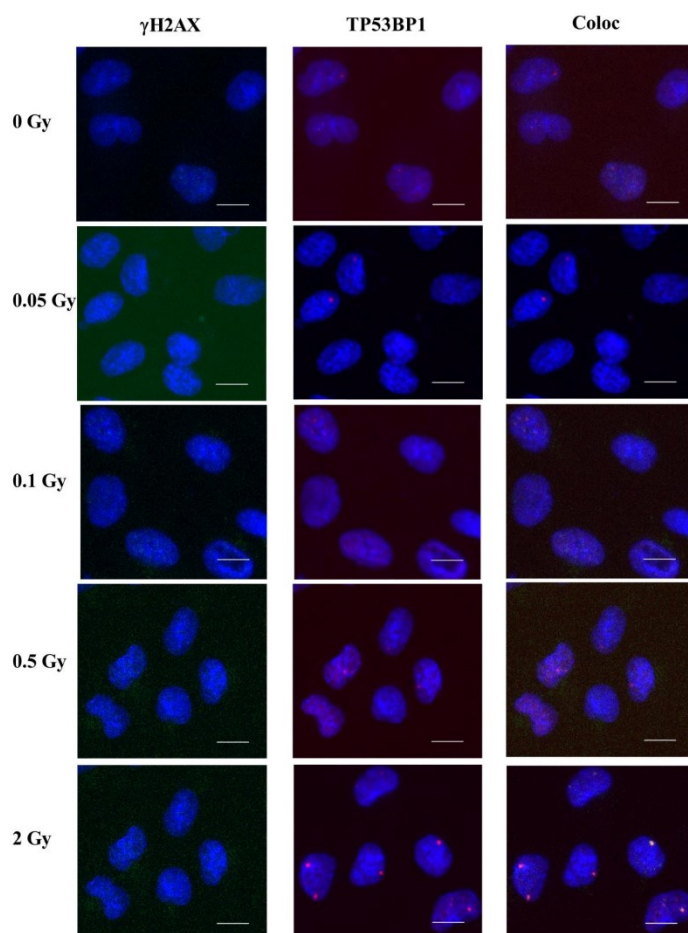
Supplementary Figure 2. Representative images showing γ H2AX (green), TP53BP1 (red) and γ H2AX+TP53BP1 (yellow) foci in DAPI stained nuclei (blue) of TICAE cells 30 minutes after irradiation with a single X-ray dose of either 0, 0.05, 0.1, 0.5 or 2 Gy. Scale bar, 10 μ m.



Supplementary Figure 3. Representative images showing γ H2AX (green), TP53BP1 (red) and γ H2AX+TP53BP1 (yellow) foci in DAPI stained nuclei (blue) of TICAE cells 1 hour after irradiation with a single X-ray dose of either 0, 0.05, 0.1, 0.5 or 2 Gy. Scale bar, 10 μ m



Supplementary Figure 4. Representative images showing γ H2AX (green), TP53BP1 (red) and γ H2AX+TP53BP1 (yellow) foci in DAPI stained nuclei (blue) of TICAE cells 4 hours after irradiation with a single X-ray dose of either 0, 0.05, 0.1, 0.5 or 2 Gy. Scale bar, 10 μ m.



Supplementary Figure 5. Representative images showing γ H2AX (green), TP53BP1 (red) and γ H2AX+TP53BP1 (yellow) foci in DAPI stained nuclei (blue) of TICAE cells 24 hours after irradiation with a single X-ray dose of either 0, 0.05, 0.1, 0.5 or 2 Gy. Scale bar, 10 μ m

Chapter 2

*Differential impact of single-dose Fe ion
and X-ray irradiation on endothelial cell
transcriptomic and proteomic responses*

1 **Differential impact of single-dose Fe ion and X-ray irradiation on**
2 **endothelial cell transcriptomic and proteomic responses**

3 **Bjorn Baselet^{1,2}, Omid Azimzadeh³, Nadine Erbeltinger^{4,5}, Mayur V Bakshi³, Till Dettmering⁴,**
4 **Ann Janssen¹, Svetlana Kitareva⁴, Donna Lowe⁶, Arlette Michaux¹, Kenneth Raj⁶, Marco**
5 **Durante^{4,5}, Claudia Fournier⁴, Mohammed A Benotmane¹, Sarah Baatout^{1,7}, Pierre Sonveaux²,**
6 **Soile Tapio³, An Aerts^{1,*}**

7 ¹Radiobiology Unit, Institute for Environment, Health and Safety, Belgian Nuclear Research Centre
8 (SCK•CEN), Mol, Belgium

9 ²Pole of Pharmacology and Therapeutics, Institut de Recherche Expérimentale et Clinique (IREC),
10 Université catholique de Louvain (UCL), Brussels, Belgium

11 ³Institute of Radiation Biology, Helmholtz Zentrum Munich, German Research Center for
12 Environmental Health, Neuherberg, Germany

13 ⁴GSI Helmholtz Centre for Heavy Ion Research, Darmstadt, Germany

14 ⁵Technical University Darmstadt, Darmstadt, Germany

15 ⁶Radiation Effects Department, Centre for Radiation, Chemical and Environmental Hazards, Public
16 Health England, Didcot, Oxfordshire, UK

17 ⁷Department of Molecular Biotechnology, Ghent University, Ghent, Belgium.

18 *** Correspondence:**

19 An Aerts
20 an.aerts@sckcen.be

21 **Keywords:** Irradiation, radiotherapy, X-rays, Fe ions, linear energy transfer, endothelial cells,
22 cardiovascular disease

23 **Abstract word count:** 311/350

24 **Word count:** 4,933/12,000

25 **#Figures:** 3

26 **#Tables:** 4

27

28

29

30

31

Radiation Quality Effect on Endothelial Cells

32 Abstract

33 *Background and Purpose.* Radiotherapy is an essential tool for cancer treatment. In order to spare
34 normal tissues and to reduce the risk of normal tissue complications, particle therapy is a method of
35 choice. Although a large part of healthy tissues can be spared due to improved depth dose
36 characteristics, little is known about the biological and molecular mechanisms altered after particle
37 irradiation in healthy tissues. Elucidation of these effects is also required in the context of long term
38 space flights, as particle radiation is the main contributor to the radiation effects observed in space.
39 Endothelial cells, forming the inner layer of all vascular structures, are especially sensitive to
40 irradiation and, if damaged, contribute to radiation-induced cardiovascular disease.

41 *Materials and Methods.* Transcriptomics, proteomics and cytokine analyses were used to compare the
42 response of endothelial cells irradiated or not with a single 2 Gy dose of X-rays or Fe ions measured
43 one and seven days post-irradiation. To support the observed inflammatory effects, monocyte adhesion
44 on endothelial cells was also assessed.

45 *Results.* Experimental data indicate time- and radiation quality-dependent changes of the endothelial
46 cell response to irradiation. The irradiation impact was more pronounced and longer lasting for Fe ions
47 than for X-rays. Both radiation qualities decreased the expression of genes involved in cell-cell
48 adhesion and enhanced the expression of proteins involved in caveolar mediated endocytosis signaling.
49 Endothelial inflammation and adhesiveness were increased with X-rays, but decreased after Fe ion
50 exposure.

51 *Conclusions.* Fe ions induce pro-atherosclerotic processes in endothelial cells that are different in
52 nature and kinetics than those induced by X-rays, highlighting radiation quality-dependent differences
53 which can be linked to the induction and progression of cardiovascular diseases. Our findings give a
54 better understanding of the underlying processes triggered by particle irradiation in endothelial cells, a
55 crucial aspect for the development of protective measures for cancer patients undergoing particle
56 therapy and for astronauts in space.

57

58

59

60

61

62

63

64

65

66

67

68 **1 Introduction**

69 The main goal of radiotherapy is to efficiently target and eradicate tumors while sparing surrounding
 70 healthy tissues (Bentzen, 2006; Barnett et al., 2009). One of the recent developments in radiotherapy
 71 modalities is high linear energy transfer (LET) particle therapy (Stone et al., 2003). In this technique,
 72 accelerated charged particle beams, such as proton and carbon ions, are used (Wilson, 1946), which
 73 have improved depth dose characteristics in comparison to low LET radiotherapy (Durante and
 74 Loeffler, 2010). In this way, tumors can be irradiated with great precision, minimizing the dose to
 75 surrounding healthy tissues. Besides their physical advantage, charged particle beams induce more
 76 damage per unit of dose, i.e., demonstrate a higher relative biological effectiveness (RBE) compared
 77 to conventional low LET X-ray radiotherapy (Kramer et al., 2003; Schulz-Ertner and Tsujii, 2007).
 78 Despite this advantage, particle therapy is not commonly used due to its complex and expensive nature.
 79 Consequently, particle therapy currently focuses on localized tumors in proximity to critical organs
 80 and tumors resistant to conventional treatments, such as uveal melanoma, pediatric tumors, head-and-
 81 neck cancer and prostate cancer (Schulz-Ertner and Tsujii, 2007; Durante and Loeffler, 2010). In the
 82 last ten years, however, there has been an exponential growth of new facilities (Jermann, 2015), a rapid
 83 increase in the number of patients treated (Jermann, 2015) and several new indications including lung
 84 cancer (Chang et al., 2016), breast cancer (Akamatsu et al., 2014) and pancreatic cancer (Nichols et
 85 al., 2015). Nonetheless, due to the limited number of patients treated with particle therapy at present,
 86 induction of normal tissue damage cannot be predicted correctly as molecular pathways and biological
 87 functions altered by high LET radiotherapy are still largely unknown (Schulz-Ertner and Tsujii, 2007;
 88 Durante and Loeffler, 2010; Newhauser and Durante, 2011). Identification and characterization of
 89 these processes is not only imperative for the development of protective measures for cancer patients
 90 undergoing high LET radiotherapy, but also for astronauts in space. Indeed, high LET particles are
 91 omnipresent in space as part of cosmic radiation. Among these particles, iron (Fe) ions are the major
 92 contributor to biological radiation effects due to their high LET value (Moreels et al., 2012; Fernandez-
 93 Gonzalo et al., 2017).

94 One of the known consequences of conventional low LET radiotherapy is an increased risk of
 95 cardiovascular diseases (CVD), especially when the heart is located within the radiation field (Darby
 96 et al., 2013; Aleman et al., 2014). For example, low LET radiation exposure during breast cancer
 97 therapy has been shown to accelerate atherosclerosis leading to CVD (Darby et al., 2013). CVD is an
 98 umbrella term for several types of disorders that affect the heart, such as cardiomyopathy and heart
 99 failure, or blood vessels, such as coronary artery disease (Kumar et al., 2013). Although many aspects
 100 of the mechanisms by which ionizing radiation (IR) causes CVD are still unknown, evidence indicates
 101 that it acts at least in part by inducing endothelial cell (EC) dysfunction leading to increased oxidative
 102 stress, inflammation, coagulation, senescence and EC death (Vita and Keaney, 2002; Corre et al., 2013;
 103 Rombouts et al., 2013; Yentrapalli et al., 2013a; Yentrapalli et al., 2013b; Rombouts et al., 2014;
 104 Widmer and Lerman, 2014; Azimzadeh et al., 2015; Baselet et al., 2017). These responses may
 105 eventually lead to the onset and/or progression of atherosclerosis, the leading cause of CVD (Schultz-
 106 Hector and Trott, 2007; Borghini et al., 2013). Compared to low LET, even less is known about the
 107 effects of high LET irradiation in the context of radiation-induced CVD. High LET irradiation was
 108 nevertheless found to be more damaging for ECs (Grabham et al., 2011; Helm et al., 2016) and to
 109 inhibit blood vessel formation differently than low LET irradiation (Grabham et al., 2013).
 110 Furthermore, atherogenesis was accelerated in obese apoE^{-/-} mice at both 13 and 40 weeks after
 111 exposure to 2 and 5 Gy Fe ions (Yu et al., 2011). In rats, 1 Gy of Fe ions has been shown to relaxation,
 112 increased reactive oxygen species levels and decreased nitric oxide production, indicating endothelial
 113 dysfunction, which was associated with increased aortic stiffness and impaired endothelial-dependent

Radiation Quality Effect on Endothelial Cells

114 (Soucy et al., 2011). Taking into account the increasing use of high LET radiation in cancer therapy
115 (Jermann, 2015), there is an obvious necessity to further study its possible cardiovascular effects.

116 In this study, we hypothesized that high LET exposure would induce more endothelial cell dysfunction
117 related processes in exposed ECs when compared to low LET exposure. Therefore, we aimed to
118 compare the transcriptomic, proteomic and pro-inflammatory response of endothelial cells irradiated
119 with either Fe ions or X-rays. We identified differences in signaling pathways and response
120 mechanisms influenced by low (X-ray) compared to high (Fe ion) LET radiation in telomerase-
121 immortalized human coronary artery ECs. ECs were irradiated or not with a single dose of 2 Gy and
122 changes were measured after 1 and 7 days. We conducted both transcriptomic and proteomic analyses,
123 which were complemented with pro-inflammatory cytokine quantification and monocyte adhesion
124 tests on irradiated ECs. We report time- and radiation quality-dependent changes in the EC response
125 after exposure to IR.

126 2 Materials and methods

127 2.1 Cells, reagents and irradiation

128 ECs from human coronary artery were purchased from European Cell Culture Collection (HCAECs
129 Cat. No: 300-05) and transduced with retroviruses bearing the est2 gene, a yeast homologue of the
130 human TERT protein. ECs were grown in Human MesoEndo Endothelial Cell Medium (Cat. No. 212-
131 500, Cell Applications) and cultured at 37°C with 5% CO₂ in a humidified incubator as described
132 previously (Lowe and Raj, 2014). Cell were counted (Beckman Coulter counter) and seeding was
133 carried out 2 days prior to irradiation with 40,000 cells/cm² in 0.4 ml medium/cm². This resulted in a
134 confluence of 90-100% at the time of irradiation visualized on a Leica DMI4000b microscope (Leica
135 Microsystems). ECs were exposed to 2 Gy of X-ray irradiation using an AGO HS320/250 X-ray
136 cabinet (250 kV, 13 mA, 1.5 mm Al, 1.2 mm Cu, 3 KeV/μm) or Fe ions (1 GeV/u, 155 keV/μm), both
137 with a dose rate of 1.5 Gy/min. Fe ion irradiation of EC monolayers was performed in the entrance
138 channel of the beam to mimic the effects on healthy tissues. 1 GeV Fe ions occurs in the plateau region
139 of the depth dose profile and has a penetration depth of 25 cm in water (Scholz, 2003; Lee et al.,
140 2011). Cells were not passaged during experiments to simulate normal, quiescent endothelium, but
141 medium was changed regularly to ensure viability (three times per week after X-ray and twice per week
142 after Fe ion irradiation).

143 2.2 Transcriptomic analysis

144 2.2.1 Microarray preparation, analysis and statistics

145 Total RNA of ECs was extracted according to manufacturer's instructions using the AllPrep
146 DNA/RNA/protein mini kit (Qiagen). RNA was quantified using a NanoDrop Spectrophotometer and
147 its quality assessed with an Agilent 2100 Bioanalyzer. Samples with a RNA integrity number > 8 were
148 used for hybridization onto Affymetrix Human Gene 2.0 ST arrays, following manufacturer's
149 instructions. Raw data were uploaded to the Partek Genomics Suite (version 6.6) and normalized using
150 a customized Robust Multi-chip Analysis algorithm (background correction for entire probe sequence,
151 quantile normalization, log₂ transformation of intensity signals). Microarray data were filtered to
152 exclude genes expressed below the background signal in at least 67% of all samples and analyzed using
153 three-way ANOVA. Differentially expressed genes were identified as those with a fold change > |1.2|
154 and p < 0.05 after correction for multiple testing according to Benjamini and Hochberg (Benjamini and
155 Hochberg, 1995). The data have been deposited in the ArrayExpress database
156 (<http://www.ebi.ac.uk/arrayexpress>; accession number E-MTAB-5754).

Radiation Quality Effect on Endothelial Cells

157 2.2.2 Functional enrichment analysis

158 Functional gene enrichment was performed and visualized using the GOrilla tool (Eden et al., 2007;
159 Eden et al., 2009). Settings were: organism: *Homo sapiens*; running mode: two unranked lists of genes
160 (target list: differentially expressed genes, background list: genes expressed above background in at
161 least 33% of all samples); p value < 0.001. To exclude redundant gene ontology terms, results were
162 reduced using REVIGO (Rudjer Boskovic Institute, Croatia) with an allowed similarity of 0.4 (Supek
163 et al., 2011). The version of Gene Ontology used was go_201507-termdb.obo-xml.gz
164 (<http://archive.geneontology.org/full/2015-07-01/>).

165 2.3 Proteomic analysis

166 2.3.1 Protein labeling

167 Protein labeling with isotope-coded protein labels (ICPL) was done as previously reported (Azimzadeh
168 et al., 2013). Briefly, triplicate aliquots of 25 µg of cell lysate proteins obtained from either sham or
169 irradiated ECs were labeled with ICPL reagents (SERVA) following manufacturer's instructions.
170 ICPL0 was used for sham-irradiated ECs and ICPL6 for irradiated cells. Labeling was done using three
171 biological replicates per condition. Heavy and light labeled samples were combined and separated by
172 12 % SDS gel electrophoresis before staining with colloidal Coomassie solution.

173 2.3.2 Protein analysis

174 After staining, SDS-PAGE lanes were cut into 5 slices and subjected to in-gel digestion with trypsin
175 (SERVA), as previously described (Merl et al., 2012). Digested peptides were separated by reversed
176 phase liquid chromatography (LC), and mass spectrometry (MS) analyses were done with a linear
177 quadrupole ion trap-Orbitrap (LTQ Orbitrap XL) mass spectrometer (ThermoFisher) equipped with a
178 nano-ESI source (Hauck et al., 2010). This method allowed for sequential isolation of up to ten most
179 intense ions, depending on signal intensity, for fragmentation on the linear ion trap using collision-
180 induced dissociation at a target value of 100,000 ions. High resolution MS scans in the Orbitrap and
181 MS/MS scans in the linear ion trap were performed in parallel. Target peptides already selected for
182 MS/MS were dynamically excluded for 30 s. Acquired MS/MS spectra were searched against the
183 Ensembl Human database using Mascot (Matrix Science, version 2.3.02; 20140909, Number of
184 sequences: 100607) with the following parameters: MS/MS spectra were searched with a precursor
185 mass tolerance of 10 ppm and a fragment tolerance of 0.8 Da; Arg-C was selected as enzyme. One
186 missed cleavage was allowed, and carbamidomethylation was set as a fixed modification. Oxidized
187 methionine and the heavy and light ICPL labeled lysines as well as heavy and light labels of proteins
188 were set as variable modifications.

189 2.3.3 Protein identification and quantification

190 Data processing for protein identification and quantification of ICPL pairs was performed using
191 Proteome Discoverer version 1.3 (Thermo Fisher). This software provides automated strict statistical
192 analysis of the protein quantification using unique peptides only. To minimize experimental bias, the
193 software was set to normalize on the protein median (minimum protein count: 20). Complete peptide
194 and protein profiles were filtered using high peptide confidence and top one peptide rank filters. False
195 discovery rate (FDR) was calculated at the peptide level for all experimental runs using the Decoy
196 option in Mascot; this rate was estimated to be lower than 1% using the identity threshold as the scoring
197 threshold system. Differentially labeled isotopic pairs were detected with a mass precision of 2 ppm
198 and a retention time window of 0.3 min. Proteins identified by at least two unique peptides in two out
199 of three replicates, with ratios of heavy / light (H/L) label greater than 1.50-fold or less than 0.66-fold
200 (t test, p<0.05) were defined as significantly differentially expressed. Raw MS data have been

5

Radiation Quality Effect on Endothelial Cells

201 deposited in the STORE^{DB} database (<http://www.storedb.org>; dataset identifier
202 DOI:10.20348/STOREDB/1086).

203 2.3.4 Protein-Protein Interaction and Signaling Networks

204 Analysis of possible protein-protein interactions and signaling networks was performed with the
205 INGENUITY Pathway Analysis (IPA) software tool (INGENUITY System,
206 <http://www.INGENUITY.com>). IPA is a knowledge database generated from peer-reviewed scientific
207 publications that enables to discover highly represented functions and pathways ($p < 0.001$) from large
208 quantitative data sets (Wu et al., 2007).

209 2.3.5 Western blotting

210 For the validation of proteomics data, 10 μg of cell protein extract was separated on 12% SDS
211 polyacrylamide gels according to Laemmli (Laemmli, 1970) before being transferred onto PVDF
212 membranes and labeled with primary antibodies against caveolin-1 (#3238, cell signalling) and α -
213 tubulin (#GTX72291, GeneTex). Secondary antibodies were horseradish peroxidase-conjugated anti-
214 rabbit and anti-mouse, respectively, and was detected using the ECL system (GE Healthcare). Signals
215 were quantified using ImageJ software and normalized to the α -tubulin expression.

216 2.4 Functional analyses

217 2.4.1 Cytokine release assays

218 The release of interleukin (IL)-6, IL-8 and C-C motif chemokine ligand 2 (CCL2) was determined with
219 enzyme-linked immunosorbent assays (ELISAs; eBioscience). Cell culture supernatant was collected
220 at the indicated time points after irradiation and frozen at -80°C . Medium was replaced 24 h before
221 each time point to ensure cell viability and consistency. ELISAs were performed according to
222 manufacturer's instructions. Measured cytokine concentrations were normalized to the cell number
223 (Beckman Coulter counter), as total protein content per cell was dependent on irradiation dose, and the
224 volume of supernatant at the time of collection, and calculated as fold change compared to control cells
225 at matched time points.

226 2.4.2 Monocyte adhesion assay

227 Monocyte adhesion on ECs was tested as previously described (Lowe and Raj, 2014; Lowe and Raj,
228 2015). In brief, ECs were seeded on fibronectin-coated glass coverslips and cultured until confluent.
229 Seven days after irradiation, 500,000 Cell Tracker-labeled HL-60 monocytes (ThermoFisher
230 Scientific) were added to the coverslip and incubated at 37°C . After 30 min, coverslips were washed
231 with HBSS, fixed in formalin and embedded in Vectashield Hard Set mounting medium with 4'-
232 diamidino-2-phenylindole (Vectorlabs H-1500). Monocytes adhering to ECs were microscopically
233 quantified.

234 2.4.3 Statistics

235 The data show means \pm SEM. Differences between sham and irradiated samples at different time-
236 points were determined by two-sided t-test (Welch-test). X-ray and Fe ion data are shown from three
237 and one independent experiments, respectively. For Fe ion experiments, data represent 2 biological
238 replicates with 2-3 technical replicates each. For X-ray experiments, data represent 9 biological
239 replicates with 3 technical replicates each. $P < 0.05$ was considered to be statistically significant.

240

241 **3 Results**242 **3.1 The transcriptional response of Fe ion-irradiated ECs is more pronounced and persistent**
243 **than the X-ray radiation response**

244 Little is known about the effects of high LET irradiation in the context of radiation-induced CVD. To
245 gain more knowledge on the molecular pathways affected high LET irradiation, we tested whether
246 irradiation of ECs with a single 2 Gy Fe ion dose induced different effects after 1 and 7 days in
247 comparison to a single 2 Gy X-ray dose. Using a genome-wide gene expression analysis, we observed
248 time- and radiation quality-dependent changes in gene expression. Differentially expressed genes (up
249 or down-regulated) using Fe ion or X-ray irradiation are listed in **Supplementary Data file 1**. The
250 number of deregulated genes and the shared deregulated genes between radiation qualities or time
251 points are shown in **figure 1**. A single X-ray dose of 2 Gy caused a profound effect on the gene
252 expression on day 1 (1042 genes), which significantly decreased on day 7 (455 genes) (**Figure 1A**).
253 Comparatively, Fe ions caused a smaller effect on gene expression at day 1 (977 genes), but this effect
254 increased in size at day 7 (1401 genes) and demonstrated a larger overlap between both time points
255 (**Figure 1B**). When comparing the samples irradiated with either X-rays or Fe ions, a lot of
256 differentially expressed genes were shared at day 1 (418 genes), which was lost for the most part at
257 day 7 (157 genes) (**Figures 1C and D**).

258 **3.2 Irradiation of ECs represses the expression of genes involved in cell cycling and cell-cell**
259 **adhesion**

260 Functional enrichment analysis revealed that, one day after exposure to a single X-ray dose of 2 Gy,
261 upregulated differentially expressed genes were involved in cell-cell adhesion, whereas downregulated
262 differentially expressed genes associated with in cell cycle-related processes such as DNA replication
263 and chromosome segregation (**Table 1, upper panel and Supplementary Data file 2**). On day 7 after
264 exposure to a single X-ray dose of 2 Gy, gene ontology analysis highlighted the acute nature of the
265 induced transcriptional changes. Upregulated differentially expressed genes were involved in cell
266 cycle-related processes (top 10 upregulated: *CCNA1*, *UBE2S*, *CDC6*, *MAD2L1*, *QRC1*, *AURKA*,
267 *MCMA4*, *CKS2*, *SPAG5* and *CDC48*; **Figure 2**), whereas downregulated differentially expressed genes
268 played a role in cell-cell adhesion (top 10 downregulated: *VWF*, *SNED1*, *ITGA10*, *ICAMI*, *FAT4*,
269 *LAMA2*, *PCDHB14*, *HAPLN3*, *FBLN5* and *BCAM*; **Figure 3**) (**Table 1, lower panel**). The
270 transcriptional response to low LET irradiation was then compared to that of a same 2 Gy dose of high
271 LET IR. On day 1, Fe ion-exposed ECs upregulated the expression of genes involved in cell cycle
272 arrest, such as genes related to p53 signal DNA damage signal transduction, which was associated to
273 a downregulation of genes involved in cell cycle-related processes, such as DNA replication and
274 chromosome segregation (**Table 2, upper panel**). Fe ions also upregulated the expression of genes
275 controlling apoptosis at day 1 post-irradiation (top 10 upregulated: *MIR21*, *YBX3*, *MDM2*, *MIR222*,
276 *ACER2*, *TP53INP1*, *ZMAT3*, *BTG2*, *GDF5* and *PHLDA3*; **Figure 4**). Seven days after exposure to a
277 single 2 Gy dose of Fe ions, ECs demonstrated a downregulation of gene expression involved in cell
278 cycle-related processes, indicating a persistent cell cycle response (**Table 2, lower panel**). As opposed
279 to day 1, downregulation of the expression of genes involved in cell death regulation and cell-cell
280 adhesion was observed.

281 **3.3 Fe ion-irradiated ECs have more differentially expressed proteins in comparison to X-**
282 **rays, indicating a pronounced and persistent radiation response in comparison**

283 To determine if the proteomic effects in ECs are dependent on radiation quality, proteins derived from
284 ECs irradiated with either a single 2 Gy Fe ion dose or a single 2 Gy X-ray dose were studied at 1 and

Radiation Quality Effect on Endothelial Cells

285 7 days after radiation exposure using a global proteomics analysis. The list of differentially expressed
286 proteins is displayed in **Supplementary Data File 3**. The numbers of deregulated proteins using the
287 two radiation qualities and time points are shown in **Figure 5**. While there was virtually no change in
288 the number of differentially expressed proteins (up and down-regulated) between day 1 (70) and day 7
289 (74) after exposure to X-rays (**Figure 5A**), the number of differentially expressed proteins induced by
290 Fe ion exposure almost doubled between day 1 and 7 (**Figure 5B**). In addition, compared to X-rays,
291 Fe ions induced more differentially expressed proteins at day 1 (**Figure 5C**) and at day 7 post-
292 irradiation (**Figure 5D**). The number of shared proteins between the two types of exposure was small,
293 indicating a different protein fingerprint with the two radiation qualities in question.

294 **3.4 Although with different kinetics, Fe ions and X-ray irradiation both induce protein** 295 **expression involved in caveolar mediated endocytosis signaling and cell-cell adhesion**

296 At one day after exposure to a single X-ray dose of 2 Gy, a detailed analysis of altered biological
297 pathways revealed that differentially expressed proteins played a role in caveolar mediated endocytosis
298 signaling (FLOT2, FLNC, PTPN1 and CAV1; **Figure 6**) and in cell-cell adhesion, including integrin
299 signaling (PFN1, ARF4, CAV1 and TLN1; **Figure 6**) and epithelial adherence junction signaling
300 (CDH2 and CTNBN1; **Figure 6**) (**Table 3, left panels** and **Supplementary Data File 4**). Fe ion
301 irradiation induced in general similar pathway changes, with differentially expressed proteins involved
302 in endocytosis signaling and cell-cell adhesion, but at a later time point (day 7) (**Table 3, right panels**).
303 While X-rays markedly deregulated proteins involved in endocytosis signaling at both days, Fe ions
304 only induced a marked effect at day 7 and merely a small but significant effect on day 1. Furthermore,
305 differentially expressed proteins involved in cell-cell adhesion were mostly observed at day 7 after X-
306 ray exposure, whereas they were mostly observed on day 1 following Fe ion exposure (**Table 3, right**
307 **panels**). In addition to analysis of altered pathways, differentially expressed proteins were classified
308 based on their molecular function (**Table 4** and **Supplementary Data File 5**). Proteomic alterations
309 covered a broad range of cellular events, including cell death and survival, cell cycle, cellular
310 movement and cell-cell signaling. In light of the bidirectional regulation of proteins, all the shown
311 pathways were derived from the entire proteomics data as no separation was performed between up-
312 and downregulated proteins. To better document alteration of caveolar-mediated endocytosis
313 signaling, we focused on caveolin-1, which is the main protein component of caveolae (Frank, 2010).
314 EC exposure to X-rays induced a persistent downregulation of caveolin 1 expression detected using
315 western blotting day 1 and day 7 (**Figure 7A** and **B**). Comparatively, Fe ions only upregulated of
316 caveolin 1 expression at day 7 after exposure, indicating a difference between both radiation types.

317 **3.5 X-ray and Fe ion exposure induces cytokine release and alters monocyte adhesion**

318 In order to study the functional effect of irradiation on inflammatory processes in ECs, we focused on
319 3 pro-inflammatory cytokines known to be involved in atherosclerosis: IL-6 (Schuett et al., 2009), IL-
320 8 (Boisvert et al., 1998) and CCL2 (Harrington, 2000). At 4 hours after X-ray exposure and on day 1
321 after exposure to either X-rays or Fe ions, there was no significant change in IL-6 and IL-8 levels
322 measured using ELISA (**Figure 8A-C**). However, secreted CCL2 levels on day 1 increased only after
323 exposure to X-rays. Seven days after exposure to a single dose of X-rays, ECs released more IL-6
324 (**Figure 8A**) and IL-8 (**Figure 8B**) but not CCL2 (**Figure 8C**) in comparison to control cells. In
325 contrast, Fe ions did not significantly alter the secretion of IL-6 (**Figure 8A**) or IL-8 (**Figure 8B**), and
326 CCL2 levels were below the detection threshold of ELISA assays (**Figure 4C**). When testing monocyte
327 adhesion on ECs as a functional outcome of EC inflammation, X-rays were found to induce whilst Fe
328 ions reduced monocyte adhesion on irradiated ECs 7 days post-irradiation (**Figure 8D**). Furthermore,

Radiation Quality Effect on Endothelial Cells

329 irradiation with both X-rays and Fe ions significantly reduced the number of ECs 7 days after exposure
330 (Figure 8E).

331 4 Discussion

332 Our study aimed at investigating differences in signaling pathways and radiation response mechanisms
333 in ECs irradiated with a single 2 Gy dose of either X-rays or Fe ions. We report time- and radiation
334 type-dependent changes in the expression of genes and protein involved in cell cycle progression, cell-
335 cell adhesion and caveolar-mediated endocytosis signaling. Furthermore, we found that X-ray
336 irradiation induces EC release of pro-inflammatory cytokines IL-6 and IL-8 and increases monocyte
337 adhesiveness of ECs, whilst Fe ions were found not to significantly induce cytokine secretion and
338 reduced monocyte adhesiveness of ECs. These changes are indicative of a radiation quality-dependent
339 changes in ECs, which can be linked to atherosclerosis and underscores the importance of conducting
340 future research to better understand processes altered in healthy tissues exposed to high LET radiation.

341 It is generally accepted that high LET radiation (e.g. Fe ions) has a higher RBE in comparison to low
342 LET radiation (e.g. X-rays) (ICRP, 2007). In accordance, we found that the transcriptional and
343 proteomic impact of irradiation was more pronounced and longer lasting for Fe ions in comparison to
344 X-rays. At the gene expression level, both radiation qualities were shown to repress the expression of
345 genes involved in cell cycling on day 1, as previously demonstrated for X-rays using the same *in vitro*
346 model (Baselet et al., 2017). However, X-ray-irradiated ECs induced the expression of cell-cycle genes
347 on day 7, indicating a reactivation of the cell cycle process (Baselet et al., 2017). In contrast, Fe ion
348 irradiation persistently repressed the expression of genes associated with cell cycle regulation. A
349 permanent cell cycle arrest after high LET exposure has also been demonstrated by others (Fournier
350 and Taucher-Scholz, 2004; Suetens et al., 2016) and is believed to be a consequence of the complex,
351 clustered hard-to-repair DNA damage it induces (Hada and Georgakilas, 2008; Asaithamby and Chen,
352 2011).

353 The observed changes of transcriptional and proteomic signaling involved in adhesion pathways in
354 irradiated ECs may have two biological interpretations. Diminished EC adhesion signaling, as
355 observed on day 7 after irradiation with both X-rays and Fe ions, can be a result of angiogenic
356 activation, a process initiating vascular extension from preexisting blood vessels and maintained by
357 proliferating ECs (Folkman, 1971). Emerging evidence indicates that high LET inhibits (Takahashi et
358 al., 2003; Mao et al., 2010; Grabham et al., 2013) and low LET radiation promotes angiogenesis
359 (Sonveaux et al., 2003; Sofia Vala et al., 2010). However, angiogenic activation is less likely to have
360 occurred after X-ray and Fe ion irradiation in our model because cell numbers were decreased. Cell
361 number reduction in Fe ion-treated samples was accompanied by decreased transcriptional and
362 proteomic signaling linked to EC death and reduced proliferation, making angiogenic activation even
363 less likely. A more likely explanation would be compromised EC integrity, corroborated by the
364 observed decrease in EC number and adhesiveness in combination with signaling linked to increased
365 EC death and reduced proliferation. In line with this, nickel ion radiation of ECs *in vitro* was found to
366 induce the expression of genes involved in endothelial permeability and apoptosis (Beck et al., 2014).
367 Furthermore, Fe ions induced a decreased EC number *in vivo* twelve months after exposure to a single
368 2 Gy dose (Mao et al., 2010). Loss of EC integrity may induce a number of adverse effects, including
369 thrombus formation, and could predispose to the development of chronic pathologies such as
370 atherosclerosis leading to CVD (Widlansky et al., 2003; Deanfield et al., 2007; Munzel et al., 2008).

371 Another observation is the potential involvement of caveolar mediated endocytosis signaling in the EC
372 response to IR exposure. Indeed, caveolin-1 (cav-1) protein expression was decreased on days 1 and 7

Radiation Quality Effect on Endothelial Cells

373 after X-ray exposure, whereas Fe ion exposure increased cav-1 expression on day 7. During
374 endocytosis, plasma membrane invagination leads to the formation of intracellular carrier vesicles that
375 allow the engulfment of particles or fluids from the extracellular environment (de Duve, 1983).
376 Although this process is known to occur during oxidative stress in ECs (Sundqvist and Liu, 1993; Liu
377 and Sundqvist, 1995), less is known about caveolar mediated endocytosis during cellular responses to
378 IR. The principal component protein of caveolae, caveolin-1 (Cav-1), has been shown to play a role in
379 DNA damage repair (Zhu et al., 2010) and is therefore related to EC radiosensitivity (Klein et al.,
380 2015). In addition, Caveolin 1 expression has been shown to suppress cell-cycle progression (Hulit et
381 al., 2000) and inhibits angiogenesis (Liu et al., 1999; Morais et al., 2012) by mediating contact
382 inhibition (Galbiati et al., 1998) and by reducing endothelial nitric oxide synthase abundance and
383 activity (Sbaa et al., 2005). Consequently, an elevated endothelial expression of Cav-1 has been linked
384 to processes underlying the development and progression of atherosclerosis (Fernandez-Hernando et
385 al., 2010; Pavlides et al., 2014).

386 Inflammation plays a central role in the development, progression and final outcome of atherosclerosis
387 (Libby, 2002). In this study, we evidenced that a single 2 Gy X-ray dose induces inflammation in ECs
388 at day 7 after exposure, whereas 2 Gy Fe ions did not significantly induce inflammation. The pro-
389 inflammatory effect of X-ray exposure was previously evidenced in the same *in vitro* model (Baselet
390 et al., 2017). In accordance, others observed elevated IL-6 and IL-8 levels in 2-10 Gy X-ray-irradiated
391 EC cultures (Meeren et al., 1997), elevated IL-6 levels in EC cultures after chronic irradiation with a
392 total dose of 2 Gy (Ebrahimian et al., 2015) and elevated blood levels of IL-6 were detected in A-bomb
393 survivors (Hayashi et al., 2003). These changes were previously demonstrated to increase EC
394 adhesiveness to monocytes 1 day after exposure to X-ray doses higher than 5 Gy (Khaled et al., 2012).
395 In contrast, reduced EC adhesiveness to monocytes in response to high LET IR is more controversial,
396 since others have reported increased monocyte adherence to ECs 1 day after 2 and 5 Gy Fe ion exposure
397 (Kucik et al., 2010; Khaled, 2011). In these studies, ECs were pretreated with tumor necrosis factor α ,
398 known to induce EC adhesiveness to monocytes (Ikuta et al., 1991; Mackay et al., 1993), which may
399 have caused a bias. Nonetheless, these authors used a flow chamber system that provides an
400 environment with fluid shear stress resembling the *in vivo* blood vessel environment. In contrast to our
401 findings, high LET radiation exposure has been shown to increase the *in vitro* expression of adhesion
402 molecules (Kiyohara et al., 2011), which can lead to accelerated development and progression of
403 atherosclerosis in obese apoE^{-/-} mice (Yu et al., 2011). These conflicting results highlight the need for
404 further research with a particular focus on radiation dose and timing after exposure to univocally
405 determine the effects of high LET radiation on EC inflammation in the frame of CVD.

406 In this study, we determined the effects of radiation quality on human coronary artery ECs seeing their
407 importance in radiation-induced CVD (Vita and Keaney, 2002; Darby et al., 2013; Widmer and
408 Lerman, 2014). As the Fe ions in this study were accelerated to 1 GeV and had a penetration depth of
409 up to 25 cm in water (Scholz, 2003; Lee et al., 2011), they are able to reach endothelial linings in the
410 human body since tissue is generally considered to be similar to water. Although immortalized, these
411 cells retain a normal EC phenotype, including genome stability (unpublished data), normal cell cycle
412 regulation (Baselet et al., 2017), responsiveness to IR (Lowe and Raj, 2014) and the expression of all
413 major EC phenotypic markers (e.g., von Willebrand factor and cadherin-5; unpublished data). Due to
414 the large phenotypic heterogeneity between ECs derived from different vascular beds, care should be
415 taken before generalizing our findings (Aird, 2007a; b). Furthermore, our *in vitro* model is not adapted
416 to provide the entire complexity of the development of radiation-induced CVD in humans. Although
417 Fe ions are a form of high LET radiation that is more relevant for the space environment than medical
418 practice, they can provide valuable insights into the endothelial response to high LET exposure.

Radiation Quality Effect on Endothelial Cells

419 In conclusion, we found a time- and radiation quality dependent endothelial radiation response. In
420 general, the radiation impact was more pronounced and longer lasting for Fe ions than for X-rays.
421 Observed transcriptional and proteomic changes were involved in cell cycle regulation, cell death,
422 caveolar mediated endocytosis signaling and EC permeability. In contrast to Fe ions, X-rays were
423 found to induce EC inflammation and adhesiveness to monocytes. Besides the link with CVD
424 development and progression, these findings are indicative of a different molecular response induced
425 by the two types of irradiation. In the context of the ProCardio FP7 project, our findings will be
426 integrated with other *in vitro*, *in vivo* and epidemiological data to increase our understanding of
427 radiation-induced CVD. Although studies on the effect of high LET particles are scarce due to limited
428 access to the radiation facilities, future research should continue aiming at elucidating the underlying
429 molecular mechanisms induced by high LET radiation in ECs. Before exploring details of each
430 modified pathway, our findings should be confirmed with independent irradiated EC samples. Besides
431 the quality effect, emphasis should also be placed on the dose effect, as low and high dose irradiation
432 may have different outcomes. Furthermore, radiation doses of Fe ions and X-rays should be identified
433 with an equal relative biological effectiveness in order to compare cellular responses to the 2 radiation
434 types on the same scale of biological damage. A better understanding of the radiation-induced CVD
435 risk is necessary for the protection of radiotherapy patients but also astronauts in space.

436 **5 Acknowledgements**

437 Authors thank Stefanie Winkler for skillful technical assistance.

438 **6 Conflict of Interest**

439 The authors declare that the research was conducted in the absence of any commercial or financial
440 relationships that could be construed as a potential conflict of interest.

441 **7 Author contributions**

442 BB performed microarray analysis (functional enrichment analysis). Microarrays were performed by
443 AJ and AM. OA and MVB performed the proteomic analysis. NE, TD and SK quantified cytokines
444 and endothelial adhesiveness. DL and KR created and validated the human coronary artery endothelial
445 cell line. All authors helped with data interpretation, scientific guidance and preparation of the
446 manuscript.

447 **8 Funding**

448 This work was funded by EU FP7 DoReMi network of excellence (grant #249689), EU FP7 project
449 ProCardio (grant #295823), the Belgian Federal Agency for Nuclear Control FANC-AFCN (grant
450 #CO-90-13-3289-00) and the Belgian Fonds National de la Recherche Scientifique (F.R.S.-FNRS).
451 BB, NB and EC are supported by a doctoral SCK•CEN grant. PS is a F.R.S.-FNRS Senior Research
452 Associate. Funding sources had no role in study design, data collection analysis and interpretation, the
453 writing and submission of the manuscript for publication.

454

455

456

457 **9 References**

- 458 Aird, W.C. (2007a). Phenotypic heterogeneity of the endothelium: I. Structure, function, and
459 mechanisms. *Circ Res* 100(2), 158-173. 10.1161/01.RES.0000255691.76142.4a.
- 460 Aird, W.C. (2007b). Phenotypic heterogeneity of the endothelium: II. Representative vascular beds.
461 *Circ Res* 100(2), 174-190. 10.1161/01.RES.0000255690.03436.ae.
- 462 Akamatsu, H., Karasawa, K., Omatsu, T., Isobe, Y., Ogata, R., and Koba, Y. (2014). First experience
463 of carbon-ion radiotherapy for early breast cancer. *Jpn J Radiol* 32(5), 288-295.
464 10.1007/s11604-014-0300-6.
- 465 Aleman, B.M., Moser, E.C., Nuver, J., Suter, T.M., Maraldo, M.V., Specht, L., et al. (2014).
466 Cardiovascular disease after cancer therapy. *EJC Suppl* 12(1), 18-28.
467 10.1016/j.ejcsup.2014.03.002.
- 468 Asaithamby, A., and Chen, D.J. (2011). Mechanism of cluster DNA damage repair in response to
469 high-atomic number and energy particles radiation. *Mutat Res* 711(1-2), 87-99.
470 10.1016/j.mrfmmm.2010.11.002.
- 471 Azimzadeh, O., Sievert, W., Sarioglu, H., Merl-Pham, J., Yentrapalli, R., Bakshi, M.V., et al. (2015).
472 Integrative proteomics and targeted transcriptomics analyses in cardiac endothelial cells
473 unravel mechanisms of long-term radiation-induced vascular dysfunction. *J Proteome Res*
474 14(2), 1203-1219. 10.1021/pr501141b.
- 475 Azimzadeh, O., Sievert, W., Sarioglu, H., Yentrapalli, R., Barjaktarovic, Z., Sriharshan, A., et al.
476 (2013). PPAR alpha: a novel radiation target in locally exposed Mus musculus heart revealed
477 by quantitative proteomics. *J Proteome Res* 12(6), 2700-2714. 10.1021/pr400071g.
- 478 Barnett, G.C., West, C.M., Dunning, A.M., Elliott, R.M., Coles, C.E., Pharoah, P.D., et al. (2009).
479 Normal tissue reactions to radiotherapy: towards tailoring treatment dose by genotype. *Nat*
480 *Rev Cancer* 9(2), 134-142. 10.1038/nrc2587.
- 481 Baselet, B., Belmans, N., Coninx, E., Lowe, D., Janssen, A., Michaux, A., et al. (2017). Functional
482 Gene Analysis Reveals Cell Cycle Changes and Inflammation in Endothelial Cells Irradiated
483 with a Single X-ray Dose. *Frontiers in Pharmacology* 8(213). 10.3389/fphar.2017.00213.
- 484 Beck, M., Rombouts, C., Moreels, M., Aerts, A., Quintens, R., Tabury, K., et al. (2014). Modulation
485 of gene expression in endothelial cells in response to high LET nickel ion irradiation. *Int J*
486 *Mol Med* 34(4), 1124-1132. 10.3892/ijmm.2014.1893.
- 487 Benjamini, Y., and Hochberg, Y. (1995). Controlling the False Discovery Rate - a Practical and
488 Powerful Approach to Multiple Testing. *Journal of the Royal Statistical Society Series B-*
489 *Methodological* 57(1), 289-300.
- 490 Bentzen, S.M. (2006). Preventing or reducing late side effects of radiation therapy: radiobiology
491 meets molecular pathology. *Nat Rev Cancer* 6(9), 702-713. 10.1038/nrc1950.
- 492 Boisvert, W.A., Santiago, R., Curtiss, L.K., and Terkeltaub, R.A. (1998). A leukocyte homologue of
493 the IL-8 receptor CXCR-2 mediates the accumulation of macrophages in atherosclerotic
494 lesions of LDL receptor-deficient mice. *J Clin Invest* 101(2), 353-363. 10.1172/JCI11195.
- 495 Borghini, A., Gianicolo, E.A., Picano, E., and Andreassi, M.G. (2013). Ionizing radiation and
496 atherosclerosis: current knowledge and future challenges. *Atherosclerosis* 230(1), 40-47.
497 10.1016/j.atherosclerosis.2013.06.010.

Radiation Quality Effect on Endothelial Cells

- 498 Chang, J.Y., Jabbour, S.K., De Ruyscher, D., Schild, S.E., Simone, C.B., 2nd, Rengan, R., et al.
499 (2016). Consensus Statement on Proton Therapy in Early-Stage and Locally Advanced Non-
500 Small Cell Lung Cancer. *Int J Radiat Oncol Biol Phys* 95(1), 505-516.
501 10.1016/j.ijrobp.2016.01.036.
- 502 Corre, I., Guillonneau, M., and Paris, F. (2013). Membrane signaling induced by high doses of
503 ionizing radiation in the endothelial compartment. Relevance in radiation toxicity. *Int J Mol*
504 *Sci* 14(11), 22678-22696. 10.3390/ijms141122678.
- 505 Darby, S.C., Ewertz, M., McGale, P., Bennet, A.M., Blom-Goldman, U., Bronnum, D., et al. (2013).
506 Risk of ischemic heart disease in women after radiotherapy for breast cancer. *N Engl J Med*
507 368(11), 987-998. 10.1056/NEJMoa1209825.
- 508 de Duve, C. (1983). Lysosomes revisited. *Eur J Biochem* 137(3), 391-397.
- 509 Deanfield, J.E., Halcox, J.P., and Rabelink, T.J. (2007). Endothelial function and dysfunction: testing
510 and clinical relevance. *Circulation* 115(10), 1285-1295.
511 10.1161/CIRCULATIONAHA.106.652859.
- 512 Durante, M., and Loeffler, J.S. (2010). Charged particles in radiation oncology. *Nat Rev Clin Oncol*
513 7(1), 37-43. 10.1038/nrclinonc.2009.183.
- 514 Ebrahimian, T., Le Gallic, C., Stefani, J., Dublineau, I., Yentrapalli, R., Harms-Ringdahl, M., et al.
515 (2015). Chronic Gamma-Irradiation Induces a Dose-Rate-Dependent Pro-inflammatory
516 Response and Associated Loss of Function in Human Umbilical Vein Endothelial Cells.
517 *Radiat Res* 183(4), 447-454. 10.1667/RR13732.1.
- 518 Eden, E., Lipson, D., Yogev, S., and Yakhini, Z. (2007). Discovering motifs in ranked lists of DNA
519 sequences. *PLoS Comput Biol* 3(3), e39. 10.1371/journal.pcbi.0030039.
- 520 Eden, E., Navon, R., Steinfeld, I., Lipson, D., and Yakhini, Z. (2009). GOrilla: a tool for discovery
521 and visualization of enriched GO terms in ranked gene lists. *BMC Bioinformatics* 10, 48.
522 10.1186/1471-2105-10-48.
- 523 Fernandez-Gonzalo, R., Baatout, S., and Moreels, M. (2017). Impact of Particle Irradiation on the
524 Immune System: From the Clinic to Mars. *Front Immunol* 8, 177.
525 10.3389/fimmu.2017.00177.
- 526 Fernandez-Hernando, C., Yu, J., Davalos, A., Prendergast, J., and Sessa, W.C. (2010). Endothelial-
527 specific overexpression of caveolin-1 accelerates atherosclerosis in apolipoprotein E-deficient
528 mice. *Am J Pathol* 177(2), 998-1003. 10.2353/ajpath.2010.091287.
- 529 Folkman, J. (1971). Tumor angiogenesis: therapeutic implications. *N Engl J Med* 285(21), 1182-
530 1186. 10.1056/NEJM197111182852108.
- 531 Fournier, C., and Taucher-Scholz, G. (2004). Radiation induced cell cycle arrest: an overview of
532 specific effects following high-LET exposure. *Radiother Oncol* 73 Suppl 2, S119-122.
- 533 Frank, P.G. (2010). Endothelial caveolae and caveolin-1 as key regulators of atherosclerosis. *Am J*
534 *Pathol* 177(2), 544-546. 10.2353/ajpath.2010.100247.
- 535 Galbiati, F., Volonte, D., Engelman, J.A., Watanabe, G., Burk, R., Pestell, R.G., et al. (1998).
536 Targeted downregulation of caveolin-1 is sufficient to drive cell transformation and
537 hyperactivate the p42/44 MAP kinase cascade. *EMBO J* 17(22), 6633-6648.
538 10.1093/emboj/17.22.6633.

Radiation Quality Effect on Endothelial Cells

- 539 Grabham, P., Hu, B., Sharma, P., and Geard, C. (2011). Effects of ionizing radiation on three-
540 dimensional human vessel models: differential effects according to radiation quality and
541 cellular development. *Radiat Res* 175(1), 21-28. 10.1667/RR2289.1.
- 542 Grabham, P., Sharma, P., Bigelow, A., and Geard, C. (2013). Two distinct types of the inhibition of
543 vasculogenesis by different species of charged particles. *Vasc Cell* 5(1), 16. 10.1186/2045-
544 824X-5-16.
- 545 Hada, M., and Georgakilas, A.G. (2008). Formation of clustered DNA damage after high-LET
546 irradiation: a review. *J Radiat Res* 49(3), 203-210.
- 547 Harrington, J.R. (2000). The role of MCP-1 in atherosclerosis. *Stem Cells* 18(1), 65-66.
548 10.1634/stemcells.18-1-65.
- 549 Hauck, S.M., Dietter, J., Kramer, R.L., Hofmaier, F., Zipplies, J.K., Amann, B., et al. (2010).
550 Deciphering membrane-associated molecular processes in target tissue of autoimmune uveitis
551 by label-free quantitative mass spectrometry. *Mol Cell Proteomics* 9(10), 2292-2305.
552 10.1074/mcp.M110.001073.
- 553 Hayashi, T., Kusunoki, Y., Hakoda, M., Morishita, Y., Kubo, Y., Maki, M., et al. (2003). Radiation
554 dose-dependent increases in inflammatory response markers in A-bomb survivors. *Int J*
555 *Radiat Biol* 79(2), 129-136.
- 556 Helm, A., Lee, R., Durante, M., and Ritter, S. (2016). The Influence of C-Ions and X-rays on Human
557 Umbilical Vein Endothelial Cells. *Front Oncol* 6, 5. 10.3389/fonc.2016.00005.
- 558 Hulit, J., Bash, T., Fu, M., Galbiati, F., Albanese, C., Sage, D.R., et al. (2000). The cyclin D1 gene is
559 transcriptionally repressed by caveolin-1. *J Biol Chem* 275(28), 21203-21209.
560 10.1074/jbc.M000321200.
- 561 ICRP (2007). The 2007 Recommendations of the International Commission on Radiological
562 Protection. ICRP publication 103. *Ann ICRP* 37(2-4), 1-332. 10.1016/j.icrp.2007.10.003.
- 563 Ikuta, S., Kirby, J.A., Shenton, B.K., Givan, A.L., and Lennard, T.W. (1991). Human endothelial
564 cells: effect of TNF-alpha on peripheral blood mononuclear cell adhesion. *Immunology* 73(1),
565 71-76.
- 566 Jermann, M. (2015). Particle Therapy Statistics in 2014. *International Journal of Particle Therapy*
567 2(1), 50-54. 10.14338/ijpt-15-00013.
- 568 Khaled, S. (2011). *Low and high LET irradiation of human aortic endothelial cells induces dose and*
569 *time dependent adhesion of monocytes which is mediated by chemokines expressed by the*
570 *irradiated endothelium*. Doctor of Philosophy, The University of Alabama.
- 571 Khaled, S., Gupta, K.B., and Kucik, D.F. (2012). Ionizing radiation increases adhesiveness of human
572 aortic endothelial cells via a chemokine-dependent mechanism. *Radiat Res* 177(5), 594-601.
- 573 Kiyohara, H., Ishizaki, Y., Suzuki, Y., Katoh, H., Hamada, N., Ohno, T., et al. (2011). Radiation-
574 induced ICAM-1 expression via TGF-beta1 pathway on human umbilical vein endothelial
575 cells; comparison between X-ray and carbon-ion beam irradiation. *J Radiat Res* 52(3), 287-
576 292.
- 577 Klein, D., Schmitz, T., Verhelst, V., Panic, A., Schenck, M., Reis, H., et al. (2015). Endothelial
578 Caveolin-1 regulates the radiation response of epithelial prostate tumors. *Oncogenesis* 4,
579 e148. 10.1038/oncsis.2015.9.

Radiation Quality Effect on Endothelial Cells

- 580 Kramer, M., Weyrather, W.K., and Scholz, M. (2003). The increased biological effectiveness of
581 heavy charged particles: from radiobiology to treatment planning. *Technol Cancer Res Treat*
582 2(5), 427-436.
- 583 Kucik, D.F., Khaled, S., Gupta, K., Wu, X., Yu, T., and Chang, P.Y. (2010). X-ray, proton and iron
584 ion irradiation all increase adhesiveness of aortic endothelium and may accelerate
585 development of atherosclerosis. *The FASEB Journal* 24(1 Supplement), 1028.1011.
- 586 Kumar, V., Abbas, A.K., Aster, J.C., and Robbins, S.L. (2013). *Robbins basic pathology*.
587 Philadelphia, PA: Elsevier/Saunders.
- 588 Laemmli, U.K. (1970). Cleavage of structural proteins during the assembly of the head of
589 bacteriophage T4. *Nature* 227(259), 680-685.
- 590 Lee, R., Nasonova, E., Hartel, C., Durante, M., and Ritter, S. (2011). Chromosome aberration
591 measurements in mitotic and G2-PCC lymphocytes at the standard sampling time of 48 h
592 underestimate the effectiveness of high-LET particles. *Radiat Environ Biophys* 50(3), 371-
593 381. 10.1007/s00411-011-0360-2.
- 594 Libby, P. (2002). Inflammation in atherosclerosis. *Nature* 420(6917), 868-874. 10.1038/nature01323.
- 595 Liu, J., Razani, B., Tang, S., Terman, B.I., Ware, J.A., and Lisanti, M.P. (1999). Angiogenesis
596 activators and inhibitors differentially regulate caveolin-1 expression and caveolae formation
597 in vascular endothelial cells. Angiogenesis inhibitors block vascular endothelial growth
598 factor-induced down-regulation of caveolin-1. *J Biol Chem* 274(22), 15781-15785.
- 599 Liu, S.M., and Sundqvist, T. (1995). Effects of hydrogen peroxide and phorbol myristate acetate on
600 endothelial transport and F-actin distribution. *Exp Cell Res* 217(1), 1-7.
601 10.1006/excr.1995.1056.
- 602 Lowe, D., and Raj, K. (2014). Premature aging induced by radiation exhibits pro-atherosclerotic
603 effects mediated by epigenetic activation of CD44 expression. *Aging Cell* 13(5), 900-910.
604 10.1111/acel.12253.
- 605 Lowe, D.J., and Raj, K. (2015). Quantitation of Endothelial Cell Adhesiveness In Vitro. *J Vis Exp*
606 (100), e52924. 10.3791/52924.
- 607 Mackay, F., Loetscher, H., Stueber, D., Gehr, G., and Lesslauer, W. (1993). Tumor necrosis factor
608 alpha (TNF-alpha)-induced cell adhesion to human endothelial cells is under dominant
609 control of one TNF receptor type, TNF-R55. *J Exp Med* 177(5), 1277-1286.
- 610 Mao, X.W., Favre, C.J., Fike, J.R., Kubinova, L., Anderson, E., Campbell-Beachler, M., et al.
611 (2010). High-LET radiation-induced response of microvessels in the Hippocampus. *Radiat*
612 *Res* 173(4), 486-493. 10.1667/RR1728.1.
- 613 Meeren, A.V., Bertho, J.M., Vandamme, M., and Gaugler, M.H. (1997). Ionizing radiation enhances
614 IL-6 and IL-8 production by human endothelial cells. *Mediators Inflamm* 6(3), 185-193.
615 10.1080/09629359791677.
- 616 Merl, J., Ueffing, M., Hauck, S.M., and von Toerne, C. (2012). Direct comparison of MS-based
617 label-free and SILAC quantitative proteome profiling strategies in primary retinal Muller
618 cells. *Proteomics* 12(12), 1902-1911. 10.1002/pmic.201100549.
- 619 Morais, C., Ebrahim, Q., Anand-Apte, B., and Parat, M.O. (2012). Altered angiogenesis in caveolin-
620 1 gene-deficient mice is restored by ablation of endothelial nitric oxide synthase. *Am J Pathol*
621 180(4), 1702-1714. 10.1016/j.ajpath.2011.12.018.

Radiation Quality Effect on Endothelial Cells

- 622 Moreels, M., de Saint-Georges, L., Vanhavere, F., and Baatout, S. (2012). "Stress and Radiation
623 Responsiveness," in *Stress challenges and immunity in space : from mechanisms to monitoring,
624 and preventive strategies*, ed. A. Choukèr. (Heidelberg ; New York: Springer), pp 239-260.
- 625 Munzel, T., Sinning, C., Post, F., Warnholtz, A., and Schulz, E. (2008). Pathophysiology, diagnosis
626 and prognostic implications of endothelial dysfunction. *Ann Med* 40(3), 180-196.
627 10.1080/07853890701854702.
- 628 Newhauser, W.D., and Durante, M. (2011). Assessing the risk of second malignancies after modern
629 radiotherapy. *Nat Rev Cancer* 11(6), 438-448. 10.1038/nrc3069.
- 630 Nichols, R.C., Huh, S., Li, Z., and Rutenberg, M. (2015). Proton therapy for pancreatic cancer. *World
631 J Gastrointest Oncol* 7(9), 141-147. 10.4251/wjgo.v7.i9.141.
- 632 Pavlides, S., Gutierrez-Pajares, J.L., Iturrieta, J., Lisanti, M.P., and Frank, P.G. (2014). Endothelial
633 caveolin-1 plays a major role in the development of atherosclerosis. *Cell Tissue Res* 356(1),
634 147-157. 10.1007/s00441-013-1767-7.
- 635 Rombouts, C., Aerts, A., Beck, M., De Vos, W.H., Van Oostveldt, P., Benotmane, M.A., et al.
636 (2013). Differential response to acute low dose radiation in primary and immortalized
637 endothelial cells. *Int J Radiat Biol* 89(10), 841-850. 10.3109/09553002.2013.806831.
- 638 Rombouts, C., Aerts, A., Quintens, R., Baselet, B., El-Saghire, H., Harms-Ringdahl, M., et al. (2014).
639 Transcriptomic profiling suggests a role for IGFBP5 in premature senescence of endothelial
640 cells after chronic low dose rate irradiation. *Int J Radiat Biol* 90(7), 560-574.
641 10.3109/09553002.2014.905724.
- 642 Sbaa, E., Frerart, F., and Feron, O. (2005). The double regulation of endothelial nitric oxide synthase
643 by caveolae and caveolin: a paradox solved through the study of angiogenesis. *Trends
644 Cardiovasc Med* 15(5), 157-162. 10.1016/j.tcm.2005.05.006.
- 645 Scholz, M. (2003). "Effects of Ion Radiation on Cells and Tissues," in *Radiation Effects on Polymers
646 for Biological Use*, eds. H. Kausch, N. Anjum, Y. Chevolut, B. Gupta, D. Léonard, H.J.
647 Mathieu, L.A. Pruitt, L. Ruiz-Taylor & M. Scholz. (Berlin, Heidelberg: Springer Berlin
648 Heidelberg), 95-155.
- 649 Schuett, H., Luchtefeld, M., Grothusen, C., Grote, K., and Schieffer, B. (2009). How much is too
650 much? Interleukin-6 and its signalling in atherosclerosis. *Thromb Haemost* 102(2), 215-222.
651 10.1160/TH09-05-0297.
- 652 Schultz-Hector, S., and Trott, K.R. (2007). Radiation-induced cardiovascular diseases: is the
653 epidemiologic evidence compatible with the radiobiologic data? *Int J Radiat Oncol Biol Phys*
654 67(1), 10-18. 10.1016/j.ijrobp.2006.08.071.
- 655 Schulz-Ertner, D., and Tsujii, H. (2007). Particle radiation therapy using proton and heavier ion
656 beams. *J Clin Oncol* 25(8), 953-964. 10.1200/JCO.2006.09.7816.
- 657 Sofia Vala, I., Martins, L.R., Imaizumi, N., Nunes, R.J., Rino, J., Kuonen, F., et al. (2010). Low
658 doses of ionizing radiation promote tumor growth and metastasis by enhancing angiogenesis.
659 *PLoS One* 5(6), e11222. 10.1371/journal.pone.0011222.
- 660 Sonveaux, P., Brouet, A., Havaux, X., Gregoire, V., Dessy, C., Balligand, J.L., et al. (2003).
661 Irradiation-induced angiogenesis through the up-regulation of the nitric oxide pathway:
662 implications for tumor radiotherapy. *Cancer Res* 63(5), 1012-1019.

Radiation Quality Effect on Endothelial Cells

- 663 Soucy, K.G., Lim, H.K., Kim, J.H., Oh, Y., Attarzadeh, D.O., Sevinc, B., et al. (2011). HZE
664 (5)(6)Fe-ion irradiation induces endothelial dysfunction in rat aorta: role of xanthine oxidase.
665 *Radiat Res* 176(4), 474-485.
- 666 Stone, H.B., Coleman, C.N., Anscher, M.S., and McBride, W.H. (2003). Effects of radiation on
667 normal tissue: consequences and mechanisms. *Lancet Oncol* 4(9), 529-536.
- 668 Suetens, A., Konings, K., Moreels, M., Quintens, R., Verslegers, M., Soors, E., et al. (2016). Higher
669 Initial DNA Damage and Persistent Cell Cycle Arrest after Carbon Ion Irradiation Compared
670 to X-irradiation in Prostate and Colon Cancer Cells. *Front Oncol* 6, 87.
671 10.3389/fonc.2016.00087.
- 672 Sundqvist, T., and Liu, S.M. (1993). Hydrogen peroxide stimulates endocytosis in cultured bovine
673 aortic endothelial cells. *Acta Physiol Scand* 149(2), 127-131. 10.1111/j.1748-
674 1716.1993.tb09604.x.
- 675 Supek, F., Bosnjak, M., Skunca, N., and Smuc, T. (2011). REVIGO summarizes and visualizes long
676 lists of gene ontology terms. *PLoS One* 6(7), e21800. 10.1371/journal.pone.0021800.
- 677 Takahashi, Y., Teshima, T., Kawaguchi, N., Hamada, Y., Mori, S., Madachi, A., et al. (2003). Heavy
678 ion irradiation inhibits in vitro angiogenesis even at sublethal dose. *Cancer Res* 63(14), 4253-
679 4257.
- 680 Vita, J.A., and Keaney, J.F., Jr. (2002). Endothelial function: a barometer for cardiovascular risk?
681 *Circulation* 106(6), 640-642.
- 682 Widlansky, M.E., Gokce, N., Keaney, J.F., Jr., and Vita, J.A. (2003). The clinical implications of
683 endothelial dysfunction. *J Am Coll Cardiol* 42(7), 1149-1160.
- 684 Widmer, R.J., and Lerman, A. (2014). Endothelial dysfunction and cardiovascular disease. *Glob*
685 *Cardiol Sci Pract* 2014(3), 291-308. 10.5339/gcsp.2014.43.
- 686 Wilson, R.R. (1946). Radiological use of fast protons. *Radiology* 47(5), 487-491. 10.1148/47.5.487.
- 687 Wu, J., Liu, W., Bemis, A., Wang, E., Qiu, Y., Morris, E.A., et al. (2007). Comparative proteomic
688 characterization of articular cartilage tissue from normal donors and patients with
689 osteoarthritis. *Arthritis Rheum* 56(11), 3675-3684. 10.1002/art.22876.
- 690 Yentrapalli, R., Azimzadeh, O., Barjaktarovic, Z., Sarioglu, H., Wojcik, A., Harms-Ringdahl, M., et
691 al. (2013a). Quantitative proteomic analysis reveals induction of premature senescence in
692 human umbilical vein endothelial cells exposed to chronic low-dose rate gamma-radiation.
693 *Proteomics* 13(7), 1096-1107. 10.1002/pmic.201200463.
- 694 Yentrapalli, R., Azimzadeh, O., Sriharshan, A., Malinowsky, K., Merl, J., Wojcik, A., et al. (2013b).
695 The PI3K/Akt/mTOR pathway is implicated in the premature senescence of primary human
696 endothelial cells exposed to chronic radiation. *PLoS One* 8(8), e70024.
697 10.1371/journal.pone.0070024.
- 698 Yu, T., Parks, B.W., Yu, S., Srivastava, R., Gupta, K., Wu, X., et al. (2011). Iron-ion radiation
699 accelerates atherosclerosis in apolipoprotein E-deficient mice. *Radiat Res* 175(6), 766-773.
700 10.1667/RR2482.1.
- 701 Zhu, H., Yue, J., Pan, Z., Wu, H., Cheng, Y., Lu, H., et al. (2010). Involvement of Caveolin-1 in
702 repair of DNA damage through both homologous recombination and non-homologous end
703 joining. *PLoS One* 5(8), e12055. 10.1371/journal.pone.0012055.

704

17

Radiation Quality Effect on Endothelial Cells

705 10 Tables

706 Table 1. X-ray irradiation of ECs induces an acute gene expression signature suggestive of
707 cycle block and increased cellular adhesion.*

	Upregulated	-log10 (p-value)	Downregulated	-log10 (p-value)
	Description of process		Description of process	
2 Gy X-rays Day 1	Regulation of multicellular organismal process	9	Cell cycle process	111
	Regulation of localization	9	Chromosome organization	76
	Signal transduction	9	DNA metabolic process	54
	Regulation of cellular component movement	8	Cell division	50
	Regulation of locomotion	8	DNA replication	44
	Cell adhesion	7	Cellular component organization or biogenesis	36
	Biological adhesion	7	Chromosome segregation	26
	Response to stimulus	7	Microtubule-based process	19
	Regulation of cell proliferation	7	Regulation of chromosome segregation	18
	Developmental process	7	DNA synthesis involved in DNA repair	18
2 Gy X-rays Day 7	Mitotic cell cycle process	14	Cell-substrate adhesion	7
	Cell division	10	Extracellular matrix organization	4
	Chromosome organization	9	Extracellular structure organization	4
	DNA replication initiation	9	Ethanol oxidation	4
	Cell proliferation	6	Biological adhesion	4
	Chromosome segregation	5	Post-embryonic organ morphogenesis	4
	Cellular component organization or biogenesis	5	Maintenance of location	3
	Regulation of chromosome segregation	5	Maintenance of protein location in extracellular region	3
	Negative regulation of blood coagulation	4		
	Response to hypoxia	4		

708 *Gene ontology enrichment analysis was performed on differentially expressed genes in irradiated
709 versus sham-irradiated ECs (n = 3). Table shows the top 10 GO enrichment terms among upregulated
710 (left) and downregulated (right) differentially expressed genes at day 1 (top panel) and at day 7 after 2
711 Gy of X-rays (bottom panel).

712

713

714

715

Radiation Quality Effect on Endothelial Cells

716 **Table 2. Fe ion irradiation of ECs induces a gene expression signature suggesting persistent cell**
 717 **cycle block and decreased cellular adhesion.***

	Upregulated	-log10 (p-value)	Downregulated	-log10 (p-value)
	Description of process		Description of process	
2 Gy Fe ions Day 1	Signal transduction by p53 class mediator	11	Cell cycle process	99
	DNA damage response, signal transduction by p53 class mediator	7	Chromosome organization	67
	Positive regulation of cell cycle arrest	7	Cell division	49
	Response to radiation	7	DNA metabolic process	49
	Signal transduction in response to DNA damage	7	DNA replication	43
	Response to abiotic stimulus	7	Cellular component organization or biogenesis	38
	Regulation of cell proliferation	7	Chromosome segregation	26
	Regulation of apoptotic process	6	Microtubule-based process	19
	Response to stimulus	6	Regulation of chromosome segregation	18
Chondroblast differentiation	5	Negative regulation of gene expression, epigenetic	17	
2 Gy Fe ions Day 7	Developmental process	8	Regulation of endothelial cell migration	10
	Negative regulation of response to stimulus	8	Negative regulation of nucleic acid-templated transcription	10
	Regulation of locomotion	7	Regulation of signal transduction	9
	Regulation of cell proliferation	7	Developmental process	8
	Locomotion	7	Cytoskeleton organization	7
	Single-organism process	7	Response to endogenous stimulus	6
	Positive regulation of biological process	7	Regulation of cell death	6
	Single-organism developmental process	7	Regulation of cell cycle	6
	Regulation of multicellular organismal process	7	Regulation of cell proliferation	6
	Regulation of protein metabolic process	7	Cell adhesion	6

718 *Gene ontology enrichment analysis (process) was performed on differentially expressed genes in
 719 irradiated versus sham-irradiated ECs (n = 3). Table shows the top 10 GO enrichment terms among
 720 upregulated (left) and downregulated (right) differentially expressed genes on day 1 (top panel) or day
 721 7 after 2 Gy of Fe ions (bottom panel).

722

723

724

725

726

Radiation Quality Effect on Endothelial Cells

727 **Table 3. Fe ions and X-ray irradiation induce protein expression involved in caveolar mediated**
 728 **endocytosis signaling and cell-cell adhesion, but at different time points***

	X-rays Description of process	-log10 (p-value)	Fe ions Description of process	-log10 (p-value)
Day 1	Caveolar-mediated Endocytosis Signaling	4.1	Remodeling of Epithelial Adherens Junctions	4.8
	RAN Signaling	2.9	tRNA Charging	4.5
	Glutathione Redox Reactions I	2.6	Glutathione-mediated Detoxification	3.5
	ILK Signaling	2.4	Integrin Signaling	3.3
	Virus Entry via Endocytic Pathways	2.4	Epithelial Adherens Junction Signaling	3.2
	Integrin Signaling	2.3	Mitochondrial Dysfunction	2.9
	Palmitate Biosynthesis I (Animals)	2.2	Germ Cell-Sertoli Cell Junction Signaling	2.9
	Uridine-5'-phosphate Biosynthesis	2.2	Oxidative Phosphorylation	2.8
	Fatty Acid Biosynthesis Initiation II	2.2	Paxillin Signaling	2.7
	Cell Cycle Control of Chromosomal Replication	2.2	EIF2 Signaling	2.7
Day 7	Remodeling of Epithelial Adherens Junctions	6.9	Caveolar-mediated Endocytosis Signaling	8.9
	Cell Cycle Control of Chromosomal Replication	5.1	Virus Entry via Endocytic Pathways	8.7
	Integrin Signaling	5.0	Neuroprotective Role of THOP1 in Alzheimer's Disease	6.5
	Epithelial Adherens Junction Signaling	5.0	Ephrin Receptor Signaling	5.5
	Gap Junction Signaling	4.6	Antigen Presentation Pathway	5.3
	Germ Cell-Sertoli Cell Junction Signaling	4.6	Phagosome maturation	5.2
	Sertoli Cell-Sertoli Cell Junction Signaling	4.5	NRF2-mediated Oxidative Stress Response	5.1
	Caveolar-mediated Endocytosis Signaling	4.0	Agrin Interactions at Neuromuscular Junction	5.1
	Death Receptor Signaling	3.6	Granzyme A Signaling	5.0
	Virus Entry via Endocytic Pathways	3.4	ERK/MAPK Signaling	5.0

729 *Canonical pathway analysis was performed on differentially expressed proteins in irradiated versus
 730 sham-irradiated ECs (n = 3). Table shows the top 10 molecular functions identified on day 1 (top
 731 panels) or day 7 (bottom panels) in ECs irradiated with 2 Gy of X-rays (left panels) or Fe ions (right
 732 panels).

733
 734
 735
 736
 737

Radiation Quality Effect on Endothelial Cells

738 **Table 4. Differently expressed proteins after Fe ion and X-ray irradiation are mainly involved**
 739 **in cell death, cell cycle and cell-cell signaling***

	X-rays	-log10 (p-value)	Fe ions	-log10 (p-value)
	Description of molecular function		Description of molecular function	
Day 1	Cell Death and Survival	6.8	Cell Death and Survival	10.3
	Cell Morphology	6.8	Cellular Growth and Proliferation	5.5
	Cell-To-Cell Signaling and Interaction	6.7	Cell Morphology	4.4
	Cellular Movement	6.5	Cellular Development	4.4
	Cellular Growth and Proliferation	6.1	Cellular Function and Maintenance	4.4
	Cellular Assembly and Organization	5.7	Cellular Assembly and Organization	4.4
	Cellular Compromise	5.7	Cell-To-Cell Signaling and Interaction	4.3
	DNA Replication, Recombination, and Repair	4.8	Cell Cycle	3.9
	Cellular Development	4.7	Cellular Movement	3.9
	Cell Cycle	4.1	Post-Translational Modification	3.8
Day 7	Cell Death and Survival	8.5	Cell Death and Survival	14.9
	Cellular Movement	6.4	Cell-To-Cell Signaling and Interaction	9.2
	Cell Morphology	6.2	Cellular Movement	7.6
	Cellular Growth and Proliferation	5.8	Cellular Growth and Proliferation	7.0
	Cell Cycle	5.4	Cell Cycle	6.5
	Cellular Function and Maintenance	5.0	Cellular Development	6.3
	Cell-To-Cell Signaling and Interaction	4.9	Cellular Function and Maintenance	5.7
	DNA Replication, Recombination, and Repair	4.8	Cell Morphology	5.3
	Cellular Development	4.3	Cellular Assembly and Organization	5.2
	Gene Expression	3.9	Protein Degradation	4.5

740 *Protein ontology analysis was performed on differentially expressed proteins in irradiated versus
 741 sham-irradiated ECs (n = 3). Table shows the top 10 molecular functions identified on day 1 (top
 742 panels) or day 7 (bottom panels) in ECs after a 2 Gy irradiation with X-ray (left panels) or Fe ions
 743 (right panels).

744 11 Figure legends

745 **Figure 1. Fe ion irradiation induces a more pronounced and persistent transcriptional response**
 746 **in ECs in comparison to X-ray irradiation.** Venn diagrams indicate the number of differentially
 747 expressed genes after exposure to a single 2.0 Gy dose of X-rays (A) or Fe ions (B). The gene
 748 expression changes after low and high LET irradiation are compared on day 1 (C) and on day 7 (D).
 749 Changes are compared gene expression in sham irradiated cells, as described in Materials and Methods
 750 (N = 3, n = 12).

751 **Figure 2. Upregulated genes involved in cell cycle regulated processes at 1 day after a single dose**
 752 **of 2 Gy X-rays.** Arborecence diagram indicates cell cycle pathway with the identified upregulated
 753 genes indicated in green. Pathway diagram was adapted from Wikipathways and modified with
 754 Pathvisio. Changes are shown compared to gene expression in sham irradiated cells (N = 3, n = 12).

Radiation Quality Effect on Endothelial Cells

755 **Figure 3. Downregulated genes involved in cell-cell adhesion processes at 1 day after a single dose**
756 **of 2 Gy X-rays.** Arborescence diagram indicates cell-cell adhesion pathway with the identified
757 downregulated genes indicated in red. Pathway diagram was adapted from Wikipathways and modified
758 with Pathvisio. Changes are shown compared to gene expression in sham irradiated cells (N = 3, n =
759 12).

760 **Figure 4. Upregulated genes involved in apoptosis signaling at 1 day after a single dose of 2 Gy**
761 **Fe ions.** Arborescence diagram indicates apoptosis pathway with the identified upregulated genes
762 indicated in green. Pathway diagram was adapted from Wikipathways and modified with Pathvisio.
763 Changes are shown compared to gene expression in sham irradiated cells (N = 3, n = 12).

764

765 **Figure 5. Irradiated ECs demonstrate a larger number of differentially expressed proteins after**
766 **Fe ion exposure in comparison to X-ray exposure.** Venn diagrams indicate the numbers of
767 differentially expressed proteins after exposure to a single 2.0 Gy dose of X-rays (A) or Fe ions (B).
768 The protein expression changes after low and high LET irradiation are compared on day 1 (C) and on
769 day 7 (D). Changes are shown compared to protein expression in sham irradiated cells, as described in
770 Materials and Methods (N = 3, n = 12).

771 **Figure 6. Irradiated ECs differentially expressed proteins after X-ray exposure involved in**
772 **caveolar-mediated endocytosis and cell-cell adhesion.** Arborescence diagram indicates caveolar-
773 mediated endocytosis signaling and cell-cell adhesion pathways with the identified upregulated genes
774 indicated in green and downregulated genes in red. Pathway diagram was adapted from Wikipathways
775 and modified with Pathvisio. Changes are shown compared to gene expression in sham irradiated cells
776 (N = 3, n = 12).

777 **Figure 7. X-ray irradiated ECs exhibit a persistent downregulation of caveolin-1, whereas Fe ion**
778 **exposure induces a caveolin 1 upregulation.** (A) Caveolin-1 (cav-1) and α -tubulin protein expression
779 analyzed using western blot after cell exposure to a single 2.0 Gy dose fo X-ray or Fe ions. (B) Data
780 represent the cav-1/ α -tubulin ratio in control and irradiated samples after background correction and
781 normalization to α -tubulin expression. Data show means \pm SEM (N = 3, n = 12). * $p \leq 0.05$ using two-
782 sided t-test (Welch-test).

783 **Figure 8. X-ray irradiation causes EC inflammation and adhesiveness to monocytes, whilst Fe**
784 **ion irradiation reduces cellular number and decreases EC adhesiveness to monocytes.** The levels
785 of IL-6 , IL-8 and CCL2 secreted by EC on 4 hours and day 1 plus day 7 (B-D) are shown after
786 exposure to X-rays (n = 18-27) and Fe ions (n = 4-6). Data were normalized to cell numbers,
787 supernatant volume and control values. (D) The numbers of monocytes adhering to EC on day 7 are
788 shown after exposure to X-rays (n = 90-225) and Fe ions (n = 30). Data was normalized to cell numbers
789 and control values of sham-irradiated ECs. (E) EC numbers on day 7 using either X-rays (n = 18-27)
790 or Fe ions (n = 4-6) are shown. (A-E). Data show mean \pm SEM. ns, not significant, * $p \leq 0.05$, ** $p \leq$
791 0.005, *** $p \leq 0.001$ using two-sided t-test (Welch-test).

Figure 1.TIF

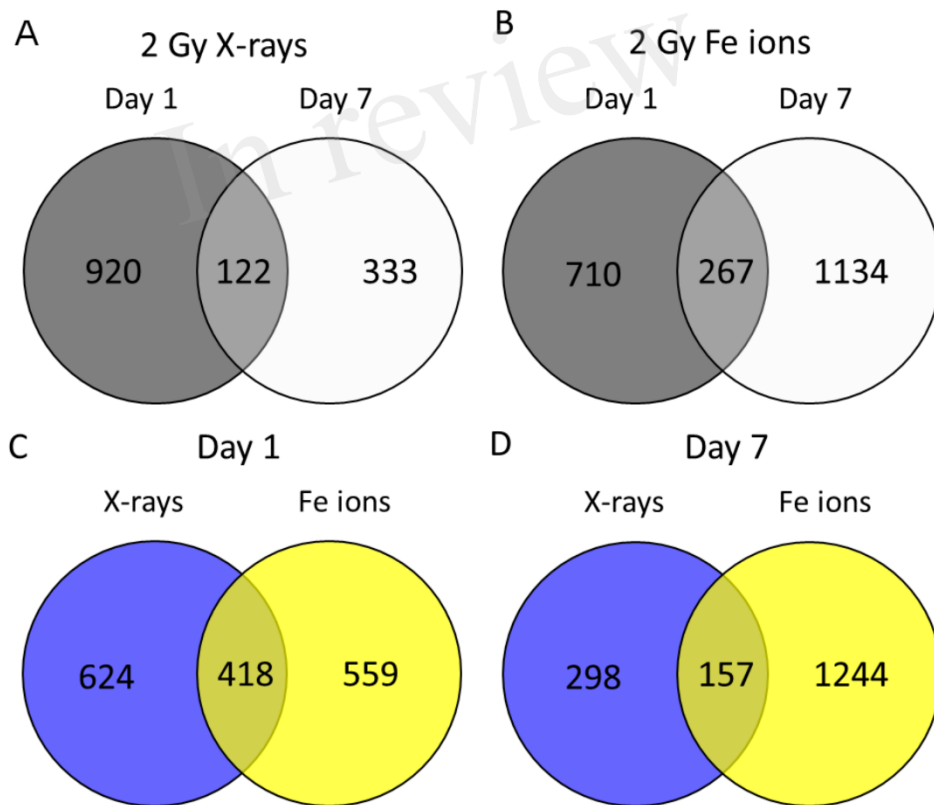


Figure 2.TIFF

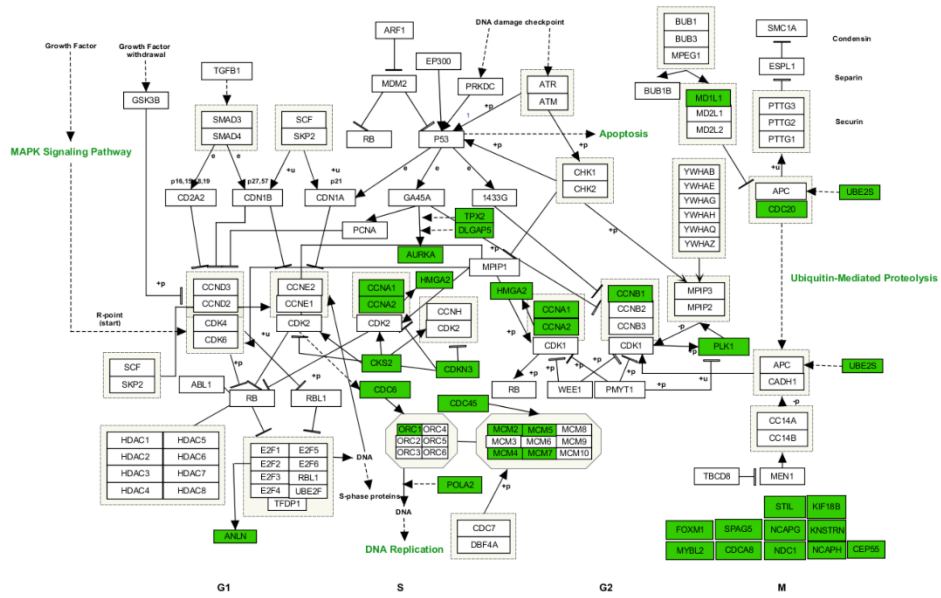


Figure 3.TIFF

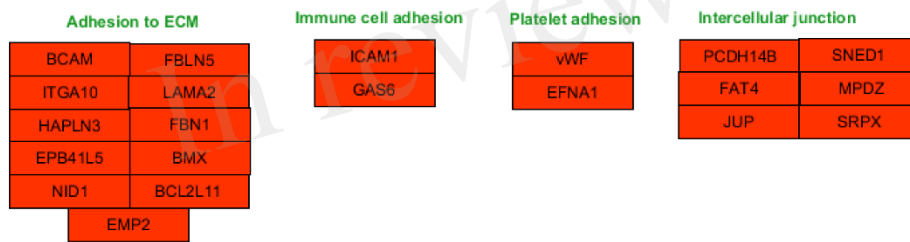


Figure 4.TIFF

In review

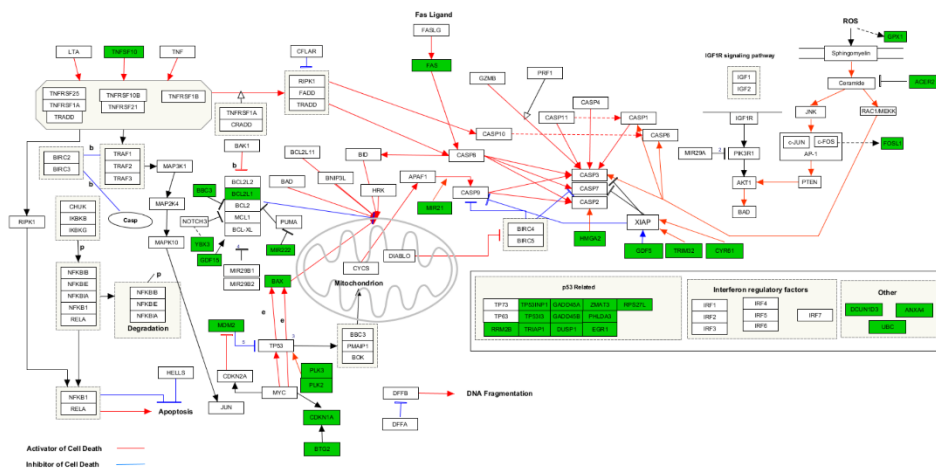


Figure 5.TIF

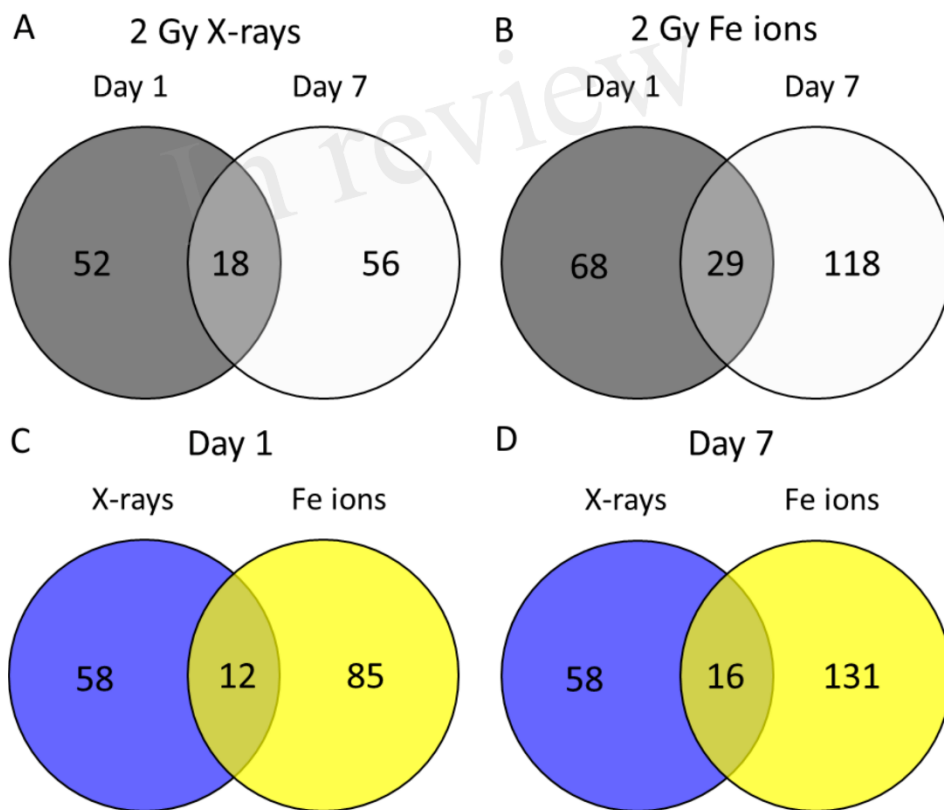


Figure 6.TIFF

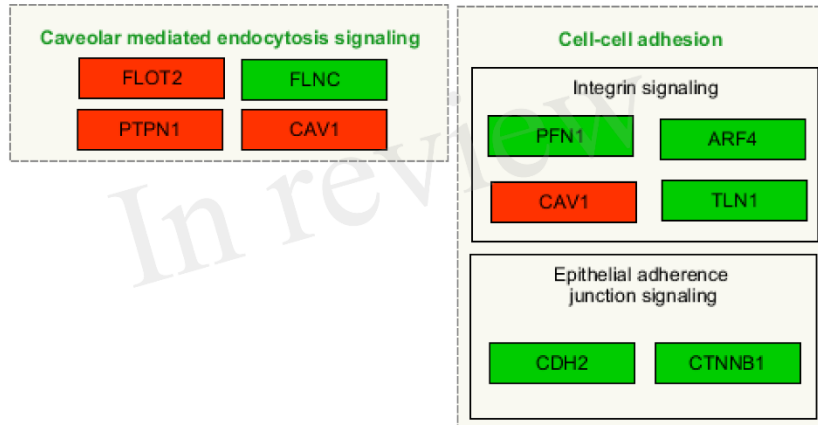


Figure 7.TIF

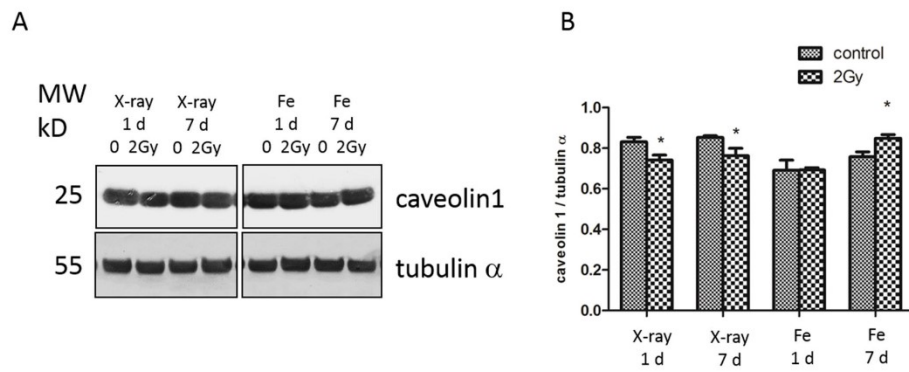
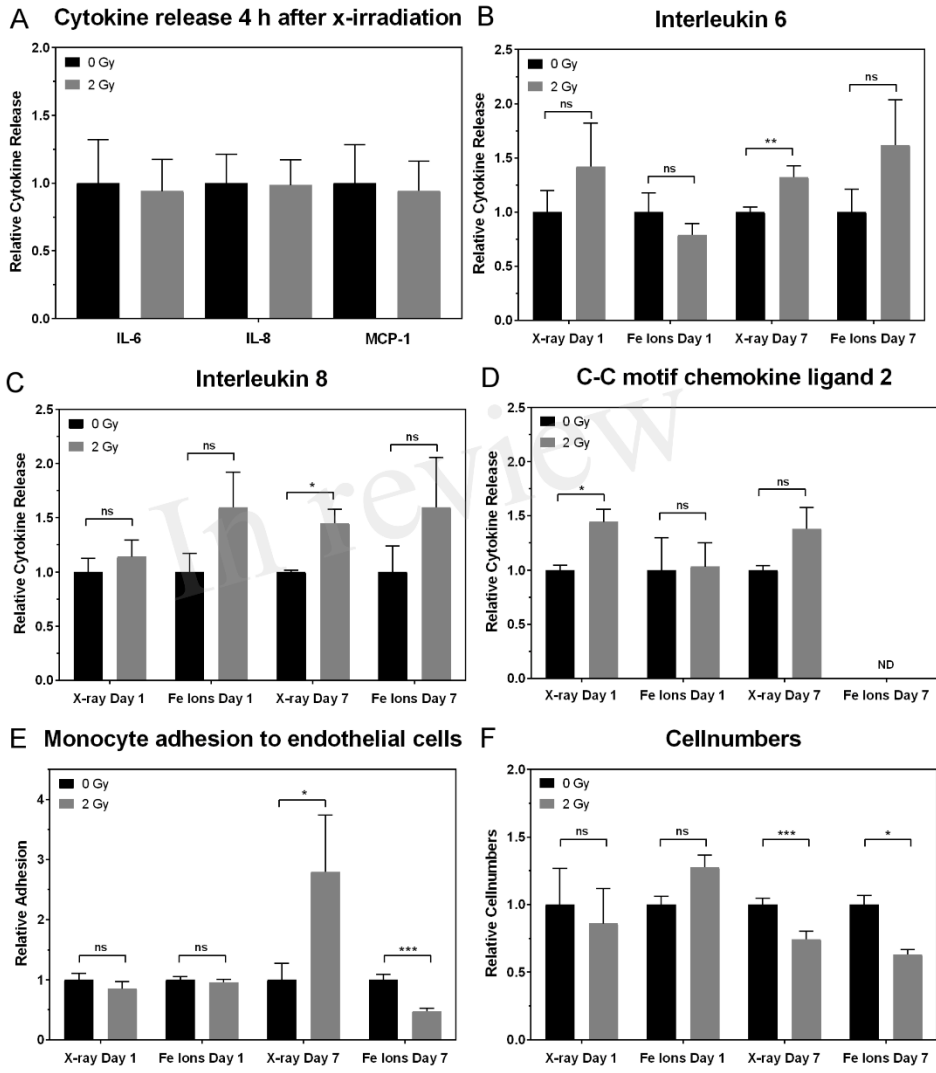


Figure 8.TIFF



*Discussion and
perspectives*

Discussion and perspectives

1. Dose-, time- and radiation quality-dependent changes in irradiated endothelial cells linked to a pro-atherosclerotic phenotype

The necessity to provide adequate protection of mankind and the environment to hazardous effects of ionizing radiation exposure is at the core of the current radiation protection system (14). To optimally protect humans, however, a good understanding of radiation-related health risks and molecular mechanisms altered by irradiation is essential (569). In this regard, epidemiological studies provided part of the puzzle by obtaining evidence for increased cardiovascular risks above 0.5 Gy (151, 171, 172). However, these studies have low statistical power, lack the control of potential confounders and deal with uncertainty in dose assessments, making it difficult to draw any conclusion about cardiovascular risks following exposure to lower doses (166, 570). As a consequence, the impact of ionizing radiation on human health could be underestimated. If true, then exposed people would potentially be underprotected. Furthermore, biological mechanisms accounting for radiation-induced cardiovascular effects are unclear (570). In order to mechanistically validate these epidemiological studies and to ameliorate the radiation protection system if necessary, there is a need for molecular radiobiological research that can give insights into radiation-induced cardiovascular effects.

In this PhD thesis, we aimed to better characterize molecular determinants of radiation-induced CVDs. Previous information suggested that ionizing radiation accelerates the development of age-related atherosclerosis in coronary arteries (145, 171), *i.e.*, a pathological inflammatory process of the vascular wall characterized by loss of endothelial functions and vascular integrity (181, 183). We therefore irradiated Est2-immortalized human coronary artery endothelial cells with different doses of X-rays and Fe ions. Early after X-ray irradiation, microarray analysis and validation experiments showed activation of the DNA damage response associated with cell cycle repression, decreased endothelial cell proliferation and an increased inflammatory state. Identification of radiation-induced endothelial activation is in agreement with other findings, explaining the molecular effects observed one day after endothelial exposure to high doses (≥ 5 Gy) of ionizing radiation (338-341). Our study evidenced that inflammation is also

induced in endothelial cells exposed to lower radiation doses (0.5 and 2 Gy), and has a more chronic nature since it persisted up to 7 days after single dose irradiation. Interestingly, others observed that atomic bomb survivors also have signs of a general increased chronic state of inflammation, with increased levels of IL-6 and C-reactive protein in their blood (571). A question that arises from our study is: what caused the pro-inflammatory reaction in endothelial cells after radiation exposure? A plausible explanation would be the release of DAMPs by stressed and dying endothelial cells (335). Another explanation would be linked to radiation-induced chronic oxidative stress, which has been shown to induce endothelial activation by activating redox-sensitive transcription factors NF- κ B, AP-1 and Nrf2 (323-327). Inflammation plays a key role in the development, progression and final outcome of atherosclerosis (572). Our *in vitro* findings that endothelial inflammation occurs at low single X-ray doses is a first milestone indicating that low dose irradiation could constitute a health risk. Of course, this possibility must now be verified with more refined models.

Fourteen days after exposure to a single X-ray dose, inflammation levels resumed to levels of sham-irradiated samples. At this time, however, we identified induction of premature endothelial senescence at all radiation doses tested. Radiation-induced senescence can be due to persistent p53 signaling, as evidenced by our data at 1 and 7 days after exposure, which is usually associated with persistent DNA damage (573). In addition to radiation-induced activation of the p53 pathway, others identified reduced activity of the PI3K/Akt/mTOR pathway after 10 weeks of chronic low-dose rate exposure (4.1 mGy/h) of HUVECs, leading to p16 overexpression associated with senescence induction (528). Furthermore, chronic inflammation, observed from day 1 until day 7 after X-ray irradiation in our model, can in theory be a cause of cellular senescence (574, 575). Briefly, chronic inflammation can cause cellular senescence by inducing the expression of p53 and related family members p21, p16 and p14 by persistent NF- κ B activation and oxidative stress (576). However, this cannot explain induction of senescence at low X-ray doses, at which we did not observe endothelial activation. Identification of radiation-induced endothelial senescence at higher doses is in agreement with other findings. Chronic low-dose rate γ radiation (4.1 mGy/h) led to premature senescence in HUVECs by the induction of the p53/p21 pathway (577). Further analysis revealed PI3K/Akt/mTOR pathway inactivation, which can directly induce premature senescence by increasing the expression of p21 (528). At the gene

expression level of these cells, a role for IGFBP5 was identified, which is known to inhibit cell proliferation through a p53-dependent mechanism (526, 578). In addition, a dose of 10 Gy of X-ray to Est2-immortalized human coronary artery endothelial cells was found to induce premature aging by epigenetic activation of CD44 expression (519). Senescent endothelial cells are an emerging contributor to the pathogenesis of atherosclerosis (468) and have been shown to be present in human atherosclerotic plaques (515). Fundamental research with anti-senescent and anti-inflammatory drugs is thus needed to evaluate whether or not they could act as radioprotectors.

Identification of a pro-atherosclerotic phenotype in X-ray-irradiated endothelial cells led us to wonder whether other radiation qualities could have similar effects in the context of particle radiotherapy and space missions. For this reason, we compared 2 Gy Fe ion-irradiated and 2 Gy X-ray-irradiated Est2-immortalized human coronary artery endothelial cells. Probably due to the higher RBE of Fe ions, we observed a more profound and longer lasting radiation response after exposure to Fe ions in comparison to X-rays. In contrast to X-rays, Fe ions indeed persistently repressed the expression of genes associated with cell cycle regulation, a finding also observed in other cell types exposed to high LET radiation (579, 580) and that is thought to be the consequence of complex, clustered, hard-to-repair DNA damage (581, 582).

Both X-rays and Fe ions repressed transcriptional and proteomic changes associated with endothelial-monocyte adhesion pathways 7 days after exposure. While these changes could indicate an angiogenic activation of X-ray-irradiated endothelial cells, supported by independent observations (361, 583), this is less likely to be the case for Fe ion-irradiated endothelial cells that had a lower alteration of proteomic and transcriptomic pathways involved in cell proliferation. In accordance, 0.1 Gy of C ions was shown to decrease angiogenesis, partly by reducing the expression level or activity of angiogenesis-related molecules integrins and matrix metalloproteinases (584). Others identified that 1 Gy of Fe or proton radiation did not affect the early stages, but well the later stages, of vasculogenesis when endothelial cells migrate to form tubes (585). Furthermore, irradiation with 0.5 Gy and 2 Gy of Fe ions mediated 34% and 29% loss of endothelial cells in the brain microvasculature, respectively, 12 months after exposure (586). The mechanisms by which high LET irradiation inhibits angiogenesis are to date

unknown (587). One explanation, however, is enhanced induction of cytogenetic damage, decreased cell proliferation and deteriorated mitochondrial activity seen in HUVECs when comparing 0.75 – 1.5 Gy of X-rays to 0.25 - 0.75 Gy of C ions (500). Changes associated with endothelial cell-cell adhesion are more likely to be due to compromised integrity of Fe ion-irradiated endothelial cells, as observed by others (586, 588) and supported by our findings that endothelial number and monocyte adhesiveness are decreased after high LET irradiation, in combination with signaling linked to increased cell death and reduced proliferation.

Proteomics further revealed altered caveolar mediated endocytosis signaling after exposure to both X-rays and Fe ions. The principal component protein of caveolae, caveolin-1, plays a role in DNA damage response/repair and confers radiosensitivity (Figure 28). At least 4 lines of evidence support this conclusion. First, caveolin-1 down-regulation resulted in a delayed resolution of γ H2AX foci, but did not alter the early activation of the DNA damage response, as measured by phospho-ATM in human cells derived from breast, ovarian and prostate cancer as well as normal mammary epithelium (589, 590). It mediated a decrease in HR and NHEJ DSB DNA repair after irradiation, thus contributing to maintenance of genomic integrity (589, 590). Effects of caveolin-1 on DNA damage repair might be related to accumulation of BRCA1 foci in the nucleus after DNA damage and to phosphorylation of protein kinase DNA-activated catalytic polypeptide (589, 590). Second, caveolin-1 is able to suppress *cyclin D1* gene expression and inhibits the activity of the *cdc25A* promoter, resulting in a block in cell cycle progression (591). Third, protein levels of caveolin-1 are upregulated at cellular confluence, where it is able to mediate contact inhibition by suppression of the cell cycle (592). Fourth, caveolin-1 interacts with various receptors and signaling molecules, *i.e.*, G-protein-coupled receptors, receptor tyrosine kinases, integrins, steroid hormone receptors, and downstream molecules such as heterotrimeric G-proteins, ion channels and NOS (593). For example, caveolin-1 depletion in pancreatic cancer cells activated the JAK/STAT pathway that is involved in stress-induced proliferation and survival (590). Downregulation of caveolin-1 has also been shown to activate MAPK signaling pathways, resulting in cell survival and proliferation (592).

Caveolin-1 is also crucial in the normal function of endothelial cells and reduced levels can be linked to endothelial activation, dysfunction and increased radiationsensitivity. First, caveolin-1 inhibits angiogenesis by reducing eNOS activity

(594) and vascular endothelial growth factor receptor (VEGFR) activity (595). As a consequence, caveolin-1 knock down resulted in impaired endothelial cell migration, tube formation, cell sprouting from aortic rings, tumor growth, and angiogenesis (596). Second, loss of caveolin-1 expression was reported to result in increased endothelial radiosensitivity by increasing radiation-induced apoptosis and reducing clonogenic survival (597). Third, angiogenesis activators and inhibitors decrease and increase the expression of caveolin-1, respectively, indicating that it is an important element that controls endothelial cell proliferation (598). Fourth, caveolin-1 overexpression in ApoE^{-/-} mice has been shown to accelerate atherosclerosis development and progression by reducing endothelial cell proliferation, migration and NO production, and increased expression of VCAM-1 (599). Others also identified diminished LDL endocytosis and decreased VCAM-1 protein levels due to reduced signaling *via* the NF-κB inflammatory pathway in HUVECs overexpressing caveolin-1 (600, 601). In addition, endocytosis regulates endothelial adhesion through cadherin endocytosis, affecting adherens junction turnover in endothelial cells (602-604). Because caveolin-1 enhances DNA damage response/repair, blocks cell cycle progression and modulates cell survival pathways, it could also play a role in the response to radiation. Accordingly, caveolin-1 was found to be upregulated in human bronchial carcinoma cells 20 - 40 minutes after exposure to 4 Gy of X-rays (605). Ionizing radiation also induced caveolin-1 expression and the formation of caveolin-1-positive caveolae in pancreatic cancer cells 12 and 24 h after exposure to 2 and 6 Gy of X-rays (606). Similarly, malignant glioma cells exposed to 10 Gy of X-rays underwent a 4.5 fold increase in caveolin-1 expression (607). However, caveolin-1 levels were found reduced at 96 h and 10 days after exposure in 10 Gy X-ray irradiated endothelial cells, which was linked to endothelial cell death and reduced clonogenic survival (597). It is evident that, based on our findings, functional validation of irradiation-altered endothelial adhesion and caveolar mediated endocytosis is now needed.

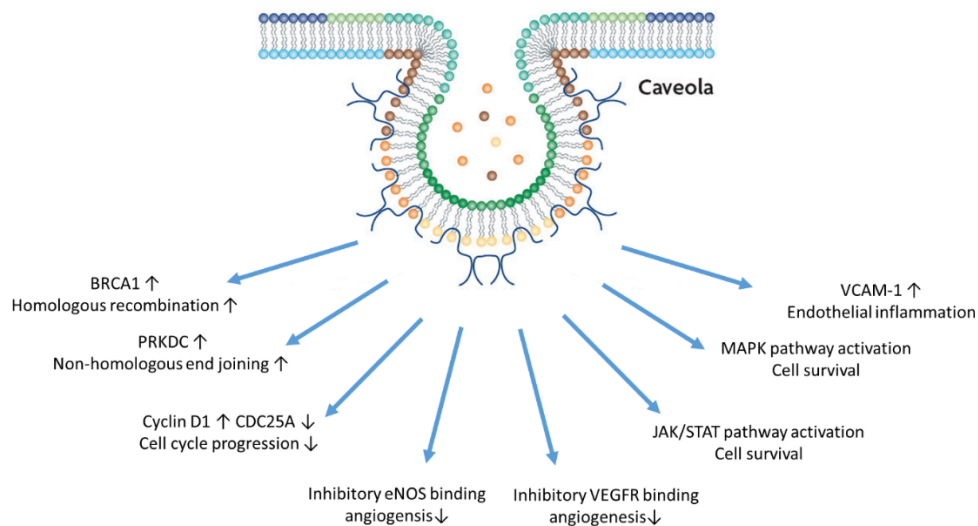


Figure 28. Overview of the wide range of caveolin-1 mechanisms, related to radiation sensitivity and cardiovascular disease. Caveolins (blue binding linkers) are integrated plasma membrane proteins, present in caveola, that are complex signaling regulators with numerous partners. By interacting with BRCA1, PRKDC, cyclin D1, *CDC25A* and affecting the JAK/STAT and MAPK signalling, caveolin is able to induce radiation resistance. In endothelial cells, caveolin is also linked to endothelial inflammation and reduced angiogenesis, indicating its link with endothelial dysfunction and CVD. Figure is partly based on (608).

Lastly, we report radiation quality-dependent effects on cytokine secretion by irradiated endothelial cells, and increased adhesiveness to monocytes. Briefly, X-ray irradiation induced an inflammatory state characterized by elevated levels of IL-6 and IL-8 with increased monocyte adhesion, similar to what was previously observed by others at higher doses (5 – 10 Gy) and/or after chronic exposure (4.1 mGy/h for 10 weeks) (571, 609-611). Unlike other observations using 2 and 5 Gy of Fe ions (612, 613), Fe ions in our hands induced no significant release of pro-inflammatory cytokines by endothelial cells and decreased endothelial monocyte adhesion. This observation could be due to loss of endothelial integrity caused by Fe ion irradiation.

In conclusion, our experimental work provides new knowledge on molecular events, potentially causes, of irradiation-induced CVD. When exposed to a single dose of radiation, endothelial cells indeed acquire a dose-, time- and radiation quality-dependent pro-atherosclerotic phenotype supported by transcriptional and

proteomic changes affecting cell cycling, senescence, inflammation, adhesion and endocytosis signaling. Our molecular data constitute an initial step in the exploration of these paradigms, and many more experiments are needed to confirm findings at molecular and functional levels and to explore these responses in different types of endothelial cells and in more complex *in vitro*, *ex vivo* and *in vivo* models. Although we did not identify whether or not a threshold exists between radiation dose and endothelial responses, we believe that our data could constitute a basis on which to build new knowledge in order to ultimately optimize radiation protection systems.

2. Preclinical significance

Our study evidenced the presence of a dose-, time- and radiation quality-dependent pro-atherosclerotic phenotype in irradiated endothelial cells. This conclusion was drawn using immortalized human endothelial cells derived from the coronary arteries, which were chosen as a model based on previous data that evidenced induction of coronary artery disease by ionizing radiation (145, 171, 210, 614). These immortalized endothelial cells were previously shown to retain the radiation responsiveness (519), genomic stability, and all major phenotypic markers of normal coronary endothelial cells. Human atherosclerosis is a chronic process (181) that can take up to 10 or more years to manifest after radiation exposure depending on the dose (148, 615). We therefore determined radiation-induced changes after short (1 day), intermediate (7 days) and long (14 days) timespans. Our data indicate that exposure to ionizing radiation induces initial endothelial activation and dysfunction, which can be linked to initiation of *de novo* and the progression of already existing atherosclerotic plaques. In our first study (365), X-ray doses ranged from low doses of 0.05 Gy and 0.1 Gy, which corresponds to doses given during repeated coronary CT angiographs (range: 5 mSv to 30 mSv per trial(616)), to intermediate dose of 0.5 Gy, which corresponds to the dose received by endothelial cells during irradiation of normal tissues outside the treated volume of patients treated by radiation, and to a high dose of 2 Gy, corresponding to a single fraction dose of radiotherapy given to malignant tissues (171, 617). We believe that these doses are clinically relevant seeing the increasing use of CT scans (618) as well as an increase in the incidence of myocardial infarction worldwide (619). Comparatively, the mean dose delivered to the heart during left breast cancer therapy is estimated to be around 4-8 Gy, with part of the heart and

probably the left anterior descending coronary artery receiving more than a total dose of 20 Gy in some patients undergoing fractionated radiotherapy (171, 620-622). To represent a normal physiological state of endothelial cells, we irradiated confluent endothelial cell cultures as they recapitulate the *in vivo* quiescent state. We did not use pro-inflammatory stimuli, such as TNF- α or LPS, to activate the cells prior to irradiation. Because our projects are part of the European 7th framework ProCardio project, our findings are intended to be integrated with other *in vitro*, *in vivo* and epidemiological data in order to increase the current understanding of radiation-induced CVDs.

Of important note, care should be taken about the clinical significance of our findings. Irradiation in our models was delivered to confluent cells, during which cell-cell contact normally induces a quiescent state. However, due to the presence of growth factors in media, cell division was maintained at a low rate and the resulting overconfluent state was not adapted for long term cultures. The maximal life-time of a confluent endothelial cell culture in our hands was 14 days, after which viability significantly decreased. Thus, in contrast to atherosclerosis that takes years to develop, we could only study mechanisms associated to atherosclerosis initiation and progression in a limited time frame. As endothelial cells do not readily divide in the human body (546) and proliferating cells are believed to be more sensitive than quiescent cells (116), cellular division in our endothelial models could also influence radiation outcome. Furthermore, studying a limited number of radiation-induced endothelial-derived factors *in vitro* evidently does not explain all the molecular mechanisms of a multifactorial and complex pathological condition such as atherosclerosis. Given the complex interactions of endothelial cells with other cell types in their microenvironment (*e.g.* fibroblasts, pericytes, VSMCs and circulating cells), our study does not appreciate all the molecular events leading to CVDs. In addition, our experimental data are relevant only to single radiation dose exposure within the available dose range, whereas dose fractionation is most often used in radiotherapy setting (617). Based on preliminary findings in our group, when the total dose given to endothelial cells is fractionated, this ameliorated the outcome of radiation exposure as cells have time to repair the induced cellular damage (Figure 29). Moreover, we cannot exclude differential effects at doses higher than 2 Gy after a single dose irradiation. Based on the literature, one we can postulate that higher irradiation doses worsen cellular outcome after irradiation, leading to a higher probability to develop

atherosclerosis. For example, when compared to low doses, a single fraction of high doses (> 8 -10 Gy) of ionizing radiation has been shown to primarily induce endothelial cell death *via* ceramide-based mechanisms (443, 623). Lower dose effects (< 8 – 10 Gy) are more subtle and activate different pathways (386, 624). Previous work of our group showed that 5 Gy of X-rays induces more apoptosis and aberrant cellular morphology than a single dose \leq 0.5 Gy (449). In respect to irradiation beam quality, while Fe ion irradiation is a type of high LET radiation relevant for the space environment, it is not used for particle radiotherapy due its tendency for fragmentation, high LET values at entrance channel and the need for enormous accelerators to produce them. Nonetheless, they can provide valuable insights into the general effects of high LET exposure in endothelial cells. Of note, due to limited time access to an Fe ion irradiator, we could not yet validate the proteomic and transcriptomic data reported in results chapter 2. We believe that our findings nevertheless give a first line of understanding of radiation-induced endothelial effects necessary to evaluate protection of radiotherapy patients and astronauts in space.

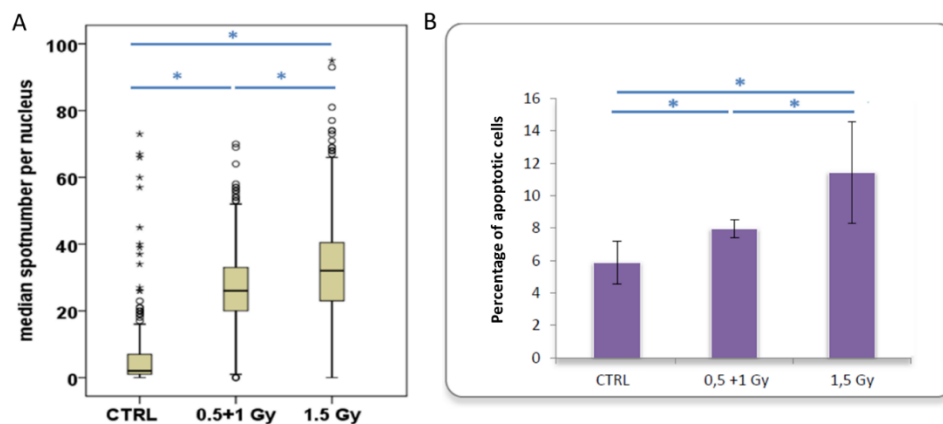


Figure 29. Dose fractionation results in reduced foci formation and apoptosis in EA.hy926 cells. A. Fractionation of a total dose of 1.5 Gy of X-rays leads to reduced levels of nuclear γ H2AX foci 30 min after radiation exposure, as measured by immunocytochemistry. Data show boxplots \pm minimum and maximum of all data (n = 4). **B.** Radiation dose fractionation induces less apoptosis in comparison to unfractionated higher dose, as measured with flowcytometric annexin-V/propidium iodide double staining (n = 6). Data show means \pm SEM. * p < 0.05 using two-sided t-test (Kruskal-Wallis). Time between repeated irradiation was 4 h. Data collected by Nerea Talavera Moreno.

In conclusion, we identified a dose-, time- and radiation quality-dependent pro-atherosclerotic phenotype induced by irradiation that can form a foundation on which to build new scientific knowledge in order to understand how ionizing radiations can induce CVD. With follow-up studies, this might in turn lead to the development of risk-reducing strategies, such as identification of pharmaceutical agents or detection methods (*e.g.* biomarkers) to prevent radiation-induced CVD. Future research may thus ameliorate the current radiation protection system, alleviating radiation-induced CVDs in exposed people.

3 Endothelial cells are a critical target for radiation-induced atherosclerosis

We focused on the endothelium as a key integrator of vascular risk and as the critical target of ionizing radiation. Endothelial activation and dysfunction are initiators of atherosclerosis, which, together with the response-to-injury theory that prevails in radiobiology, explained the occurrence of radiation-induced CVDs since many years (625-627). This view is based on *in vitro* and *in vivo* findings (628-630). However, the entire microenvironment of the endothelium is evidently irradiated as well and has the potential to be damaged by ionizing radiation. When comparing radiation sensitivity at doses between 2.5 and 20 Gy, it was observed that endothelial cells are more sensitive than VSMCs and fibroblasts (631-633). These cells do undergo the same acute irradiation effects as endothelial cells, such as a dose-dependent DNA damage, cell cycle block and micronuclei formation (395, 634-641). Conversely, fibrosis and SMC hypertrophy can also be a consequence of endothelial dysfunction (145, 147, 177), and fibrosis arrhythmia in heart known consequences of endothelial damage in the cardiac microcirculatory system (143, 642). Interactions between different cell types could further influence the response to ionizing radiations. For example, endothelial cells were shown to induce a more proliferative and fibrogenic phenotype in VSMCs after irradiation (341, 643). In conclusion, while different cell types in the vascular system determine the final outcome of blood vessel irradiation, the endothelium is able to process pathogenic signals that may converge to several common pathways in the genesis of CVD (313).

4. Future directions of research in the field of irradiation-induced atherosclerosis

4.1. Novel targets

In this work, we identified dose-, time-, and radiation quality dependent involvement of DNA damage, cell cycle blockage, inflammation, premature senescence, cell-cell adhesion and caveolar mediated endocytosis signaling in the endothelial cell response to ionizing radiation. These effects observed *in vitro* could provide a link between endothelial damage caused by irradiation and initiation and/or progression of atherosclerosis *in vivo*. However, it is a long way to bridge *in vitro* data to actual human responses to ionizing radiation. Differences in transcriptomics and proteomics related to cell-cell adhesion and caveolar mediated endocytosis should be initially validated with independent samples, including with different endothelial cell types. Furthermore, more complex *in vitro* cultures (2D and 3D coculture systems and spheroids containing perivascular cells such as fibroblasts and VSMCs), *ex vivo* and animal studies are needed, as they provide a step-forward in the translation of *in vitro* findings to the human situation. Care should be taken to select adapted animal models. In this context, porcine models are interesting as they spontaneously demonstrate atherosclerosis with a pathophysiology resembling that of humans. Using these models is, however, rather expensive. Candidate biomarkers related to the pathways that we identified in this study should be assessed in humans as well.

4.2. Biomarkers

Identification of biomarkers for radiation-related CVD would be of clinical value. A main interest lies in the detection of a panel of specific biomarkers that would enable early detection of radiation-induced CVD before the presentation of symptoms, with the possibility for early treatment and prevention (644, 645). Due to the multifactorial nature of CVD and the subtle effects of low dose radiation exposure, this aim has proven to be difficult to reach (644, 645). Because no single biomarker identified so far is specific of radiation-induced CVD, a panel of biomarkers should be assembled that would be specific and sensitive enough to detect radiation-induced defects. To increase its clinical utility, this panel should be obtained *via* easy manners of sampling, such as blood or saliva collection (644, 645). Although specific biomarkers were not identified in our project, several pathways were identified that may provide biomarkers upon further research. An interesting

tool to study endothelial function in patient blood samples is the detection of endothelial microparticles, heterogeneous (0.1-5 μm) vesicular structures derived from plasma membranes of activated or dying endothelial cells (646, 647). Structural and functional characterization of these microparticles after radiation exposure can prove valuable as they are also linked to chronic diseases such as coronary artery disease, diabetes and hypertension (648). In this context, the number of endothelial microparticles in 2D and 3D models was found to be increased after 5 Gy of X-rays (432), whereas others only identify a slight increase (649). Because these microparticles contain parts of the endothelial cytoplasm and cellular membrane, it would be interesting to explore content of inflammatory and senescence markers as a possible use as biomarker for radiation-related CVD. Traditional markers for cardiovascular disease risk already applied in the clinics should be tested as well. Examples of such biomarkers are lipoprotein A, apolipoprotein A1, apolipoprotein B, fibrinogen, N-terminal-pro-B-type natriuretic peptide, LDL-associated phospholipase A2, cardiac troponins I and T, C-reactive protein and the urine albumin/creatinine ratio (650). In addition to early detection, biomarkers could also in theory be used for implementation of strategies to reduce radiation-induced CVD risk by individual risk characterization and the development of countermeasures (644, 645). These strategies might prove valuable for exposed individuals, not only radiotherapy patients but also occupationally exposed individuals, radiologists and interventional cardiologists. Furthermore, biomarkers can be utilized in molecular epidemiological studies in order to improve the understanding of the pathogenesis and the risk estimation of radiation-induced circulatory disease at low doses (570).

4.3. Pharmaceutical agents

Radioprotectants can protect irradiated individuals against the development of detrimental radiation effects. This could be of importance for cancer patients undergoing radiotherapy, and also for accidentally or occupationally exposed individuals receiving smaller doses of ionizing radiation. Several radioprotective strategies exist, from reducing the amount of oxidative stress to maintaining genomic integrity in the affected cells (651-653). When used to reduce normal tissue toxicity during radiotherapy, care should be taken that the radioprotectant is selective for protecting normal tissues but not tumors, can be delivered with relative ease and with minimal toxicity and is able to protect normal tissues that

are considered to be the most sensitive (651). Due to organ and tissue-specific factors that include radiation sensitivity, cellular turnover rate and differences in mechanisms of injury manifestation and damage response, successful development of radioprotectants should address these site-specific differences (652).

While a number of compounds meet most or all of these criteria in preclinical studies or in early clinical trials (651), to date only amifostine is approved for clinical prevention of mouth dryness during fractionated radiotherapy (654, 655). Amifostine is a prodrug that needs to be dephosphorylated to its active form WR-1065 by intracellular membrane-bound alkaline phosphatases, (656). Once dephosphorylated, the agent acts as a free radical scavenger targeting *e.g.* superoxide and nitric oxide (651). It has a preference for normal *versus* tumor tissues (657), presumably due to tumor acidosis, aberrant tumor blood flow and lower expression of alkaline phosphatase by tumor blood vessels (658). Amifostine has been shown to provide radiation protection to *in vitro* human microvascular endothelial cells after exposure to a single dose of 10 and 20 Gy (659, 660), murine salivary glands after exposures to 100-141MBq Technetium-99 (661). In addition, amifostine is also able to protect against formation of acute radiation-induced dermatitis (662), nephrotoxicity (663) and esophagitis(664) in patients. By changing the redox state of endothelial cells, it can also inhibit endothelial activation by attenuating NF- κ B activation (665). It also has anti-angiogenic effects by reducing the expression and activity of VEGF (666-669), and has proven useful in the context of radiation-induced CVD as it reduces radiation-induced fibrosis, restores cardiac output and abolishes the effect of ionizing radiation on coronary and aortic flow in the irradiated rat heart, abolishing most of these effects after high single dose exposure (up to 22.5 Gy) (670). Unfortunately, current data do not support its use in chemoradiotherapy (654), and concerns about tumor protection and normal tissue toxicity have led to controversy regarding appropriate setting for its use (671). As amifostine experimentally showed some potential benefit in preventing morphologic and functional deterioration of the cardiovascular system, future research is warranted to demonstrate its clinical usefulness in the context of irradiation-induced CVD.

We also evidenced endothelial activation after radiation exposure, leading to elevated levels of secreted IL-6 and CCL2. Interestingly, amifostine reduces NF- κ B activity in endothelial cells, thereby attenuating their pro-inflammatory

phenotype (665). Another option for radioprotection is to use non-specific anti-inflammatory drugs, such as methylprednisolone and ibuprofen. Both were shown to reduce radiation-induced heart disease in rabbits, but studies on their clinical usefulness are still lacking (672). In one of our ongoing studies, hydrocortisone showed potential to decrease irradiation-induced endothelial senescence, which might be linked to inhibition of endothelial inflammation (673). Besides general anti-inflammatory drugs, IL-6 and CCL-2 levels could also be reduced directly by the use of blocking antibodies. Siltuximab is a chimeric anti-IL-6 monoclonal antibody in phase I and II clinical trials for adjuvant treatment of multiple myeloma (674) and prostate cancer (675). It holds promise as an adjuvant cancer therapy, and may also prove valuable for protecting the heart and its vessels from radiation-induced defects. Carlumab, an anti-CCL2 monoclonal antibody, is also currently tested as an anti-inflammatory agent in clinical trials in patients with prostate cancer (676, 677). This monoclonal antibody is well-tolerated by patients, but only decreases free CCL2 serum concentrations for a brief duration, after which it stimulates CCL2 secretion to levels exceeding those before delivery (rebound effect) (677). As an alternative to CCL2 inhibition, it would be wise to target CCL2 receptors or downstream intracellular signaling intermediates (677). It is crucial, however, to verify that anti-inflammatory therapies do not influence the antitumor response by changing the composition of the tumor inflammatory microenvironment that has a pivotal influence on disease outcome (678).

Finally, our data indicate that X-ray radiotherapy can induce endothelial senescence. Because senescence can cause tissue dysfunction, blocking radiation-induced senescence has the potential to preserve normal tissue biological activities (679). In the context of radiation-induced increase in IGFBP7 secretion by endothelial cells, abrogation of insulin-like growth factor-1 receptor (IGF-1R) signaling has been shown to prevent irradiation-induced primary endothelial cell senescence (680). In addition, IGF-1R-targeting monoclonal antibodies and small molecule tyrosine kinase inhibitors against the IGF-1R pathway are in phase I and II clinical trials for patients with non-small cell lung cancer, breast cancer, and pancreatic cancer (681, 682). The PI3K/Akt/mTOR pathway is also involved in endothelial senescence (526, 528, 577) and could be targeted therapeutically. For instance, pharmacological inhibition of mTOR in epithelial stem cells has been shown to be sufficient to prevent radiation-induced senescence (683). Statins, which are known for their cholesterol-lowering action, can also prevent endothelial

senescence (684, 685). To determine whether statins could reduce radiation-induced endothelial senescence, we recently tested atorvastatin. We observed signs of decreased endothelial senescence, but these data are too preliminary to reach significance. Of note, some clinical evidence also suggests beneficial effect of a statins on the treatment of prostate (686), liver (687), colorectal (688) cancer, although exact mechanisms and targets are to date unknown. Randomized, placebo-controlled clinical trials are warranted because available data are largely derived from observational case-control studies (686).

The use of pharmaceutical agents to protect or mitigate normal tissues from damage after radiation exposure may have the ability to minimize radiation toxicity for patients and may provide a treatment option for accidentally exposed individuals. Important considerations in the development of these agents are evidenced efficacy, absence of tumor protection and acceptable toxicity levels (652, 689). As chronic treatment with amifostine, ibuprofen and other drugs listed above induces severe normal tissue toxicity (671, 690), their clinical applicability should be restricted to the treatment of radiation-induced injury. As a consequence, the best approach to minimize the impact of radiation toxicity on the quality of life in patients still remains preventive strategies (652, 689). In respect to irradiation-induced CVD, radiotherapy treatment should be accompanied by a reduction in lifestyle-associated CVD risks for patients. Strategies should be individually tailored and should focus on the implementation of a healthy diet, increasing physical activity, smoking cessation, limited alcohol use, treating hypertension, lowering too high total cholesterol levels and losing weight when having a high BMI (691-693).

4.4 Impact on clinical practice and radiation protection system

Our data on the dose-, time- and radiation quality-dependent molecular changes of the endothelial cell response to ionizing radiation could prove valuable for the clinical practice in the future. The identified involvement of DNA damage, cell cycle blockage, inflammation, premature senescence, cell-cell adhesion and caveolar mediated endocytosis signaling could urge new research projects aimed at better detailing the endothelial cell response to ionizing radiation and its relation to ionizing radiation-related CVDs, especially at low doses. Our findings after independent confirmation could also be used to identify druggable targets in order to prevent the occurrence of CVD after accidental, occupational or therapeutic

exposure to ionizing radiation. Although we cannot conclude from our data that there is no threshold effect of irradiation-induced cardiovascular risk, our findings give an incentive for further research on the shape of the dose-response curve. However, a lot of unanswered questions need to be answered before one can speak of a proper radiation protection system. Open questions notably are: which dose of ionizing radiation requires protection? In which case is it justified to use a high therapeutic dose of ionizing radiation? Is there a patient heterogeneity in respect to the development of irradiation-induced CVD?

5. General conclusion

The molecular mechanisms accounting for the cardiovascular effects observed after ionizing radiation exposure are not completely understood and need to be elucidated to optimize the current radiation protection system. We show that ionizing radiation induces pro-atherosclerotic processes in endothelial cells in a dose-, time- and radiation quality-dependent manner. Functional gene analysis revealed cell cycle changes and inflammation in endothelial cells irradiated with a single X-ray dose. In addition, premature endothelial senescence at later time points was evidenced even at low doses. Dedicated gene and protein analysis indicated a more pronounced and longer lasting radiation impact for Fe ions than for X-rays, linked with loss of endothelial integrity and signaling in caveolar mediated endocytosis signaling and endothelial adhesion. These findings may form the basis for new experimental research into the molecular mechanisms underlying the pathogenesis of radiation-induced CVD.

References

1. Hall EJ, Giaccia AJ. Radiobiology for the radiologist. 7th ed. Philadelphia: Lippincott, Williams & Wilkins; 2012.
2. Martin A, Harbison S, Beach K, Cole P. An Introduction to Radiation Protection. 6th ed. London: Hodder Arnold; 2012. 256 p.
3. Dendy PP, Heaton B. Physics for diagnostic radiology. 3rd ed. Bosa Roca, US: Taylor & Francis Inc; 2012. 695 p.
4. Kudriashov IB, Kudriashov YB. Radiation Biophysics (Ionizing radiations). 1st ed. New York: Nova Science Publishers Inc 2008. 327 p.
5. Maalouf M, Durante M, Foray N. Biological effects of space radiation on human cells: history, advances and outcomes. *J Radiat Res.* 2011;52(2):126-46.
6. Durante M, Loeffler JS. Charged particles in radiation oncology. *Nat Rev Clin Oncol.* 2010;7(1):37-43.
7. Zagorski ZP, Kornacka EM. Ionizing radiation: friend or foe of the origins of life? *Orig Life Evol Biosph.* 2012;42(5):503-5.
8. ICRP. The 2007 Recommendations of the International Commission on Radiological Protection. ICRP Publication 103. *Ann ICRP.* 2007;37(2-4).
9. Einstein AJ. Effects of radiation exposure from cardiac imaging: how good are the data? *J Am Coll Cardiol.* 2012;59(6):553-65.
10. Lin EC. Radiation risk from medical imaging. *Mayo Clin Proc.* 2010;85(12):1142-6; quiz 6.
11. Mullenders L, Atkinson M, Paretzke H, Sabatier L, Bouffler S. Assessing cancer risks of low-dose radiation. *Nat Rev Cancer.* 2009;9(8):596-604.
12. Brenner DJ, Doll R, Goodhead DT, Hall EJ, Land CE, Little JB, et al. Cancer risks attributable to low doses of ionizing radiation: assessing what we really know. *Proc Natl Acad Sci U S A.* 2003;100(24):13761-6.
13. Paterick TE, Jan MF, Paterick ZR, Tajik AJ, Gerber TC. Cardiac imaging modalities with ionizing radiation: the role of informed consent. *JACC: Cardiovascular Imaging* 2012;5(6):634-40.
14. ICRP. The 2007 Recommendations of the International Commission on Radiological Protection. ICRP publication 103. *Ann ICRP.* 2007;37(2-4):1-332.
15. Fazel R, Krumholz HM, Wang Y, Ross JS, Chen J, Ting HH, et al. Exposure to low-dose ionizing radiation from medical imaging procedures. *N Engl J Med.* 2009;361(9):849-57.
16. Wilson RR. Radiological use of fast protons. *Radiology.* 1946;47(5):487-91.
17. Joiner M, Kogel Avd. Basic clinical radiobiology. 4th ed. London: Hodder Arnold; 2009. 375 p.

18. Task Group on Radiation Quality Effects in Radiological Protection CoREICoRP. Relative biological effectiveness (RBE), quality factor (Q), and radiation weighting factor ($w(R)$). A report of the International Commission on Radiological Protection. *Ann ICRP*. 2003;33(4):1-117.
19. Advisory Group on Ionising Radiation. Circulatory disease risk. Chilton; 2010.
20. Committee to Assess Health Risks from Exposure to Low Levels of Ionizing Radiation. National Research Council. Health Risks from Exposure to Low Levels of Ionizing Radiation: BEIR VII - Phase 2. Washington, DC: National Academy Press; 2006. p. 1–406.
21. McGuire S. World Cancer Report 2014. Geneva, Switzerland: World Health Organization, International Agency for Research on Cancer, WHO Press, 2015. *Adv Nutr*. 2016;7(2):418-9.
22. Dale RG, Jones B, Carabe-Fernandez A. Why more needs to be known about RBE effects in modern radiotherapy. *Appl Radiat Isot*. 2009;67(3):387-92.
23. Sikora K, Price P. Treatment of cancer. 6th ed. Boca Raton: CRC Press, Taylor & Francis Group; 2015. 825 p.
24. Lievens Y, Grau C. Health economics in radiation oncology: introducing the ESTRO HERO project. *Radiother Oncol*. 2012;103(1):109-12.
25. Schulz-Ertner D, Tsujii H. Particle radiation therapy using proton and heavier ion beams. *J Clin Oncol*. 2007;25(8):953-64.
26. Kramer M, Weyrather WK, Scholz M. The increased biological effectiveness of heavy charged particles: from radiobiology to treatment planning. *Technol Cancer Res Treat*. 2003;2(5):427-36.
27. Skarsgard LD. Radiobiology with heavy charged particles: a historical review. *Phys Med*. 1998;14 Suppl 1:1-19.
28. Benton ER, Benton EV. Space radiation dosimetry in low-Earth orbit and beyond. *Nucl Instrum Methods Phys Res B*. 2001;184(1-2):255-94.
29. Moding EJ, Kastan MB, Kirsch DG. Strategies for optimizing the response of cancer and normal tissues to radiation. *Nat Rev Drug Discov*. 2013;12(7):526-42.
30. Reisz JA, Bansal N, Qian J, Zhao W, Furdui CM. Effects of ionizing radiation on biological molecules--mechanisms of damage and emerging methods of detection. *Antioxid Redox Signal*. 2014;21(2):260-92.
31. Munro TR. The site of the target region for radiation-induced mitotic delay in cultured mammalian cells. *Radiat Res*. 1970;44(3):747-57.
32. Barnett GC, West CM, Dunning AM, Elliott RM, Coles CE, Pharoah PD, et al. Normal tissue reactions to radiotherapy: towards tailoring treatment dose by genotype. *Nat Rev Cancer*. 2009;9(2):134-42.
33. Mitchell G. The rationale for fractionation in radiotherapy. *Clin J Oncol Nurs*. 2013;17(4):412-7.

34. Corner J, Bailey C. Cancer nursing: care in context. 2nd ed. Oxford ; Malden, MA: Blackwell Pub.; 2008. 724 p.
35. Cox JD, Ang KK. Radiation oncology: rationale, technique, results. 9th ed. Philadelphia: Mosby; 2010. 1072 p.
36. Pawlik TM, Keyomarsi K. Role of cell cycle in mediating sensitivity to radiotherapy. *Int J Radiat Oncol Biol Phys.* 2004;59(4):928-42.
37. Fyles A, Milosevic M, Hedley D, Pintilie M, Levin W, Manchul L, et al. Tumor hypoxia has independent predictor impact only in patients with node-negative cervix cancer. *J Clin Oncol.* 2002;20(3):680-7.
38. Gray LH, Conger AD, Ebert M, Hornsey S, Scott OCA. The Concentration of Oxygen Dissolved in Tissues at the Time of Irradiation as a Factor in Radiotherapy. *The British Journal of Radiology.* 1953;26(312):638-48.
39. Zolzer F, Streffer C. Increased radiosensitivity with chronic hypoxia in four human tumor cell lines. *Int J Radiat Oncol Biol Phys.* 2002;54(3):910-20.
40. Harrington K, Jankowska P, Hingorani M. Molecular biology for the radiation oncologist: the 5Rs of radiobiology meet the hallmarks of cancer. *Clin Oncol (R Coll Radiol).* 2007;19(8):561-71.
41. Bese NS, Sut PA, Ober A. The effect of treatment interruptions in the postoperative irradiation of breast cancer. *Oncology.* 2005;69(3):214-23.
42. Ng W-L, Huang Q, Liu X, Zimmerman M, Li F, Li C-Y. Molecular mechanisms involved in tumor repopulation after radiotherapy. *Translational cancer research.* 2013;2(5):442-8.
43. OpenStax. Chemistry.2016. Date Accessed:29 May 2017. Available from: <https://opentextbc.ca/chemistry/>.
44. Kempner ES. Direct Effects of Ionizing Radiation on Macromolecules. *J Polym Sci B Polym Phys.* 2011;49(12):827-31.
45. Le Caër S. Water Radiolysis: Influence of Oxide Surfaces on H₂ Production under Ionizing Radiation. *Water.* 2011;3(1):235.
46. Ahmad SI. Reactive oxygen species in biology and human health. Boca Raton: CRC Press, Taylor & Francis Group; 2016. 543 p.
47. Azzam EI, Jay-Gerin JP, Pain D. Ionizing radiation-induced metabolic oxidative stress and prolonged cell injury. *Cancer Lett.* 2012;327(1-2):48-60.
48. Singh A, Singh H. Time-scale and nature of radiation-biological damage: approaches to radiation protection and post-irradiation therapy. *Progress in biophysics and molecular biology.* 1982;39(2):69-107.
49. Reth M. Hydrogen peroxide as second messenger in lymphocyte activation. *Nat Immunol.* 2002;3(12):1129-34.
50. Halliwell B, Clement MV, Long LH. Hydrogen peroxide in the human body. *FEBS Lett.* 2000;486(1):10-3.
51. Halliwell B, Gutteridge JM. Role of free radicals and catalytic metal ions in human disease: an overview. *Methods Enzymol.* 1990;186:1-85.

52. Jay-Gerin JP, Ferradini C. Are there protective enzymatic pathways to regulate high local nitric oxide (NO) concentrations in cells under stress conditions? *Biochimie*. 2000;82(2):161-6.
53. Shah AM, Channon KM. Free radicals and redox signalling in cardiovascular disease. *Heart*. 2004;90(5):486-7.
54. D'Autreaux B, Toledano MB. ROS as signalling molecules: mechanisms that generate specificity in ROS homeostasis. *Nat Rev Mol Cell Biol*. 2007;8(10):813-24.
55. Ganguly NK. *Studies on respiratory disorders*. New York: Humana Press; 2014. 394 p.
56. Holmstrom KM, Finkel T. Cellular mechanisms and physiological consequences of redox-dependent signalling. *Nat Rev Mol Cell Biol*. 2014;15(6):411-21.
57. Brieger K, Schiavone S, Miller FJ, Jr., Krause KH. Reactive oxygen species: from health to disease. *Swiss Med Wkly*. 2012;142:w13659.
58. Aprioku JS. Pharmacology of free radicals and the impact of reactive oxygen species on the testis. *J Reprod Infertil*. 2013;14(4):158-72.
59. Zelko IN, Mariani TJ, Folz RJ. Superoxide dismutase multigene family: a comparison of the CuZn-SOD (SOD1), Mn-SOD (SOD2), and EC-SOD (SOD3) gene structures, evolution, and expression. *Free Radic Biol Med*. 2002;33(3):337-49.
60. Mannervik B. The enzymes of glutathione metabolism: an overview. *Biochem Soc Trans*. 1987;15(4):717-8.
61. Powis G, Montfort WR. Properties and biological activities of thioredoxins. *Annu Rev Biophys Biomol Struct*. 2001;30:421-55.
62. Arner ES, Holmgren A. Physiological functions of thioredoxin and thioredoxin reductase. *Eur J Biochem*. 2000;267(20):6102-9.
63. Wood ZA, Schroder E, Robin Harris J, Poole LB. Structure, mechanism and regulation of peroxiredoxins. *Trends Biochem Sci*. 2003;28(1):32-40.
64. Hall A, Nelson K, Poole LB, Karplus PA. Structure-based insights into the catalytic power and conformational dexterity of peroxiredoxins. *Antioxid Redox Signal*. 2011;15(3):795-815.
65. Chae HZ, Kim HJ, Kang SW, Rhee SG. Characterization of three isoforms of mammalian peroxiredoxin that reduce peroxides in the presence of thioredoxin. *Diabetes Res Clin Pract*. 1999;45(2-3):101-12.
66. Rhee SG. Overview on Peroxiredoxin. *Mol Cells*. 2016;39(1):1-5.
67. Department of Biochemistry. Accessed on 29 May 2017. Available from: <http://biochem.otago.ac.nz/our-people/academic-teaching-staff/liz-ledgerwood/>.
68. Pastore A, Federici G, Bertini E, Piemonte F. Analysis of glutathione: implication in redox and detoxification. *Clin Chim Acta*. 2003;333(1):19-39.

69. Meister A. Glutathione metabolism and its selective modification. *J Biol Chem.* 1988;263(33):17205-8.
70. Padayatty SJ, Katz A, Wang Y, Eck P, Kwon O, Lee JH, et al. Vitamin C as an antioxidant: evaluation of its role in disease prevention. *J Am Coll Nutr.* 2003;22(1):18-35.
71. Meister A. Glutathione-ascorbic acid antioxidant system in animals. *J Biol Chem.* 1994;269(13):9397-400.
72. Traber MG, Atkinson J. Vitamin E, antioxidant and nothing more. *Free Radic Biol Med.* 2007;43(1):4-15.
73. Reiter R, Tang L, Garcia JJ, Munoz-Hoyos A. Pharmacological actions of melatonin in oxygen radical pathophysiology. *Life Sci.* 1997;60(25):2255-71.
74. Shenkin A. The key role of micronutrients. *Clin Nutr.* 2006;25(1):1-13.
75. Glantzounis GK, Tsimoyiannis EC, Kappas AM, Galaris DA. Uric acid and oxidative stress. *Curr Pharm Des.* 2005;11(32):4145-51.
76. Jansen T, Hortmann M, Oelze M, Opitz B, Steven S, Schell R, et al. Conversion of biliverdin to bilirubin by biliverdin reductase contributes to endothelial cell protection by heme oxygenase-1-evidence for direct and indirect antioxidant actions of bilirubin. *J Mol Cell Cardiol.* 2010;49(2):186-95.
77. Armstrong JS, Rajasekaran M, Hellstrom WJ, Sikka SC. Antioxidant potential of human serum albumin: role in the recovery of high quality human spermatozoa for assisted reproductive technology. *J Androl.* 1998;19(4):412-9.
78. McDermott JH. Antioxidant nutrients: current dietary recommendations and research update. *J Am Pharm Assoc (Wash).* 2000;40(6):785-99.
79. Martinez MC, Andriantsitohaina R. Reactive nitrogen species: molecular mechanisms and potential significance in health and disease. *Antioxid Redox Signal.* 2009;11(3):669-702.
80. Patwari P, Lee RT. Thioredoxins, mitochondria, and hypertension. *Am J Pathol.* 2007;170(3):805-8.
81. Brigelius-Flohe R. Glutathione peroxidases and redox-regulated transcription factors. *Biol Chem.* 2006;387(10-11):1329-35.
82. Johnson F, Giulivi C. Superoxide dismutases and their impact upon human health. *Mol Aspects Med.* 2005;26(4-5):340-52.
83. Huseby NE, Asare N, Wetting S, Mikkelsen IM, Mortensen B, Sveinbjornsson B, et al. Nitric oxide exposure of CC531 rat colon carcinoma cells induces gamma-glutamyltransferase which may counteract glutathione depletion and cell death. *Free Radic Res.* 2003;37(1):99-107.
84. Jeggo P. The role of the DNA damage response mechanisms after low-dose radiation exposure and a consideration of potentially sensitive individuals. *Radiat Res.* 2010;174(6):825-32.

85. Helleday T, Eshtad S, Nik-Zainal S. Mechanisms underlying mutational signatures in human cancers. *Nat Rev Genet.* 2014;15(9):585-98.
86. Murphy MP. How mitochondria produce reactive oxygen species. *Biochem J.* 2009;417(1):1-13.
87. De Zio D, Cianfanelli V, Cecconi F. New insights into the link between DNA damage and apoptosis. *Antioxid Redox Signal.* 2013;19(6):559-71.
88. Bekker-Jensen S, Mailand N. Assembly and function of DNA double-strand break repair foci in mammalian cells. *DNA Repair (Amst).* 2010;9(12):1219-28.
89. Jackson SP. Sensing and repairing DNA double-strand breaks. *Carcinogenesis.* 2002;23(5):687-96.
90. Richardson C, Jasin M. Frequent chromosomal translocations induced by DNA double-strand breaks. *Nature.* 2000;405(6787):697-700.
91. Vamvakas S, Vock EH, Lutz WK. On the role of DNA double-strand breaks in toxicity and carcinogenesis. *Crit Rev Toxicol.* 1997;27(2):155-74.
92. Khanna KK, Jackson SP. DNA double-strand breaks: signaling, repair and the cancer connection. *Nat Genet.* 2001;27(3):247-54.
93. Medici Enterprises. Accessed on 2017-05-29. Available from: <http://medicenterprises.com/2013/09/07/fukushima-danger-myths-and-realities-exposed-9713/>.
94. Sulli G, Di Micco R, d'Adda di Fagagna F. Crosstalk between chromatin state and DNA damage response in cellular senescence and cancer. *Nat Rev Cancer.* 2012;12(10):709-20.
95. Zhang J, de Toledo SM, Pandey BN, Guo G, Pain D, Li H, et al. Role of the translationally controlled tumor protein in DNA damage sensing and repair. *Proc Natl Acad Sci U S A.* 2012;109(16):E926-33.
96. Kinner A, Wu W, Staudt C, Iliakis G. Gamma-H2AX in recognition and signaling of DNA double-strand breaks in the context of chromatin. *Nucleic Acids Res.* 2008;36(17):5678-94.
97. Fernandez-Capetillo O, Lee A, Nussenzweig M, Nussenzweig A. H2AX: the histone guardian of the genome. *DNA Repair (Amst).* 2004;3(8-9):959-67.
98. Kobayashi J, Tauchi H, Chen B, Burma S, Tashiro S, Matsuura S, et al. Histone H2AX participates the DNA damage-induced ATM activation through interaction with NBS1. *Biochem Biophys Res Commun.* 2009;380(4):752-7.
99. Rogakou EP, Boon C, Redon C, Bonner WM. Megabase chromatin domains involved in DNA double-strand breaks in vivo. *J Cell Biol.* 1999;146(5):905-16.
100. Rogakou EP, Pilch DR, Orr AH, Ivanova VS, Bonner WM. DNA double-stranded breaks induce histone H2AX phosphorylation on serine 139. *J Biol Chem.* 1998;273(10):5858-68.

101. Kuo LJ, Yang LX. Gamma-H2AX - a novel biomarker for DNA double-strand breaks. *In Vivo*. 2008;22(3):305-9.
102. Rothkamm K, Lobrich M. Evidence for a lack of DNA double-strand break repair in human cells exposed to very low x-ray doses. *Proc Natl Acad Sci U S A*. 2003;100(9):5057-62.
103. de Feraudy S, Revet I, Bezrookove V, Feeney L, Cleaver JE. A minority of foci or pan-nuclear apoptotic staining of gammaH2AX in the S phase after UV damage contain DNA double-strand breaks. *Proc Natl Acad Sci U S A*. 2010;107(15):6870-5.
104. Ciccio A, Elledge SJ. The DNA damage response: making it safe to play with knives. *Mol Cell*. 2010;40(2):179-204.
105. Horn S, Barnard S, Rothkamm K. Gamma-H2AX-based dose estimation for whole and partial body radiation exposure. *PLoS One*. 2011;6(9):e25113.
106. Redon CE, Weyemi U, Parekh PR, Huang D, Burrell AS, Bonner WM. gamma-H2AX and other histone post-translational modifications in the clinic. *Biochim Biophys Acta*. 2012;1819(7):743-56.
107. Solier S, Sordet O, Kohn KW, Pommier Y. Death receptor-induced activation of the Chk2- and histone H2AX-associated DNA damage response pathways. *Mol Cell Biol*. 2009;29(1):68-82.
108. Panier S, Boulton SJ. Double-strand break repair: 53BP1 comes into focus. *Nat Rev Mol Cell Biol*. 2014;15(1):7-18.
109. Lane DP. Cancer. p53, guardian of the genome. *Nature*. 1992;358(6381):15-6.
110. Bartek J, Lukas J. Chk1 and Chk2 kinases in checkpoint control and cancer. *Cancer Cell*. 2003;3(5):421-9.
111. Jeggo P, Lavin MF. Cellular radiosensitivity: how much better do we understand it? *Int J Radiat Biol*. 2009;85(12):1061-81.
112. Chowdhury D, Choi YE, Brault ME. Charity begins at home: non-coding RNA functions in DNA repair. *Nat Rev Mol Cell Biol*. 2013;14(3):181-9.
113. Bartek J, Lukas J. Pathways governing G1/S transition and their response to DNA damage. *FEBS Lett*. 2001;490(3):117-22.
114. Weber TS, Jaehnert I, Schichor C, Or-Guil M, Carneiro J. Quantifying the length and variance of the eukaryotic cell cycle phases by a stochastic model and dual nucleoside pulse labelling. *PLoS Comput Biol*. 2014;10(7):e1003616.
115. Lobrich M, Jeggo PA. The impact of a negligent G2/M checkpoint on genomic instability and cancer induction. *Nat Rev Cancer*. 2007;7(11):861-9.
116. Sinclair WK, Morton RA. X-ray sensitivity during the cell generation cycle of cultured Chinese hamster cells. *Radiat Res*. 1966;29(3):450-74.

117. Comprehensive System for Life Science Education. A comprehensive approach to life science.2011. Available from: <http://csls-text3.c.u-tokyo.ac.jp/>.
118. Surova O, Zhivotovsky B. Various modes of cell death induced by DNA damage. *Oncogene*. 2013;32(33):3789-97.
119. Golstein P, Kroemer G. Cell death by necrosis: towards a molecular definition. *Trends Biochem Sci*. 2007;32(1):37-43.
120. Panganiban RA, Snow AL, Day RM. Mechanisms of radiation toxicity in transformed and non-transformed cells. *Int J Mol Sci*. 2013;14(8):15931-58.
121. Kong Y, Cui H, Ramkumar C, Zhang H. Regulation of senescence in cancer and aging. *J Aging Res*. 2011;2011:963172.
122. Minamino T, Komuro I. Vascular cell senescence: contribution to atherosclerosis. *Circ Res*. 2007;100(1):15-26.
123. Itahana K, Dimri G, Campisi J. Regulation of cellular senescence by p53. *Eur J Biochem*. 2001;268(10):2784-91.
124. Vitale I, Galluzzi L, Castedo M, Kroemer G. Mitotic catastrophe: a mechanism for avoiding genomic instability. *Nat Rev Mol Cell Biol*. 2011;12(6):385-92.
125. Eriksson D, Stigbrand T. Radiation-induced cell death mechanisms. *Tumour Biol*. 2010;31(4):363-72.
126. Rathore S, Datta G, Kaur I, Malhotra P, Mohmmmed A. Disruption of cellular homeostasis induces organelle stress and triggers apoptosis like cell-death pathways in malaria parasite. *Cell Death Dis*. 2015;6:e1803.
127. Maier P, Hartmann L, Wenz F, Herskind C. Cellular Pathways in Response to Ionizing Radiation and Their Targetability for Tumor Radiosensitization. *Int J Mol Sci*. 2016;17(1).
128. Elmore S. Apoptosis: a review of programmed cell death. *Toxicol Pathol*. 2007;35(4):495-516.
129. Muller M, Strand S, Hug H, Heinemann EM, Walczak H, Hofmann WJ, et al. Drug-induced apoptosis in hepatoma cells is mediated by the CD95 (APO-1/Fas) receptor/ligand system and involves activation of wild-type p53. *J Clin Invest*. 1997;99(3):403-13.
130. Harms K, Nozell S, Chen X. The common and distinct target genes of the p53 family transcription factors. *Cell Mol Life Sci*. 2004;61(7-8):822-42.
131. Sheard MA. Ionizing radiation as a response-enhancing agent for CD95-mediated apoptosis. *Int J Cancer*. 2001;96(4):213-20.
132. Scaffidi C, Fulda S, Srinivasan A, Friesen C, Li F, Tomaselli KJ, et al. Two CD95 (APO-1/Fas) signaling pathways. *EMBO J*. 1998;17(6):1675-87.
133. Chen YR, Meyer CF, Tan TH. Persistent activation of c-Jun N-terminal kinase 1 (JNK1) in gamma radiation-induced apoptosis. *J Biol Chem*. 1996;271(2):631-4.

134. Kolesnick R. The therapeutic potential of modulating the ceramide/sphingomyelin pathway. *J Clin Invest.* 2002;110(1):3-8.
135. Kolesnick RN. 1,2-Diacylglycerols but not phorbol esters stimulate sphingomyelin hydrolysis in GH3 pituitary cells. *J Biol Chem.* 1987;262(35):16759-62.
136. Okazaki T, Bell RM, Hannun YA. Sphingomyelin turnover induced by vitamin D3 in HL-60 cells. Role in cell differentiation. *J Biol Chem.* 1989;264(32):19076-80.
137. Lin T, Genestier L, Pinkoski MJ, Castro A, Nicholas S, Mogil R, et al. Role of acidic sphingomyelinase in Fas/CD95-mediated cell death. *J Biol Chem.* 2000;275(12):8657-63.
138. Ch'ang HJ, Maj JG, Paris F, Xing HR, Zhang J, Truman JP, et al. ATM regulates target switching to escalating doses of radiation in the intestines. *Nat Med.* 2005;11(5):484-90.
139. Verheij M, Ruiter GA, Zerp SF, van Blitterswijk WJ, Fuks Z, Haimovitz-Friedman A, et al. The role of the stress-activated protein kinase (SAPK/JNK) signaling pathway in radiation-induced apoptosis. *Radiother Oncol.* 1998;47(3):225-32.
140. Panayi ND, Mendoza EE, Breshears ES, Burd R. Aberrant Death Pathways in Melanoma. 2013. Accessed. In: *Aberrant Death Pathways in Melanoma, Recent Advances in the Biology, Therapy and Management of Melanoma* [Internet]. InTech. Available from: <https://www.intechopen.com/books/recent-advances-in-the-biology-therapy-and-management-of-melanoma/aberrant-death-pathways-in-melanoma>.
141. Thariat J, Hannoun-Levi JM, Sun Myint A, Vuong T, Gerard JP. Past, present, and future of radiotherapy for the benefit of patients. *Nat Rev Clin Oncol.* 2013;10(1):52-60.
142. Walker JS. *Permissible dose : a history of radiation protection in the twentieth century.* Berkeley: University of California Press; 2000. xii, 168 p.
143. Stewart JR, Fajardo LF. Radiation-induced heart disease. Clinical and experimental aspects. *Radiologic Clinics of North America.* 1971;9(3):511-31.
144. Stewart FA. Mechanisms and dose-response relationships for radiation-induced cardiovascular disease. *Ann ICRP.* 2012;41(3-4):72-9.
145. Schultz-Hector S, Trott KR. Radiation-induced cardiovascular diseases: is the epidemiologic evidence compatible with the radiobiologic data? *Int J Radiat Oncol Biol Phys.* 2007;67(1):10-8.
146. Clarke M, Collins R, Darby S, Davies C, Elphinstone P, Evans E, et al. Effects of radiotherapy and of differences in the extent of surgery for early breast

- cancer on local recurrence and 15-year survival: an overview of the randomised trials. *Lancet*. 2005;366(9503):2087-106.
147. Darby SC, Cutter DJ, Boerma M, Constine LS, Fajardo LF, Kodama K, et al. Radiation-related heart disease: current knowledge and future prospects. *Int J Radiat Oncol Biol Phys*. 2010;76(3):656-65.
 148. Darby SC, McGale P, Taylor CW, Peto R. Long-term mortality from heart disease and lung cancer after radiotherapy for early breast cancer: prospective cohort study of about 300,000 women in US SEER cancer registries. *Lancet Oncology*. 2005;6(8):557-65.
 149. McGale P, Darby SC, Hall P, Adolfsson J, Bengtsson NO, Bennet AM, et al. Incidence of heart disease in 35,000 women treated with radiotherapy for breast cancer in Denmark and Sweden. *Radiother Oncol*. 2011;100(2):167-75.
 150. Carr ZA, Land CE, Kleinerman RA, Weinstock RW, Stovall M, Griem ML, et al. Coronary heart disease after radiotherapy for peptic ulcer disease. *Int J Radiat Oncol Biol Phys*. 2005;61(3):842-50.
 151. Shimizu Y, Kodama K, Nishi N, Kasagi F, Suyama A, Soda M, et al. Radiation exposure and circulatory disease risk: Hiroshima and Nagasaki atomic bomb survivor data, 1950-2003. *BMJ*. 2010;340:b5349.
 152. Radiation AGol, editor *Circulatory disease risk. Report of the independent Advisory Group on Ionising Radiation 2010*: Health Protection Agency.
 153. Takahashi I, Abbott RD, Ohshita T, Takahashi T, Ozasa K, Akahoshi M, et al. A prospective follow-up study of the association of radiation exposure with fatal and non-fatal stroke among atomic bomb survivors in Hiroshima and Nagasaki (1980-2003). *BMJ Open*. 2012;2(1):e000654.
 154. Vrijheid M, Cardis E, Ashmore P, Auvinen A, Bae JM, Engels H, et al. Mortality from diseases other than cancer following low doses of ionizing radiation: results from the 15-Country Study of nuclear industry workers. *Int J Epidemiol*. 2007;36(5):1126-35.
 155. Muirhead CR, O'Hagan JA, Haylock RG, Phillipson MA, Willcock T, Berridge GL, et al. Mortality and cancer incidence following occupational radiation exposure: third analysis of the National Registry for Radiation Workers. *Br J Cancer*. 2009;100(1):206-12.
 156. Ashmore JP, Krewski D, Zielinski JM, Jiang H, Semenciw R, Band PR. First analysis of mortality and occupational radiation exposure based on the National Dose Registry of Canada. *Am J Epidemiol*. 1998;148(6):564-74.
 157. Ivanov VK, Maksioutov MA, Chekin SY, Petrov AV, Biryukov AP, Kruglova ZG, et al. The risk of radiation-induced cerebrovascular disease in Chernobyl emergency workers. *Health Phys*. 2006;90(3):199-207.

158. Azizova TV, Muirhead CR, Druzhinina MB, Grigoryeva ES, Vlasenko EV, Sumina MV, et al. Cardiovascular diseases in the cohort of workers first employed at Mayak PA in 1948-1958. *Radiat Res.* 2010;174(2):155-68.
159. Azizova TV, Day RD, Wald N, Muirhead CR, O'Hagan JA, Sumina MV, et al. The "clinic" medical-dosimetric database of Mayak production association workers: structure, characteristics and prospects of utilization. *Health Phys.* 2008;94(5):449-58.
160. Azizova TV, Muirhead CR, Moseeva MB, Grigoryeva ES, Vlasenko EV, Hunter N, et al. Ischemic heart disease in nuclear workers first employed at the Mayak PA in 1948-1972. *Health Phys.* 2012;103(1):3-14.
161. Krestinina LY, Epifanova S, Silkin S, Mikryukova L, Degteva M, Shagina N, et al. Chronic low-dose exposure in the Techa River Cohort: risk of mortality from circulatory diseases. *Radiation and environmental biophysics.* 2013;52(1):47-57.
162. Grosche B, Lackland DT, Land CE, Simon SL, Apsalikov KN, Pivina LM, et al. Mortality from cardiovascular diseases in the Semipalatinsk historical cohort, 1960-1999, and its relationship to radiation exposure. *Radiat Res.* 2011;176(5):660-9.
163. Chargari C, Riet F, Mazevet M, Morel E, Lepechoux C, Deutsch E. Complications of thoracic radiotherapy. *Presse Med.* 2013;42(9 Pt 2):e342-51.
164. Mancuso M, Pasquali E, Braga-Tanaka I, 3rd, Tanaka S, Pannicelli A, Giardullo P, et al. Acceleration of atherogenesis in ApoE^{-/-} mice exposed to acute or low-dose-rate ionizing radiation. *Oncotarget.* 2015;6(31):31263-71.
165. United Nations. Scientific Committee on the Effects of Atomic Radiation. Sources and effects of ionizing radiation : United Nations Scientific Committee on the Effects of Atomic Radiation : UNSCEAR 2008 report to the General Assembly, with scientific annexes. New York: United Nations; 2010.
166. United Nations. Scientific Committee on the Effects of Atomic Radiation. Sources and effects of ionizing radiation : United Nations Committee on the Effects of Atomic Radiation : UNSCEAR 1993 report to the General Assembly, with scientific annexes. New York: United Nations; 1993. 922 p.
167. Committee to assess Health Risks from Exposure to Low Levels of Ionizing Radiation Research NRC. Health risks from exposure to low levels of ionizing radiation: BEIR VII - Phase 2. 2006.
168. Martin CJ. The LNT model provides the best approach for practical implementation of radiation protection. *The British journal of radiology.* 2005;78:14-6.

169. Martin CJ, Sutton DG, West CM, Wright EG. The radiobiology/radiation protection interface in healthcare. *Journal of radiological protection: official journal of the Society for Radiological Protection*. 2009;29:A1-A20.
170. Hildebrandt G. Non-cancer diseases and non-targeted effects. *Mutat Res*. 2010;687(1-2):73-7.
171. Darby SC, Ewertz M, McGale P, Bennet AM, Blom-Goldman U, Bronnum D, et al. Risk of ischemic heart disease in women after radiotherapy for breast cancer. *N Engl J Med*. 2013;368(11):987-98.
172. Little MP, Azizova TV, Bazyka D, Bouffler SD, Cardis E, Chekin S, et al. Systematic review and meta-analysis of circulatory disease from exposure to low-level ionizing radiation and estimates of potential population mortality risks. *Environ Health Perspect*. 2012;120(11):1503-11.
173. UNSCEAR. UNSCEAR 2006 report: Volume 1, Annex B: epidemiological evaluation of cardiovascular diseases and other non-cancer diseases. 2006.
174. Wilkins E, Wilson L, Wickramasinghe K, Bhatnagar P, Leal J, Luengo-Fernandez R, et al. *European Cardiovascular Disease Statistics 2017*. European Heart Network, Brussels; 2017.
175. Montgomery JE, Brown JR. Metabolic biomarkers for predicting cardiovascular disease. *Journal of Vascular Health and Risk Management*. 2013;9:37-45.
176. Heidenreich PA, Kapoor JR. Radiation induced heart disease. *Heart*. 2009;95(3):252-8.
177. Adams MJ, Hardenbergh PH, Constine LS, Lipshultz SE. Radiation-associated cardiovascular disease. *Crit Rev Oncol Hematol*. 2003;45(1):55-75.
178. Adams MJ, Lipshultz SE, Schwartz C, Fajardo LF, Coen V, Constine LS. Radiation-associated cardiovascular disease: manifestations and management. *Semin Radiat Oncol*. 2003;13(3):346-56.
179. Taunk NK, Haffty BG, Kostis JB, Goyal S. Radiation-induced heart disease: pathologic abnormalities and putative mechanisms. *Front Oncol*. 2015;5:39.
180. Lusis AJ. Atherosclerosis. *Nature*. 2000;407(6801):233-41.
181. Libby P, Ridker PM, Hansson GK. Progress and challenges in translating the biology of atherosclerosis. *Nature*. 2011;473(7347):317-25.
182. Cullen P, Rauterberg J, Lorkowski S. The pathogenesis of atherosclerosis. *Handb Exp Pharmacol*. 2005(170):3-70.
183. Bentzon JF, Otsuka F, Virmani R, Falk E. Mechanisms of plaque formation and rupture. *Circ Res*. 2014;114(12):1852-66.
184. Osterud B, Bjorklid E. Role of monocytes in atherogenesis. *Physiol Rev*. 2003;83(4):1069-112.
185. Gottfried K-LD, Penn G, U.S. Nuclear Regulatory Commission. Medical Use Program., Institute of Medicine (U.S.). Committee for Review and Evaluation of the Medical Use Program of the Nuclear Regulatory

- Commission. Radiation in medicine : a need for regulatory reform. Washington, D.C.: National Academy Press; 1996. 308 p.
186. Reinders JG, Heijmen BJ, Olofsen-van Acht MJ, van Putten WL, Levendag PC. Ischemic heart disease after mantlefield irradiation for Hodgkin's disease in long-term follow-up. *Radiother Oncol.* 1999;51(1):35-42.
 187. Lee WC. Excess relative risk as an effect measure in case-control studies of rare diseases. *PLoS One.* 2014;10(4):e0121141.
 188. Azizova TV, Grigorieva ES, Hunter N, Pikulina MV, Moseeva MB. Risk of mortality from circulatory diseases in Mayak workers cohort following occupational radiation exposure. *J Radiol Prot.* 2015;35(3):517-38.
 189. Borghini A, Gianicolo EA, Picano E, Andreassi MG. Ionizing radiation and atherosclerosis: current knowledge and future challenges. *Atherosclerosis.* 2013;230(1):40-7.
 190. Yamada M, Wong FL, Fujiwara S, Akahoshi M, Suzuki G. Noncancer disease incidence in atomic bomb survivors, 1958-1998. *Radiat Res.* 2004;161(6):622-32.
 191. Grant EJ, Brenner A, Sugiyama H, Sakata R, Sadakane A, Utada M, et al. Solid Cancer Incidence among the Life Span Study of Atomic Bomb Survivors: 1958-2009. *Radiat Res.* 2017;187(5):513-37.
 192. Preston DL, Shimizu Y, Pierce DA, Suyama A, Mabuchi K. Studies of mortality of atomic bomb survivors. Report 13: Solid cancer and noncancer disease mortality: 1950-1997. *Radiat Res.* 2003;160(4):381-407.
 193. Little MP, Lipshultz SE. Low dose radiation and circulatory diseases: a brief narrative review. *Cardio-Oncology.* 2015;1(1):1-10.
 194. Simonetto C, Azizova TV, Grigoryeva ES, Kaiser JC, Schollnberger H, Eidemuller M. Ischemic heart disease in workers at Mayak PA: latency of incidence risk after radiation exposure. *PLoS One.* 2014;9(5):e96309.
 195. Boron WF, Boulpaep EL. *Medical physiology.* 3rd ed. Philadelphia, PA: Elsevier; 2017. 1297 p.
 196. Sender R, Fuchs S, Milo R. Revised Estimates for the Number of Human and Bacteria Cells in the Body. *PLoS Biol.* 2016;14(8):e1002533.
 197. Jaffe EA. Cell biology of endothelial cells. *Hum Pathol.* 1987;18(3):234-9.
 198. Fishman AP. Endothelium: a distributed organ of diverse capabilities. *Ann N Y Acad Sci.* 1982;401:1-8.
 199. Creager MA, Cooke JP, Mendelsohn ME, Gallagher SJ, Coleman SM, Loscalzo J, et al. Impaired vasodilation of forearm resistance vessels in hypercholesterolemic humans. *J Clin Invest.* 1990;86(1):228-34.
 200. Masumoto A, Hirooka Y, Hironaga K, Eshima K, Setoguchi S, Egashira K, et al. Effect of pravastatin on endothelial function in patients with coronary artery disease (cholesterol-independent effect of pravastatin). *Am J Cardiol.* 2001;88(11):1291-4.

201. Bragulat E, de la Sierra A, Antonio MT, Coca A. Endothelial dysfunction in salt-sensitive essential hypertension. *Hypertension*. 2001;37(2 Pt 2):444-8.
202. Yoshida M, Imaizumi T, Ando S, Hirooka Y, Harada S, Takeshita A. Impaired forearm vasodilatation by acetylcholine in patients with hypertension. *Heart Vessels*. 1991;6(4):218-23.
203. Gilligan DM, Guetta V, Panza JA, Garcia CE, Quyyumi AA, Cannon RO, 3rd. Selective loss of microvascular endothelial function in human hypercholesterolemia. *Circulation*. 1994;90(1):35-41.
204. Panza JA, Quyyumi AA, Brush JE, Jr., Epstein SE. Abnormal endothelium-dependent vascular relaxation in patients with essential hypertension. *N Engl J Med*. 1990;323(1):22-7.
205. Bergholm R, Leirisalo-Repo M, Vehkavaara S, Makimattila S, Taskinen MR, Yki-Jarvinen H. Impaired responsiveness to NO in newly diagnosed patients with rheumatoid arthritis. *Arterioscler Thromb Vasc Biol*. 2002;22(10):1637-41.
206. Datta D, Ferrell WR, Sturrock RD, Jadhav ST, Sattar N. Inflammatory suppression rapidly attenuates microvascular dysfunction in rheumatoid arthritis. *Atherosclerosis*. 2007;192(2):391-5.
207. Piper MK, Raza K, Nuttall SL, Stevens R, Toescu V, Heaton S, et al. Impaired endothelial function in systemic lupus erythematosus. *Lupus*. 2007;16(2):84-8.
208. Sari I, Okan T, Akar S, Cece H, Altay C, Secil M, et al. Impaired endothelial function in patients with ankylosing spondylitis. *Rheumatology (Oxford)*. 2006;45(3):283-6.
209. Deanfield J, Donald A, Ferri C, Giannattasio C, Halcox J, Halligan S, et al. Endothelial function and dysfunction. Part I: Methodological issues for assessment in the different vascular beds: a statement by the Working Group on Endothelin and Endothelial Factors of the European Society of Hypertension. *J Hypertens*. 2005;23(1):7-17.
210. Widmer RJ, Lerman A. Endothelial dysfunction and cardiovascular disease. *Glob Cardiol Sci Pract*. 2014;2014(3):291-308.
211. Davignon J, Ganz P. Role of endothelial dysfunction in atherosclerosis. *Circulation*. 2004;109(23 Suppl 1):III27-32.
212. Suwaidi JA, Hamasaki S, Higano ST, Nishimura RA, Holmes DR, Jr., Lerman A. Long-term follow-up of patients with mild coronary artery disease and endothelial dysfunction. *Circulation*. 2000;101(9):948-54.
213. OpenStax. *Anatomy and Physiology*. 2016. Date Accessed: 29 May 2017: OpenStax CNX. Available from: <http://cnx.org/contents/14fb4ad7-39a1-4eee-ab6e-3ef2482e3e22@8.24>.

214. Furchgott RF, Zawadzki JV. The obligatory role of endothelial cells in the relaxation of arterial smooth muscle by acetylcholine. *Nature*. 1980;288(5789):373-6.
215. Palmer RM, Ferrige AG, Moncada S. Nitric oxide release accounts for the biological activity of endothelium-derived relaxing factor. *Nature*. 1987;327(6122):524-6.
216. Furchgott RF. Studies on relaxation of rabbit aorta by sodium nitrite. The basis for the proposal that the acid activatable inhibitory factor from bovine retractor penis is inorganic nitrite and the endothelium-derived relaxing factor is nitric oxide. In: Vanhoutte PM, editor. *Vasodilatation : vascular smooth muscle, peptides, autonomic nerves, and endothelium*. New York: Raven Press; 1988. p. pp. 401-14.
217. Palmer RM, Ashton DS, Moncada S. Vascular endothelial cells synthesize nitric oxide from L-arginine. *Nature*. 1988;333(6174):664-6.
218. Kwon NS, Nathan CF, Stuehr DJ. Reduced biopterin as a cofactor in the generation of nitrogen oxides by murine macrophages. *J Biol Chem*. 1989;264(34):20496-501.
219. Hemmens B, Mayer B. Enzymology of nitric oxide synthases. *Methods Mol Biol*. 1998;100:1-32.
220. Sowa G, Pypaert M, Sessa WC. Distinction between signaling mechanisms in lipid rafts vs. caveolae. *Proc Natl Acad Sci U S A*. 2001;98(24):14072-7.
221. Gratton JP, Fontana J, O'Connor DS, Garcia-Cardena G, McCabe TJ, Sessa WC. Reconstitution of an endothelial nitric-oxide synthase (eNOS), hsp90, and caveolin-1 complex in vitro. Evidence that hsp90 facilitates calmodulin stimulated displacement of eNOS from caveolin-1. *J Biol Chem*. 2000;275(29):22268-72.
222. Drab M, Verkade P, Elger M, Kasper M, Lohn M, Lauterbach B, et al. Loss of caveolae, vascular dysfunction, and pulmonary defects in caveolin-1 gene-disrupted mice. *Science*. 2001;293(5539):2449-52.
223. Garcia-Cardena G, Fan R, Shah V, Sorrentino R, Cirino G, Papapetropoulos A, et al. Dynamic activation of endothelial nitric oxide synthase by Hsp90. *Nature*. 1998;392(6678):821-4.
224. McCabe TJ, Fulton D, Roman LJ, Sessa WC. Enhanced electron flux and reduced calmodulin dissociation may explain "calcium-independent" eNOS activation by phosphorylation. *J Biol Chem*. 2000;275(9):6123-8.
225. Fleming I, Busse R. Molecular mechanisms involved in the regulation of the endothelial nitric oxide synthase. *Am J Physiol Regul Integr Comp Physiol*. 2003;284(1):R1-12.
226. Forstermann U, Sessa WC. Nitric oxide synthases: regulation and function. *Eur Heart J*. 2012;33(7):829-37, 37a-37d.

227. Fleming I. Molecular mechanisms underlying the activation of eNOS. *Pflugers Arch.* 2010;459(6):793-806.
228. Forstermann U, Closs EI, Pollock JS, Nakane M, Schwarz P, Gath I, et al. Nitric oxide synthase isozymes. Characterization, purification, molecular cloning, and functions. *Hypertension.* 1994;23(6 Pt 2):1121-31.
229. Saha RN, Pahan K. Regulation of inducible nitric oxide synthase gene in glial cells. *Antioxid Redox Signal.* 2006;8(5-6):929-47.
230. Davies PF. Flow-mediated endothelial mechanotransduction. *Physiol Rev.* 1995;75(3):519-60.
231. Angus JA, Campbell GR, Cocks TM, Manderson JA. Vasodilatation by acetylcholine is endothelium-dependent: a study by sonomicrometry in canine femoral artery in vivo. *The Journal of physiology.* 1983;344:209-22.
232. Haberl RL, Anneser F, Villringer A, Einhaupl KM. Angiotensin II induces endothelium-dependent vasodilation of rat cerebral arterioles. *Am J Physiol.* 1990;258(6 Pt 2):H1840-6.
233. Ku DD. Mechanism of thrombin-induced endothelium-dependent coronary vasodilation in dogs: role of its proteolytic enzymatic activity. *J Cardiovasc Pharmacol.* 1986;8(1):29-36.
234. Houston DA, Burnstock G, Vanhoutte PM. Different P2-purinergic receptor subtypes of endothelium and smooth muscle in canine blood vessels. *J Pharmacol Exp Ther.* 1987;241(2):501-6.
235. Kennedy C, Delbro D, Burnstock G. P2-purinoceptors mediate both vasodilation (via the endothelium) and vasoconstriction of the isolated rat femoral artery. *Eur J Pharmacol.* 1985;107(2):161-8.
236. Antonio A, Rocha ESM. Coronary vasodilation produced by bradykinin on isolated mammalian heart. *Circ Res.* 1962;11:910-5.
237. Denninger JW, Marletta MA. Guanylate cyclase and the .NO/cGMP signaling pathway. *Biochim Biophys Acta.* 1999;1411(2-3):334-50.
238. Moncada S, Gryglewski R, Bunting S, Vane JR. An enzyme isolated from arteries transforms prostaglandin endoperoxides to an unstable substance that inhibits platelet aggregation. *Nature.* 1976;263(5579):663-5.
239. Majed BH, Khalil RA. Molecular mechanisms regulating the vascular prostacyclin pathways and their adaptation during pregnancy and in the newborn. *Pharmacol Rev.* 2012;64(3):540-82.
240. Marrelli SP. Mechanisms of endothelial P2Y(1)- and P2Y(2)-mediated vasodilatation involve differential [Ca²⁺]_i responses. *Am J Physiol Heart Circ Physiol.* 2001;281(4):H1759-66.
241. Rath G, Saliez J, Behets G, Romero-Perez M, Leon-Gomez E, Bouzin C, et al. Vascular hypoxic preconditioning relies on TRPV4-dependent calcium influx and proper intercellular gap junctions communication. *Arterioscler Thromb Vasc Biol.* 2012;32(9):2241-9.

242. Jia G, Durante W, Sowers JR. Endothelium-Derived Hyperpolarizing Factors: A Potential Therapeutic Target for Vascular Dysfunction in Obesity and Insulin Resistance. *Diabetes*. 2016;65(8):2118-20.
243. Mokhtar SS, Rasool AH. Role of endothelium-dependent hyperpolarisation and prostacyclin in diabetes. *Malays J Med Sci*. 2015;22(2):8-17.
244. Hickey KA, Rubanyi G, Paul RJ, Highsmith RF. Characterization of a coronary vasoconstrictor produced by cultured endothelial cells. *Am J Physiol*. 1985;248(5 Pt 1):C550-6.
245. Bouallegue A, Daou GB, Srivastava AK. Endothelin-1-induced signaling pathways in vascular smooth muscle cells. *Curr Vasc Pharmacol*. 2007;5(1):45-52.
246. Tsihlis ND, Oustwani CS, Vavra AK, Jiang Q, Keefer LK, Kibbe MR. Nitric oxide inhibits vascular smooth muscle cell proliferation and neointimal hyperplasia by increasing the ubiquitination and degradation of Ubch10. *Cell Biochem Biophys*. 2011;60(1-2):89-97.
247. Berk BC, Rao GN. Angiotensin II-induced vascular smooth muscle cell hypertrophy: PDGF A-chain mediates the increase in cell size. *J Cell Physiol*. 1993;154(2):368-80.
248. Yu SM, Hung LM, Lin CC. cGMP-elevating agents suppress proliferation of vascular smooth muscle cells by inhibiting the activation of epidermal growth factor signaling pathway. *Circulation*. 1997;95(5):1269-77.
249. Chen L, Daum G, Chitale K, Coats SA, Bowen-Pope DF, Eigenthaler M, et al. Vasodilator-stimulated phosphoprotein regulates proliferation and growth inhibition by nitric oxide in vascular smooth muscle cells. *Arterioscler Thromb Vasc Biol*. 2004;24(8):1403-8.
250. Pifarre P, Baltrons MA, Foldi I, Garcia A. NO-sensitive guanylyl cyclase beta1 subunit is peripherally associated to chromosomes during mitosis. Novel role in chromatin condensation and cell cycle progression. *Int J Biochem Cell Biol*. 2009;41(8-9):1719-30.
251. Illi B, Dello Russo C, Colussi C, Rosati J, Pallaoro M, Spallotta F, et al. Nitric oxide modulates chromatin folding in human endothelial cells via protein phosphatase 2A activation and class II histone deacetylases nuclear shuttling. *Circ Res*. 2008;102(1):51-8.
252. Batista WL, Ogata FT, Curcio MF, Miguel RB, Arai RJ, Matsuo AL, et al. S-nitrosoglutathione and endothelial nitric oxide synthase-derived nitric oxide regulate compartmentalized ras S-nitrosylation and stimulate cell proliferation. *Antioxid Redox Signal*. 2013;18(3):221-38.
253. Schulman IH, Hare JM. Regulation of cardiovascular cellular processes by S-nitrosylation. *Biochim Biophys Acta*. 2012;1820(6):752-62.

254. Yang Z, Krasnici N, Luscher TF. Endothelin-1 potentiates human smooth muscle cell growth to PDGF: effects of ETA and ETB receptor blockade. *Circulation*. 1999;100(1):5-8.
255. Gomez Sandoval YH, Levesque LO, Li Y, Anand-Srivastava MB. Role of epidermal growth factor receptor transactivation in endothelin-1-induced enhanced expression of Gi protein and proliferation in A10 vascular smooth muscle cells. *Can J Physiol Pharmacol*. 2013;91(3):221-7.
256. Davie N, Haleen SJ, Upton PD, Polak JM, Yacoub MH, Morrell NW, et al. ET(A) and ET(B) receptors modulate the proliferation of human pulmonary artery smooth muscle cells. *Am J Respir Crit Care Med*. 2002;165(3):398-405.
257. Mii S, Khalil RA, Morgan KG, Ware JA, Kent KC. Mitogen-activated protein kinase and proliferation of human vascular smooth muscle cells. *Am J Physiol*. 1996;270(1 Pt 2):H142-50.
258. Bokemeyer D, Schmitz U, Kramer HJ. Angiotensin II-induced growth of vascular smooth muscle cells requires an Src-dependent activation of the epidermal growth factor receptor. *Kidney Int*. 2000;58(2):549-58.
259. Lavallee M, Takamura M, Parent R, Thorin E. Crosstalk between endothelin and nitric oxide in the control of vascular tone. *Heart Fail Rev*. 2001;6(4):265-76.
260. Garcia JG, Painter RG, Fenton JW, 2nd, English D, Callahan KS. Thrombin-induced prostacyclin biosynthesis in human endothelium: role of guanine nucleotide regulatory proteins in stimulus/coupling responses. *J Cell Physiol*. 1990;142(1):186-93.
261. Boulanger CM, Luscher TF. Hirudin and nitrates inhibit the thrombin-induced release of endothelin from the intact porcine aorta. *Circ Res*. 1991;68(6):1768-72.
262. Michiels C. Endothelial cell functions. *J Cell Physiol*. 2003;196(3):430-43.
263. Rucker HK, Wynder HJ, Thomas WE. Cellular mechanisms of CNS pericytes. *Brain Res Bull*. 2000;51(5):363-9.
264. Dodge AB, Hechtman HB, Shepro D. Microvascular endothelial-derived autacoids regulate pericyte contractility. *Cell Motil Cytoskeleton*. 1991;18(3):180-8.
265. Matsugi T, Chen Q, Anderson DR. Contractile responses of cultured bovine retinal pericytes to angiotensin II. *Arch Ophthalmol*. 1997;115(10):1281-5.
266. Haefliger IO, Zschauer A, Anderson DR. Relaxation of retinal pericyte contractile tone through the nitric oxide-cyclic guanosine monophosphate pathway. *Invest Ophthalmol Vis Sci*. 1994;35(3):991-7.
267. Chen Q, Anderson DR. Effect of CO₂ on intracellular pH and contraction of retinal capillary pericytes. *Invest Ophthalmol Vis Sci*. 1997;38(3):643-51.

268. Yamanishi S, Katsumura K, Kobayashi T, Puro DG. Extracellular lactate as a dynamic vasoactive signal in the rat retinal microvasculature. *Am J Physiol Heart Circ Physiol*. 2006;290(3):H925-34.
269. Matsugi T, Chen Q, Anderson DR. Adenosine-induced relaxation of cultured bovine retinal pericytes. *Invest Ophthalmol Vis Sci*. 1997;38(13):2695-701.
270. de Graaf JC, Banga JD, Moncada S, Palmer RM, de Groot PG, Sixma JJ. Nitric oxide functions as an inhibitor of platelet adhesion under flow conditions. *Circulation*. 1992;85(6):2284-90.
271. Saniabadi AR, Lowe GD, Belch JJ, Barbenel JC, Forbes CD. Effect of prostacyclin (epoprostenol) on the aggregation of human platelets in whole blood in vitro. *Haemostasis*. 1984;14(6):487-94.
272. Smolenski A. Novel roles of cAMP/cGMP-dependent signaling in platelets. *J Thromb Haemost*. 2012;10(2):167-76.
273. Esmon CT. The endothelial protein C receptor. *Curr Opin Hematol*. 2006;13(5):382-5.
274. Sadler JE. Thrombomodulin structure and function. *Thromb Haemost*. 1997;78(1):392-5.
275. Stern DM, Esposito C, Gerlach H, Gerlach M, Ryan J, Handley D, et al. Endothelium and regulation of coagulation. *Diabetes Care*. 1991;14(2):160-6.
276. Marcum JA, McKenney JB, Rosenberg RD. Acceleration of thrombin-antithrombin complex formation in rat hindquarters via heparinlike molecules bound to the endothelium. *J Clin Invest*. 1984;74(2):341-50.
277. Kato H. Regulation of functions of vascular wall cells by tissue factor pathway inhibitor: basic and clinical aspects. *Arterioscler Thromb Vasc Biol*. 2002;22(4):539-48.
278. Ho G, Toomey JR, Broze GJ, Jr., Schwartz AL. Receptor-mediated endocytosis of coagulation factor Xa requires cell surface-bound tissue factor pathway inhibitor. *J Biol Chem*. 1996;271(16):9497-502.
279. Loskutoff DJ, Edgington TE. Synthesis of a fibrinolytic activator and inhibitor by endothelial cells. *Proc Natl Acad Sci U S A*. 1977;74(9):3903-7.
280. Bachmann F, Kruithof IE. Tissue plasminogen activator: chemical and physiological aspects. *Semin Thromb Hemost*. 1984;10(1):6-17.
281. Emeis J. The Control of tPA and PAI-1 Secretion from the Vessel Wall. *Vascular Medicine Review*. 1995;vmr-6(2):153-66.
282. Gross PL, Aird WC. The endothelium and thrombosis. *Semin Thromb Hemost*. 2000;26(5):463-78.
283. Zimmerman GA, McIntyre TM, Mehra M, Prescott SM. Endothelial cell-associated platelet-activating factor: a novel mechanism for signaling intercellular adhesion. *J Cell Biol*. 1990;110(2):529-40.

284. Denis CV. Molecular and cellular biology of von Willebrand factor. *Int J Hematol.* 2002;75(1):3-8.
285. Ruggeri ZM. Structure of von Willebrand factor and its function in platelet adhesion and thrombus formation. *Best Pract Res Clin Haematol.* 2001;14(2):257-79.
286. Colucci M, Balconi G, Lorenzet R, Pietra A, Locati D, Donati MB, et al. Cultured human endothelial cells generate tissue factor in response to endotoxin. *J Clin Invest.* 1983;71(6):1893-6.
287. Maynard JR, Dreyer BE, Stemerman MB, Pitlick FA. Tissue-factor coagulant activity of cultured human endothelial and smooth muscle cells and fibroblasts. *Blood.* 1977;50(3):387-96.
288. Rahman A, Fazal F. Blocking NF-kappaB: an inflammatory issue. *Proc Am Thorac Soc.* 2011;8(6):497-503.
289. Nathan C. Points of control in inflammation. *Nature.* 2002;420(6917):846-52.
290. Mako V, Czucz J, Weiszhar Z, Herczenik E, Matko J, Prohaszka Z, et al. Proinflammatory activation pattern of human umbilical vein endothelial cells induced by IL-1beta, TNF-alpha, and LPS. *Cytometry A.* 2010;77(10):962-70.
291. Collins T, Read MA, Neish AS, Whitley MZ, Thanos D, Maniatis T. Transcriptional regulation of endothelial cell adhesion molecules: NF-kappa B and cytokine-inducible enhancers. *FASEB J.* 1995;9(10):899-909.
292. Muller WA. Leukocyte-endothelial cell interactions in the inflammatory response. *Lab Invest.* 2002;82(5):521-33.
293. Pober JS, Cotran RS. Cytokines and endothelial cell biology. *Physiol Rev.* 1990;70(2):427-51.
294. Mantovani A, Bussolino F, Dejana E. Cytokine regulation of endothelial cell function. *FASEB J.* 1992;6(8):2591-9.
295. Krishnaswamy G, Kelley J, Yerra L, Smith JK, Chi DS. Human endothelium as a source of multifunctional cytokines: molecular regulation and possible role in human disease. *J Interferon Cytokine Res.* 1999;19(2):91-104.
296. Vestweber D. How leukocytes cross the vascular endothelium. *Nat Rev Immunol.* 2015;15(11):692-704.
297. Dudek SM, Garcia JG. Cytoskeletal regulation of pulmonary vascular permeability. *Journal of applied physiology.* 2001;91(4):1487-500.
298. Mehta D, Malik AB. Signaling mechanisms regulating endothelial permeability. *Physiol Rev.* 2006;86(1):279-367.
299. Levick JR. *An introduction to cardiovascular physiology.* 5th ed. London: Hodder Arnold; 2010. xii, 414 p. p.
300. Simionescu N, Simionescu M, Palade GE. Open junctions in the endothelium of the postcapillary venules of the diaphragm. *J Cell Biol.* 1978;79(1):27-44.

301. Giannotta M, Trani M, Dejana E. VE-cadherin and endothelial adherens junctions: active guardians of vascular integrity. *Dev Cell*. 2013;26(5):441-54.
302. Dejana E. Endothelial adherens junctions: implications in the control of vascular permeability and angiogenesis. *J Clin Invest*. 1997;100(11 Suppl):S7-10.
303. Hawkins BT, Davis TP. The blood-brain barrier/neurovascular unit in health and disease. *Pharmacol Rev*. 2005;57(2):173-85.
304. Campbell M, Humphries P. The blood-retina barrier: tight junctions and barrier modulation. *Adv Exp Med Biol*. 2012;763:70-84.
305. Mruk DD, Cheng CY. Tight junctions in the testis: new perspectives. *Philos Trans R Soc Lond B Biol Sci*. 2010;365(1546):1621-35.
306. Unterberg A, Wahl M, Baethmann A. Effects of bradykinin on permeability and diameter of pial vessels in vivo. *J Cereb Blood Flow Metab*. 1984;4(4):574-85.
307. Curry FR. Microvascular solute and water transport. *Microcirculation*. 2005;12(1):17-31.
308. Sukriti S, Tauseef M, Yazbeck P, Mehta D. Mechanisms regulating endothelial permeability. *Pulm Circ*. 2014;4(4):535-51.
309. Wallez Y, Huber P. Endothelial adherens and tight junctions in vascular homeostasis, inflammation and angiogenesis. *Biochim Biophys Acta*. 2008;1778(3):794-809.
310. Van Rijen H, van Kempen MJ, Analbers LJ, Rook MB, van Ginneken AC, Gros D, et al. Gap junctions in human umbilical cord endothelial cells contain multiple connexins. *Am J Physiol*. 1997;272(1 Pt 1):C117-30.
311. Figueroa XF, Duling BR. Gap junctions in the control of vascular function. *Antioxid Redox Signal*. 2009;11(2):251-66.
312. Deanfield JE, Halcox JP, Rabelink TJ. Endothelial function and dysfunction: testing and clinical relevance. *Circulation*. 2007;115(10):1285-95.
313. Steyers CM, 3rd, Miller FJ, Jr. Endothelial dysfunction in chronic inflammatory diseases. *Int J Mol Sci*. 2014;15(7):11324-49.
314. Bonetti PO, Lerman LO, Lerman A. Endothelial dysfunction: a marker of atherosclerotic risk. *Arterioscler Thromb Vasc Biol*. 2003;23(2):168-75.
315. Liao JK. Linking endothelial dysfunction with endothelial cell activation. *J Clin Invest*. 2013;123(2):540-1.
316. Collins-Underwood JR, Zhao W, Sharpe JG, Robbins ME. NADPH oxidase mediates radiation-induced oxidative stress in rat brain microvascular endothelial cells. *Free Radic Biol Med*. 2008;45(6):929-38.
317. Choi SH, Kim M, Lee HJ, Kim EH, Kim CH, Lee YJ. Effects of NOX1 on fibroblastic changes of endothelial cells in radiation-induced pulmonary fibrosis. *Mol Med Rep*. 2016;13(5):4135-42.

318. Large M, Reichert S, Hehlhans S, Fournier C, Rodel C, Rodel F. A non-linear detection of phospho-histone H2AX in EA.hy926 endothelial cells following low-dose X-irradiation is modulated by reactive oxygen species. *Radiat Oncol.* 2014;9:80.
319. Surh YJ, Kundu JK, Na HK, Lee JS. Redox-sensitive transcription factors as prime targets for chemoprevention with anti-inflammatory and antioxidative phytochemicals. *J Nutr.* 2005;135(12 Suppl):2993S-3001S.
320. Nguyen T, Nioi P, Pickett CB. The Nrf2-antioxidant response element signaling pathway and its activation by oxidative stress. *J Biol Chem.* 2009;284(20):13291-5.
321. Angel P, Karin M. The role of Jun, Fos and the AP-1 complex in cell-proliferation and transformation. *Biochim Biophys Acta.* 1991;1072(2-3):129-57.
322. Wisdom R. AP-1: one switch for many signals. *Exp Cell Res.* 1999;253(1):180-5.
323. Gaboury JP, Anderson DC, Kubes P. Molecular mechanisms involved in superoxide-induced leukocyte-endothelial cell interactions in vivo. *Am J Physiol.* 1994;266(2 Pt 2):H637-42.
324. Rahman A, Bando M, Kefer J, Anwar KN, Malik AB. Protein kinase C-activated oxidant generation in endothelial cells signals intercellular adhesion molecule-1 gene transcription. *Mol Pharmacol.* 1999;55(3):575-83.
325. Marui N, Offermann MK, Swerlick R, Kunsch C, Rosen CA, Ahmad M, et al. Vascular cell adhesion molecule-1 (VCAM-1) gene transcription and expression are regulated through an antioxidant-sensitive mechanism in human vascular endothelial cells. *J Clin Invest.* 1993;92(4):1866-74.
326. Awad EM, Khan SY, Sokolikova B, Brunner PM, Olcaydu D, Wojta J, et al. Cold induces reactive oxygen species production and activation of the NF-kappa B response in endothelial cells and inflammation in vivo. *J Thromb Haemost.* 2013;11(9):1716-26.
327. Griendling KK, Sorescu D, Lassegue B, Ushio-Fukai M. Modulation of protein kinase activity and gene expression by reactive oxygen species and their role in vascular physiology and pathophysiology. *Arterioscler Thromb Vasc Biol.* 2000;20(10):2175-83.
328. Fiuza C, Bustin M, Talwar S, Tropea M, Gerstenberger E, Shelhamer JH, et al. Inflammation-promoting activity of HMGB1 on human microvascular endothelial cells. *Blood.* 2003;101(7):2652-60.
329. Land WG. The Role of Damage-Associated Molecular Patterns (DAMPs) in Human Diseases: Part II: DAMPs as diagnostics, prognostics and therapeutics in clinical medicine. *Sultan Qaboos Univ Med J.* 2015;15(2):e157-70.

330. Jirik FR, Podor TJ, Hirano T, Kishimoto T, Loskutoff DJ, Carson DA, et al. Bacterial lipopolysaccharide and inflammatory mediators augment IL-6 secretion by human endothelial cells. *J Immunol.* 1989;142(1):144-7.
331. Goebeler M, Gillitzer R, Kilian K, Utzel K, Brocker EB, Rapp UR, et al. Multiple signaling pathways regulate NF-kappaB-dependent transcription of the monocyte chemoattractant protein-1 gene in primary endothelial cells. *Blood.* 2001;97(1):46-55.
332. Yoshida A, Yoshida S, Khalil AK, Ishibashi T, Inomata H. Role of NF-kappaB-mediated interleukin-8 expression in intraocular neovascularization. *Invest Ophthalmol Vis Sci.* 1998;39(7):1097-106.
333. Kim I, Moon SO, Kim SH, Kim HJ, Koh YS, Koh GY. Vascular endothelial growth factor expression of intercellular adhesion molecule 1 (ICAM-1), vascular cell adhesion molecule 1 (VCAM-1), and E-selectin through nuclear factor-kappa B activation in endothelial cells. *J Biol Chem.* 2001;276(10):7614-20.
334. Wang L, He L, Bao G, He X, Fan S, Wang H. Ionizing Radiation Induces HMGB1 Cytoplasmic Translocation and Extracellular Release. *Guo Ji Fang She Yi Xue He Yi Xue Za Zhi.* 2016;40(2):91-9.
335. Sun W, Jiao Y, Cui B, Gao X, Xia Y, Zhao Y. Immune complexes activate human endothelium involving the cell-signaling HMGB1-RAGE axis in the pathogenesis of lupus vasculitis. *Lab Invest.* 2013;93(6):626-38.
336. Halle M, Gabrielsen A, Paulsson-Berne G, Gahm C, Agardh HE, Farnebo F, et al. Sustained inflammation due to nuclear factor-kappa B activation in irradiated human arteries. *J Am Coll Cardiol.* 2010;55(12):1227-36.
337. Anders HJ, Schaefer L. Beyond tissue injury-damage-associated molecular patterns, toll-like receptors, and inflammasomes also drive regeneration and fibrosis. *J Am Soc Nephrol.* 2014;25(7):1387-400.
338. Hildebrandt G, Maggiorella L, Rodel F, Rodel V, Willis D, Trott KR. Mononuclear cell adhesion and cell adhesion molecule liberation after X-irradiation of activated endothelial cells in vitro. *Int J Radiat Biol.* 2002;78(4):315-25.
339. Hallahan DE, Virudachalam S, Kuchibhotla J. Nuclear factor kappaB dominant negative genetic constructs inhibit X-ray induction of cell adhesion molecules in the vascular endothelium. *Cancer Res.* 1998;58(23):5484-8.
340. Van Der Meeren A, Squiban C, Gourmelon P, Lafont H, Gaugler MH. Differential regulation by IL-4 and IL-10 of radiation-induced IL-6 and IL-8 production and ICAM-1 expression by human endothelial cells. *Cytokine.* 1999;11(11):831-8.
341. Milliat F, Francois A, Isoir M, Deutsch E, Tamarat R, Tarlet G, et al. Influence of endothelial cells on vascular smooth muscle cells phenotype after

- irradiation: implication in radiation-induced vascular damages. *Am J Pathol.* 2006;169(4):1484-95.
342. Stewart FA, Heeneman S, Te Poele J, Kruse J, Russell NS, Gijbels M, et al. Ionizing radiation accelerates the development of atherosclerotic lesions in ApoE^{-/-} mice and predisposes to an inflammatory plaque phenotype prone to hemorrhage. *Am J Pathol.* 2006;168(2):649-58.
 343. Hayashi T, Morishita Y, Khattree R, Misumi M, Sasaki K, Hayashi I, et al. Evaluation of systemic markers of inflammation in atomic-bomb survivors with special reference to radiation and age effects. *FASEB J.* 2012;26(11):4765-73.
 344. Kern PM, Keilholz L, Forster C, Hallmann R, Herrmann M, Seegenschmiedt MH. Low-dose radiotherapy selectively reduces adhesion of peripheral blood mononuclear cells to endothelium in vitro. *Radiother Oncol.* 2000;54(3):273-82.
 345. Large M, Hehlhans S, Reichert S, Gaipf US, Fournier C, Rodel C, et al. Study of the anti-inflammatory effects of low-dose radiation: The contribution of biphasic regulation of the antioxidative system in endothelial cells. *Strahlenther Onkol.* 2015;191(9):742-9.
 346. Rodel F, Frey B, Capalbo G, Gaipf U, Keilholz L, Voll R, et al. Discontinuous induction of X-linked inhibitor of apoptosis in EA.hy.926 endothelial cells is linked to NF-kappaB activation and mediates the anti-inflammatory properties of low-dose ionising-radiation. *Radiother Oncol.* 2010;97(2):346-51.
 347. Rodel F, Hofmann D, Auer J, Keilholz L, Rollinghoff M, Sauer R, et al. The anti-inflammatory effect of low-dose radiation therapy involves a diminished CCL20 chemokine expression and granulocyte/endothelial cell adhesion. *Strahlenther Onkol.* 2008;184(1):41-7.
 348. Rodel F, Kamprad F, Sauer R, Hildebrandt G. [Functional and molecular aspects of anti-inflammatory effects of low-dose radiotherapy]. *Strahlenther Onkol.* 2002;178(1):1-9.
 349. Rodel F, Keilholz L, Herrmann M, Sauer R, Hildebrandt G. Radiobiological mechanisms in inflammatory diseases of low-dose radiation therapy. *Int J Radiat Biol.* 2007;83(6):357-66.
 350. Rodel F, Schaller U, Schultze-Mosgau S, Beuscher HU, Keilholz L, Herrmann M, et al. The induction of TGF-beta(1) and NF-kappaB parallels a biphasic time course of leukocyte/endothelial cell adhesion following low-dose X-irradiation. *Strahlenther Onkol.* 2004;180(4):194-200.
 351. Le Gallic C, Phalente Y, Manens L, Dublineau I, Benderitter M, Gueguen Y, et al. Chronic Internal Exposure to Low Dose ¹³⁷Cs Induces Positive Impact on the Stability of Atherosclerotic Plaques by Reducing Inflammation in ApoE^{-/-} Mice. *PLoS One.* 2015;10(6):e0128539.

352. Trott KR, Kamprad F. Radiobiological mechanisms of anti-inflammatory radiotherapy. *Radiother Oncol.* 1999;51(3):197-203.
353. Seegenschmiedt MH, Katalinic A, Makoski HB, Haase W, Gademann G, Hassenstein E. Radiotherapy of benign diseases: a pattern of care study in Germany. *Strahlenther Onkol.* 1999;175(11):541-7.
354. Lerman A, Burnett JC, Jr. Intact and altered endothelium in regulation of vasomotion. *Circulation.* 1992;86(6 Suppl):III12-9.
355. Tousoulis D, Kampoli AM, Tentolouris C, Papageorgiou N, Stefanadis C. The role of nitric oxide on endothelial function. *Curr Vasc Pharmacol.* 2012;10(1):4-18.
356. Mombouli JV, Vanhoutte PM. Endothelial dysfunction: from physiology to therapy. *J Mol Cell Cardiol.* 1999;31(1):61-74.
357. Vanhoutte PM, Shimokawa H, Feletou M, Tang EH. Endothelial dysfunction and vascular disease - a 30th anniversary update. *Acta Physiol (Oxf).* 2017;219(1):22-96.
358. Gisone P, Dubner D, Del Perez Rosario M, Michelin S, Puntarulo S. The role of nitric oxide in the radiation-induced effects in the developing brain. *In Vivo.* 2004;18(3):281-92.
359. Kobayashi K, Miki M. Frontiers of reactive oxygen species in biology and medicine : proceedings of the 6th International Conference on Superoxide and Superoxide Dismutase, Kyoto, Japan, October 11-15, 1993. In: Asada K, Yoshikawa T, editors. International congress series. Amsterdam ; New York: Excerpta Medica; 1994. p. 223-4.
360. Pathak R, Cheema AK, Boca SM, Krager KJ, Hauer-Jensen M, Aykin-Burns N. Modulation of Radiation Response by the Tetrahydrobiopterin Pathway. *Antioxidants (Basel).* 2015;4(1):68-81.
361. Sonveaux P, Brouet A, Havaux X, Gregoire V, Dessy C, Balligand JL, et al. Irradiation-induced angiogenesis through the up-regulation of the nitric oxide pathway: implications for tumor radiotherapy. *Cancer Res.* 2003;63(5):1012-9.
362. Sonveaux P, Dessy C, Brouet A, Jordan BF, Gregoire V, Gallez B, et al. Modulation of the tumor vasculature functionality by ionizing radiation accounts for tumor radiosensitization and promotes gene delivery. *FASEB J.* 2002;16(14):1979-81.
363. Sonveaux P, Frerart F, Bouzin C, Brouet A, Dewever J, Jordan BF, et al. Irradiation promotes Akt-targeting therapeutic gene delivery to the tumor vasculature. *Int J Radiat Oncol Biol Phys.* 2007;67(4):1155-62.
364. Nagane M, Yasui H, Sakai Y, Yamamori T, Niwa K, Hattori Y, et al. Activation of eNOS in endothelial cells exposed to ionizing radiation involves components of the DNA damage response pathway. *Biochem Biophys Res Commun.* 2015;456(1):541-6.

365. Baselet B, Belmans N, Coninx E, Lowe D, Janssen A, Michaux A, et al. Functional Gene Analysis Reveals Cell Cycle Changes and Inflammation in Endothelial Cells Irradiated with a Single X-ray Dose. *Front Pharmacol.* 2017;8(213).
366. Hong CW, Kim YM, Pyo H, Lee JH, Kim S, Lee S, et al. Involvement of inducible nitric oxide synthase in radiation-induced vascular endothelial damage. *J Radiat Res.* 2013;54(6):1036-42.
367. Qi F, Sugihara T, Hattori Y, Yamamoto Y, Kanno M, Abe K. Functional and morphological damage of endothelium in rabbit ear artery following irradiation with cobalt60. *Br J Pharmacol.* 1998;123(4):653-60.
368. Maynard KI, Stewart-Lee AL, Milner P, Burnstock G. X-irradiation attenuates relaxant responses in the rabbit ear artery. *Br J Pharmacol.* 1992;105(1):126-8.
369. Soloviev AI, Tishkin SM, Parshikov AV, Ivanova IV, Goncharov EV, Gurney AM. Mechanisms of endothelial dysfunction after ionized radiation: selective impairment of the nitric oxide component of endothelium-dependent vasodilation. *Br J Pharmacol.* 2003;138(5):837-44.
370. Carrier S, Hricak H, Lee SS, Baba K, Morgan DM, Nunes L, et al. Radiation-induced decrease in nitric oxide synthase--containing nerves in the rat penis. *Radiology.* 1995;195(1):95-9.
371. Menendez JC, Casanova D, Amado JA, Salas E, Garcia-Unzueta MT, Fernandez F, et al. Effects of radiation on endothelial function. *Int J Radiat Oncol Biol Phys.* 1998;41(4):905-13.
372. Sugihara T, Hattori Y, Yamamoto Y, Qi F, Ichikawa R, Sato A, et al. Preferential impairment of nitric oxide-mediated endothelium-dependent relaxation in human cervical arteries after irradiation. *Circulation.* 1999;100(6):635-41.
373. Beckman JA, Thakore A, Kalinowski BH, Harris JR, Creager MA. Radiation therapy impairs endothelium-dependent vasodilation in humans. *J Am Coll Cardiol.* 2001;37(3):761-5.
374. Verheij M, Koomen GC, van Mourik JA, Dewit L. Radiation reduces cyclooxygenase activity in cultured human endothelial cells at low doses. *Prostaglandins.* 1994;48(6):351-66.
375. Hosoi Y, Yamamoto M, Ono T, Sakamoto K. Prostacyclin production in cultured endothelial cells is highly sensitive to low doses of ionizing radiation. *Int J Radiat Biol.* 1993;63(5):631-8.
376. Friedman M, Saunders DS, Madden MC, Chaney EL, Kwock L. The effects of ionizing radiation on the pulmonary endothelial cell uptake of alpha-aminoisobutyric acid and synthesis of prostacyclin. *Radiat Res.* 1986;106(2):171-81.

377. Rubin DB, Drab EA, Ts'ao CH, Gardner D, Ward WF. Prostacyclin synthesis in irradiated endothelial cells cultured from bovine aorta. *J Appl Physiol.* 1985;58(2):592-7.
378. Eldor A, Vlodavsky I, HyAm E, Atzmon R, Fuks Z. The effect of radiation on prostacyclin (PGI₂) production by cultured endothelial cells. *Prostaglandins.* 1983;25(2):263-79.
379. Hahn GL, Menconi MJ, Cahill M, Polgar P. The influence of gamma radiation on arachidonic acid release and prostacyclin synthesis. *Prostaglandins.* 1983;25(6):783-91.
380. Sinzinger H, Firbas W, Cromwell M. Radiation induced alterations in rabbit aortic prostacyclin formation. *Prostaglandins.* 1982;24(3):323-9.
381. Allen JB, Sagerman RH, Stuart MJ. Irradiation decreases vascular prostacyclin formation with no concomitant effect on platelet thromboxane production. *Lancet.* 1981;2(8257):1193-6.
382. Sinzinger H, Cromwell M, Firbas W. Long-lasting depression of rabbit aortic prostacyclin formation by single-dose irradiation. *Radiat Res.* 1984;97(3):533-6.
383. Estrada-Garcia L, Carrera-Rotllan J, Puig-Parellada P. Effects of oxidative stress and antioxidant treatments on eicosanoid synthesis and lipid peroxidation in long term human umbilical vein endothelial cells culture. *Prostaglandins Other Lipid Mediat.* 2002;67(1):13-25.
384. Eldor A, Vlodavsky I, Riklis E, Fuks Z. Recovery of prostacyclin capacity of irradiated endothelial cells and the protective effect of vitamin C. *Prostaglandins.* 1987;34(2):241-55.
385. Ivanova IV, Kislova OV, Soloviev AI. Endothelium-Derived Hyperpolarizing Factor as a Reserve Defense Mechanism of the Vascular Control under Ionizing Radiation Impact. 2012;3(2):161-73.
386. Lanza V, Fadda P, Iannone C, Negri R. Low-dose ionizing radiation stimulates transcription and production of endothelin by human vein endothelial cells. *Radiat Res.* 2007;168(2):193-8.
387. Lanza V, Pretazzoli V, Olivieri G, Pascarella G, Panconesi A, Negri R. Transcriptional response of human umbilical vein endothelial cells to low doses of ionizing radiation. *J Radiat Res.* 2005;46(2):265-76.
388. Fardid R, Najafi M, Salajegheh A, Kazemi E, Rezaeyan A. Radiation-induced non-targeted effect in vivo: Evaluation of cyclooxygenase-2 and endothelin-1 gene expression in rat heart tissues. *J Cancer Res Ther.* 2017;13(1):51-5.
389. Merlin SL, Brock GB, Begin LR, Hiou Tim FF, Macramalla AN, Seyam RM, et al. New insights into the role of endothelin-1 in radiation-associated impotence. *Int J Impot Res.* 2001;13(2):104-9.
390. Papapetropoulos A, Burch SE, Topouzis S, Catravas JD. Radiation-induced alterations in angiotensin converting enzyme activity in cultured bovine

- pulmonary arterial endothelial cell monolayers. *Toxicol Appl Pharmacol*. 1993;120(1):96-105.
391. Wei J, Xu H, Liu Y, Li B, Zhou F. Effect of captopril on radiation-induced TGF-beta1 secretion in EA.Hy926 human umbilical vein endothelial cells. *Oncotarget*. 2017;8(13):20842-50.
 392. Ward WF, Kim YT, Molteni A, Solliday NH. Radiation-induced pulmonary endothelial dysfunction in rats: modification by an inhibitor of angiotensin converting enzyme. *Int J Radiat Oncol Biol Phys*. 1988;15(1):135-40.
 393. Cao S, Wu R. Expression of Angiotensin II and Aldosterone in Radiation-induced Lung Injury. *Cancer Biol Med*. 2012;9(4):254-60.
 394. Heckenkamp J, Leszczynski D, Schiereck J, Kung J, LaMuraglia GM. Different effects of photodynamic therapy and gamma-irradiation on vascular smooth muscle cells and matrix : implications for inhibiting restenosis. *Arterioscler Thromb Vasc Biol*. 1999;19(9):2154-61.
 395. Gajdusek CM, Tian H, London S, Zhou D, Rasey J, Mayberg MR. Gamma radiation effect on vascular smooth muscle cells in culture. *Int J Radiat Oncol Biol Phys*. 1996;36(4):821-8.
 396. Keller PF, Verin V, Ziegler T, Mermillod B, Popowski Y, Delafontaine P. Gamma-irradiation markedly inhibits the hydrated collagen gel contradiction by arterial smooth muscle cells. *J Investig Med*. 2001;49(3):258-64.
 397. Heckenkamp J, Nigri GR, Waterman PR, Overhaus M, Kossodo SC, Lamuraglia GM. Gamma-irradiation modulates vascular smooth muscle cell and extracellular matrix function: Implications for neointimal development. *J Vasc Surg*. 2004;39(5):1097-103.
 398. Rudijanto A. The role of vascular smooth muscle cells on the pathogenesis of atherosclerosis. *Acta Med Indones*. 2007;39(2):86-93.
 399. Soloviev A, Tishkin S, Ivanova I, Zelensky S, Dosenko V, Kyrychenko S, et al. Functional and molecular consequences of ionizing irradiation on large conductance Ca²⁺-activated K⁺ channels in rat aortic smooth muscle cells. *Life Sci*. 2009;84(5-6):164-71.
 400. Soloviev AI, Tishkin SM, Zelensky SN, Ivanova IV, Kizub IV, Pavlova AA, et al. Ionizing radiation alters myofilament calcium sensitivity in vascular smooth muscle: potential role of protein kinase C. *Am J Physiol Regul Integr Comp Physiol*. 2005;289(3):R755-62.
 401. Roveri A, Coassin M, Maiorino M, Zamburlini A, van Amsterdam FT, Ratti E, et al. Effect of hydrogen peroxide on calcium homeostasis in smooth muscle cells. *Arch Biochem Biophys*. 1992;297(2):265-70.
 402. Satoh K, Nigro P, Berk BC. Oxidative stress and vascular smooth muscle cell growth: a mechanistic linkage by cyclophilin A. *Antioxid Redox Signal*. 2010;12(5):675-82.

403. Ruef J, Rao GN, Li F, Bode C, Patterson C, Bhatnagar A, et al. Induction of rat aortic smooth muscle cell growth by the lipid peroxidation product 4-hydroxy-2-nonenal. *Circulation*. 1998;97(11):1071-8.
404. Rao GN, Alexander RW, Runge MS. Linoleic acid and its metabolites, hydroperoxyoctadecadienoic acids, stimulate c-Fos, c-Jun, and c-Myc mRNA expression, mitogen-activated protein kinase activation, and growth in rat aortic smooth muscle cells. *J Clin Invest*. 1995;96(2):842-7.
405. Pearson JD. Endothelial cell function and thrombosis. *Baillieres Best Pract Res Clin Haematol*. 1999;12(3):329-41.
406. Cines DB, Pollak ES, Buck CA, Loscalzo J, Zimmerman GA, McEver RP, et al. Endothelial cells in physiology and in the pathophysiology of vascular disorders. *Blood*. 1998;91(10):3527-61.
407. Verheij M, Dewit LG, van Mourik JA. The effect of ionizing radiation on endothelial tissue factor activity and its cellular localization. *Thromb Haemost*. 1995;73(5):894-5.
408. Wang J, Zheng H, Ou X, Albertson CM, Fink LM, Herbert JM, et al. Hirudin ameliorates intestinal radiation toxicity in the rat: support for thrombin inhibition as strategy to minimize side-effects after radiation therapy and as countermeasure against radiation exposure. *J Thromb Haemost*. 2004;2(11):2027-35.
409. van Kleef E, Verheij M, te Poele H, Oussoren Y, Dewit L, Stewart F. In vitro and in vivo expression of endothelial von Willebrand factor and leukocyte accumulation after fractionated irradiation. *Radiat Res*. 2000;154(4):375-81.
410. Boerma M, Kruse JJ, van Loenen M, Klein HR, Bart CI, Zurcher C, et al. Increased deposition of von Willebrand factor in the rat heart after local ionizing irradiation. *Strahlenther Onkol*. 2004;180(2):109-16.
411. Stewart FA, Te Poele JA, Van der Wal AF, Oussoren YG, Van Kleef EM, Kuin A, et al. Radiation nephropathy--the link between functional damage and vascular mediated inflammatory and thrombotic changes. *Acta Oncol*. 2001;40(8):952-7.
412. Sporn LA, Rubin P, Marder VJ, Wagner DD. Irradiation induces release of von Willebrand protein from endothelial cells in culture. *Blood*. 1984;64(2):567-70.
413. Jahroudi N, Ardekani AM, Greenberger JS. Ionizing irradiation increases transcription of the von Willebrand factor gene in endothelial cells. *Blood*. 1996;88(10):3801-14.
414. McManus LM, Ostrom KK, Lear C, Luce EB, Gander DL, Pinckard RN, et al. Radiation-induced increased platelet-activating factor activity in mixed saliva. *Lab Invest*. 1993;68(1):118-24.
415. Wang J, Zheng H, Ou X, Fink LM, Hauer-Jensen M. Deficiency of microvascular thrombomodulin and up-regulation of protease-activated

- receptor-1 in irradiated rat intestine: possible link between endothelial dysfunction and chronic radiation fibrosis. *Am J Pathol.* 2002;160(6):2063-72.
416. Zhou Q, Zhao Y, Li P, Bai X, Ruan C. Thrombomodulin as a marker of radiation-induced endothelial cell injury. *Radiat Res.* 1992;131(3):285-9.
 417. Leigh PJ, Cramp WA, MacDermot J. Identification of the prostacyclin receptor by radiation inactivation. *J Biol Chem.* 1984;259(20):12431-6.
 418. Henderson BW, Bicher HI, Johnson RJ. Loss of vascular fibrinolytic activity following irradiation of the liver--an aspect of late radiation damage. *Radiat Res.* 1983;95(3):646-52.
 419. Svanberg L, Astedt B, Kullander S. On radiation-decreased fibrinolytic activity of vessel walls. *Acta Obstet Gynecol Scand.* 1976;55(1):49-51.
 420. Ts'ao CH, Ward WF, Port CD. Radiation injury in rat lung. III. Plasminogen activator and fibrinolytic inhibitor activities. *Radiat Res.* 1983;96(2):301-8.
 421. Wang HF, Li XD, Chen YM, Yuan LB, Foye WO. Radiation-protective and platelet aggregation inhibitory effects of five traditional Chinese drugs and acetylsalicylic acid following high-dose gamma-irradiation. *J Ethnopharmacol.* 1991;34(2-3):215-9.
 422. Schneider MD. Functional aspects of blood platelets in irradiated burros. *Am J Vet Res.* 1977;38(2):209-16.
 423. Bicher HI, D'Agostino L, Doss LL, Kaufman N, Amigone J. Prevention of ionizing radiation-induced liver microcirculation changes by the use of flow improvers. *Adv Exp Med Biol.* 1977;94:383-9.
 424. Kennedy AR, Maity A, Sanzari JK. A Review of Radiation-Induced Coagulopathy and New Findings to Support Potential Prevention Strategies and Treatments. *Radiat Res.* 2016;186(2):121-40.
 425. Kerr R, Stirling D, Ludlam CA. Interleukin 6 and haemostasis. *Br J Haematol.* 2001;115(1):3-12.
 426. Inoue K-i, Takano H, Yanagisawa R, Shimada A, Yoshikawa T. Role of interleukin-6 in coagulatory and hemostatic disturbance during inflammation. *Ensho Saisei.* 2006;26(1):40-3.
 427. Neumann FJ, Ott I, Marx N, Luther T, Kenngott S, Gawaz M, et al. Effect of human recombinant interleukin-6 and interleukin-8 on monocyte procoagulant activity. *Arterioscler Thromb Vasc Biol.* 1997;17(12):3399-405.
 428. Hoving S, Heeneman S, Gijbels MJ, Te Poele JA, Visser N, Cleutjens J, et al. Irradiation induces different inflammatory and thrombotic responses in carotid arteries of wildtype C57BL/6J and atherosclerosis-prone ApoE(-/-) mice. *Radiother Oncol.* 2012;105(3):365-70.
 429. Wiig H. Pathophysiology of tissue fluid accumulation in inflammation. *J Physiol.* 2011;589(Pt 12):2945-53.

430. Scallan J, Huxley V, Korthuis R. Pathophysiology of Edema Formation. 2010. Accessed. In: Capillary Fluid Exchange: Regulation, Functions, and Pathology [Internet]. San Rafael (CA): Morgan & Claypool Life Sciences. Available from: <https://www.ncbi.nlm.nih.gov/books/NBK53445/>.
431. Sharma P, Templin T, Grabham P. Short term effects of gamma radiation on endothelial barrier function: uncoupling of PECAM-1. *Microvasc Res.* 2013;86:11-20.
432. Templin T, Sharma P, Guida P, Grabham P. Short-Term Effects of Low-LET Radiation on the Endothelial Barrier: Uncoupling of PECAM-1 and the Production of Endothelial Microparticles. *Radiat Res.* 2016;186(6):602-13.
433. Gabrys D, Greco O, Patel G, Prise KM, Tozer GM, Kanthou C. Radiation effects on the cytoskeleton of endothelial cells and endothelial monolayer permeability. *Int J Radiat Oncol Biol Phys.* 2007;69(5):1553-62.
434. Waters CM, Taylor JM, Molteni A, Ward WF. Dose-response effects of radiation on the permeability of endothelial cells in culture. *Radiat Res.* 1996;146(3):321-8.
435. Kantak SS, Diglio CA, Onoda JM. Low dose radiation-induced endothelial cell retraction. *Int J Radiat Biol.* 1993;64(3):319-28.
436. Onoda JM, Kantak SS, Diglio CA. Radiation induced endothelial cell retraction in vitro: correlation with acute pulmonary edema. *Pathol Oncol Res.* 1999;5(1):49-55.
437. Asai K, Kudej RK, Shen YT, Yang GP, Takagi G, Kudej AB, et al. Peripheral vascular endothelial dysfunction and apoptosis in old monkeys. *Arterioscler Thromb Vasc Biol.* 2000;20(6):1493-9.
438. Yu E, Mercer J, Bennett M. Mitochondria in vascular disease. *Cardiovasc Res.* 2012;95(2):173-82.
439. Franken NA, Rodermond HM, Stap J, Haveman J, van Bree C. Clonogenic assay of cells in vitro. *Nat Protoc.* 2006;1(5):2315-9.
440. Park MT, Oh ET, Song MJ, Lee H, Park HJ. Radio-sensitivities and angiogenic signaling pathways of irradiated normal endothelial cells derived from diverse human organs. *J Radiat Res.* 2012;53(4):570-80.
441. Riquier H, Wera AC, Heuskin AC, Feron O, Lucas S, Michiels C. Comparison of X-ray and alpha particle effects on a human cancer and endothelial cells: survival curves and gene expression profiles. *Radiother Oncol.* 2013;106(3):397-403.
442. Haimovitz-Friedman A, Kan CC, Ehleiter D, Persaud RS, McLoughlin M, Fuks Z, et al. Ionizing radiation acts on cellular membranes to generate ceramide and initiate apoptosis. *J Exp Med.* 1994;180(2):525-35.
443. Kolesnick R, Fuks Z. Radiation and ceramide-induced apoptosis. *Oncogene.* 2003;22(37):5897-906.

444. Yabu T, Shiba H, Shibasaki Y, Nakanishi T, Imamura S, Touhata K, et al. Stress-induced ceramide generation and apoptosis via the phosphorylation and activation of nSMase1 by JNK signaling. *Cell Death Differ.* 2015;22(2):258-73.
445. Haimovitz-Friedman A, Kolesnick RN, Fuks Z. Ceramide signaling in apoptosis. *Br Med Bull.* 1997;53(3):539-53.
446. Dikomey E, Dahm-Daphi J, Brammer I, Martensen R, Kaina B. Correlation between cellular radiosensitivity and non-repaired double-strand breaks studied in nine mammalian cell lines. *Int J Radiat Biol.* 1998;73(3):269-78.
447. Langley RE, Bump EA, Quartuccio SG, Medeiros D, Braunhut SJ. Radiation-induced apoptosis in microvascular endothelial cells. *Br J Cancer.* 1997;75(5):666-72.
448. Pluder F, Barjaktarovic Z, Azimzadeh O, Mortl S, Kramer A, Steininger S, et al. Low-dose irradiation causes rapid alterations to the proteome of the human endothelial cell line EA.hy926. *Radiat Environ Biophys.* 2011;50(1):155-66.
449. Rombouts C, Aerts A, Beck M, De Vos WH, Van Oostveldt P, Benotmane MA, et al. Differential response to acute low dose radiation in primary and immortalized endothelial cells. *Int J Radiat Biol.* 2013;89(10):841-50.
450. Hirase T, Node K. Endothelial dysfunction as a cellular mechanism for vascular failure. *Am J Physiol Heart Circ Physiol.* 2012;302(3):H499-505.
451. Chistiakov DA, Orekhov AN, Bobryshev YV. Endothelial Barrier and Its Abnormalities in Cardiovascular Disease. *Front Physiol.* 2015;6:365.
452. Davidson SM, Duchon MR. Endothelial mitochondria: contributing to vascular function and disease. *Circ Res.* 2007;100(8):1128-41.
453. Groschner LN, Waldeck-Weiermair M, Malli R, Graier WF. Endothelial mitochondria--less respiration, more integration. *Pflugers Arch.* 2012;464(1):63-76.
454. Kluge MA, Fetterman JL, Vita JA. Mitochondria and endothelial function. *Circ Res.* 2013;112(8):1171-88.
455. Tang X, Luo YX, Chen HZ, Liu DP. Mitochondria, endothelial cell function, and vascular diseases. *Front Physiol.* 2014;5:175.
456. Szewczyk A, Jarmuszkiewicz W, Koziel A, Sobieraj I, Nobik W, Lukasiak A, et al. Mitochondrial mechanisms of endothelial dysfunction. *Pharmacol Rep.* 2015;67(4):704-10.
457. Blouin A, Bolender RP, Weibel ER. Distribution of organelles and membranes between hepatocytes and nonhepatocytes in the rat liver parenchyma. A stereological study. *J Cell Biol.* 1977;72(2):441-55.
458. Culic O, Gruwel ML, Schrader J. Energy turnover of vascular endothelial cells. *Am J Physiol.* 1997;273(1 Pt 1):C205-13.

459. De Bock K, Georgiadou M, Schoors S, Kuchnio A, Wong BW, Cantelmo AR, et al. Role of PFKFB3-driven glycolysis in vessel sprouting. *Cell*. 2013;154(3):651-63.
460. Krutzfeldt A, Spahr R, Mertens S, Siegmund B, Piper HM. Metabolism of exogenous substrates by coronary endothelial cells in culture. *J Mol Cell Cardiol*. 1990;22(12):1393-404.
461. Quintero M, Colombo SL, Godfrey A, Moncada S. Mitochondria as signaling organelles in the vascular endothelium. *Proc Natl Acad Sci U S A*. 2006;103(14):5379-84.
462. Gunter KK, Gunter TE. Transport of calcium by mitochondria. *J Bioenerg Biomembr*. 1994;26(5):471-85.
463. Gunter TE, Pfeiffer DR. Mechanisms by which mitochondria transport calcium. *Am J Physiol*. 1990;258(5 Pt 1):C755-86.
464. Griffiths EJ, Rutter GA. Mitochondrial calcium as a key regulator of mitochondrial ATP production in mammalian cells. *Biochim Biophys Acta*. 2009;1787(11):1324-33.
465. Zou H, Henzel WJ, Liu X, Lutschg A, Wang X. Apaf-1, a human protein homologous to *C. elegans* CED-4, participates in cytochrome c-dependent activation of caspase-3. *Cell*. 1997;90(3):405-13.
466. Kluck RM, Bossy-Wetzler E, Green DR, Newmeyer DD. The release of cytochrome c from mitochondria: a primary site for Bcl-2 regulation of apoptosis. *Science*. 1997;275(5303):1132-6.
467. Li P, Nijhawan D, Budihardjo I, Srinivasula SM, Ahmad M, Alnemri ES, et al. Cytochrome c and dATP-dependent formation of Apaf-1/caspase-9 complex initiates an apoptotic protease cascade. *Cell*. 1997;91(4):479-89.
468. Wang Y, Boerma M, Zhou D. Ionizing Radiation-Induced Endothelial Cell Senescence and Cardiovascular Diseases. *Radiat Res*. 2016;186(2):153-61.
469. Czabotar PE, Lessene G, Strasser A, Adams JM. Control of apoptosis by the BCL-2 protein family: implications for physiology and therapy. *Nat Rev Mol Cell Biol*. 2014;15(1):49-63.
470. Balaban RS, Nemoto S, Finkel T. Mitochondria, oxidants, and aging. *Cell*. 2005;120(4):483-95.
471. Little MP, Tawn EJ, Tzoulaki I, Wakeford R, Hildebrandt G, Paris F, et al. A systematic review of epidemiological associations between low and moderate doses of ionizing radiation and late cardiovascular effects, and their possible mechanisms. *Radiat Res*. 2008;169(1):99-109.
472. Sena LA, Chandel NS. Physiological roles of mitochondrial reactive oxygen species. *Mol Cell*. 2012;48(2):158-67.
473. Riley PA. Free radicals in biology: oxidative stress and the effects of ionizing radiation. *Int J Radiat Biol*. 1994;65(1):27-33.

474. Lee K, Park JS, Kim YJ, Soo Lee YS, Sook Hwang TS, Kim DJ, et al. Differential expression of Prx I and II in mouse testis and their up-regulation by radiation. *Biochem Biophys Res Commun.* 2002;296(2):337-42.
475. Mikkelsen RB, Wardman P. Biological chemistry of reactive oxygen and nitrogen and radiation-induced signal transduction mechanisms. *Oncogene.* 2003;22(37):5734-54.
476. McDonald JT, Kim K, Norris AJ, Vlashi E, Phillips TM, Lagadec C, et al. Ionizing radiation activates the Nrf2 antioxidant response. *Cancer Res.* 2010;70(21):8886-95.
477. Patwardhan RS, Checker R, Sharma D, Sandur SK, Sainis KB. Involvement of ERK-Nrf-2 signaling in ionizing radiation induced cell death in normal and tumor cells. *PLoS One.* 2013;8(6):e65929.
478. Kensler TW, Wakabayashi N, Biswal S. Cell survival responses to environmental stresses via the Keap1-Nrf2-ARE pathway. *Annu Rev Pharmacol Toxicol.* 2007;47:89-116.
479. Kang KW, Lee SJ, Kim SG. Molecular mechanism of nrf2 activation by oxidative stress. *Antioxid Redox Signal.* 2005;7(11-12):1664-73.
480. Chen N, Wu L, Yuan H, Wang J. ROS/Autophagy/Nrf2 Pathway Mediated Low-Dose Radiation Induced Radio-Resistance in Human Lung Adenocarcinoma A549 Cell. *Int J Biol Sci.* 2015;11(7):833-44.
481. Jayakumar S, Pal D, Sandur SK. Nrf2 facilitates repair of radiation induced DNA damage through homologous recombination repair pathway in a ROS independent manner in cancer cells. *Mutat Res.* 2015;779:33-45.
482. Khan NM, Sandur SK, Checker R, Sharma D, Poduval TB, Sainis KB. Pro-oxidants ameliorate radiation-induced apoptosis through activation of the calcium-ERK1/2-Nrf2 pathway. *Free Radic Biol Med.* 2011;51(1):115-28.
483. Sekhar KR, Freeman ML. Nrf2 promotes survival following exposure to ionizing radiation. *Free Radic Biol Med.* 2015;88(Pt B):268-74.
484. Singh A, Bodas M, Wakabayashi N, Bunz F, Biswal S. Gain of Nrf2 function in non-small-cell lung cancer cells confers radioresistance. *Antioxid Redox Signal.* 2010;13(11):1627-37.
485. Zhao Q, Mao A, Yan J, Sun C, Di C, Zhou X, et al. Downregulation of Nrf2 promotes radiation-induced apoptosis through Nrf2 mediated Notch signaling in non-small cell lung cancer cells. *Int J Oncol.* 2016;48(2):765-73.
486. Anuranjani, Bala M. Concerted action of Nrf2-ARE pathway, MRN complex, HMGB1 and inflammatory cytokines - implication in modification of radiation damage. *Redox Biol.* 2014;2:832-46.
487. Chen B, Lu Y, Chen Y, Cheng J. The role of Nrf2 in oxidative stress-induced endothelial injuries. *J Endocrinol.* 2015;225(3):R83-99.

488. Hoshi Y, Tanooka H, Miyazaki K, Wakasugi H. Induction of thioredoxin in human lymphocytes with low-dose ionizing radiation. *Biochim Biophys Acta*. 1997;1359(1):65-70.
489. Chen WC, McBride WH, Iwamoto KS, Barber CL, Wang CC, Oh YT, et al. Induction of radioprotective peroxiredoxin-I by ionizing irradiation. *J Neurosci Res*. 2002;70(6):794-8.
490. An JH, Kim J, Seong J. Redox signaling by ionizing radiation in mouse liver. *Ann N Y Acad Sci*. 2004;1030:86-94.
491. Gao MC, Jia XD, Wu QF, Cheng Y, Chen FR, Zhang J. Silencing Prx1 and/or Prx5 sensitizes human esophageal cancer cells to ionizing radiation and increases apoptosis via intracellular ROS accumulation. *Acta Pharmacol Sin*. 2011;32(4):528-36.
492. Woolston CM, Storr SJ, Ellis IO, Morgan DA, Martin SG. Expression of thioredoxin system and related peroxiredoxin proteins is associated with clinical outcome in radiotherapy treated early stage breast cancer. *Radiother Oncol*. 2011;100(2):308-13.
493. Yamamori T, Yasui H, Yamazumi M, Wada Y, Nakamura Y, Nakamura H, et al. Ionizing radiation induces mitochondrial reactive oxygen species production accompanied by upregulation of mitochondrial electron transport chain function and mitochondrial content under control of the cell cycle checkpoint. *Free Radic Biol Med*. 2012;53(2):260-70.
494. Yakes FM, Van Houten B. Mitochondrial DNA damage is more extensive and persists longer than nuclear DNA damage in human cells following oxidative stress. *Proc Natl Acad Sci U S A*. 1997;94(2):514-9.
495. Prithivirajsingh S, Story MD, Bergh SA, Geara FB, Ang KK, Ismail SM, et al. Accumulation of the common mitochondrial DNA deletion induced by ionizing radiation. *FEBS Lett*. 2004;571(1-3):227-32.
496. Leach JK, Van Tuyle G, Lin PS, Schmidt-Ullrich R, Mikkelsen RB. Ionizing radiation-induced, mitochondria-dependent generation of reactive oxygen/nitrogen. *Cancer Res*. 2001;61(10):3894-901.
497. Wang L, Kuwahara Y, Li L, Baba T, Shin RW, Ohkubo Y, et al. Analysis of Common Deletion (CD) and a novel deletion of mitochondrial DNA induced by ionizing radiation. *Int J Radiat Biol*. 2007;83(7):433-42.
498. Schilling-Toth B, Sandor N, Kis E, Kadhim M, Safrany G, Hegyesi H. Analysis of the common deletions in the mitochondrial DNA is a sensitive biomarker detecting direct and non-targeted cellular effects of low dose ionizing radiation. *Mutat Res*. 2011;716(1-2):33-9.
499. Hu S, Gao Y, Zhou H, Kong F, Xiao F, Zhou P, et al. New insight into mitochondrial changes in vascular endothelial cells irradiated by gamma ray. *Int J Radiat Biol*. 2017;93(5):470-6.

500. Helm A, Lee R, Durante M, Ritter S. The Influence of C-Ions and X-rays on Human Umbilical Vein Endothelial Cells. *Front Oncol.* 2016;6:5.
501. Lafargue A, Degorre C, Corre I, Alves-Guerra MC, Gaugler MH, Vallette F, et al. Ionizing radiation induces long-term senescence in endothelial cells through mitochondrial respiratory complex II dysfunction and superoxide generation. *Free Radic Biol Med.* 2017;108:750-9.
502. Barjaktarovic Z, Shyla A, Azimzadeh O, Schulz S, Haagen J, Dorr W, et al. Ionising radiation induces persistent alterations in the cardiac mitochondrial function of C57BL/6 mice 40 weeks after local heart exposure. *Radiother Oncol.* 2013;106(3):404-10.
503. Kempf SJ, Moertl S, Sepe S, von Toerne C, Hauck SM, Atkinson MJ, et al. Low-dose ionizing radiation rapidly affects mitochondrial and synaptic signaling pathways in murine hippocampus and cortex. *J Proteome Res.* 2015;14(5):2055-64.
504. Ungvari Z, Kaley G, de Cabo R, Sonntag WE, Csiszar A. Mechanisms of vascular aging: new perspectives. *J Gerontol A Biol Sci Med Sci.* 2010;65(10):1028-41.
505. Voghel G, Thorin-Trescases N, Farhat N, Mamarbachi AM, Villeneuve L, Fortier A, et al. Chronic treatment with N-acetyl-cystein delays cellular senescence in endothelial cells isolated from a subgroup of atherosclerotic patients. *Mech Ageing Dev.* 2008;129(5):261-70.
506. Voghel G, Thorin-Trescases N, Farhat N, Nguyen A, Villeneuve L, Mamarbachi AM, et al. Cellular senescence in endothelial cells from atherosclerotic patients is accelerated by oxidative stress associated with cardiovascular risk factors. *Mech Ageing Dev.* 2007;128(11-12):662-71.
507. Campisi J, d'Adda di Fagagna F. Cellular senescence: when bad things happen to good cells. *Nature Reviews Molecular Cell Biology.* 2007;8(9):729-40.
508. Hayflick L. The Limited in Vitro Lifetime of Human Diploid Cell Strains. *Exp Cell Res.* 1965;37:614-36.
509. Zhu H, Belcher M, van der Harst P. Healthy aging and disease: role for telomere biology? *Clinical science (London, England : 1979).* 2011;120(10):427-40.
510. Ben-Porath I, Weinberg RA. The signals and pathways activating cellular senescence. *Int J Biochem Cell Biol.* 2005;37(5):961-76.
511. Kurz DJ, Decary S, Hong Y, Trivier E, Akhmedov A, Erusalimsky JD. Chronic oxidative stress compromises telomere integrity and accelerates the onset of senescence in human endothelial cells. *J Cell Sci.* 2004;117(Pt 11):2417-26.

512. El Assar M, Angulo J, Vallejo S, Peiro C, Sanchez-Ferrer CF, Rodriguez-Manas L. Mechanisms involved in the aging-induced vascular dysfunction. *Front Physiol.* 2012;3:132.
513. Erusalimsky JD. Vascular endothelial senescence: from mechanisms to pathophysiology. *J Appl Physiol.* 2009;106(1):326-32.
514. Chen J, Huang X, Halicka D, Brodsky S, Avram A, Eskander J, et al. Contribution of p16(INK4a) and p21(CIP1) pathways to induction of premature senescence of human endothelial cells: permissive role of p53. *Am J Physiol-Heart C.* 2006;290(4):H1575-H86.
515. Minamino T, Miyauchi H, Yoshida T, Ishida Y, Yoshida H, Komuro I. Endothelial cell senescence in human atherosclerosis: role of telomere in endothelial dysfunction. *Circulation.* 2002;105(13):1541-4.
516. Coppe JP, Desprez PY, Krtolica A, Campisi J. The senescence-associated secretory phenotype: the dark side of tumor suppression. *Annu Rev Pathol.* 2010;5:99-118.
517. Sabatino L, Picano E, Andreassi MG. Telomere shortening and ionizing radiation: a possible role in vascular dysfunction? *Int J Radiat Biol.* 2012;88(11):830-9.
518. Vavrova J, Rezacova M. The importance of senescence in ionizing radiation-induced tumour suppression. *Folia Biol (Praha).* 2011;57(2):41-6.
519. Lowe D, Raj K. Premature aging induced by radiation exhibits pro-atherosclerotic effects mediated by epigenetic activation of CD44 expression. *Aging Cell.* 2014;13(5):900-10.
520. Dong X, Tong F, Qian C, Zhang R, Dong J, Wu G, et al. NEMO modulates radiation-induced endothelial senescence of human umbilical veins through NF-kappaB signal pathway. *Radiat Res.* 2015;183(1):82-93.
521. Igarashi K, Miura M. Inhibition of a radiation-induced senescence-like phenotype: a possible mechanism for potentially lethal damage repair in vascular endothelial cells. *Radiat Res.* 2008;170(4):534-9.
522. Igarashi K, Sakimoto I, Kataoka K, Ohta K, Miura M. Radiation-induced senescence-like phenotype in proliferating and plateau-phase vascular endothelial cells. *Exp Cell Res.* 2007;313(15):3326-36.
523. Kim KS, Kim JE, Choi KJ, Bae S, Kim DH. Characterization of DNA damage-induced cellular senescence by ionizing radiation in endothelial cells. *Int J Radiat Biol.* 2014;90(1):71-80.
524. Panganiban RA, Mungunsukh O, Day RM. X-irradiation induces ER stress, apoptosis, and senescence in pulmonary artery endothelial cells. *Int J Radiat Biol.* 2013;89(8):656-67.
525. Oh CW, Bump EA, Kim JS, Janigro D, Mayberg MR. Induction of a senescence-like phenotype in bovine aortic endothelial cells by ionizing radiation. *Radiat Res.* 2001;156(3):232-40.

526. Rombouts C, Aerts A, Quintens R, Baselet B, El-Saghire H, Harms-Ringdahl M, et al. Transcriptomic profiling suggests a role for IGFBP5 in premature senescence of endothelial cells after chronic low dose rate irradiation. *Int J Radiat Biol.* 2014;90(7):560-74.
527. Yentrapalli R, Azimzadeh O, Barjaktarovic Z, Sarioglu H, Wojcik A, Harms-Ringdahl M, et al. Quantitative proteomic analysis reveals induction of premature senescence in human umbilical vein endothelial cells exposed to chronic low-dose rate gamma radiation. *Proteomics.* 2013;13(7):1096-107.
528. Yentrapalli R, Azimzadeh O, Sriharshan A, Malinowsky K, Merl J, Wojcik A, et al. The PI3K/Akt/mTOR pathway is implicated in the premature senescence of primary human endothelial cells exposed to chronic radiation. *PLoS One.* 2013;8(8):e70024.
529. Jaffe EA, Nachman RL, Becker CG, Minick CR. Culture of human endothelial cells derived from umbilical veins. Identification by morphologic and immunologic criteria. *J Clin Invest.* 1973;52(11):2745-56.
530. Onat D, Brillon D, Colombo PC, Schmidt AM. Human vascular endothelial cells: a model system for studying vascular inflammation in diabetes and atherosclerosis. *Curr Diab Rep.* 2011;11(3):193-202.
531. Hauser S, Jung F, Pietzsch J. Human Endothelial Cell Models in Biomaterial Research. *Trends Biotechnol.* 2017;35(3):265-77.
532. Bouis D, Hospers GA, Meijer C, Molema G, Mulder NH. Endothelium in vitro: a review of human vascular endothelial cell lines for blood vessel-related research. *Angiogenesis.* 2001;4(2):91-102.
533. Navab M, Hough GP, Berliner JA, Frank JA, Fogelman AM, Haberland ME, et al. Rabbit beta-migrating very low density lipoprotein increases endothelial macromolecular transport without altering electrical resistance. *J Clin Invest.* 1986;78(2):389-97.
534. Comhair SA, Xu W, Mavrakis L, Aldred MA, Asosingh K, Erzurum SC. Human primary lung endothelial cells in culture. *Am J Respir Cell Mol Biol.* 2012;46(6):723-30.
535. Duthu GS, Smith JR. In vitro proliferation and lifespan of bovine aorta endothelial cells: effect of culture conditions and fibroblast growth factor. *J Cell Physiol.* 1980;103(3):385-92.
536. Aird WC. Phenotypic heterogeneity of the endothelium: II. Representative vascular beds. *Circ Res.* 2007;100(2):174-90.
537. Aird WC. Phenotypic heterogeneity of the endothelium: I. Structure, function, and mechanisms. *Circ Res.* 2007;100(2):158-73.
538. Aird WC. Endothelial cell heterogeneity. *Cold Spring Harb Perspect Med.* 2012;2(1):a006429.

539. Edgell CJ, McDonald CC, Graham JB. Permanent cell line expressing human factor VIII-related antigen established by hybridization. *Proc Natl Acad Sci U S A*. 1983;80(12):3734-7.
540. Bishop ET, Bell GT, Bloor S, Broom IJ, Hendry NF, Wheatley DN. An in vitro model of angiogenesis: basic features. *Angiogenesis*. 1999;3(4):335-44.
541. Donovan D, Brown NJ, Bishop ET, Lewis CE. Comparison of three in vitro human 'angiogenesis' assays with capillaries formed in vivo. *Angiogenesis*. 2001;4(2):113-21.
542. Wallace CS, Truskey GA. Direct-contact co-culture between smooth muscle and endothelial cells inhibits TNF-alpha-mediated endothelial cell activation. *Am J Physiol Heart Circ Physiol*. 2010;299(2):H338-46.
543. Rainger GE, Nash GB. Cellular pathology of atherosclerosis: smooth muscle cells prime cocultured endothelial cells for enhanced leukocyte adhesion. *Circ Res*. 2001;88(6):615-22.
544. Acheva A, Aerts A, Baatout S, Rombouts C, Salomaa S, Manda K, et al. Human 3-D tissue models in radiation biology – current status and future perspectives. *International Journal of Radiation Research*. 2014;12(2):81-98.
545. Heiss M, Hellstrom M, Kalen M, May T, Weber H, Hecker M, et al. Endothelial cell spheroids as a versatile tool to study angiogenesis in vitro. *FASEB J*. 2015;29(7):3076-84.
546. Hobson B, Denekamp J. Endothelial proliferation in tumours and normal tissues: continuous labelling studies. *Br J Cancer*. 1984;49(4):405-13.
547. Collier HA, Sang L, Roberts JM. A new description of cellular quiescence. *PLoS Biol*. 2006;4(3):e83.
548. Pfisterer L, Korff T. Spheroid-Based In Vitro Angiogenesis Model. *Methods Mol Biol*. 2016;1430:167-77.
549. Rezvan A, Ni CW, Alberts-Grill N, Jo H. Animal, in vitro, and ex vivo models of flow-dependent atherosclerosis: role of oxidative stress. *Antioxid Redox Signal*. 2011;15(5):1433-48.
550. Spiers A, Padmanabhan N. A guide to wire myography. *Methods Mol Med*. 2005;108:91-104.
551. Lu X, Kassab GS. Assessment of endothelial function of large, medium, and small vessels: a unified myograph. *Am J Physiol Heart Circ Physiol*. 2011;300(1):H94-H100.
552. Steinmetz M, Van Le T, Bierer S, De Mey JG, Schlatter E. Prior vasorelaxation enhances diadenosine polyphosphate-induced contractility of rat mesenteric resistance arteries. *Naunyn Schmiedeberg's Arch Pharmacol*. 2005;371(5):359-63.
553. Rodriguez-Manas L, El-Assar M, Vallejo S, Lopez-Doriga P, Solis J, Petidier R, et al. Endothelial dysfunction in aged humans is related with oxidative stress and vascular inflammation. *Aging Cell*. 2009;8(3):226-38.

554. Baker M, Robinson SD, Lechertier T, Barber PR, Tavora B, D'Amico G, et al. Use of the mouse aortic ring assay to study angiogenesis. *Nat Protoc.* 2011;7(1):89-104.
555. Camare C, Pucelle M, Negre-Salvayre A, Salvayre R. Angiogenesis in the atherosclerotic plaque. *Redox Biol.* 2017;12:18-34.
556. Erbel C, Okuyucu D, Akhavanpoor M, Zhao L, Wangler S, Hakimi M, et al. A human ex vivo atherosclerotic plaque model to study lesion biology. *J Vis Exp.* 2014(87).
557. Akhtar R, Sherratt MJ, Cruickshank JK, Derby B. Characterizing the elastic properties of tissues. *Mater Today (Kidlington).* 2011;14(3):96-105.
558. Wang D, Iversen J, Strandgaard S. Endothelium-dependent relaxation of small resistance vessels is impaired in patients with autosomal dominant polycystic kidney disease. *J Am Soc Nephrol.* 2000;11(8):1371-6.
559. Zadelaar S, Kleemann R, Verschuren L, de Vries-Van der Weij J, van der Hoorn J, Princen HM, et al. Mouse models for atherosclerosis and pharmaceutical modifiers. *Arterioscler Thromb Vasc Biol.* 2007;27(8):1706-21.
560. Ohashi R, Mu H, Yao Q, Chen C. Cellular and molecular mechanisms of atherosclerosis with mouse models. *Trends Cardiovasc Med.* 2004;14(5):187-90.
561. Zaragoza C, Gomez-Guerrero C, Martin-Ventura JL, Blanco-Colio L, Lavin B, Mallavia B, et al. Animal models of cardiovascular diseases. *J Biomed Biotechnol.* 2011;2011:497841.
562. Skold BH, Getty R, Ramsey FK. Spontaneous atherosclerosis in the arterial system of aging swine. *Am J Vet Res.* 1966;27(116):257-73.
563. Reiser R, Sorrels MF, Williams MC. Influence of high levels of dietary fats and cholesterol on atherosclerosis and lipid distribution in swine. *Circ Res.* 1959;7:833-46.
564. Koskinas KC, Feldman CL, Chatzizisis YS, Coskun AU, Jonas M, Maynard C, et al. Natural history of experimental coronary atherosclerosis and vascular remodeling in relation to endothelial shear stress: a serial, in vivo intravascular ultrasound study. *Circulation.* 2010;121(19):2092-101.
565. Gerrity RG, Natarajan R, Nadler JL, Kimsey T. Diabetes-induced accelerated atherosclerosis in swine. *Diabetes.* 2001;50(7):1654-65.
566. Getz GS, Reardon CA. Animal models of atherosclerosis. *Arterioscler Thromb Vasc Biol.* 2012;32(5):1104-15.
567. Xiangdong L, Yuanwu L, Hua Z, Liming R, Qiuyan L, Ning L. Animal models for the atherosclerosis research: a review. *Protein Cell.* 2011;2(3):189-201.
568. Jermann M. Particle Therapy Statistics in 2014. *Int J Part Ther.* 2015;2(1):50-4.

569. Boyd MA. A regulatory perspective on whether the system of radiation protection is fit for purpose. *Annals of the ICRP*. 2012;41(3):57-63.
570. Kreuzer M, Auvinen A, Cardis E, Hall J, Jourdain JR, Laurier D, et al. Low-dose ionising radiation and cardiovascular diseases--Strategies for molecular epidemiological studies in Europe. *Mutat Res Rev Mutat Res*. 2015;764:90-100.
571. Hayashi T, Kusunoki Y, Hakoda M, Morishita Y, Kubo Y, Maki M, et al. Radiation dose-dependent increases in inflammatory response markers in A-bomb survivors. *Int J Radiat Biol*. 2003;79(2):129-36.
572. Libby P. Inflammation in atherosclerosis. *Nature*. 2002;420(6917):868-74.
573. Rufini A, Tucci P, Celardo I, Melino G. Senescence and aging: the critical roles of p53. *Oncogene*. 2013;32(43):5129-43.
574. Freund A, Orjalo AV, Desprez PY, Campisi J. Inflammatory networks during cellular senescence: causes and consequences. *Trends Mol Med*. 2010;16(5):238-46.
575. Kojima H, Inoue T, Kunimoto H, Nakajima K. IL-6-STAT3 signaling and premature senescence. *JAKSTAT*. 2013;2(4):e25763.
576. Ren JL, Pan JS, Lu YP, Sun P, Han J. Inflammatory signaling and cellular senescence. *Cell Signal*. 2009;21(3):378-83.
577. Yentrapalli R, Azimzadeh O, Barjaktarovic Z, Sarioglu H, Wojcik A, Harms-Ringdahl M, et al. Quantitative proteomic analysis reveals induction of premature senescence in human umbilical vein endothelial cells exposed to chronic low-dose rate gamma-radiation. *Proteomics*. 2013;13(7):1096-107.
578. Kim KS, Seu YB, Baek SH, Kim MJ, Kim KJ, Kim JH, et al. Induction of cellular senescence by insulin-like growth factor binding protein-5 through a p53-dependent mechanism. *Mol Biol Cell*. 2007;18(11):4543-52.
579. Fournier C, Taucher-Scholz G. Radiation induced cell cycle arrest: an overview of specific effects following high-LET exposure. *Radiother Oncol*. 2004;73 Suppl 2:S119-22.
580. Suetens A, Konings K, Moreels M, Quintens R, Verslegers M, Soors E, et al. Higher Initial DNA Damage and Persistent Cell Cycle Arrest after Carbon Ion Irradiation Compared to X-irradiation in Prostate and Colon Cancer Cells. *Front Oncol*. 2016;6:87.
581. Hada M, Georgakilas AG. Formation of clustered DNA damage after high-LET irradiation: a review. *J Radiat Res*. 2008;49(3):203-10.
582. Asaithamby A, Chen DJ. Mechanism of cluster DNA damage repair in response to high-atomic number and energy particles radiation. *Mutat Res*. 2011;711(1-2):87-99.
583. Sofia Vala I, Martins LR, Imaizumi N, Nunes RJ, Rino J, Kuonen F, et al. Low doses of ionizing radiation promote tumor growth and metastasis by enhancing angiogenesis. *PLoS One*. 2010;5(6):e11222.

584. Takahashi Y, Teshima T, Kawaguchi N, Hamada Y, Mori S, Madachi A, et al. Heavy ion irradiation inhibits in vitro angiogenesis even at sublethal dose. *Cancer Res.* 2003;63(14):4253-7.
585. Grabham P, Sharma P, Bigelow A, Geard C. Two distinct types of the inhibition of vasculogenesis by different species of charged particles. *Vasc Cell.* 2013;5(1):16.
586. Mao XW, Favre CJ, Fike JR, Kubinova L, Anderson E, Campbell-Beachler M, et al. High-LET radiation-induced response of microvessels in the Hippocampus. *Radiat Res.* 2010;173(4):486-93.
587. Grabham P, Sharma P. The effects of radiation on angiogenesis. *Vasc Cell.* 2013;5(1):19.
588. Beck M, Rombouts C, Moreels M, Aerts A, Quintens R, Tabury K, et al. Modulation of gene expression in endothelial cells in response to high LET nickel ion irradiation. *Int J Mol Med.* 2014;34(4):1124-32.
589. Zhu H, Yue J, Pan Z, Wu H, Cheng Y, Lu H, et al. Involvement of Caveolin-1 in repair of DNA damage through both homologous recombination and non-homologous end joining. *PLoS One.* 2010;5(8):e12055.
590. Chatterjee M, Ben-Josef E, Thomas DG, Morgan MA, Zalupski MM, Khan G, et al. Caveolin-1 is Associated with Tumor Progression and Confers a Multi-Modality Resistance Phenotype in Pancreatic Cancer. *Sci Rep.* 2015;5:10867.
591. Hult J, Bash T, Fu M, Galbiati F, Albanese C, Sage DR, et al. The cyclin D1 gene is transcriptionally repressed by caveolin-1. *J Biol Chem.* 2000;275(28):21203-9.
592. Galbiati F, Volonte D, Engelman JA, Watanabe G, Burk R, Pestell RG, et al. Targeted downregulation of caveolin-1 is sufficient to drive cell transformation and hyperactivate the p42/44 MAP kinase cascade. *EMBO J.* 1998;17(22):6633-48.
593. Shankar J, Boscher C, Nabi IR. Caveolin-1, galectin-3 and lipid raft domains in cancer cell signalling. *Essays Biochem.* 2015;57:189-201.
594. Sbaa E, Frerart F, Feron O. The double regulation of endothelial nitric oxide synthase by caveolae and caveolin: a paradox solved through the study of angiogenesis. *Trends Cardiovasc Med.* 2005;15(5):157-62.
595. Labrecque L, Royal I, Surprenant DS, Patterson C, Gingras D, Beliveau R. Regulation of vascular endothelial growth factor receptor-2 activity by caveolin-1 and plasma membrane cholesterol. *Mol Biol Cell.* 2003;14(1):334-47.
596. Morais C, Ebrahim Q, Anand-Apte B, Parat MO. Altered angiogenesis in caveolin-1 gene-deficient mice is restored by ablation of endothelial nitric oxide synthase. *Am J Pathol.* 2012;180(4):1702-14.

597. Klein D, Schmitz T, Verhelst V, Panic A, Schenck M, Reis H, et al. Endothelial Caveolin-1 regulates the radiation response of epithelial prostate tumors. *Oncogenesis*. 2015;4:e148.
598. Liu J, Razani B, Tang S, Terman BI, Ware JA, Lisanti MP. Angiogenesis activators and inhibitors differentially regulate caveolin-1 expression and caveolae formation in vascular endothelial cells. Angiogenesis inhibitors block vascular endothelial growth factor-induced down-regulation of caveolin-1. *J Biol Chem*. 1999;274(22):15781-5.
599. Fernandez-Hernando C, Yu J, Davalos A, Prendergast J, Sessa WC. Endothelial-specific overexpression of caveolin-1 accelerates atherosclerosis in apolipoprotein E-deficient mice. *Am J Pathol*. 2010;177(2):998-1003.
600. Pavlides S, Gutierrez-Pajares JL, Iturrieta J, Lisanti MP, Frank PG. Endothelial caveolin-1 plays a major role in the development of atherosclerosis. *Cell Tissue Res*. 2014;356(1):147-57.
601. Qin L, Zhu N, Ao BX, Liu C, Shi YN, Du K, et al. Caveolae and Caveolin-1 Integrate Reverse Cholesterol Transport and Inflammation in Atherosclerosis. *Int J Mol Sci*. 2016;17(3):429.
602. Kowalczyk AP, Nanes BA. Adherens junction turnover: regulating adhesion through cadherin endocytosis, degradation, and recycling. *Subcell Biochem*. 2012;60:197-222.
603. Xiao K, Allison DF, Kottke MD, Summers S, Sorescu GP, Faundez V, et al. Mechanisms of VE-cadherin processing and degradation in microvascular endothelial cells. *J Biol Chem*. 2003;278(21):19199-208.
604. Zhang Y, Zhang L, Li Y, Sun S, Tan H. Different contributions of clathrin- and caveolae-mediated endocytosis of vascular endothelial cadherin to lipopolysaccharide-induced vascular hyperpermeability. *PLoS One*. 2014;9(9):e106328.
605. Dittmann K, Mayer C, Kehlbach R, Rodemann HP. Radiation-induced caveolin-1 associated EGFR internalization is linked with nuclear EGFR transport and activation of DNA-PK. *Mol Cancer*. 2008;7:69.
606. Cordes N, Frick S, Brunner TB, Pilarsky C, Grutzmann R, Sipos B, et al. Human pancreatic tumor cells are sensitized to ionizing radiation by knockdown of caveolin-1. *Oncogene*. 2007;26(48):6851-62.
607. McLaughlin N, Annabi B, Bouzeghrane M, Temme A, Bahary JP, Mouldjian R, et al. The Survivin-mediated radioresistant phenotype of glioblastomas is regulated by RhoA and inhibited by the green tea polyphenol (-)-epigallocatechin-3-gallate. *Brain Res*. 2006;1071(1):1-9.
608. Parton RG, Simons K. The multiple faces of caveolae. *Nat Rev Mol Cell Biol*. 2007;8(3):185-94.

609. Meeren AV, Bertho JM, Vandamme M, Gaugler MH. Ionizing radiation enhances IL-6 and IL-8 production by human endothelial cells. *Mediators Inflamm.* 1997;6(3):185-93.
610. Ebrahimian T, Le Gallic C, Stefani J, Dublineau I, Yentrapalli R, Harms-Ringdahl M, et al. Chronic Gamma-Irradiation Induces a Dose-Rate-Dependent Pro-inflammatory Response and Associated Loss of Function in Human Umbilical Vein Endothelial Cells. *Radiat Res.* 2015;183(4):447-54.
611. Khaled S, Gupta KB, Kucik DF. Ionizing radiation increases adhesiveness of human aortic endothelial cells via a chemokine-dependent mechanism. *Radiat Res.* 2012;177(5):594-601.
612. Kucik DF, Khaled S, Gupta K, Wu X, Yu T, Chang PY. X-ray, proton and iron ion irradiation all increase adhesiveness of aortic endothelium and may accelerate development of atherosclerosis. *The FASEB Journal.* 2010;24(1 Supplement):1028.11.
613. Khaled S. Low and high LET irradiation of human aortic endothelial cells induces dose and time dependent adhesion of monocytes which is mediated by chemokines expressed by the irradiated endothelium. Birmingham: The University of Alabama; 2011.
614. Vita JA, Keaney JF, Jr. Endothelial function: a barometer for cardiovascular risk? *Circulation.* 2002;106(6):640-2.
615. Baker JE, Moulder JE, Hopewell JW. Radiation as a risk factor for cardiovascular disease. *Antioxid Redox Signal.* 2011;15(7):1945-56.
616. Hausleiter J, Meyer T, Hermann F, Hadamitzky M, Krebs M, Gerber TC, et al. Estimated radiation dose associated with cardiac CT angiography. *JAMA.* 2009;301(5):500-7.
617. Pedraza Muriel V. The biological basis of fractionation in radiotherapy. *Clinical & Translational Oncology.* 2002;4(3):161-5.
618. Dincer Y, Sezgin Z. Medical radiation exposure and human carcinogenesis-genetic and epigenetic mechanisms. *Biomed Environ Sci.* 2014;27(9):718-28.
619. Sanchis-Gomar F, Perez-Quilis C, Leischik R, Lucia A. Epidemiology of coronary heart disease and acute coronary syndrome. *Ann Transl Med.* 2016;4(13):256.
620. Sautter-Bihl ML, Hultenschmidt B, Melcher U, Ulmer HU. Radiotherapy of internal mammary lymph nodes in breast cancer. Principle considerations on the basis of dosimetric data. *Strahlenther Onkol.* 2002;178(1):18-24.
621. Fuller SA, Haybittle JL, Smith RE, Dobbs HJ. Cardiac doses in post-operative breast irradiation. *Radiother Oncol.* 1992;25(1):19-24.
622. Gyenes G, Gagliardi G, Lax I, Fornander T, Rutqvist LE. Evaluation of irradiated heart volumes in stage I breast cancer patients treated with postoperative adjuvant radiotherapy. *J Clin Oncol.* 1997;15(4):1348-53.

623. Corre I, Guillonneau M, Paris F. Membrane signaling induced by high doses of ionizing radiation in the endothelial compartment. Relevance in radiation toxicity. *Int J Mol Sci.* 2013;14(11):22678-96.
624. Azimzadeh O, Azizova T, Merl-Pham J, Subramanian V, Bakshi MV, Moseeva M, et al. A dose-dependent perturbation in cardiac energy metabolism is linked to radiation-induced ischemic heart disease in Mayak nuclear workers. *Oncotarget.* 2016.
625. Phillips TL, Benak S, Ross G. Ultrastructural and cellular effects of ionizing radiation. *Front Radiat Ther Oncol* 6: 21-43(1972). 1972:Medium: X.
626. McReynolds RA, Gold GL, Roberts WC. Coronary heart disease after mediastinal irradiation for Hodgkin's disease. *Am J Med.* 1976;60(1):39-45.
627. Hopewell JW, Campling D, Calvo W, Reinhold HS, Wilkinson JH, Yeung TK. Vascular irradiation damage: its cellular basis and likely consequences. *Br J Cancer Suppl.* 1986;7:181-91.
628. Phillips TL. An ultrastructural study of the development of radiation injury in the lung. *Radiology.* 1966;87(1):49-54.
629. Fajardo LF, Stewart JR. Pathogenesis of radiation-induced myocardial fibrosis. *Lab Invest.* 1973;29(2):244-57.
630. Konings AW, Smit Sibinga CT, Aarnoudse MW, de Wit SS, Lamberts HB. Initial events in radiation-induced atheromatosis. II. Damage to intimal cells. *Strahlentherapie.* 1978;154(11):795-800.
631. Johnson LK, Longenecker JP, Fajardo LF. Differential radiation response of cultured endothelial cells and smooth myocytes. *Anal Quant Cytol.* 1982;4(3):188-98.
632. Fischer-Dzoga K, Dimitrievich GS, Griem ML. Radiosensitivity of vascular tissue. II. Differential radiosensitivity of aortic cells in vitro. *Radiat Res.* 1984;99(3):536-46.
633. Rubin DB, Drab EA, Ward WF, Smith LJ, Fowell SM. Enzymatic responses to radiation in cultured vascular endothelial and smooth muscle cells. *Radiat Res.* 1984;99(2):420-32.
634. Rosen EM, Goldberg ID, Myrick KV, Levenson S. Radiation survival properties of cultured vascular smooth muscle cells. *Radiat Res.* 1984;100(1):182-91.
635. Rosen EM, Goldberg ID, Myrick KV, Levenson SE. Radiation survival of vascular smooth muscle cells as a function of age. *Int J Radiat Biol Relat Stud Phys Chem Med.* 1985;48(1):71-9.
636. Bertrand OF, Mongrain R, Thorin E, Lehnert S. Effects of low-dose-rate beta-irradiation on vascular smooth muscle cells: comparison with high-dose-rate exposure. *Cardiovasc Radiat Med.* 1999;1(2):125-30.

637. Kim SJ, Masaki T, Rowley R, Leyboldt JK, Mohammad SF, Cheung AK. Different responses by cultured aortic and venous smooth muscle cells to gamma radiation. *Kidney Int.* 2005;68(1):371-7.
638. Mahrhofer H, Burger S, Oppitz U, Flentje M, Djuzenova CS. Radiation induced DNA damage and damage repair in human tumor and fibroblast cell lines assessed by histone H2AX phosphorylation. *Int J Radiat Oncol Biol Phys.* 2006;64(2):573-80.
639. Dimitrijevic-Bussod M, Balzaretto-Maggi VS, Gadbois DM. Extracellular matrix and radiation G1 cell cycle arrest in human fibroblasts. *Cancer Res.* 1999;59(19):4843-7.
640. DeSimone JN, Dolezalova H, Redpath JL, Stanbridge EJ. Prolonged cell cycle arrest in irradiated human diploid skin fibroblasts: the role of nutrient deprivation. *Radiat Res.* 2000;153(2):131-43.
641. Kim HS, Cho HJ, Cho HJ, Park SJ, Park KW, Chae IH, et al. The essential role of p21 in radiation-induced cell cycle arrest of vascular smooth muscle cell. *J Mol Cell Cardiol.* 2004;37(4):871-80.
642. Stewart JR, Fajardo LF, Gillette SM, Constine LS. Radiation injury to the heart. *Int J Radiat Oncol Biol Phys.* 1995;31(5):1205-11.
643. de Crom R, Wulf P, van Nimwegen H, Kutryk MJ, Visser P, van der Kamp A, et al. Irradiated versus nonirradiated endothelial cells: effect on proliferation of vascular smooth muscle cells. *J Vasc Interv Radiol.* 2001;12(7):855-61.
644. Hall J, Jeggo PA, West C, Gomolka M, Quintens R, Badie C, et al. Ionizing radiation biomarkers in epidemiological studies - An update. *Mutat Res.* 2017;771:59-84.
645. Pernot E, Hall J, Baatout S, Benotmane MA, Blanchardon E, Bouffler S, et al. Ionizing radiation biomarkers for potential use in epidemiological studies. *Mutat Res.* 2012;751(2):258-86.
646. Serban KA, Rezaia S, Petrusca DN, Poirier C, Cao D, Justice MJ, et al. Structural and functional characterization of endothelial microparticles released by cigarette smoke. *Sci Rep.* 2016;6:31596.
647. Dignat-George F, Boulanger CM. The many faces of endothelial microparticles. *Arterioscler Thromb Vasc Biol.* 2011;31(1):27-33.
648. Horstman LL, Jy W, Jimenez JJ, Ahn YS. Endothelial microparticles as markers of endothelial dysfunction. *Front Biosci.* 2004;9:1118-35.
649. Neuber C, Pufe J, Pietzsch J. Influence of irradiation on release of endothelial microparticles (EMP) in vitro. *Clin Hemorheol Microcirc.* 2015;61(2):291-9.
650. van Holten TC, Waanders LF, de Groot PG, Vissers J, Hofer IE, Pasterkamp G, et al. Circulating biomarkers for predicting cardiovascular disease risk; a

- systematic review and comprehensive overview of meta-analyses. *PLoS One*. 2013;8(4):e62080.
651. Citrin D, Cotrim AP, Hyodo F, Baum BJ, Krishna MC, Mitchell JB. Radioprotectors and mitigators of radiation-induced normal tissue injury. *Oncologist*. 2010;15(4):360-71.
 652. Prasanna PG, Stone HB, Wong RS, Capala J, Bernhard EJ, Vikram B, et al. Normal tissue protection for improving radiotherapy: Where are the Gaps? *Transl Cancer Res*. 2012;1(1):35-48.
 653. Koukourakis MI. Radiation damage and radioprotectants: new concepts in the era of molecular medicine. *Br J Radiol*. 2012;85(1012):313-30.
 654. Hensley ML, Hagerty KL, Kewalramani T, Green DM, Meropol NJ, Wasserman TH, et al. American Society of Clinical Oncology 2008 clinical practice guideline update: use of chemotherapy and radiation therapy protectants. *J Clin Oncol*. 2009;27(1):127-45.
 655. Brizel DM, Wasserman TH, Henke M, Strnad V, Rudat V, Monnier A, et al. Phase III randomized trial of amifostine as a radioprotector in head and neck cancer. *J Clin Oncol*. 2000;18(19):3339-45.
 656. Kouvaris JR, Kouloulis VE, Vlahos LJ. Amifostine: the first selective-target and broad-spectrum radioprotector. *Oncologist*. 2007;12(6):738-47.
 657. Yuhas JM. Active versus passive absorption kinetics as the basis for selective protection of normal tissues by S-2-(3-aminopropylamino)-ethylphosphorothioic acid. *Cancer Res*. 1980;40(5):1519-24.
 658. Wasserman TH, Brizel DM. The role of amifostine as a radioprotector. *Oncology (Williston Park)*. 2001;15(10):1349-54; discussion 57-60.
 659. Andreopoulos D, Schleicher UM, Cotarelo CL, Hand S, Ammon J. Radioprotection of human endothelial cells with amifostine. *Strahlenther Onkol*. 1999;175 Suppl 4:34-6.
 660. Grdina DJ, Murley JS, Kataoka Y, Calvin DP. Differential activation of nuclear transcription factor kappaB, gene expression, and proteins by amifostine's free thiol in human microvascular endothelial and glioma cells. *Semin Radiat Oncol*. 2002;12(1 Suppl 1):103-11.
 661. Bohuslavizki KH, Brenner W, Klutmann S, Hubner RH, Lassmann S, Feyerabend B, et al. Radioprotection of salivary glands by amifostine in high-dose radioiodine therapy. *J Nucl Med*. 1998;39(7):1237-42.
 662. Dunst J, Semlin S, Pigorsch S, Muller AC, Reese T. Intermittent use of amifostine during postoperative radiochemotherapy and acute toxicity in rectal cancer patients. *Strahlenther Onkol*. 2000;176(9):416-21.
 663. Kanter M, Topcu-Tarladacalisir Y, Uzal C. Role of amifostine on acute and late radiation nephrotoxicity: a histopathological study. *In Vivo*. 2011;25(1):77-85.

664. Tannehill SP, Mehta MP, Larson M, Storer B, Pellet J, Kinsella TJ, et al. Effect of amifostine on toxicities associated with sequential chemotherapy and radiation therapy for unresectable non-small-cell lung cancer: results of a phase II trial. *J Clin Oncol*. 1997;15(8):2850-7.
665. Fu P, Birukova AA, Xing J, Sammani S, Murley JS, Garcia JG, et al. Amifostine reduces lung vascular permeability via suppression of inflammatory signalling. *Eur Respir J*. 2009;33(3):612-24.
666. Giannopoulou E, Katsoris P, Kardamakis D, Papadimitriou E. Amifostine inhibits angiogenesis in vivo. *J Pharmacol Exp Ther*. 2003;304(2):729-37.
667. Giannopoulou E, Papadimitriou E. Amifostine has antiangiogenic properties in vitro by changing the redox status of human endothelial cells. *Free Radic Res*. 2003;37(11):1191-9.
668. Akel SM, Atoum MF, Saleh SA, Awadallah SM. Amifostine exerts anti-angiogenic activity and suppresses vascular endothelial growth factor secreted by hemopoietic stem/progenitor cells. *Saudi Med J*. 2005;26(10):1523-8.
669. Dedieu S, Canron X, Rezvani HR, Bouche-careilh M, Mazurier F, Sinisi R, et al. The cytoprotective drug amifostine modifies both expression and activity of the pro-angiogenic factor VEGF-A. *BMC Med*. 2010;8:19.
670. Kruse JJ, Strootman EG, Wondergem J. Effects of amifostine on radiation-induced cardiac damage. *Acta Oncol*. 2003;42(1):4-9.
671. Brizel DM, Overgaard J. Does amifostine have a role in chemoradiation treatment? *Lancet Oncol*. 2003;4(6):378-81.
672. Reeves WC, Cunningham D, Schwiter EJ, Abt A, Skarlatos S, Wood MA, et al. Myocardial hydroxyproline reduced by early administration of methylprednisolone or ibuprofen to rabbits with radiation-induced heart disease. *Circulation*. 1982;65(5):924-7.
673. Zielinska KA, Van Moortel L, Opdenakker G, De Bosscher K, Van den Steen PE. Endothelial Response to Glucocorticoids in Inflammatory Diseases. *Front Immunol*. 2016;7:592.
674. Orłowski RZ, Gercheva L, Williams C, Sutherland H, Robak T, Masszi T, et al. A Phase II, Randomized, Double-Blind, Placebo-Controlled Study of Siltuximab (Anti-IL-6 mAb) and Bortezomib versus Bortezomib Alone in Patients with Relapsed or Refractory Multiple Myeloma. *Am J Hematol*. 2015;90(1):42-9.
675. Dorff TB, Goldman B, Pinski JK, Mack PC, Lara PN, Jr., Van Veldhuizen PJ, Jr., et al. Clinical and correlative results of SWOG S0354: a phase II trial of CNT0328 (siltuximab), a monoclonal antibody against interleukin-6, in chemotherapy-pretreated patients with castration-resistant prostate cancer. *Clin Cancer Res*. 2010;16(11):3028-34.

676. Brana I, Calles A, LoRusso PM, Yee LK, Puchalski TA, Seetharam S, et al. Carlumab, an anti-C-C chemokine ligand 2 monoclonal antibody, in combination with four chemotherapy regimens for the treatment of patients with solid tumors: an open-label, multicenter phase 1b study. *Target Oncol.* 2015;10(1):111-23.
677. Pienta KJ, Machiels JP, Schrijvers D, Alekseev B, Shkolnik M, Crabb SJ, et al. Phase 2 study of carlumab (CNTO 888), a human monoclonal antibody against CC-chemokine ligand 2 (CCL2), in metastatic castration-resistant prostate cancer. *Invest New Drugs.* 2013;31(3):760-8.
678. Crusz SM, Balkwill FR. Inflammation and cancer: advances and new agents. *Nat Rev Clin Oncol.* 2015;12(10):584-96.
679. Rosen EM, Day R, Singh VK. New Approaches to Radiation Protection. *Frontiers in Oncology.* 2014;4:381.
680. Panganiban RA, Day RM. Inhibition of IGF-1R prevents ionizing radiation-induced primary endothelial cell senescence. *PLoS One.* 2013;8(10):e78589.
681. Chen HX, Sharon E. IGF-1R as an anti-cancer target--trials and tribulations. *Chin J Cancer.* 2013;32(5):242-52.
682. Weroha SJ, Haluska P. IGF-1 receptor inhibitors in clinical trials--early lessons. *J Mammary Gland Biol Neoplasia.* 2008;13(4):471-83.
683. Iglesias-Bartolome R, Patel V, Cotrim A, Leelahavanichkul K, Molinolo AA, Mitchell JB, et al. mTOR inhibition prevents epithelial stem cell senescence and protects from radiation-induced mucositis. *Cell Stem Cell.* 2012;11(3):401-14.
684. Assmus B, Urbich C, Aicher A, Hofmann WK, Haendeler J, Rossig L, et al. HMG-CoA reductase inhibitors reduce senescence and increase proliferation of endothelial progenitor cells via regulation of cell cycle regulatory genes. *Circ Res.* 2003;92(9):1049-55.
685. Ota H, Eto M, Kano MR, Kahyo T, Setou M, Ogawa S, et al. Induction of endothelial nitric oxide synthase, SIRT1, and catalase by statins inhibits endothelial senescence through the Akt pathway. *Arterioscler Thromb Vasc Biol.* 2010;30(11):2205-11.
686. Babcook MA, Joshi A, Montellano JA, Shankar E, Gupta S. Statin Use in Prostate Cancer: An Update. *Nutr Metab Insights.* 2016;9:43-50.
687. Kawata S, Yamasaki E, Nagase T, Inui Y, Ito N, Matsuda Y, et al. Effect of pravastatin on survival in patients with advanced hepatocellular carcinoma. A randomized controlled trial. *Br J Cancer.* 2001;84(7):886-91.
688. Lochhead P, Chan AT. Statins and colorectal cancer. *Clin Gastroenterol Hepatol.* 2013;11(2):109-e14.
689. Rosen EM, Day R, Singh VK. New approaches to radiation protection. *Front Oncol.* 2014;4:381.

690. Dajani EZ, Islam K. Cardiovascular and gastrointestinal toxicity of selective cyclo-oxygenase-2 inhibitors in man. *J Physiol Pharmacol.* 2008;59 Suppl 2:117-33.
691. Kirkham AA, Davis MK. Exercise Prevention of Cardiovascular Disease in Breast Cancer Survivors. *J Oncol.* 2015;2015:917606.
692. Singla A, Kumar G, Bardia A. Personalizing cardiovascular disease prevention among breast cancer survivors. *Curr Opin Cardiol.* 2012;27(5):515-24.
693. Daher IN, Daigle TR, Bhatia N, Durand JB. The prevention of cardiovascular disease in cancer survivors. *Tex Heart Inst J.* 2012;39(2):190-8.

Annexes

CURRICULUM VITAE OF BJORN BASELET

NAME BASELET, Bjorn (born October 26 th , 1990)	POSITION TITLE PhD Student		
eRA COMMONS USER NAME (credential, e.g., agency login)			
EDUCATION/TRAINING			
INSTITUTION AND LOCATION	DEGREE <i>(if applicable)</i>	MM/YY	FIELD OF STUDY
University of Hasselt, Belgium	B.S.	2011	Biomedical Science
University of Hasselt, Belgium	Master	2013	Clinical Molecular Sciences
Université catholique de Louvain (UCL) & Belgian Nuclear Research Centre (SCK•CEN)	PhD Student	ongoing	Radiobiology

Contact: Bjorn Baselet, Institute of Clinical and Experimental Research (IREC), Pole of Pharmacology & Therapeutics (FATH), Université catholique de Louvain (UCL), Avenue Emmanuel Mounier 52 box B1.53.09, Brussels, 1200, Belgium. Phone: +32 (0)2 764 52 67, Fax: +32 (0)2.764 52 69, Email: bjorn.baselet@uclouvain.be

Total cumulated impact factor: 25,809 H-index (Scopus August 2 nd , 2017): 3 Total number of citations (Scopus August 2 nd , 2017): 40

A. Positions and Honors

Positions & Employment

- 2011 Student Researcher in Biomedical Sciences, Department of Human Biology, Maastricht University, Maastricht, NL. *Topic:* Effect of feeding frequency on glucose and insulin metabolism and substrate partitioning in impaired glucose tolerant men. *Promotors:* Prof. Wim Saris and Dr. Marjet Munsters
- 2012 Student Researcher in Biomedical Sciences, Biomedical Research Institute, University of Hasselt, Diepenbeek, BE. *Topic:* Role of cholesterol and its receptors in experimental autoimmune encephalomyelitis. *Promotors:* Prof. Niels Hellings, Prof. Veerle Somers and Dr. Silke Timmermans
- 2013 Summer intern in Biomedical Sciences, Epsilon Biotech BVBA, Zonhoven, BE. *Topic:* Early detection of Sepsis via nanoelectronics using cytokine quantification. *Promotor:* Dr. Eugene Bosmans
- 2013 Research Fellow in Biomedical Sciences, Epsilon Biotech BVBA, Zonhoven, BE. *Topic:* Biomarkers in male subfertility: a flow cytometric approach. *Promotors:* Prof. Niels Hellings, Prof. Veerle Somers and Dr. Eugene Bosmans
- 2013 - PhD fellow at the Institute of Experimental and Clinical Research (IREC) affiliated to Université catholique de Louvain (UCL) & Belgian Nuclear Research Centre (SCK•CEN). *Directors:* Prof. Pierre Sonveaux and Dr An Aerts.

Honors & Awards

- 2013 Competitive travel grant to participate in the DoReMi European training course in Radiobiology: Inter-individual variability of radiation-sensitivity (CEA, France)
- 2013 Doctoral SCK•CEN/Université catholique de Louvain grant (4 years)
- 2014 Young investigator award from the European Radiation Research Society (ERR2014), Greece.
- 2015 Excellent Poster Award for the poster "Effect of ionizing radiation on coronary artery endothelial cells" presented at the 15th International Congress of Radiation Research (ICRR 2015) in Kyoto, Japan.
- 2015 DoReMi Ad Hoc Travel grant to attend the 15th International Congress of Radiation Research (ICRR 2015) in Kyoto, Japan.
- 2015 Young Investigators Travel Award to attend the 15th International Congress of Radiation Research (ICRR 2015) in Kyoto, Japan.
- 2016 3rd Prize at the photo competition "Tous connectés" of Confluent des Savoires (UNamur) with the picture entitled: "Circle of connectivity and vitality"
- 2016 CONCERT Travel grant to attend the "FEBS Advanced Lecture Course on Redox Regulation of Metabolic Processes" in Spetses, Greece
- 2016 DoReMi Ad Hoc Travel grant to attend the "Mitochondria and low dose radiation workshop" in Munich, Germany
- 2016 DoReMi Ad Hoc Travel grant to attend the "Low dose radiation and endothelium workshop" in Krakow, Poland

Other Experience and Professional Memberships

- 2012 Course on Laboratory Animal Science (FELASA B & C) at UHasselt (8 weeks)
- 2012 Radiation protection (ackd. by Federal Agency for Nuclear Control) at UHasselt (5 days)
- 2013 - Member of the Belgian Society of Pharmaceutical Sciences (BSPS)
- 2013 - Member of the European Radiation Research Association for Young Scientists (EURAYS)
- 2013 International School on Radiation Protection (SCK•CEN Academy, Mol, BE) (5 days)
- 2013 European training course in Radiobiology: Inter-individual variability of radiation-sensitivity: Mechanisms and Biomarkers (FP 7; CEA, Paris, France)
- 2014 - Member of the Belgian Society for Advancements in Cytometry (BSAC)
- 2014 - Member of the Belgian Association for Radiological Protection (BVS/ABR)
- 2014 PARTEK workshop: Microarray analysis (Affymetrix, Rotterdam, The Netherlands)

- 2014 Eur MSc Radiation Biology: part Radiation-induced effects (FP7; SCK•CEN, Mol, BE) (10 days)
- 2014 - Member of the European Radiation Research Society (ERRS)
- 2014 - Member of the Belgian Society for Analytical Cytology (BVAC/ABCA)
- 2017 - Member of the community of young space enthusiasts in Belgium (beSPACE)
- 2017 - Member of YouSpace platform
- 2017 - Member of the Student European Low Gravity Research Association (SELGRA)

B. Bibliography

Dissertations

- 2011 Bachelor dissertation: "Effect of feeding frequency on glucose and insulin metabolism and substrate partitioning in impaired glucose tolerant men."
- 2012 Junior dissertation: "Role of cholesterol and its receptors in experimental autoimmune encephalomyelitis"
- 2013 Master dissertation: "Biomarkers in male subfertility: a flow cytometric approach".

Publications in peer-reviewed journals

1. Rombouts C, Aerts A, Quintens R, Baselet B, El Saghire H, Harms-Ringdahl M, Haghdoost S, Janssen A, Yentrapalli R, Benotmane MA, Van Oostveldt P, Baatout S. Transcriptomic profiling suggests a role for IGFBP5 in premature senescence of endothelial cells after chronic low dose rate irradiation. *Int J Radiat Biol.* 2014;90(7):560-74. JCR IF2016: **1.992**
2. Payen VL, Porporato PE, Baselet B, Sonveaux P. Metabolic changes associated with tumor metastasis, part 1: tumor pH, glycolysis and the pentose phosphate pathway. *Cell Mol Life Sci.* 2016;73(7):1333-48. JCR IF2016: **5.788**
3. Baselet B, Rombouts C, Benotmane MA, Baatout S, Aerts A. Cardiovascular diseases related to ionizing radiation: the risk of low-dose exposure. *Int J Mol Med.* 2016; 38(6):1623-41. JCR IF2016: **2.341**
4. Porporato PE, Payen VL, Baselet B, Sonveaux P. Metabolic changes associated with tumor metastasis, part 2: Mitochondria, lipid and amino acid metabolism. *Cell Mol Life Sci.* 2016;73(7):1349-63. JCR IF2016: **5.788**
5. Hall J, Penny A, West C, Gomolka M, Quintens R, Badie C, Laurent O, Aerts A, Anastasov N, Azimzadeh O, Azizova T, Baatout S, Baselet B, Benotmane R, Blanchardon E, Guéguen Y, Haghdoost S, Harms-Ringhdahl M, Hess J, Kreuzer M, Laurier D, Macaeva E, Manning G, Pernot E, Ravanat J-L, Sabatie L, Tack K, Tapio S, Zitzelsberger H, Cardis E. Ionizing radiation biomarkers in epidemiological studies - An update. *Mutat Res.* 2017;771:59-84. JCR IF2016: **5.500**

6. Baselet B, Belmans N, Coninx E, Lowe D, Janssen A, Michaux A, Tabury K, Raj K, Quintens R, Benotmane MA, Baatout S, Sonveaux P, Aerts A. Functional gene analysis reveals cell cycle changes and inflammation in endothelial cells irradiated with a single X-ray dose. *Front. Pharmacol.* 2017;8:213 JCRIF2016: **4.400**

Submitted Manuscript

7. Baselet B, Azimzadeh O, Erbeltinger N, Bakshi M, Dettmering T, Janssen A, Ktitareva S, Lowe D, Michaux A, Quintens R, Raj K, Durante M, Fournier C, Benotmane AM, Baatout S, Sonveaux P, Tapio S, Aerts A. Single Dose Fe Ion and X-ray Irradiation Highlights the Radiation Quality Dependent Nature of the Endothelial Cell Response Single dose Fe ion irradiation highlights the radiation quality dependent nature of the endothelial cell response to ionizing radiation exposure. *Front. Pharmacol.* (resubmitted after revision).

Oral presentations

(*Denotes contribution as presenting author)

1. Baselet B*, Aerts A, Sonveaux P, Baatout S. Ionizing radiation: What does the heart say? SCK•CEN lunchtalk, 2017/05/19, Mol, Belgium.
2. Baselet B*, Aerts A, Janssen A, Michaux A, Quintens R, Benotmane R, Lowe D, Raj K, Sonveaux P, Baatout S. Effects of ionizing radiation on mitochondrial function in human endothelial cells. RDB Belgian Society for Advancement in Cytometry Annual Meeting 2016, 2016/10/21, Brussels, Belgium.
3. Baselet Bjorn*, Aerts A, Janssen A, Michaux A, Quintens R, Benotmane R, Lowe D, Raj K, Sonveaux P, Baatout S. Effects of ionizing radiation on mitochondrial function in human endothelial cells. RDB seminars in radiobiology, 2016/10/03 Brussels, Belgium.
4. Baselet B*, Aerts A, Janssen A, Michaux A, Quintens R, Benotmane R, Lowe D, Raj K, Sonveaux P, Baatout S. Effects of ionizing radiation on mitochondrial function in human endothelial cells. FEBS Advanced Lecture Course on Redox Regulation of Metabolic Processes, 2016/09/19-25, Spetses, Greece.
5. Baselet B*, Aerts A, Janssen A, Michaux A, Quintens R, Benotmane R, Lowe D, Raj K, Sonveaux P, Baatout S. Endothelial cell response after exposure to low dose X-ray radiation. PhD day of Institut de Recherche Expérimentale et Clinique (IREC), 2016/03/04 Brussels, Belgium.
6. Baselet B*, Aerts A, Janssen A, Michaux A, Quintens R, Benotmane R, Lowe D, Raj K, Sonveaux P, Baatout S. Effects of ionizing radiation on mitochondrial function in human endothelial cells. DoReMi workshop “Mitochondria and Radiation”, 2015/12/14-15, Munich, Germany.
7. Baselet B*, Aerts A, Janssen A, Michaux A, Quintens R, Benotmane R, Lowe D, Raj K, Sonveaux P, Baatout S. Transcriptomic profiling suggests a role for

- IGFBP5 in premature senescence of endothelial cells after chronic low dose rate irradiation. ICRR2015 conference, 2015/05/25-29, Kyoto, Japan.
8. Baselet B*, Aerts A, Janssen A, Michaux A, Quintens R, Benotmane R, Lowe D, Raj K, Sonveaux P, Baatout S. The vascular endothelial cell response following exposure to low doses of ionizing radiation. SCK•CEN PhD day, 2015/04/28, Mol, Belgium.
 9. Baselet B*, Aerts A, Janssen A, Michaux A, Quintens R, Benotmane R, Lowe D, Raj K, Sonveaux P, Baatout S. Evaluation of high and low LET radiation on human coronary artery endothelial cells. ProCardio final meeting, 2015/02/18-20, Rome, Italy.
 10. Baselet B*, Rombouts C, Aerts A, Sonveaux P, Baatout S. Radiation-induced cardiovascular risks and the potential prophylactic effects of statins. Séminaire de l'école doctorale en sciences pharmaceutiques et biomédicales, 2015/01/20, UCL, Brussels, Belgium.
 11. Baselet B, Aerts A, Janssen A, Michaux A, Quintens R, Benotmane R, Lowe D, Raj K, Sonveaux P, Baatout S*. Ionizing radiation induces a gene expression profile resembling a pro-atherosclerotic state in endothelial cells. 6th International MELODI Workshop, 2014/10/07-09, Barcelona, Spain.
 12. Baselet B*, Aerts A, Janssen A, Michaux A, Quintens R, Benotmane R, Lowe D, Raj K, Sonveaux P, Baatout S. Ionizing radiation induces a gene expression profile resembling a pro-atherosclerotic state in endothelial cells. ERRS conference, 2014/09/15-19, Rhodes, Greece.
 13. Baselet B*, Aerts A, Sonveaux P. Radiation-induced endothelial cell reprogramming. FATH retreat, 2014/05/09, Pepinster, Belgium.
 14. Baselet B*, Aerts A, Sonveaux P, Baatout S. Microarray results of the ProCardio study. IREC, UCL, Brussels, BE.
 15. Baselet B*, Aerts A, Sonveaux P, Baatout S. Caveats in the detection of the mitochondrial common deletion in endothelial cells. TUMETABO meeting, 2014/03/12, IREC, UCL, Brussels, BE.
 16. Baselet B*, Rombouts C, Aerts A, Sonveaux P, Baatout S. Radiation/induced cardiovascular risks and the potential prophylactic effects of statins. Séminaire de l'école doctorale en sciences pharmaceutiques et biomédicales, 2014/01/20, UCL, Brussels, BE.
 17. Baselet B*, Rombouts C, Aerts A, Sonveaux P, Baatout S. Radiation-induced cardiovascular risks and the potential prophylactic effects of statins. TUMETABO meeting, 2013/11/26, UCL, Brussels, BE.
 18. Baselet B*, Rombouts C, Aerts A, Sonveaux P, Baatout S. Radiation-induced cardiovascular risks and the potential prophylactic effects of statins. Meet and Greet meeting for the new scientists of the Institute for Environment, Health and Safety, 2013/11/22, SCK•CEN, BE.

19. Baselet B*, Rombouts C, Aerts A, Sonveaux P, Baatout S. Cardiovascular risks upon low dose exposure: endothelial cell response. Radiobiology seminars, 2013/11/04, SCK•CEN, Mol, BE.
20. Baselet B*, Rombouts C, Aerts A, Sonveaux P, Baatout S. Cardiovascular risks upon low dose exposure: endothelial cell response. Kick-off meeting LowX/Endotox, 2013/10/22, Agence Fédérale de Contrôle Nucléaire, Brussels, BE.

Poster communications

(*Denotes contribution as presenting author)

1. Baselet B*, Coninx E, Belmans N, Baatout S, Sonveaux P, Aerts A. Effects of ionizing radiation on mitochondrial function in human endothelial cells. SCK•CEN PhD day, 2016/10/27, Mol, Belgium.
2. Baselet B, Aerts A, Janssen A, Michaux A, Quintens R, Benotmane R, Lowe D, Raj K, Sonveaux Pierre, Baatout S. Effects of ionizing radiation on mitochondrial function in human endothelial cells. Radiation protection week, 2016/09/19-23, Oxford, UK.
3. Baselet B*, Aerts A, Janssen A, Michaux A, Quintens R, Benotmane R, Lowe D, Raj K, Sonveaux P, Baatout S. Effects of ionizing radiation on mitochondrial function in human endothelial cells. FEBS Advanced Lecture Course on Redox Regulation of Metabolic Processes, 2016/09/19-25, Spetses, Greece.
4. Baselet B*, Aerts An, Janssen Ann, Michaux Arlette, Quintens Roel, Benotmane Rafi, Lowe Donna, Raj Ken, Sonveaux Pierre, Baatout Sarah. Acute exposure to ionizing radiation induces a glycolytic switch, senescence and inflammation in endothelial cells. Interuniversity attraction pole meeting, 2016/05/24, Brussels, Belgium.
5. Baselet B*, Aerts A, Janssen A, Michaux A, Quintens R, Benotmane R, Lowe D, Raj K, Sonveaux P, Baatout S. Effects of ionizing radiation on mitochondrial function in human endothelial cells. Spring meeting of the FNRS contact group "oxidative processes and antioxidants", 2016/04/22, Louvain-la-Neuve, Belgium.
6. Baselet B*, Aerts A, Janssen A, Michaux A, Quintens R, Benotmane R, Lowe D, Raj K, Sonveaux P, Baatout S. Effect of ionizing radiation on human coronary artery endothelial cells. BACR annual meeting, 2016/01/30, Anderlecht, Belgium.
7. Baselet B, Aerts A, Janssen A, Michaux A, Quintens R, Benotmane R, Lowe D, Raj K, Sonveaux P, Baatout S*. Effect of ionizing radiation on human coronary artery endothelial cells. 20th annual meeting "Advances in Immunomonitoring by Flow Cytometry", 2015/11/19, Antwerp, Belgium.

8. Baselet B*, Aerts A, Janssen A, Michaux A, Quintens R, Benotmane R, Lowe D, Raj K, Sonveaux P, Baatout S. Effect of ionizing radiation on human coronary artery endothelial cells. 7th MELODI Workshop, 2015/11/09-11, Munich, Germany.
9. Baselet B*, Aerts A, Janssen A, Michaux A, Quintens R, Benotmane R, Lowe D, Raj K, Sonveaux P, Baatout S. Ionizing radiation induces a pro-atherosclerotic state in endothelial cells. Metabolism in Cancer and Stromal Cells (VIB meeting), 2015/09/8-10, Leuven, Belgium.
10. Baselet B*, Aerts A, Janssen A, Michaux A, Quintens R, Benotmane R, Lowe D, Raj K, Sonveaux P, Baatout S. Ionizing radiation induces a gene expression profile resembling a pro-atherosclerotic state in endothelial cells. IUAP-Belspo progress meeting, 2015/06/08, Ghent, Belgium.
11. Baselet B*, Aerts A, Janssen A, Michaux A, Quintens R, Benotmane R, Lowe D, Raj K, Sonveaux P, Baatout S. Cardiovascular risks after exposure to low dose ionizing radiation research at SCK•CEN. ICRR2015 conference, 2015/05/25-29, Kyoto, Japan.
12. Baselet B*, Aerts A, Janssen A, Michaux A, Quintens R, Benotmane R, Lowe D, Raj K, Sonveaux P, Baatout S. Effect of ionizing radiation on coronary artery endothelial cells. ICRR2015 conference, 2015/05/25-29, Kyoto, Japan.
13. Baselet B*, Aerts A, Janssen A, Michaux A, Quintens R, Benotmane R, Lowe D, Raj K, Sonveaux P, Baatout S. Ionizing radiation induces a gene expression profile resembling a pro-atherosclerotic state in endothelial cells. Meeting of the Belgian Association for Cancer Research (BACR-ABEC-BVSK), 2015/01/31, Antwerp, Belgium.
14. Baselet B*, Aerts A, Janssen A, Michaux A, Quintens R, Benotmane R, Lowe D, Raj K, Sonveaux P, Baatout S. Ionizing radiation induces a gene expression profile resembling a proatherosclerotic state in endothelial cells. SCK•CEN PhD day, 2014/10/23, Mol, Belgium.
15. Baselet B*, Aerts A, Janssen A, Michaux A, Quintens R, Benotmane R, Lowe D, Raj K, Sonveaux P, Baatout S. Endothelial cell reprogramming following exposure to ionizing radiations. Autumn meeting of the Belgian Society of Physiology and Pharmacology (BSPP), 2014/10/17, Brussels, Belgium.
16. Baselet B, Aerts A, Janssen A, Michaux A, Quintens R, Benotmane R, Lowe D, Raj K, Sonveaux P, Baatout S*. Radiation-induced endothelial cell reprogramming. 6th International MELODI Workshop, 2014/10/07-09, Barcelona, Spain.
17. Baselet B*, Aerts A, Janssen A, Michaux A, Quintens R, Benotmane R, Lowe D, Raj K, Sonveaux P, Baatout S. Endothelial cell reprogramming following exposure to ionizing radiation. Annual mini Symposium of the Thematic Doctoral School of Experimental Cancerology, 2014/09/2014, Liège, Belgium.

18. Baselet B*, Aerts A, Janssen A, Michaux A, Quintens R, Benotmane R, Lowe D, Raj K, Sonveaux P, Baatout S. Ionizing radiation induces a gene expression profile resembling a pro-atherosclerotic state in endothelial cells. ERR2014 conference, 2014/09/15-19, Rhodes, Greece.
19. Baselet B*, Aerts A, Janssen A, Michaux A, Quintens R, Benotmane R, Lowe D, Raj K, Sonveaux P, Baatout S. Cardiovascular risks upon low dose exposure: endothelial cell response. 3rd DoReMi Periodic meeting, 2014/07/08-10, Munich, Germany.
20. Baselet B*, Aerts A, Janssen A, Michaux A, Quintens R, Benotmane R, Lowe D, Raj K, Sonveaux P, Baatout S. Ionizing radiation induces a gene expression profile resembling a pro-atherosclerotic state in endothelial cells. ERRS conference, 2014/09/15-19, Rhodes, Greece.
21. Baselet B*, Aerts A, Janssen A, Michaux A, Quintens R, Benotmane R, Lowe D, Raj K, Sonveaux P, Baatout S*. Cardiovascular risks upon low dose exposure: endothelial cell response. 3rd DoReMi Periodic meeting, 2014/07/08-10, Munich, Germany.
22. Baselet B*, Thewissen Bart, Somers Veerle, Hellings Niels, Bosmans Eugene. Biomarkers in male subfertility: a flow cytometric approach. International Life Sciences Master Students Research Conference, 2013/06/27, Maastricht University, Maastricht, Netherlands.

Bjorn Baselet – CV & biblio – last update August 2nd, 2017

Annex 2. Online supplementary data related to Results Chapter 1: “Functional gene analysis reveals cell cycle changes and inflammation in endothelial cells irradiated with a single X-ray dose”, by Baselet B *et al.*, *Front. Pharmacol.* 2017;8:213.

Supplemental data 1. Transcriptomic comparison of irradiated and sham-irradiated Est-2 immortalized human coronary artery endothelial cells at day 1, day 7 and day 14 after a single dose of 2, 0.5, 0.1 and 0.05 Gy. Raw data with accession number E-MTAB-5054 are available online at <http://www.ebi.ac.uk/arrayexpress>.

Supplemental data 2. Gene ontology enrichment analysis of irradiated and sham-irradiated Est-2 immortalized human coronary artery endothelial cells at day 1, day 7 and day 14 after a single dose of 2, 0.5, 0.1 and 0.05 Gy. Raw data with accession number E-MTAB-5054 are available online at <http://www.ebi.ac.uk/arrayexpress>.

Supplementary table 1. Differentially expressed genes in TICAE cells irradiated with a single X-ray dose of 2 Gy.*

Day 1			Day 7			Day 14		
2 Gy vs. 0 Gy			2 Gy vs. 0 Gy			2 Gy vs. 0 Gy		
Probeset ID	Gene symbol	Fold change	Probeset ID	Gene symbol	Fold change	Probeset ID	Gene symbol	Fold change
16767115	RPSAP52	3.01	16698947	RNU5A-8P	8.96	16787362	RN7SKP255	3.60
16735751	LYVE1	2.96	17022133	LINC00577	4.01	16992789	RP11-843P14.2	3.18
17039299	HLA-B	2.77	17100711		3.65	16997676	MTRNR2L2	2.73
16753853	MDM2	2.73	16787362	RN7SKP255	2.59	16744154	RP11-25I9.2	2.42
17022133	LINC00577	2.60	16876431		2.48	16818543		2.38
17005167	RNU6-190P	2.58	16782050	MGC40069	2.42	17074080		2.33
16988913	RNU6ATAC10P	2.50	16775583	RNY3P7	2.39	16782050	MGC40069	2.31
16744154	RP11-25I9.2	2.49	16988913	RNU6ATAC10P	2.36	17005167	RNU6-190P	2.31
16966279	RNA5SP160	2.41	16735751	LYVE1	2.33	16974115		2.23
16831787		2.35	16974115		2.30	16776021	RNU6-83P	2.23
16787362	RN7SKP255	2.34	16976012		2.18	16988913	RNU6ATAC10P	2.06
16974115		2.33	16660734	MIR378F	2.16	16996800		2.03
16823889	MIR548H2	2.32	17051553	CPA4	2.11	16900737		2.01
16998510		2.26	16831787		2.08	17094586		2.00
16726880	NEAT1	2.20	17005167	RNU6-190P	2.05	16862604	CD79A	1.94
16776616	SOX1	2.18	16721566	RP11-324J3.1	2.03	16697654	MIR181A1HG	1.86
17014959	LOC102723922	2.15	17016383	HIST1H4D	1.98	16833917	LRRC3C	1.84
17074080		2.10	16698714		1.94	16920528		1.84
16848055		2.10	16967875	PARM1	1.91	16921827	MIR155HG	1.83
16696425	TNFSF4	2.08	16774053	CCNA1	1.90	16991667		1.82

16660734	MIR378F	2.05	17074080		1.90	16819792	RNA5SP428	1.81
16880254	RNU6-634P	2.01	16744154	RP11-25I9.2	1.89	17063005	PLXNA4	1.81
16897446	RNU6-439P	1.97	17059119	SEMA3C	1.87	16900709		1.79
16858310	MIR4748	1.96	16917849	THBD	1.85	16719786		1.78
16966685	SPATA18	1.94	17043843	TSPAN13	1.85	16734793	OR51E2	1.70
16983742	RNU6-760P	1.92	16875763	UBE2S	1.84	16686037	RP5-994D16.9	1.69
16877451		1.91	16776021	RNU6-83P	1.84	16785151	RNU6-1162P	1.64
16782050	MGC40069	1.91	16903140	CXCR4	1.81	17061532	SYPL1	1.64
16997676	MTRNR2L2	1.91	16904425	GRB14	1.79	16722162	PARVA	1.64
16996956		1.90	17076726	PLAT	1.79	16681884	HNRNPCL2	1.64
16829505		1.90	16966855	KIT	1.79	16782102	TRAJ10	1.62
16701877	PITRM1-AS1	1.90	17087758	NIPSNAP3A	1.78	17027679	DPCR1	1.62
17042857	AC091729.8	1.87	16660713		1.77	16908112	AC012668.3	1.62
17073066	RNA5SP278	1.86	16842219		1.76	16796406		1.57
16776021	RNU6-83P	1.85	16979985	MGARP	1.76	16828833		1.57
17047918	CROT	1.85	16702172		1.76	16856172	RNA5SP462	1.57
17084164	RP11-298E2.2	1.85	17027679	DPCR1	1.76	16943241	COL8A1	1.56
16784135	RNA5SP385	1.83	16997676	MTRNR2L2	1.76	16827041	CDH11	1.55
16721371		1.83	16788630	SNHG24	1.75	16819736		1.53
17072723	RNU1-106P	1.82	16884301	AC123886.2	1.73	16897446	RNU6-439P	1.53
16783494	SLC25A21-AS1	1.82	17010173	RNU6-411P	1.72	16682175	SPATA21	1.52
16828833		1.81	16897159	SIX2	1.72	16849623	MIR4739	-1.50
16661811		1.80	16833204	CCL2	1.71	16684579	MIR4254	-1.53
16683925	SLC9A1	1.80	16961637	NCEH1	1.70	16952769	CDCP1	-1.55
16681451	RP3-510D11.1	1.79	16993385		1.69	16963428	MFI2	-1.56
16894673	AC008278.3	1.78	16930021	MIR4534	1.67	16875968		-1.58

16993385		1.77	16828833		1.66	16979900		-1.60
16681370	ENO1	1.76	16988423	PRR16	1.64	16988984	PDLIM4	-1.60
16956613		1.73	17100771		1.64	17027504	MIR877	-1.61
16707923		1.72	16726880	NEAT1	1.63	16907621	MIR3130-1	-1.61
16660309	RP3-340N1.2	1.72	16824564		1.63	16668572	CYMP	-1.61
16819792	RNA5SP428	1.72	16855600	CCBE1	1.63	16684080	IFI6	-1.63
17027679	DPCR1	1.72	17045838	IGFBP1	1.63	16780885	FAM155A	-1.63
16738933	VWCE	1.71	17081106	GSDMC	1.63	17016366	HIST1H2AB	-1.65
16683290	ZNF436	1.71	16696425	TNFSF4	1.62	16925461	AP000696.2	-1.67
17081071	RNU4-25P	1.70	16702571	MCM10	1.62	16941998	SPATA12	-1.70
16991527	CYFIP2	1.69	16684080	IFI6	1.62	16731396	RP11-159N11.3	-1.88
16963113	APOD	1.68	17016366	HIST1H2AB	1.60	16924097		-2.01
16928988	TCN2	1.67	16719786		1.60	16989408	MIR4461	-2.23
16833917	LRRC3C	1.67	16833297	FNDC8	1.60			
16700218	TRIM17	1.66	16857258	UHRF1	1.59			
17040387	HLA-A	1.66	16905436	LINC01116	1.59			
16923805	PCBP3	1.65	16996612	CTC-436P18.3	1.59			
17084959		1.65	16762837	CAPRN2	1.58			
16819736		1.65	16725041	FAM111B	1.57			
17117604	GAS6-AS1	1.65	17110932		1.57			
16967875	PARM1	1.65	16698023	UBE2T	1.56			
17114007	APLN	1.64	17106067	VSIG1	1.55			
16797340	IGHE	1.64	16919962	SULF2	1.54			
16856172	RNA5SP462	1.64	16883690	IL1RL1	1.53			
16734339	MIR4298	1.64	17080749	ATAD2	1.53			
16719786		1.64	16686834		1.52			

17085196	ANKRD20A3	1.63	16686037	RP5-994D16.9	1.52			
16788725	MIR329-1	1.62	16861641	C19orf33	1.51			
16797444		1.62	16757324	OAS1	1.51			
16698714		1.60	16819213	MT1L	1.51			
17018720	TMEM217	1.60	16834056	CDC6	1.51			
16665932	GADD45A	1.60	16779546	DIAPH3	1.50			
16920528		1.59	16868838	SPC24	1.50			
16921827	MIR155HG	1.59	16878416	BRE	-1.50			
16774303	RGCC	1.59	16933044	ZNF70	-1.50			
16876497		1.58	17005094	GMPR	-1.51			
16824564		1.58	17067496	CTD-2647L4.4	-1.51			
17079317	TP53INP1	1.58	16915245	APCDD1L-AS1	-1.52			
16919962	SULF2	1.58	16744205	ARHGAP20	-1.52			
16991667		1.58	16934780		-1.52			
17014680	RP11-568A7.2	1.57	16732807	VWA5A	-1.52			
16813199	MESP1	1.57	17071144	SDC2	-1.52			
16920315	NFATC2	1.56	16995715	LOC100506548	-1.53			
16996937	RNU6-724P	1.56	16685875	SLFNL1	-1.53			
16991942	RN7SKP60	1.56	16669796	TXNIP	-1.55			
17099685		1.56	16675045	HMCN1	-1.55			
16769569	NUAK1	1.55	17029003	HLA-C	-1.55			
16661025	RNU6-110P	1.55	16838169	SNHG20	-1.55			
16953862	QARS	1.55	16756310	TCP11L2	-1.55			
16721280	TRIM22	1.54	17079248	KIAA1429	-1.56			
16776491		1.54	17040387	HLA-A	-1.56			
16884301	AC123886.2	1.54	16829426	DBNDD1	-1.57			
16859795	GDF15	1.54	16847676	GH2	-1.58			

16734793	OR51E2	1.54	16840113	CXCL16	-1.58			
16860386		1.53	16862284	LTBP4	-1.59			
16665796	SGIP1	1.53	16952769	CDCP1	-1.59			
17117542		1.52	16789526	ZBTB42	-1.60			
17073358	RP11-909N17.2	1.52	17088760	PTGS1	-1.60			
16864920	FAM90A27P	1.51	17059955	PDK4	-1.61			
17075014	MTUS1	1.51	16957396	CCDC80	-1.61			
16911139	PRND	1.51	16852573	NEDD4L	-1.62			
16830914	PFAS	-1.50	16959386	SLCO2A1	-1.62			
17087343	NCBP1	-1.50	16688615	SLC44A5	-1.63			
17072313	TBC1D31	-1.50	16761820	MGP	-1.64			
16687464		-1.51	16790744	SLC7A8	-1.65			
17102948	ZNF674-AS1	-1.51	16933030	GUSBP11	-1.65			
17117418		-1.51	16876147	ZNF132	-1.66			
17062502	POT1	-1.51	16806538	GOLGA8R	-1.66			
16829085	SLC7A5	-1.51	16669850	ITGA10	-1.67			
16959325	TOPBP1	-1.51	17092331	PTPRD	-1.68			
16851397	RBBP8	-1.51	16942367	RNA5SP134	-1.72			
16978995	ELOVL6	-1.51	16686640	KNCN	-1.73			
16871567	ALKBH6	-1.52	16675398	CFH	-1.74			
16852445	C18orf54	-1.52	16802022	ZNF609	-1.82			
16699877	LBR	-1.52	16671187	NPR1	-1.83			
17057413	SNHG15	-1.52	16757178	RP3-462E2.3	-1.87			
16728518	FAM86C1	-1.52	16760257	VWF	-1.89			
16772625	POLE	-1.52	16928293		-1.97			
16952769	CDCP1	-1.52	17046284	SUMF2	-2.17			

17088185	PRPF4	-1.52	16780317	CLDN10-AS1	-2.26			
16732880	SPA17	-1.52	16761776		-2.29			
16988423	PRR16	-1.52	16667155	SNORD21	-2.37			
16942991	ARL13B	-1.52	16938133	GALNT15	-2.40			
16883690	IL1RL1	-1.52						
16877888	EPT1	-1.52						
16831383	ADORA2B	-1.53						
16683875	GPN2	-1.53						
16981506	HMGB2	-1.53						
16777384	SACS	-1.53						
16722603	LDHA	-1.53						
17111594	SPIN4	-1.53						
16663033	SMAP2	-1.53						
16929199	LOC54944	-1.54						
16662338	ZMYM1	-1.54						
16799517	KNSTRN	-1.54						
17086987	PTPDC1	-1.54						
17097914	PHF19	-1.54						
16850477	TYMS	-1.54						
17021521	RNGTT	-1.55						
16731169	DLAT	-1.55						
16959148	ASTE1	-1.55						
17016506	HIST1H4L	-1.55						
16661806	RN7SKP91	-1.55						
16995705	RPL37	-1.55						
16678496	HIST3H2BB	-1.55						
16753800	NUP107	-1.56						

16683887	GPATCH3	-1.56						
17117581	LOC100128816	-1.56						
16830778	TMEM88	-1.56						
16970231	EXOSC9	-1.57						
16661117	CEP85	-1.57						
16744125	KDELC2	-1.57						
16910501	DTYMK	-1.57						
16760162	C12orf4	-1.57						
16725049	FAM111A	-1.57						
17025693	RP1-167A14.2	-1.57						
16848793	SLC25A19	-1.57						
16922495	CBR3	-1.57						
17092615	PSIP1	-1.58						
16932914	ZNF280B	-1.58						
16748490	APOLD1	-1.58						
16973693	HAUS3	-1.58						
16757347	OAS3	-1.58						
16943919	C3orf52	-1.58						
17093724	ARHGEF39	-1.58						
16735545	NRIP3	-1.59						
16785631	EIF2S1	-1.59						
16755498	TMPO	-1.59						
17051965	NUP205	-1.59						
17024227	REPS1	-1.59						
16664576		-1.59						
17005535		-1.59						
16909588	TIGD1	-1.60						

17032533	HLA-DPA1	-1.60						
16838887	SLC25A10	-1.60						
16766719	METTL1	-1.60						
17014309	ACAT2	-1.60						
16877762	CENPO	-1.61						
16908985	AP1S3	-1.61						
16747287	NCAPD2	-1.61						
16885028	TMEM177	-1.61						
16664118	NASP	-1.61						
16829464		-1.61						
17064105	EZH2	-1.62						
16907960	BARD1	-1.62						
16754917	C12orf29	-1.62						
16662945	MFSD2A	-1.62						
16766137	TIMELESS	-1.63						
16853042	TIMM21	-1.63						
16768579	CEP83	-1.63						
17117588	RP11- 669B18.1	-1.63						
16977066	NUP54	-1.63						
16922584	CHAF1B	-1.63						
16781482	PARP2	-1.63						
17086353	RMI1	-1.63						
16996645	DIMT1	-1.63						
16967031	PAICS	-1.64						
16733104	CHEK1	-1.64						
16838359	BIRC5	-1.64						

16757687	RFC5	-1.64						
17016043	MBOAT1	-1.64						
17092688	HAUS6	-1.64						
16935517	CENPM	-1.64						
16699739	PARP1	-1.64						
16673983	DARS2	-1.64						
16818600	ORC6	-1.65						
16669212	TTF2	-1.65						
16960271	HLTF	-1.65						
16987298	ANKRD32	-1.65						
17012632	ENPP1	-1.65						
16868576	DNMT1	-1.66						
17018685	PPIL1	-1.66						
17086193	PSAT1	-1.66						
16736807	CCDC34	-1.66						
16855820	RTTN	-1.66						
16869624	DDX39A	-1.66						
16954707	POC1A	-1.67						
16973263		-1.67						
17016383	HIST1H4D	-1.67						
16697196	FAM129A	-1.67						
16809596	RAB27A	-1.67						
17102230	POLA1	-1.68						
16810933	TIPIN	-1.68						
16779720	MZT1	-1.68						
16979060	ZGRF1	-1.68						
17084352	CYP4F26P	-1.69						

16729298	ACER3	-1.69						
16866951	LMNB2	-1.69						
16762661	PTHLH	-1.69						
16906440	OSGEPL1	-1.69						
16668960	DCLRE1B	-1.70						
16795304	CEP128	-1.70						
16846864	MMD	-1.71						
16775014	CKAP2	-1.71						
16783644	PNN	-1.71						
17100317	SAPCD2	-1.72						
16658987		-1.72						
17049461	POP7	-1.72						
17004273	NQO2	-1.72						
16829764	GSG2	-1.72						
16885411	GPR17	-1.72						
17070381	LRRCC1	-1.72						
16837729	NUP85	-1.72						
16785316	MTHFD1	-1.73						
17009862	PRIM2	-1.73						
17093595	FANCG	-1.73						
16803562	CHRNA5	-1.73						
16718022	PCGF6	-1.74						
16925239	DONSON	-1.74						
16860418	CCNE1	-1.74						
16703452	PDSS1	-1.74						
17068385	GINS4	-1.74						

16708097	R3HCC1L	-1.75						
17103413	SUV39H1	-1.75						
16773840	BRCA2	-1.76						
17094998	C9orf40	-1.76						
16705074	TFAM	-1.76						
16821869	CDT1	-1.77						
16833449	PIGW	-1.77						
17069976	KCNB2	-1.77						
16823229	PKMYT1	-1.78						
16877956	CENPA	-1.79						
16821239	CENPN	-1.79						
16969473	GSTCD	-1.79						
16845349	BRCA1	-1.80						
16766403	TMEM194A	-1.80						
16769481	ALDH1L2	-1.81						
17009809	KIAA1586	-1.81						
16767851	E2F7	-1.81						
16808876	CEP152	-1.81						
17016503	HIST1H3I	-1.82						
16774082	EXOSC8	-1.82						
16819678	GINS3	-1.83						
16756960	FAM216A	-1.83						
17012888	PEX7	-1.83						
16755928	PARPBP	-1.84						
16687618	DHCR24	-1.84						
16846218	HOXB2	-1.85						
16948021	ECT2	-1.85						

16984032	SKP2	-1.85						
16919044	RBL1	-1.85						
17086784	CENPP	-1.85						
16914315	UBE2C	-1.86						
16875763	UBE2S	-1.86						
16736638	E2F8	-1.87						
17112729	TIMM8A	-1.87						
16832852	ATAD5	-1.88						
16842103	SHMT1	-1.88						
16667037	CDC7	-1.89						
16798810		-1.89						
16929573	MCM5	-1.90						
16721535	ZNF215	-1.91						
16746379	NCAPD3	-1.92						
16692724	ANP32E	-1.94						
17027710	TCF19	-1.95						
16835797	EME1	-1.96						
16783047	G2E3	-1.97						
16692632	HIST2H2BE	-1.97						
17109211	FANCB	-1.97						
16987125	POLR3G	-1.97						
16985614	CENPH	-1.98						
17086634	CKS2	-1.98						
17079220	RAD54B	-1.98						
16665447	USP1	-1.98						
16792381	MIS18BP1	-1.98						
17076103	TEX15	-1.99						

16729557	DDIAS	-1.99						
16880057	CHAC2	-1.99						
16701689		-2.00						
16667206	CCDC18	-2.00						
16750761	TROAP	-2.00						
17002912	BOD1	-2.01						
16810543	KIAA0101	-2.01						
16920548	AURKA	-2.01						
16725806	INCENP	-2.02						
16664243	RAD54L	-2.02						
16671503	CKS1B	-2.03						
16992096	SPDL1	-2.03						
17020019	MCM3	-2.05						
16703478	MASTL	-2.05						
17049714	LOC101927746	-2.05						
16817824	CORO1A	-2.05						
16953279	CDC25A	-2.06						
16947556	SMC4	-2.06						
17093397	KIF24	-2.07						
17016372	HIST1H1C	-2.08						
17058617	RFC2	-2.08						
17016390	HIST1H2BG	-2.08						
16986065	TMEM171	-2.08						
16745236	H2AFX	-2.08						
16721126	RRM1	-2.09						
16829369	FANCA	-2.10						
17068782	MCM4	-2.11						

16755692	GAS2L3	-2.11						
17005560	HIST1H4I	-2.12						
16931225	RIBC2	-2.12						
16774053	CCNA1	-2.12						
16913681	FAM83D	-2.14						
17060412	MCM7	-2.14						
16687188	ORC1	-2.14						
16924966	MIS18A	-2.15						
16962493	RFC4	-2.16						
16668079	GPSM2	-2.18						
16836492	PRR11	-2.18						
16687418	NDC1	-2.18						
16670383	HIST2H2AA4	-2.19						
16858386	LDLR	-2.22						
16877473	GEN1	-2.22						
17012379	CENPW	-2.22						
16815090	CCNF	-2.22						
16858714	RNASEH2A	-2.24						
16732960	CCDC15	-2.25						
16857258	UHRF1	-2.25						
16964000	TACC3	-2.26						
16669422		-2.28						
16690067	SASS6	-2.29						
17005582	HIST1H2BF	-2.30						
16775324	BORA	-2.30						
16887810	ZAK	-2.30						
17064679	XRCC2	-2.31						

16773946	RFC3	-2.31						
16771067	CIT	-2.33						
17005396	GMNN	-2.33						
17057718	FIGNL1	-2.34						
16714504	ZWINT	-2.35						
16957951	POLQ	-2.36						
16909700	HJURP	-2.36						
16918445	E2F1	-2.36						
17016509		-2.37						
16758336	KNTC1	-2.38						
16760048	FOXMI	-2.39						
17077826	MYBL1	-2.39						
16832429	TMEM97	-2.39						
16804902	BLM	-2.39						
16996722	CENPK	-2.44						
16736891	KIF18A	-2.44						
16931384	GTSE1	-2.45						
16918976	DSN1	-2.46						
17086167	CEP78	-2.47						
16804631	TICRR	-2.48						
17080749	ATAD2	-2.49						
17024980	FBXO5	-2.50						
17104484	KIF4A	-2.50						
17020787	MB21D1	-2.52						
16845794	KIF18B	-2.53						
16877019	RRM2	-2.53						
16673557	C1orf112	-2.54						

16663958	KIF2C	-2.54						
16784299	CDKN3	-2.56						
16760621	CDCA3	-2.56						
16714998	DNA2	-2.57						
17067332	ESCO2	-2.58						
16692580	HIST2H3PS2	-2.62						
16799426	BUB1B	-2.62						
16927052	CDC45	-2.62						
16995938	C5orf34	-2.64						
16817647	KIF22	-2.64						
16793190	WDHD1	-2.65						
16945101	MCM2	-2.65						
16766318	PRIM1	-2.65						
16802204	ZWILCH	-2.66						
16982024	CENPU	-2.66						
16937505	FANCD2	-2.67						
17016496	HIST1H2AK	-2.68						
16787430	CALM1	-2.70						
16834381	TUBG1	-2.71						
16688386	DEPDC1	-2.71						
16996545	DEPDC1B	-2.73						
16685165	CLSPN	-2.74						
16889251	SGOL2	-2.75						
16779546	DIAPH3	-2.77						
16979389	MAD2L1	-2.77						
16840902	AURKB	-2.79						
16707695	HELLS	-2.80						

16985599	CCNB1	-2.80						
16847432	BRIP1	-2.82						
17096205	ZNF367	-2.82						
17038792	KIFC1	-2.82						
16698023	UBE2T	-2.84						
16913957	MYBL2	-2.84						
16830173	FAM64A	-2.88						
17087716	SMC2	-2.89						
16663514	CDC20	-2.89						
16807605	OIP5	-2.91						
16849379	TK1	-2.93						
17064939	NCAPG2	-2.93						
16705159	CDK1	-2.98						
17105401	CENPI	-2.99						
16972616	NEIL3	-3.00						
16982635	TRIP13	-3.00						
16815905	RMI2	-3.00						
16903090	MCM6	-3.02						
16692636	HIST2H2AB	-3.04						
16686796	STIL	-3.07						
16991859	HMMR	-3.08						
16751709	ESPL1	-3.11						
16697695	KIF14	-3.14						
16911212	MCM8	-3.14						
16679411	EXO1	-3.16						
16813342	PRC1	-3.17						
16725735	FEN1	-3.18						

17080595	DSCC1	-3.21						
17000439	CDC25C	-3.21						
17047965	DBF4	-3.25						
16799637	RAD51	-3.27						
16694617	IQGAP3	-3.27						
17016363	HIST1H3B	-3.29						
16826160	SHCBP1	-3.30						
16988703	LMNB1	-3.33						
16938296	SGOL1-AS1	-3.38						
16804559	FANCI	-3.41						
16842673	SPAG5	-3.46						
16702685	SUV39H2	-3.46						
16817017	PLK1	-3.46						
17067102	CDCA2	-3.46						
16800355	WDR76	-3.47						
16707221	KIF20B	-3.47						
16662648	CDCA8	-3.50						
16698984	NEK2	-3.52						
16868838	SPC24	-3.59						
16798801	ARHGAP11B	-3.60						
16677425	CENPF	-3.65						
16912379	TPX2	-3.68						
16792519	POLE2	-3.70						
16979515	CCNA2	-3.74						
17016366	HIST1H2AB	-3.75						
16673154	NUF2	-3.75						
17005589	HIST1H2AE	-3.76						

16882975	NCAPH	-3.77						
16702571	MCM10	-3.80						
16957170	KIAA1524	-3.81						
16777278	SKA3	-3.85						
16747014	RAD51AP1	-3.86						
16793225	DLGAP5	-3.88						
16677201	DTL	-3.91						
16719515	MKI67	-3.95						
17010552	TTK	-3.95						
16951485	SGOL1	-3.98						
16834056	CDC6	-3.98						
16991460	KIF4B	-3.99						
16869588	ASF1B	-4.02						
16844312	TOP2A	-4.09						
16852312	SKA1	-4.18						
17079293	CCNE2	-4.21						
16799598	CASC5	-4.22						
16978568	CENPE	-4.33						
16809748	MNS1	-4.35						
16707551	CEP55	-4.43						
16799793	NUSAP1	-4.45						
16904780	SPC25	-4.47						
16971573	MND1	-4.48						
16697544	ASPM	-4.50						
17084904	MELK	-4.54						
16850517	NDC80	-4.56						
16912192	GINS1	-4.59						

16798919	ARHGAP11A	-4.69						
16970563	PLK4	-4.70						
16901755	BUB1	-4.71						
16828886	GIN52	-4.73						
17045198	ANLN	-4.75						
16901957	CKAP2L	-4.75						
16801557	CCNB2	-4.87						
16939960	KIF15	-4.89						
16707468	KIF11	-4.89						
16965346	NCAPG	-4.99						
17005858	HIST1H2AI	-5.00						
16989636	KIF20A	-5.21						
16670387	HIST2H3A	-5.27						
17016369	HIST1H2BB	-5.64						
16802519	KIF23	-5.68						
17075776	PBK	-5.82						
17005865	HIST1H2BM	-6.49						
17016486	HIST1H2BL	-6.63						
16725041	FAM111B	-7.41						
17016499	HIST1H1B	-7.66						

*TICAE cells were analyzed at the indicated time points after irradiation with a single X-ray dose of 2 Gy. Fold changes are shown compared to sham irradiation, as described in Materials and Methods (n = 3).

Supplementary table 2. Differentially expressed genes TICAE cells irradiated with a single X-ray dose of 0.5 Gy.*

Day 1			Day 7			Day 14		
0.5 Gy vs. 0 Gy			0.5 Gy vs. 0 Gy			0.5 Gy vs. 0 Gy		
Probeset ID	Gene symbol	Fold change	Probeset ID	Gene symbol	Fold change	Probeset ID	Gene symbol	Fold change
17042857	AC091729.8	2.17	16760257	VWF	-1.60	16997676	MTRNR2L2	1.89
16974115		2.15	16787362	RN7SKP255	2.27	16862604	CD79A	1.78
16988913	RNU6ATAC10P	1.98				16782050	MGC40069	2.11
17073066	RNA5SP278	1.95				16787362	RN7SKP255	2.24
16744154	RP11-25I9.2	1.95						
17074080		1.93						
17072723	RNU1-106P	1.82						
16905115		1.79						
17005167	RNU6-190P	1.76						
16681370	ENO1	1.76						
16831787		1.75						
16897446	RNU6-439P	1.71						
16660309	RP3-340N1.2	1.66						
16956613		1.63						
16892863	AC112715.2	1.63						
16997676	MTRNR2L2	1.62						
16753853	MDM2	1.58						
16966685	SPATA18	1.58						
17056072	SKAP2	1.55						
16828833		1.55						

16991839	CCNG1	1.54						
16696425	TNFSF4	1.52						
16991164	MYOZ3	-1.50						
16829153	SNAI3	-1.50						
16815090	CCNF	-1.50						
16692724	ANP32E	-1.50						
16687418	NDC1	-1.50						
16927052	CDC45	-1.51						
16669389	PHGDH	-1.51						
17009794	BEND6	-1.53						
16847432	BRIP1	-1.53						
16821869	CDT1	-1.53						
16911212	MCM8	-1.54						
16767851	E2F7	-1.54						
16850477	TYMS	-1.55						
16910501	DTYMK	-1.55						
16992096	SPDL1	-1.55						
16663958	KIF2C	-1.56						
16838359	BIRC5	-1.56						
16909700	HJURP	-1.57						
16667206	CCDC18	-1.57						
16698023	UBE2T	-1.58						
16779546	DIAPH3	-1.58						
17067332	ESCO2	-1.58						
16775324	BORA	-1.58						
16745236	H2AFX	-1.58						

16747287	NCAPD2	-1.59						
16810543	KIAA0101	-1.59						
17068782	MCM4	-1.59						
17096205	ZNF367	-1.60						
16707468	KIF11	-1.60						
16857258	UHRF1	-1.60						
16858714	RNASEH2A	-1.60						
16799426	BUB1B	-1.61						
16804559	FANCI	-1.61						
16913681	FAM83D	-1.61						
16667037	CDC7	-1.62						
16858386	LDLR	-1.63						
17068385	GINS4	-1.63						
16679411	EXO1	-1.64						
16972616	NEIL3	-1.64						
17005865	HIST1H2BM	-1.65						
16750761	TROAP	-1.65						
16802204	ZWILCH	-1.66						
17038792	KIFC1	-1.66						
17012632	ENPP1	-1.66						
16948021	ECT2	-1.66						
16985614	CENPH	-1.67						
17064285	TMEM176B	-1.68						
16705159	CDK1	-1.68						
16688386	DEPDC1	-1.68						
16951485	SGOL1	-1.69						
16725041	FAM111B	-1.69						

16736891	KIF18A	-1.69						
17016366	HIST1H2AB	-1.70						
16869588	ASF1B	-1.70						
16739479	LRRN4CL	-1.71						
16964000	TACC3	-1.71						
17105401	CENPI	-1.71						
16995938	C5orf34	-1.71						
17086167	CEP78	-1.72						
16834056	CDC6	-1.74						
16845794	KIF18B	-1.74						
17064939	NCAPG2	-1.74						
16957951	POLQ	-1.76						
16662648	CDCA8	-1.76						
16784299	CDKN3	-1.76						
16760621	CDCA3	-1.77						
16817647	KIF22	-1.77						
16673154	NUF2	-1.78						
17067102	CDCA2	-1.78						
16982635	TRIP13	-1.78						
16828886	GINS2	-1.79						
16912192	GINS1	-1.79						
16798919	ARHGAP11A	-1.80						
16988703	LMNB1	-1.80						
16686796	STIL	-1.80						
16889251	SGOL2	-1.81						
16813342	PRC1	-1.81						
16840902	AURKB	-1.82						

17084904	MELK	-1.83						
16694617	IQGAP3	-1.84						
16807605	OIP5	-1.84						
16836492	PRR11	-1.85						
16931225	RIBC2	-1.85						
16690067	SASS6	-1.85						
16771067	CIT	-1.86						
16826160	SHCBP1	-1.86						
16760048	FOXN1	-1.87						
17087716	SMC2	-1.88						
16677201	DTL	-1.90						
17104484	KIF4A	-1.90						
16985599	CCNB1	-1.90						
16931384	GTSE1	-1.90						
16957170	KIAA1524	-1.90						
16937505	FANCD2	-1.92						
16912379	TPX2	-1.93						
16979515	CCNA2	-1.93						
16979389	MAD2L1	-1.94						
17012379	CENPW	-2.00						
16913957	MYBL2	-2.01						
16978568	CENPE	-2.03						
16751709	ESPL1	-2.05						
16965346	NCAPG	-2.05						
16904780	SPC25	-2.07						
17010552	TTK	-2.09						
16777278	SKA3	-2.09						

16668079	GPSM2	-2.09						
16830173	FAM64A	-2.11						
16707221	KIF20B	-2.11						
16849379	TK1	-2.11						
16719515	MKI67	-2.12						
16842673	SPAG5	-2.13						
16663514	CDC20	-2.14						
16991859	HMMR	-2.18						
16882975	NCAPH	-2.18						
16799598	CASC5	-2.21						
16799793	NUSAP1	-2.21						
16868838	SPC24	-2.22						
16850517	NDC80	-2.23						
16697695	KIF14	-2.26						
16901957	CKAP2L	-2.26						
16801557	CCNB2	-2.26						
16809748	MNS1	-2.27						
16939960	KIF15	-2.28						
16802519	KIF23	-2.29						
16793225	DLGAP5	-2.29						
17000439	CDC25C	-2.30						
17075776	PBK	-2.32						
16698984	NEK2	-2.34						
17049700	MIR4653	-2.34						
16817017	PLK1	-2.37						
17045198	ANLN	-2.42						
16875763	UBE2S	-2.42						

16677425	CENPF	-2.43						
16697544	ASPM	-2.49						
16844312	TOP2A	-2.50						
16707551	CEP55	-2.54						
16901755	BUB1	-2.69						
16971573	MND1	-2.83						
16989636	KIF20A	-3.14						
16991460	KIF4B	-3.38						

*TICAE cells were analyzed at the indicated time points after irradiation with a single X-ray dose of 0.5 Gy. Fold changes are shown compared to sham irradiation, as described in Materials and Methods (n = 3).

Supplementary table 3. Differentially expressed genes in TICAE cells irradiated with a single X-ray dose of 0.05 and 0.1 Gy.*

Day 14			Day 7		
0.1 Gy vs. 0 Gy			0.05 Gy vs. 0 Gy		
Probeset ID	Gene symbol	Fold change	Probeset ID	Gene symbol	Fold change
16997676	MTRNR2L2	2.02	16862604	CD79A	1.84

*TICAE cells were analyzed at the indicated time points after irradiation with a single X-ray dose of 0.1 and 0.05 Gy. Fold changes are shown compared to sham irradiation, as described in Materials and Methods (n = 3).

Annex 3. Online supplementary data related to Results Chapter 2: “Differential impact of single-dose Fe ion and X-ray irradiation on endothelial cell transcriptomic and proteomic responses” by Baselet B, *et al.*

Supplemental data 1. Transcriptomic comparison of irradiated and sham-irradiated Est-2 immortalized human coronary artery endothelial cells at day 1 and day 7 after a single dose of either 2 Gy X-rays or Fe ions. Raw data with accession number E-MTAB-5754 are available online at <http://www.ebi.ac.uk/arrayexpress> (username: Reviewer_E-MTAB-5754, password: h11qoecd).

Supplemental data 2. Gene ontology enrichment analysis of irradiated and sham-irradiated Est-2 immortalized human coronary artery endothelial at day 1 and day 7 after a single dose of either 2 Gy X-rays or Fe ions. Raw data with accession number E-MTAB-5754 are available online at <http://www.ebi.ac.uk/arrayexpress> (username: Reviewer_E-MTAB-5754, password: h11qoecd).

Supplemental data 3. Proteomic comparison of irradiated and sham-irradiated Est-2 immortalized human coronary artery endothelial cells at day 1 and day 7 after a single dose of either 2 Gy X-rays or Fe ions. Raw data with the identifier “DOI:10.20348/STOREDB/1086” are available online at <http://www.storedb.org>.

Supplemental data 4. Proteomic canonical pathway analysis of irradiated and sham-irradiated Est-2 immortalized human coronary artery endothelial cells at day 1 and day 7 after a single dose of either 2 Gy X-rays or Fe ions. Raw data with the identifier “DOI:10.20348/STOREDB/1086” are available online at <http://www.storedb.org>.

Supplemental data 5. Proteomic molecular function analysis of irradiated and sham-irradiated Est-2 immortalized human coronary artery endothelial cells at day 1 and day 7 after a single dose of either 2 Gy X-rays or Fe ions. Raw data with the identifier “DOI:10.20348/STOREDB/1086” are available online at <http://www.storedb.or>

